Perchlorate Esters and Perchloric Acid as Tools for Self-Crosslinking Thermosetting Acrylic Resins

DISSERTATION

presented by

PATRICK WIENEFELD

to the Institute of Technical and Macromolecular Chemistry
at the Faculty of Mathematics, Informatics and Natural Sciences
University of Hamburg
with the Aim of Achieving the Doctoral Degree

2026

1st reviewer: Professor Dr. Gerrit A. Luinstra

2nd reviewer: Priv. Doz. Dr. Christoph Wutz

Oral defence committee:

1. Professor Dr. Gerrit A. Luinstra
2. Professor Dr. Volker Abetz
3. Professor Dr. Wolfgang Maison

Date of oral defence: 10.04.2026

The experimental work described in this thesis was carried out at the Institute of Technical and Macromolecular Chemistry of the University of Hamburg in the research group of Professor Dr. Gerrit A. Luinstra in the period between June 2018 and December 2021.

Table of Content

I. List of Publications

Parts of this work were published in:

P. Wienefeld and G. A. Luinstra, *J. Appl. Polym. Sci.* **2025**, *142*, e56980. (https://doi.org/10.1002/app.56980)

P. Wienefeld and G. A. Luinstra, *J. Appl. Polym. Sci.* **2025**, e58087. (https://doi.org/10.1002/app.58087)

II. Abbreviations

1K/2K	one/two component
A	pre-exponential factor
AA	acrylic acid
AAEM	acetoacetoxyethyl methacrylate
ADH	adipic dihydrazide
AIBN	azobisisobutyronitril
ATR	Attenuated Total Reflection
α_g	Conversion within gel phase
BA	butyl acrylate
BDDA	1,4-butanediol diacrylate
BTFBA	3.5-bis(trifluoromethyl)benzaldehyde
CAGR	Compound Annual Growth Rate
CD	Crosslink Density
CP	Cross Polarization
CTA	Chain Transfer Agent
Đ	Dispersity
DAAM	diacetone acrylamide
DABCO	diaza bicyclo [2,2,2] octane
DBTL	dibutyltin dilaurate
DBU	1,8-diazabicyclo[5.4.0]undec-7-ene
DEM	diethyl malonate
DNNDSA	dinonylnaphthalene disulfonic acid
DSC	Differential Scanning Calorimetry
DDM	Dodecyl mercaptane
e.g.	exempli gratia
EA	ethyl acrylate
E_A	activation energy
Et	ethyl
EtOH	ethanol
exp	exponential function
f	fractional increase in diameter
f_n	average functionality
FTIR	Fourier Transform Infrared
GMA	glycidyl methacrylate
HBA	4-hydroxybutyl acrylate
HBMA	4-hydroxybutyl methacrylate
HDI	hexamethylene diisocyanato
HEA	2-hydroxyethyl acrylate
HEMA	2-hydroxyethyl methacrylate
HMMM	hexamethoxymethylmelamine
HSQC	Heteronuclear Single Quantum Coherence
IARC	International Agency of Research on Cancer
IBMAA	*N*-isobutoxymethylacrylamide
k	rate constant
MA	methyl acrylate
MAA	methacrylic acid
MAS	Magic-Angle-Spinning
M_c	number average molecular weight between crosslinks

$M_{c,cal}$	calculated number average molecular weight between crosslinks
MDI	methylene diphenyl diisocyanate
Me	methyl
MF	melamine-formaldehyde
MMA	methyl methacrylate
M_n	number average molecular weight
M_w	weight average molecular weight
n	reaction order
n-Bu	*n*-butyl
NCO	Isocyanate functional group
N_{eg}	Number of elastically active network chains per monomer unit
NMA	*N*-methylol acrylamide
NMR	Nuclear Magnetic Resonance
OEM	Original Equipment Manufacturer
OH	Hydroxy group
p_c	Gel point
P_n	Number average degree of polymerization
P_w	Weight average degree of polymerization
pCBA	4-perchloratobutyl acrylate
pCBMA	4-perchloratobutyl methacrylate
pCPA	4-perchloratopentyl acrylate
PTFE	polytetrafluoroethylene
pTSA	p-toluenesulfonic acid
Q	percentage molar ratio of crosslinker in the polymer
R	universal gas constant
SEC	Size-Exclusion-Chromatography
S_N	Nucleophilic Substitution
ST	styrene
T	absolute temperature
TCE	1,1,2,2-tetrachloroethane
TDI	toluene diisocyanate
T_g	glass transition temperature
TGA	Thermogravimetric Analysis
TGIC	triglycidylisocyanurat
THF	tetrahydrofuran
TMHDI	trimethyl hexane diisocyanato
TPA	Thermoplastic Acrylic
UV	ultraviolet
V_1	molar volume of the solvent
V_2	volume fraction of the polymer in the swollen gel at equilibrium
VOC	Volatile Organic Compound
w_g	Gel fraction
X	conversion
x_1	diameter of the sample before swelling
x_2	diameter of the sample in equilibrium swollen state
β_1	lattice constant
δ	chemical shift
δ_p	Hansen solubility parameters of the polymer
δ_s	Hansen solubility parameters of the solvent
η	dynamic viscosity

ρ	polymer density	χ	Polymer solvent interaction parameter

1 Zusammenfassung

Die Arbeit beschreibt ein neuartiges selbstvernetzendes Konzept für wärmehärtende Acrylharze, das die außergewöhnliche Reaktivität organischer Perchlorsäureester nutzt und damit eine Alternative zu Systemen bietet, die externe Vernetzer erfordern oder Katalysatorrückstände im Film hinterlassen. Ausgangspunkt war die Synthese eines Acrylmonomers mit kovalent gebundenem Perchlorsäureester. Das so entwickelte 4-Perchloratobutylacrylat (pCBA), zugänglich über eine effiziente Ein-Topf-Reaktion aus Acryloylchlorid, THF und Silberperchlorat, lässt sich mit gängigen (Meth)acrylaten radikalisch copolymerisieren und überträgt eine definierte Menge stabiler Perchlorsäureester-Gruppen in das Polymergerüst. Beim Erwärmen über 100°C ermöglichen diese Gruppen überraschenderweise eine effiziente Selbstvernetzung.

Quellexperimente zeigten, dass pCBA-haltige Copolymere bereits zwischen 105 und 135°C spontan unlösliche, dichte Netzwerke bilden. Mechanistisch erfolgt die Vernetzung nicht über oxidative Zersetzung der Perchloratspezies, sondern über eine Umesterung mit den Estergruppen des Polymers selbst. Dabei entstehen thermisch stabile 1,4-Butylendiesterbrücken, während flüchtige Alkylperchlorate entweichen. Eine Festkörper-NMR-spektroskopische Analyse bestätigte den Typus der entstehenden Vernetzungseinheiten; ergänzende FTIR-, TGA-FTIR- und Abfang-Experimente belegten die Bildung von Methyl-, Ethyl- oder Butylperchlorat sowie geringer Mengen an THF. Die Reaktion folgt einem Verlauf erster Ordnung, wobei die Aktivierungsenergien in der Reihe Methylacrylat (MA) < Ethylacrylat (EA) < *n*-Butylacrylat (BA) ansteigen. Jede pCBA-Einheit kann eine Vernetzungsstelle erzeugen, was die hohe theoretische Effizienz des Prinzips unterstreicht. Praktisch begrenzt wird der Ansatz jedoch durch die Freisetzung flüchtiger Perchlorate sowie durch die Handhabung von Silberperchlorat. In BA-reichen Copolymeren treten zudem detektierbare Nebenreaktionen auf, die zur Bildung von THF- und Carbonsäuren führen.

Um die Vorteile der Perchloratchemie ohne die Notwendigkeit eines speziellen Monomers zu nutzen, wurde das Reaktionsprinzip genutzt um unter Einsatz von Perchlorsäure hydroxyfunktionelle Acrylharze zu vernetzten. Konzentrierte Perchlorsäure bildet mit 2-Hydroxyethylacrylat (HEA)- oder 4-Hydroxybutylacrylat (HBA)-haltigen Copolymeren nach Erhitzen und dem Verdampfen des Lösungsmittels und Wasser in-situ die reaktiven Perchlorsäureester-Intermediate. Diese Intermediate reagieren analog zu pCBA und ermöglichen sowohl Veretherungen als auch Umesterungen. Ethanollösliche Harzformulierungen mit 0,6-100 mol% Perchlorsäure (relativ zur Anzahl der Hydroxylgruppen)

erwiesen sich über Monate als lagerstabil und lieferten bei 85-105°C klare, hochvernetzte Filme. FTIR-Analysen und Quellexperimente zeigten eine steigende Vernetzungsdichte mit höherem Hydroxygehalt und zunehmender Säurekonzentration. HEA-Copolymere bildeten sowohl Diethylenglykolether- als auch Ethylendiesterbrücken, während HBA-Systeme überwiegend Butylendiesterstrukturen erzeugten. Carbonsäuregruppen entstanden vor allem bei hohen Säuregehalten, vermutlich durch säurekatalysierte Dealkylierung oder partielle Hydrolyse, und führten zu Harzen mit höheren Glasübergangstemperaturen. Während der Härtung verflüchtigten sich sämtliche Perchlorat-haltige Intermediate vollständig, sodass pH-neutrale und nicht hygroskopische Filme resultierten.

Der Vernetzungsmechanismus wird durch das Zusammenspiel von Etherbildung und Umesterung geprägt, das wesentlich von der Menge Perchlorsäure pro Gramm Harz abhängt. Geringe Säurekonzentrationen führen zu flexibleren, etherreichen Netzwerken, während hohe Konzentrationen schnelle, dichter-vernetzte und thermisch stabile Strukturen begünstigen. HEA-Copolymere zeigten insgesamt ein einheitlicheres Reaktionsverhalten, während in HBA-Systemen unter bestimmten Bedingungen vermehrt THF und Carbonsäuren, Produkte von Nebenreaktionen, gebildet wurden.

Zur Entwicklung lösemittelarmer Lacke wurden niedermolekulare HEA-Copolymere mithilfe der Kettenübertragungsmittel Dodecylmercaptan (DDM) und Kohlenstofftetrabromid synthetisiert. Die resultierenden Oligomere konnten zu Filmen mit Vernetzungsdichten umgeformt werden, die denen basierend auf höhermolekularen Harzen entsprechen. Thioether-Endgruppen in den Harzen aus der Reaktion mit DDM verzögerten die Härtung aufgrund der temporären Bildung stabiler Sulfoniumperchlorate, während bromierte Endgruppen keinen Einfluss auf die Reaktivität zeigten.

2 Summary

The work concerns a new self-crosslinking concept for thermosetting acrylic resins based on perchlorate chemistry, developed as an alternative to conventional systems that require external crosslinkers or leave catalyst residues in the cured film. Initial efforts focused on the synthesis of covalently bound perchlorate ester monomers, culminating in the successful preparation of 4-perchloratobutyl acrylate (pCBA) via a one-pot reaction of acryloyl chloride, THF and silver perchlorate. This monomer polymerizes readily with common (meth)acrylates under free-radical conditions, yielding linear copolymers with controlled compositions and intact perchlorate ester groups. These groups react readily with nucleophiles, but more importantly enable efficient self-crosslinking of the copolymers upon heating above 100°C.

Curing studies revealed that pCBA-containing copolymers spontaneously form insoluble networks at 105-135°C. Mechanistic analysis showed that the perchlorate ester does not decompose oxidatively but participates in transesterification with the polymer's own ester groups, forming robust 1,4-butylene diester crosslinks and releasing volatile alkyl perchlorates. A Solid-state NMR analysis confirmed the type of crosslinks, while FTIR, TGA-FTIR and trapping experiments demonstrated evaporation of methyl, ethyl or butyl perchlorate depending on the comonomer, along with minor quantities of THF. The curing reaction follows first-order kinetics, and the activation energies increase in the order methyl acrylate (MA) < ethyl acrylate (EA) < *n*-butyl acrylate (BA), consistent with thermal stability trends. Each pCBA unit can form one crosslink, underscoring the high theoretical efficiency of the system. However, the approach poses practical limitations: silver perchlorate, used for preparation of intermediates, is expensive and hazardous; the curing process produces volatile perchlorates of toxicological concern; and side reactions in BA-rich systems generate THF and carboxylic acids, leading to undesired mass loss.

To retain the benefits of the perchlorate chemistry without relying on specialized monomers, the reaction principle was applied to crosslink hydroxy-functional acrylic resins using perchloric acid. Upon heating and evaporation of water, concentrated perchloric acid forms reactive perchlorate ester intermediates in situ with copolymers containing 2-hydroxyethyl acrylate (HEA) or 4-hydroxybutyl acrylate (HBA). These intermediates mirror the reactivity observed in pCBA copolymers, reacting either with hydroxyl groups to form ether linkages or with ester groups to form alkylene diester crosslinks. Ethanolic formulations of these resins with 0.6-100 mol% perchloric acid were stable for months and formed transparent films upon curing at 85-105°C. Swelling studies and FTIR confirmed increasing crosslink density (CD) with higher

HEA/HBA content and higher acid loadings. Solid-state NMR showed that HEA-based systems form mixtures of diethylene ether and ethylene diester linkages, whereas HBA-based systems predominantly generate butylene diester crosslinks. Carboxylic acid groups appeared in both systems, particularly at high perchloric acid concentrations, likely due to acid-induced dealkylation or hydrolysis, and led to resins of higher glass transition temperatures (T_g). Notably, all perchlorate species volatilized or decomposed during curing, leaving neutral, non-hygroscopic films.

Curing proceeds via a competition between etherification and transesterification, controlled by the amount of perchloric acid per gram resin. Low acid levels favor ether formation and yield more flexible networks, whereas higher acid concentrations promote fast curing of more densely crosslinked and thermally stable structures, dominated by alkylene diester crosslinks and higher T_g. HEA copolymers generally show a more homogeneous curing behavior, while HBA copolymers exhibit additional THF- and carboxylic acid-forming pathways under certain conditions.

To enable high-solids, low-volatile organic content (VOC) coatings, low-molecular-weight HEA copolymers were synthesized using chain transfer agents (CTA) such as dodecyl mercaptan and carbon tetrabromide. The resulting oligomers could be processed into films with CDs comparable to their high-molecular-weight analogues. Thioether end groups in the resins derived from mercaptans slowed down the curing process due to formation of sulfonium perchlorate species that temporarily bind acid, whereas brominated end groups had no measurable effect.

3 Introduction

The first records of paints and coatings date back more than ten thousand years to China[1] and Japan[2]: only in the 19th century, an industrial paint and coatings industry had developed in Europe. The global paint and coatings market size was forecasted in 2019 to reach $204 billion in 2023 with a compound annual growth rate (CAGR) of 4.9%.[3] Despite the economic downfall in early 2020, the industry is expected to recover from a 6.3% decline in 2020 and grow to $217 billion in 2028 at a CAGR of 5.4%.[4]

Today, the paint and coatings industry face several challenges: Rising concerns over volatile organic compound (VOC) and increasing regulatory pressure from legislation give the driving force and have pushed developments towards low VOC concepts comprising water-based formulations, high-solid paints, and solvent-free systems. Customer expectations have increased too and prompted manufacturers to use less raw materials and co-reactants which improve cost structures at the same time. Achieving low curing temperatures without compromising shelf-life is just one example of the challenges that manufacturers face.

Paints and coatings are majorly applied to substrates for reasons of decoration, protection and/or functional purposes. Decorative coatings will mainly serve aesthetic functions. Most commercial coating systems will fulfil multiple purposes. Protective coatings, for example in chemical reactors or pipelines, aim to prevent corrosion or degradation. Coatings in industrial applications not only provide corrosion and abrasion resistance but also impart visual appeal, and in certain sectors, such as electronics, they add functionality by adding a conductivity.

Conventional liquid paints or coatings, with a few exemptions, consists of four major components:

- binder
- solvent
- pigments
- additives

The binders constitute the film-forming component and determines most of the physical and chemical properties of the final coating. Common binder types include acrylic, alkyd, polyester, amino, epoxy, and urethane resins, each offering advantages for a specific application. Key performance parameters comprise weathering resistance, corrosion protection, gloss, colour retention, flexibility and chemical durability.

Solvents are used for dissolving or dispersing the components of a formulation and are selected based on cost, safety, evaporation rate, viscosity, solvency or odor. Aliphatic or

aromatic hydrocarbons, alcohols, ethers, esters, ketones are commonly used. Water and alcohols are the environmentally more benign options, hydrocarbons are increasingly avoided because of their flammability and toxicity.

Solid pigments are insoluble and serve as colorants or corrosion inhibitors. Common pigments are TiO_2, ZnO, red iron oxide, carbon black and aluminum. Rather insoluble organic compounds such as azo and phthalocyanine derivatives are also common pigments.[5]

Additives are added in small quantities to improve properties of the liquid formulation or the resulting film, like for example UV or microbial resistance, fire retardancy, pigment dispersion, gloss, viscosity or hardness.

Acrylic resins are among the most widely used binders and are prepared by free radical polymerization of homo- and copolymers of acrylic acid (AA) and methacrylic acid (MAA) esters. Typical resins are based on methyl, ethyl, *n*-butyl, *iso*-butyl, *tert*-butyl, 2-ethylhexyl, cyclohexyl, *n*-dodecyl and stearyl acrylic esters (Scheme 1). Styrene (ST), (meth)acrylamides, acrylonitrile, vinyl esters, and maleic anhydride are often copolymerized with the esters to tailor the resin properties. Functional monomers, including 2-hydroxyethyl (meth)acrylate (HEA, HEMA), 4-hydroxybutyl (meth)acrylate (HBA, HBMA), trimethylsiloxyethyl methacrylate, glycidyl methacrylate (GMA), isopropenyl dimethyl benzylisocyanat, dimethylaminoethyl methacrylate and methylol (meth)acrylamide contain reactive groups that enable post synthesis crosslinking of the resin.

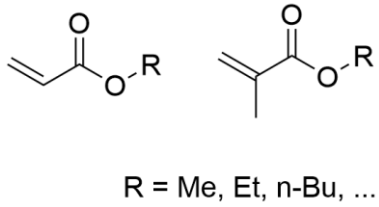

Scheme 1. General chemical structure of acrylic (left) and methacrylic esters (right); R = organic rest.

The overall performance of an acrylic polymer is governed by monomer composition. The glass transition temperature (T_g), a key design parameter, can be tuned by the monomer content of the linear copolymer according to the Fox-equation:

$$\frac{1}{T_{g,mix}} = \sum_i \frac{w_i}{T_{g,i}} \qquad (1)$$

where $T_{g,mix}$ and $T_{g,i}$ denote the glass transition temperatures of the copolymer and the homopolymer respectively and w_i is the weight fraction of the component i.

Monomers such as *n*-butyl acrylate (BA) and *n*-dodecyl acrylate lower T_g and improve ductility and adhesion. Monomers such as methyl methacrylate (MMA) increase mechanical strength and chemical resistance toughness. Copolymerization or crosslinking allows properties to be combined.

Acrylic polymers are accessible by either bulk, solution, suspension or emulsion polymerization. Bulk polymerization yields high molecular weight polymers and products with a broad molecular weight distribution. The dilution by solvents in solution polymerization results in a lower rate of chain growth with less radical transfer to polymer reaction, leading to lower molecular weight products with narrower distributions. The inherent lower viscosity of such binders is important for high-solids, low-VOC formulations. The presence of chain transfer agents (CTAs) during resin formation, commonly thiols, will further regulate the molecular weight and influence the end-group functionality. Suspension and emulsion polymerization of acrylates produce aqueous latexes, which are widely used to prepare wall paints, adhesives and inks.[6,7]

Acrylic resins are valued for their combination of flexibility, weather and impact resistance, and gloss retention. The variety of available monomers and their polymerization gives some control over the chemical and physical properties, allowing to adjust to the requirement for a plethora of applications. Their chemical structure goes along with UV stability and resistance to chemical degradation. Water-based acrylic latexes eliminate the need for organic solvents, aligning with increasingly stringent VOC regulations and environmental standards. Currently acrylic resins are widely used in the original equipment manufacturer (OEM) market, as maintenance coatings, wood coatings, architectural coatings, both interior and interior, and in inks.[5,8]

3.1 Thermosetting Acrylic Resins

Thermosetting acrylic resins are valued for their outstanding weather resistance, strong adhesion to a wide range of substrates, and overall cost efficiency.[9] Owing to this favorable balance of performance and economics, they are widely applied in architectural coatings, specialty coatings, and OEM applications. The global market size was valued at approximately $7.5 billion in 2023 and is projected to reach $11.1 billion by 2032 with an CAGR of 4.5%.[10]

Thermosetting acrylic resins are functionalized acrylic resins that undergo chemical crosslinking at elevated temperatures, typically between 80 and 250°C. The initially low-

molecular-weight polymers are converted during the curing process into a three-dimensional network of virtually infinite molecular weight. The resulting films are insoluble, exhibit good heat and chemical resistance relative to thermoplastic acrylics (TPAs). They also have a significantly higher T_g than analogous TPAs. This allows for the formulation of softer, more flexible precursor polymers with lower initial T_g values. This can e.g. be achieved by the incorporation of a higher fraction of monomers like BA.[7]

Thermosetting acrylic resins generally require less solvent than TPAs to achieve suitable processing viscosities because of their lower viscosity that comes along with their low T_g. High-solid formulations with solid contents of 70-80% and with molecular weights of approximately M_n of 2000 g mol^{-1} and M_w of 5000 g mol^{-1} are achievable, in contrast to typical TPAs with M_n of 80,000 g mol^{-1} and M_w of 180,000 g mol^{-1} and solid contents of only 20-25%. Non- or monofunctional chains must be avoided as they act as plasticisers and reduce the achievable crosslink density. Consequently, the nature of chain end groups, particularly those introduced by CTAs, play an important role with respect to curing behaviour and final film properties. High-solid thermosetting acrylic resins are widely used because they meet the requirements of VOC regulation and can be combined with other resin types such as amino resins and polyisocyanates to optimize film performance and reduce costs.[11]

Thermosetting acrylic resins are commercially available as one-component (1K) and two-component (2K) systems. All reactive components in 1K systems are pre-mixed and stored in one container. The system should have an average shelf-life of at least 6 months, and curing should be initiated only after application and heating. In contrast, 2K systems consists of components stored separately which prevents premature crosslinking. They are mixed immediately before use with pot lives of 4-8 hours corresponding to a standard work shift. Most 2K systems cure at ambient temperature, whereas some require additional heating for better performance of the resulting film. Although 1K systems offer advantages in handling and process simplicity, 2K systems remain widely used because of their superior performance and room-temperature reactivity.[11]

The principal challenge in designing 1K thermosets lies in the combination of storage stability and a high reactivity for curing at low temperatures. In practice, these requirements are often mutually exclusive: formulations stable for several months usually require curing temperatures around 180°C, whereas systems that cure at 100°C usually have shelf lives limited to less than six months. This basically reflecting the temperature dependence of reaction kinetics as described by the Arrhenius relationship.

Several strategies have been developed to overcome this limitation. One strategy uses blocking agents that reversibly deactivate reactive crosslinkers or catalysts. Upon heating the blocking agent evaporates from the film surface, regenerating the active species and enabling crosslink formation. However, blocking agents increase material costs, contribute to VOC emissions, and represent a net material loss, making them less attractive from both economic and environmental perspectives. Alternative approaches rely on the physical separation of reactive components, for example through encapsulation[12] or crystallization[13], thereby preventing premature reaction during storage. Another common strategy involves the removal of volatile species such as solvents[14] and by-products[15,16] during curing. Their evaporation shifts the equilibrium toward crosslinking by eliminating one component from the reactive mixture. The latter approach is particularly relevant for commercially available thermosetting acrylic systems, many of which can be cured at moderate temperatures and, in some cases, even under ambient conditions.

Various functional groups have been introduced in thermosetting acrylic resins to facilitate crosslinking, most prominently carboxylic acids, hydroxy groups, epoxy groups, amides, and isocyanates. Functional acrylic resins are often combined with other resins such as amino, alkyd, epoxy, and polyester resins to improve film properties and reduce costs.[11,17,18]

3.1.1 Hydroxy-Functional Acrylic Resins

Hydroxy-functional acrylic resins are the most widely used functional acrylic resins.[18,19] Although hydroxy groups are usually introduced by copolymerization of HEA, HEMA, HBA or 2-hydroxypropyl acrylate, alternative monomers[20] and strategies are available, including post-polymerization modification of a carboxylic acid functional acrylic resin with glycidyl esters[19]. The respective hydroxy-functional resins are then combined with, for example, amino resins or (poly)isocyanates.

The principal amino resins used in thermosetting acrylic resins are melamine (**1**) formaldehyde (MF) and urea (**4**) formaldehyde resins. In addition, glycoluril (**3**)-, benzoguanamine (**2**)- and carbamate (**5**)-based resins are also applied in specialized formulations (Scheme 2).

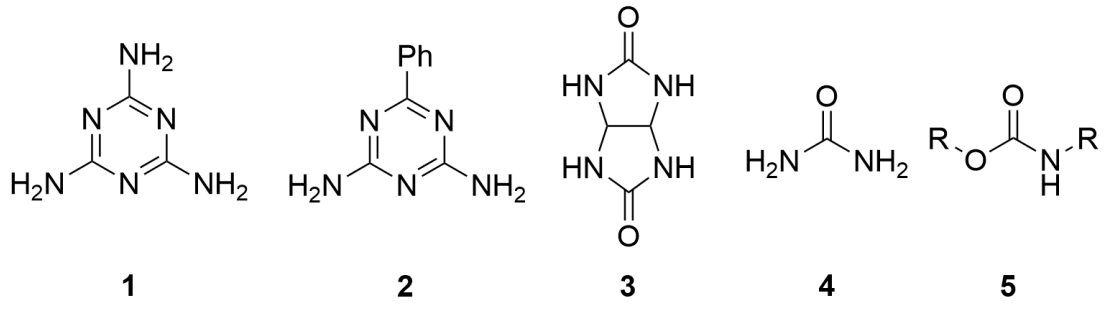

1 **2** **3** **4** **5**

Scheme 2. Chemical structures of melamine (**1**), benzogunamine (**2**), glycoluril (**3**), urea (**4**) and a carbamate (**5**); R = organic rest.

Amino resins are prepared by the condensation of the corresponding amino precursor **1**-**5** with formaldehyde and methanol. One of the most common representatives, hexamethoxymethyl melamine (HMMM, **7**), is produced by reacting **1** with formaldehyde to form methylolated melamine **6**, followed by etherification with methanol to yield the final resin (Scheme 3).

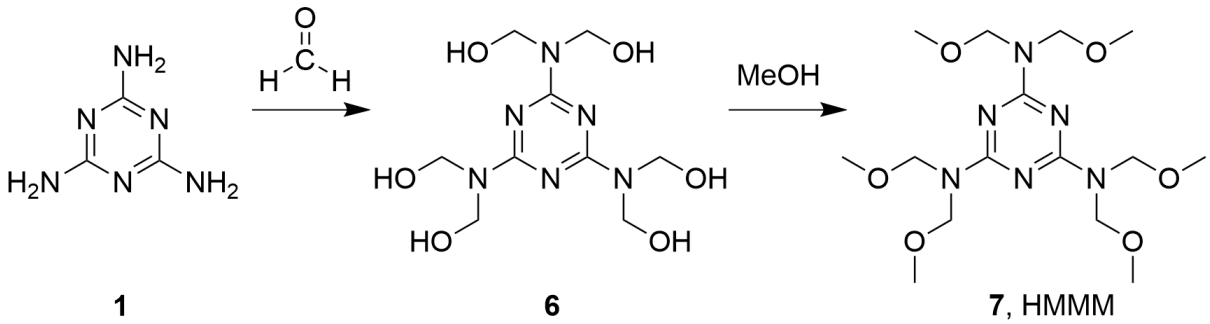

1 **6** **7**, HMMM

Scheme 3. Synthesis of HMMM (**7**) from melamine **1**, formaldehyde and methanol.

MF resins are classified according to their degree of etherification into Class I or Class II. In Class I resins, most amine groups are etherified twice, whereas in Class II resins they are etherified only once. Class II resins dominated the market during the 1940th and 1950th, but have largely been replaced by Class I resins due to their superior compatibility with other polymers, particularly hydroxy-functional acrylics, as well as with waterborne and high-solids systems.[11]

Crosslinking between amino and acrylic resins proceeds via acid-catalyzed (trans)etherification between hydroxy groups of the acrylic component and methylol or alkoxymethyl groups of the MF resin (Scheme 4). The reaction is facilitated by stabilization of the developing positive charge through electron donation from the adjacent nitrogen atom, enabling efficient ether formation. The reaction produces volatile alcohols, typically methanol or *n*-butanol, which evaporate from the film and drive the equilibrium toward crosslinking. In

cases where phenolic nucleophiles are involved, C-C bond formation may occur, leading to irreversible crosslinks.[11]

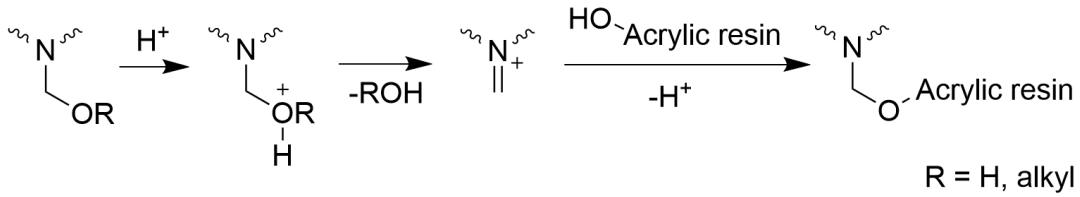

Scheme 4. Acid-catalysed crosslinking reaction between hydroxy-functional acrylic resins and methylol (R = H) or alkoxy methyl groups (R = alkyl) of amino resins such as HMMM (**7**).

In addition to co-condensation with acrylic resins, MF resins can self-condense to form dimers, trimers, oligomers and polymers. Two primary types of linkages are generated between triazine units: methylene and dimethylene ether bridges (analogous to reactions in Scheme 4). The balance between co- and self-condensation depends on the ratio of methylol and alkoxymethyl groups to hydroxy groups, and on the class of resin. Class I resins favor co-condensation whereas Class II resins tend to form self-condensed structures. Reaction conditions such as pH, catalyst type and concentration, curing time and temperature also influence the extent of self-condensation. Curing temperatures typically range from 80 to 200°C and are strongly affected by the acidity of the catalyst and its concentration. The overall rate of crosslinking depends on the molecular structure of both the acrylic and MF resin, the volatility of the generated alcohols, and the curing conditions employed.[7,11]

Catalysts are employed to reduce curing temperatures and shorten curing times, typically added in amounts between 0.1 and 1 wt% relative to the total weight of solids. Common catalyst types include carboxylic, phosphoric, and sulfonic acids. Curing in hydroxy-functional acrylic /MF Class I resin systems catalysed by sulfonic acids is typically completed within 10-30 minutes at 110-130°C. Co-condensation reactions are favoured by carboxylic acids, although curing temperatures above 140°C are required. In fast-curing applications such as coil coatings, where reaction times are on the order of seconds, high temperatures and strong acids are used. Catalysts include p-toluenesulfonic acid (pTSA, **8**), p-dodecylbenzenesulfonic acid (DDBSA, **9**), dinonylnaphthalene disulfonic acid (DNNDSA, **10**), phenyl phosphoric acid (**11**), dibutyl phosphoric acid (**12**) and maleic acid (**13**) (Scheme 5).

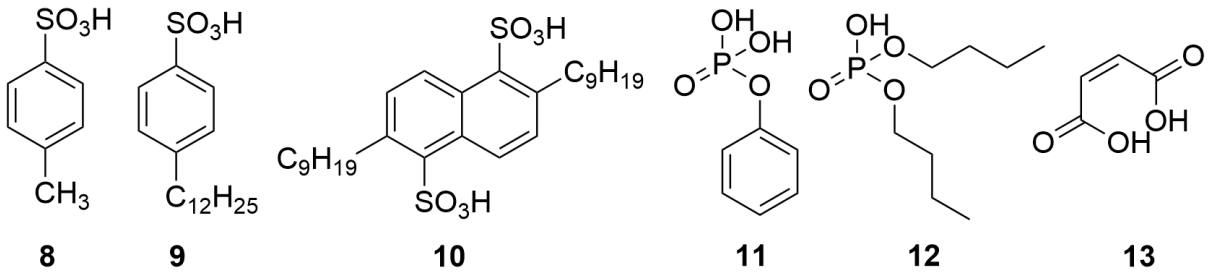

Scheme 5. Chemical structures of pTSA (**8**), DDBSA (**9**), DNNDSA (**10**), phenyl phosphoric acid (**11**), dibutyl phosphoric acid (**12**), and maleic acid (**13**).

The catalyst concentration and pH must be carefully optimized, as excessive catalyst levels can induce premature crosslinking during storage. This is commonly prevented either by formulating the system as a 2K coating or using blocked catalysts. In the latter case, strong acids, typically aryl sulfonic acids with a pk_a < 0, are neutralized with volatile amines to form amine salts (Scheme 6). These salts act as weak acids (pk_a 8-10) and are catalytically inactive during storage. Upon heating, the volatile amine evaporates, shifting the equilibrium toward the free acid and generating the active catalyst in-situ.

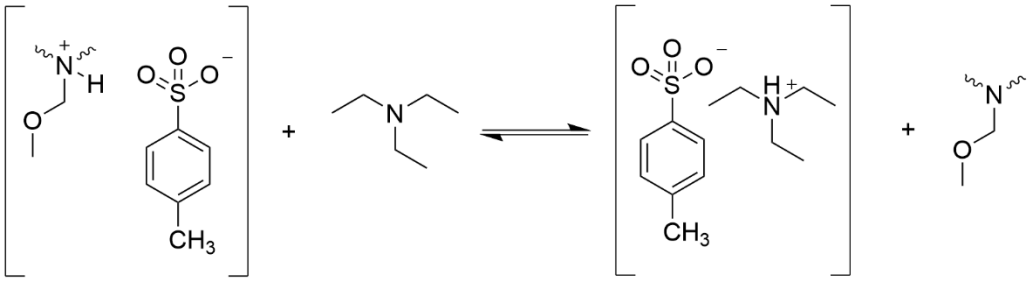

Scheme 6. Amine-blocked pTSA in storage mode (right side) and active (free) pTSA after evaporation of the volatile amine (left side).

It is important to note that the curing rate at some point cannot be increased by simply employing stronger acids, since the rate is determined by the reactions of the protonated MF resin rather than that of the free acid. Acids stronger than sulfonic acids therefore do not enhance the curing process. Catalyst selection is not only guided for curing activity and moisture matters, but also for effects on adhesion, blister formation, pigment compatibility, and substrate interaction. Residual catalysts remain in the cured film, which can promote water uptake and hydrolytic degradation of crosslinks.[21] pTSA, which is still widely used for acrylic/amino resin systems, is being replaced by more hydrophobic sulfonic acids such as DNNDSA and DDBSA, also to improve water resistance. Basic components in a formulation particular can significantly reduce catalyst performance.

Despite ongoing efforts to lower formaldehyde release[15,16,22], conventional formaldehyde-based amino resins remain widely employed in commercial coatings.[11] Amino resins continue to suffer from formaldehyde emissions during curing, posing health risks for workers and restricting their use primarily to industrial environments with exhaust treatment equipment. Also for lowering the toxicity, methanol in traditional formulations has largely been replaced by higher alcohols.

Hydroxy-functional acrylic resins are also frequently combined with (poly)isocyanates to form polyurethane networks. The reaction between alcohols and isocyanates yields urethanes and proceeds readily at room temperature or slightly elevated temperatures, which is why most polyisocyanate-based coatings are formulated as 2K systems. The curing rate can be tailored by selecting suitable combinations of isocyanates and alcohols: primary alcohols react faster than secondary or tertiary alcohols for steric reasons, and aromatic isocyanates exhibit higher reactivity than aliphatic analoges.[23]

In addition to the primary urethane forming reaction (Scheme 7a), several secondary reactions may occur depending on formulation and curing conditions. Isocyanates can react with urethanes to form allophanates (Scheme 7b); additionally isocyanates may react with atmospheric moisture to generate intermediate carbamic acids which readily decompose into amines. The resulting amines react with remaining isocyanates to yield urea moieties (Scheme 7c), a reaction much faster than the alcohols-isocyanate reaction. Ureas can further react with isocyanates to form biurets (Scheme 7d). In some cases, carboxylic acids may react with isocyanates to form amides with concurrent release of CO_2 (Scheme 7e), although this process requires elevated temperatures and can cause blistering of the coating due to gas bubble formation.[23]

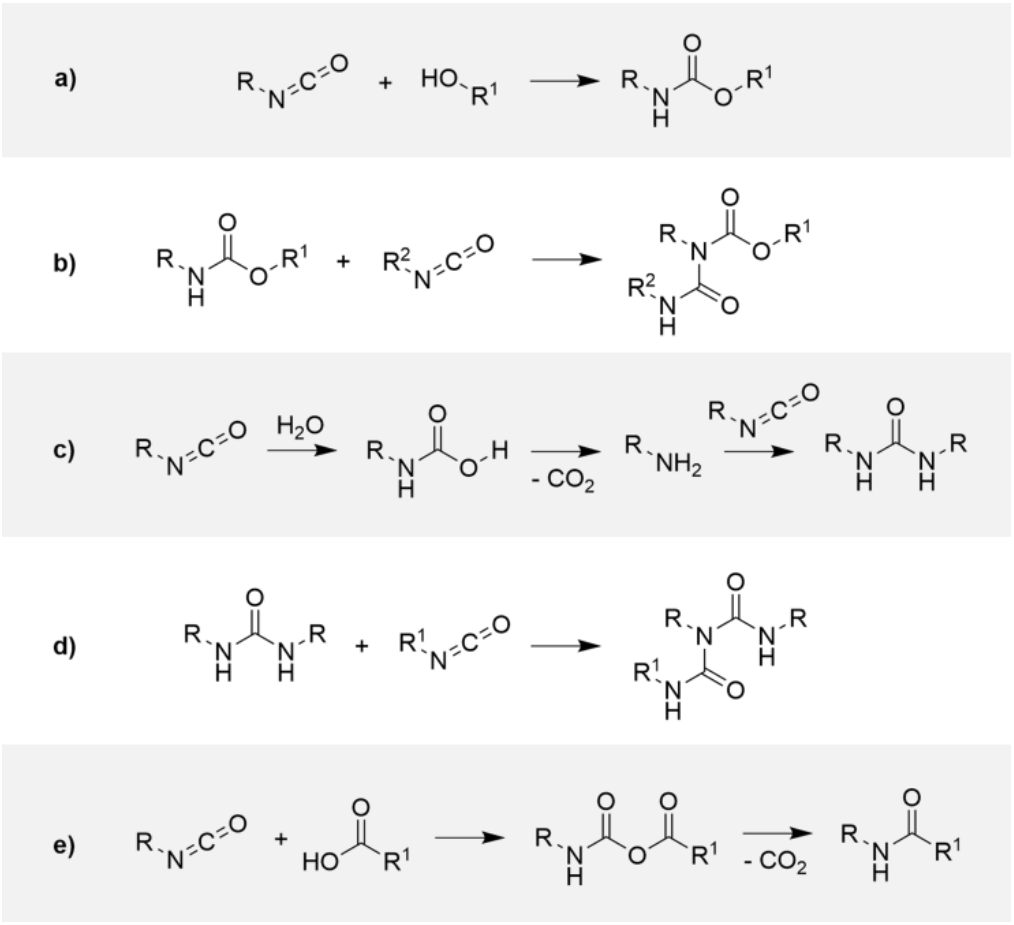

Scheme 7. Reactions in polyurethane coatings during curing; (a) reaction of isocyanate with hydoxyls; (b) reaction of urethanes with isocyanates; (c) reaction of isocyanates with water; (d) reaction of ureas with isocyanates; (e) reaction of isocyanates with carboxylic acids; R, R^1 and R^2 are organic rests.

Polyurethanes have strong intermolecular hydrogen bonding between urethane groups. Crystal domains arise in polyurethane (segments) from short diols (usually 1,4-butane diol), leading to short distances between the urethane entities. Polyurethanes formed by mixtures of short and longer diols will phase separate to yield distinct soft amorphous and hard crystalline domains. These structural features account for their excellent mechanical properties and resilience. Hydrogen bonds may temporarily dissociate under mechanical stress but will reform rapidly, preventing irreversible damage to a PU-coating. As a result, polyurethane coatings exhibit high abrasion and solvent resistance. However, the hydrophilic urethane linkages also make water uptake favorable, which can participate in the hydrogen bonding network. Coatings based on aliphatic diisocyanates show improved weathering and UV resistance, though their application is limited by their cost and toxicity of isocyanates. Volatile monomeric isocyanates have largely been replaced by high-molecular-weight polyisocyanates with low vapor pressure for their lower toxicity. Nevertheless, occupational exposure remains a concern, as even small quantities of isocyanates can cause allergic reactions such as dermatitis and asthma.[23]

Polyisocyanate crosslinkers used in coatings are based on commercial available diisocyanates such as toluene diisocyanate (TDI), methylene diphenyl diisocyanate (MDI, **15**), hexamethylene diisocyanato (HDI) and trimethyl hexane diisocyanato (TMHDI, **14**) and their reaction with polyols or other polyfunctional oligomers (Scheme 8). For example, trimethylol propane reacts with three equivalents of TDI to form the trifunctional polyurethane crosslinker **17** which is commonly employed due to its easy of handling. Catalytic dimerization or trimerization of HDI gives HDI uretdione and isocyanurate (**16**), respectively. Both are capable of regenerating isocyanates upon heating.[23]

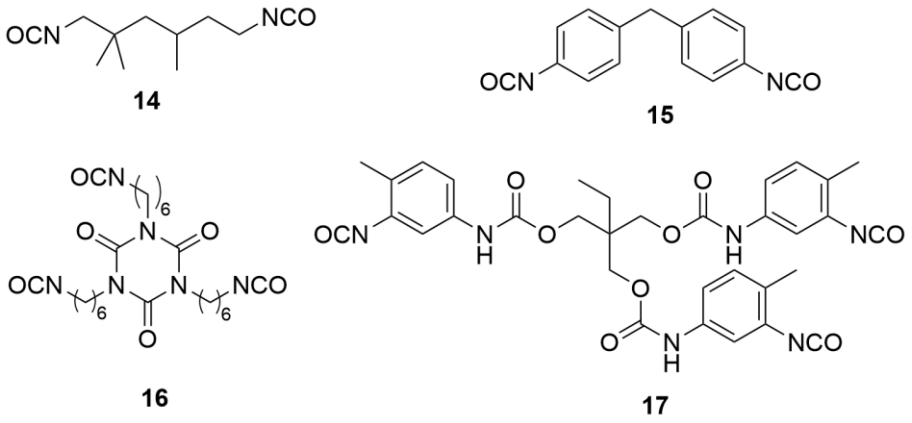

Scheme 8. Chemical structure of TMHDI (**14**), MDI (**15**), HDI isocyanurate (**16**) and TDI-based trifunctional polyurethane crosslinker (**17**).

Since the reaction between isocyanates and alcohols proceeds relatively slow at ambient temperature, catalysts are typically employed to accelerate curing. These include acids[24], bases[25], metal chelates[26] and organometallic compounds[27]. The most widely used are diazabicyclo[2,2,2]octane (DABCO) and dibutyltin dilaurate (DBTL), which act synergistically, enhancing reactivity beyond the sum of their individual effects.[28] Although required only in small quantities (0.01-0.5 wt%), DBTL is classified as toxic to humans and the environment, prompting the search for more sustainable and less hazardous alternatives.

The development of blocked isocyanate chemistry enabled the formulation of 1K polyurethane thermosets.[29] In this approach, reactive isocyanate groups are reversibly deactivated through reaction with a blocking agent, preventing premature crosslinking during storage. Upon heating, the isocyanate is released, initiating crosslinking while the blocking agent evaporates from the coating (Scheme 9). Typical blocking agents include 2-ethylhexanol, 2-butoxyethanol, ε-caprolactam, 2-butanone oxime, phenols, and malonates. The choice of blocking agent largely determines the curing temperature: the higher the stability of the blocked isocyanate, the higher the temperature required for deblocking. Conversely, if the reaction product of the

isocyanate and co-reactant is less stable than the blocked species, longer curing times are necessary. Crosslinking efficiency can be improved by selecting blocking agents with higher volatility and by employing catalysts[11,23]. In addition, blocked sulfonic acids are occasionally used together with free isocyanates and hydroxy-functional acrylic resins[30]. Unlike amino resins or unblocked polyisocyanates, they co-crosslink only through the isocyanate groups released during curing, allowing the stoichiometric OH/NCO ratio to be precisely calculated from the hydroxyl and isocyanate numbers of the respective components. When malonates such as diethyl malonate (DEM) are used as blocking agents, the resulting crosslinks are not pure polyurethanes but rather transesterification products or species derived from amide cleavage. DEM-blocked polyisocyanates are sufficiently stable to be used in waterborne systems[31] and can be co-formulated with hydroxy-functional acrylic and amino resins in a single coating system[32].

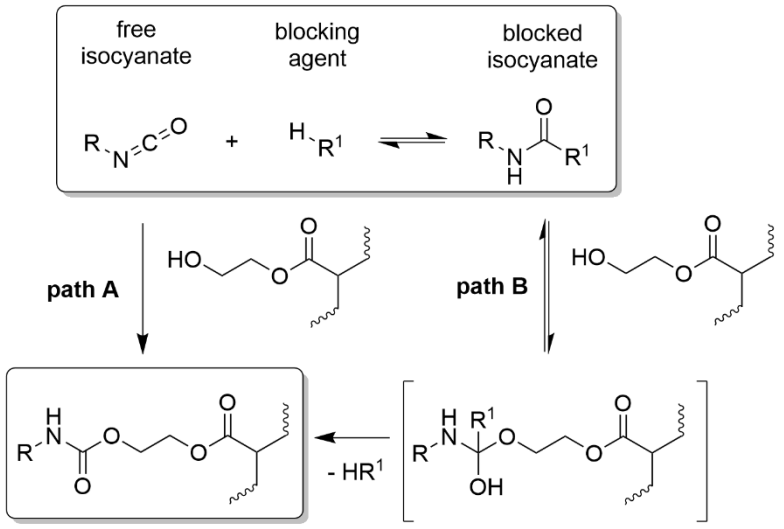

Scheme 9. Mechanism of blocking and deblocking of isocyanate functionality; path A) elimination-addition; path B) addition-elimination; R and R^1 = organic rest.

Moisture-curable polyurethanes, on the other hand, contain isocyanate-terminated polyesters, polyethers or polyacrylates that react with atmospheric moisture upon application. The resulting amine intermediates react with remaining isocyanates to form urea linkages. Polyurethane systems thus offer a wide range of possible crosslinking reactions, however, the extent to which individual pathways occur is often unpredictable, requiring extensive empirical optimization of the formulation.

A major disadvantage of blocked polyisocyanates is the loss of mass that comes along with the evaporation of the volatile blocking agent. It can account for up to 50 wt% of the crosslinker. Moreover, blocking agents with high boiling points, such as ε-caprolactam (b.p.: 270°C), may

condense at cooler sections of the curing oven, posing technical challenges during industrial processing.[23]

3.1.2 Epoxy-Functional Acrylic Resins

Epoxy-functional acrylic resins are available by copolymerizing GMA with other (meth)acrylic monomers. The resulting resins may be crosslinked by dicarboxylic acids[33] and carboxylic acid-functional resins including copolymers of AA[34] at around 200°C without or at 120-140°C with a catalyst.[35] The reaction is mostly base-catalysed. In addition to the predominant reaction (Scheme 10a) which gives a primary or secondary alcohol depending on the position of the nucleophilic attack, several other reactions may take place. The reactivity may be controlled by the type of catalyst applied.[35] Hydroxy groups can esterify carboxylic acids with elimination of water (Scheme 10b), which in turn can hydrolyse epoxy groups to form vicinal diols (Scheme 10c). Moreover, epoxy groups react with hydroxy groups to form β-hydroxy ether (Scheme 10d).[23]

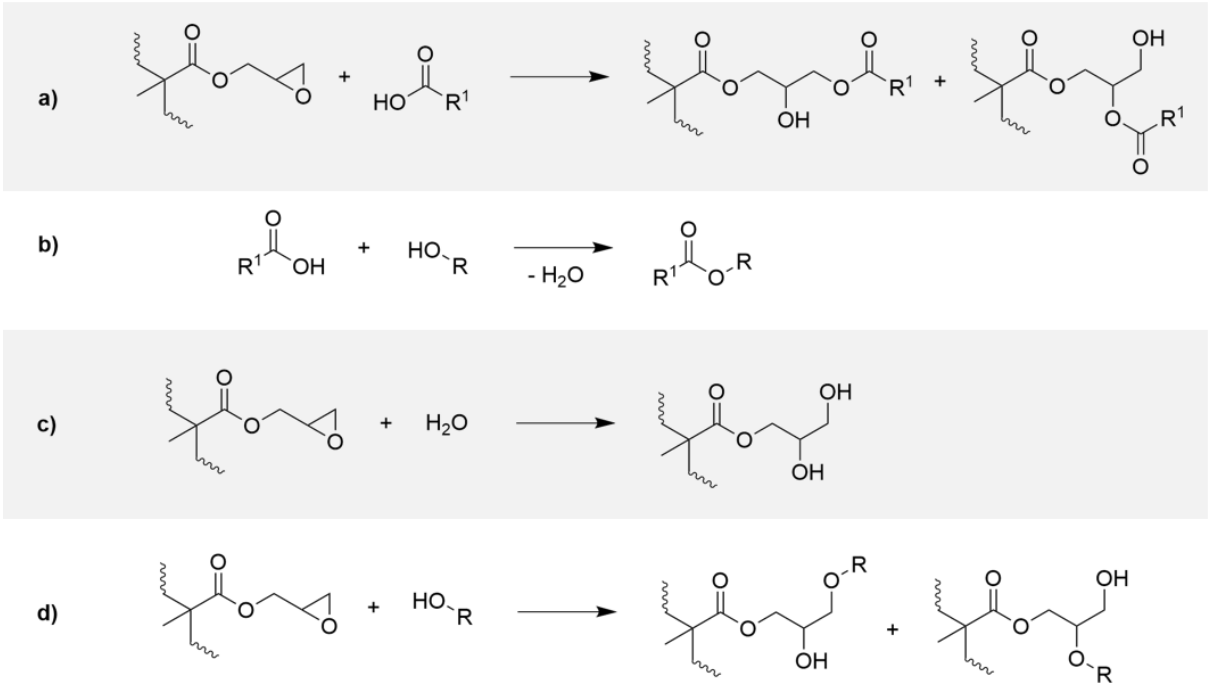

Scheme 10. Various reactions taking place during thermal curing of epoxy acrylic resins; (a) reaction of GMA-derived epoxide with carboxylic acids; (b) reaction of carboxylic acids with hydroxy-functional resins; (c) reaction of GMA-derived epoxide with water; (d) reaction of GMA-derived epoxide with hydroxy-functional resins; R and R^1 = organic rest.

A frequently used strategy combines maleic anhydride with small amounts of a hydroxy-functional monomer. Maleic anhydride is first reacted with methanol to form a half ester which at curing temperatures reforms the anhydride. The anhydride can subsequently react with hydroxy groups to give carboxylic acids that finally react with epoxy groups.[36] Carboxylic acid groups can also be formed from *tert*-butyl acrylate by elimination of isobutylene.[37]

3.1.3 Carboxylic Acid-Functional Acrylic Resins

Carboxylic acid-functional acrylic resins are generally combined with polyepoxides such as bisphenol A and F epoxy resins, epoxy novolac resins, triglycidyl isocyanurat (TGIC), polyethyleneglycol diglycidyl ether and cycloaliphatic diepoxides.[38] The underlying chemistry is the same as described above. Epoxy systems have the advantage of crosslinking without fission products and no by-products evaporate from the films or remain in the films. This results in excellent film forming properties. β-Hydroxy ether and β-hydroxy ester crosslinks are acid and heat resistant and unless aromatic compounds are used, they provide films with excellent outdoor durability. Such coatings find application as powder coatings in clear coats for automobiles.[7,23]

β-Hydroxy-alkylamide compounds have been considered as alternatives to MF resins. They yield films with similar properties but with the advantage that no formaldehyde can be formed. They give typical esterification products upon reaction with carboxylic acid-functional acrylic resins (Scheme 11). Esterification reactions are often too slow for application in coatings but β-hydroxyalkylamides like tetra-*N,N,N´,N´*-(2-hydroxyethyl)adipamide crosslink under surprisingly moderate conditions (150°C, 30 min). The reaction is not classified as an esterification reaction because it cannot be catalyzed by acids, instead, mechanistic studies suggest the reaction proceeds via an oxazolinium cation intermediate.[39] Nevertheless, the application of these systems is severely limited by the still harsh curing conditions.[11]

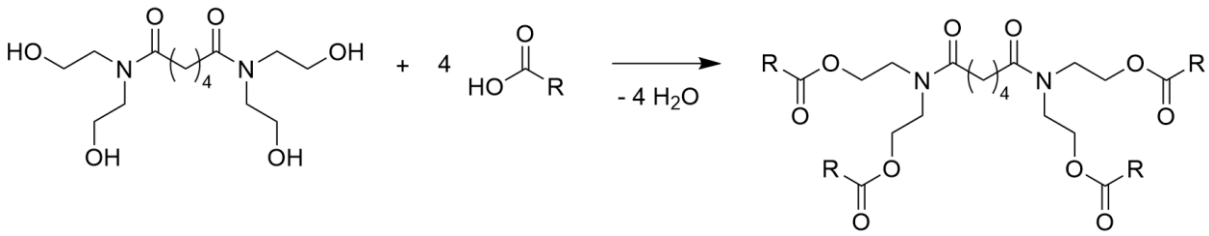

Scheme 11. Reaction of tetra-*N,N,N´,N´*-(2-hydroxyethyl)adipamide with carboxylic acid-functional acrylic resins; R = acrylic resin.

3.1.4 Other Functional Acrylic Resins

Carbamate-functional acrylic resins can be prepared by reacting isocyanato-functional acrylic resins with hydroxypropyl carbamate and crosslink with amino resins to form urethanes (Scheme 12a). Curing occurs at around 130°C in the presence of a strong acid catalyst, usually sulfonic acids. If the acid is blocked with amines, the coating may be formulated as a 1K system. Cured films have better etch resistance than hydroxy-functional acrylic resins cured with MF resins, but production costs are much higher.[40]

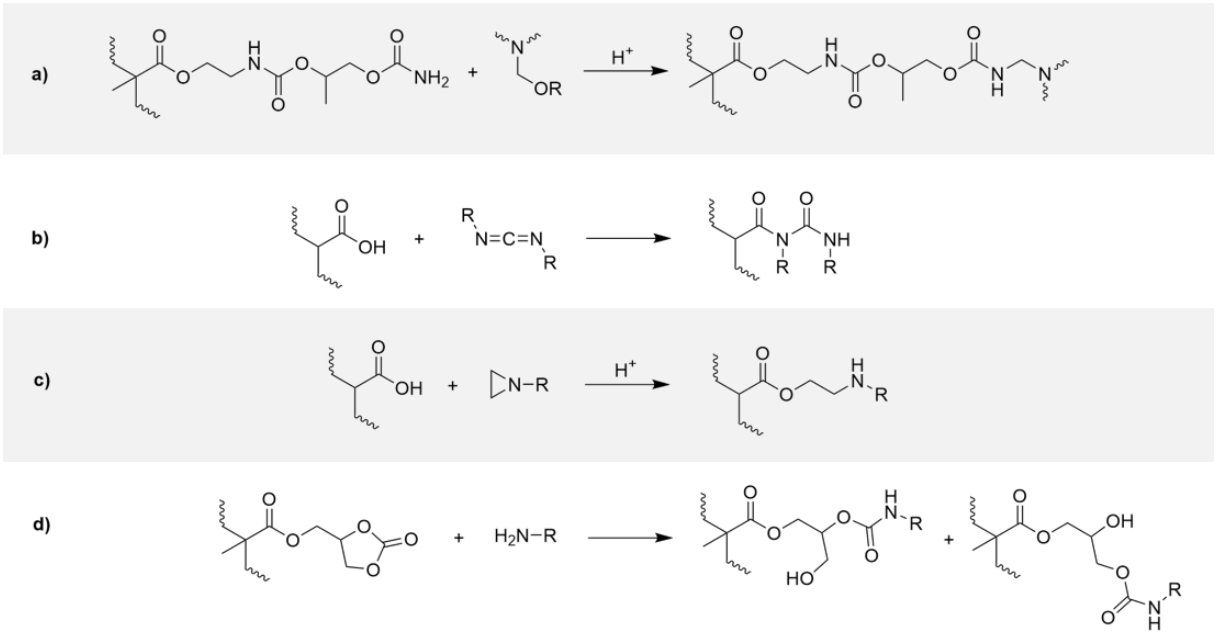

Scheme 12. Various crosslinking reactions for thermosetting acrylic resins. (a) reaction of carbamate-functional acrylic resin with amino resin; (b) reaction of carboxylic acid-functional acrylic resin with polycarbodiimides; (c) reaction of carboxylic acid-functional acrylic resin with polyaziridines; (d) reaction of carbonate-functional acrylic resin with amines crosslinkers; R = organic rest.

Other less common crosslinkers are polycarbodiimines[41] and polyaziridines[42] that can be crosslinked with carboxylic acid-functional acrylic resins to give *N*-acylureas (Scheme 12c) and β-amino ester (Scheme 12d), respectively. Cyclic carbonate-functional acrylic resins are synthesized by copolymerization of propylene carbonate (meth)acrylate or similar acrylic monomers and crosslinked by polyfunctional amines at slightly elevated temperatures (Scheme 12e).[43] Reaction products are β-hydroxy urethanes and the reaction proved to be autocatalytic as hydroxy groups catalyse the reaction. 1K Systems with this type of chemistry have also been described but needed neutralization of the amines by acids for curing.[44]

Acetoacetoxy-functional acrylic resins are prepared by copolymerization of acetoacetoxyethyl methacrylate (AAEM) with non-functional acrylic monomers. Acetoacetoxy groups act as both

nucleophiles and electrophiles; reactions of AAEM as an electrophile are discussed in section 3.1.5. They are combined with amino resins and polyisocyanates. The reaction with amino resins is acid catalysed and leads to C-C bonds, but the general film properties do not differ much from films of hydroxy-functional acrylic resins (Scheme 13a).[33]

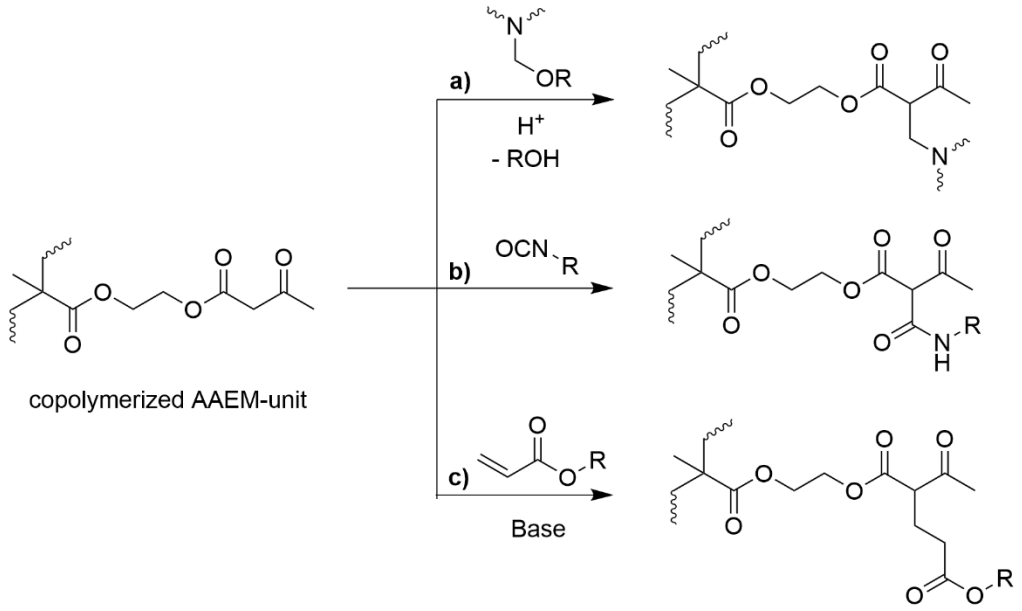

Scheme 13. Crosslinking reactions of acetoacetoxy-functional acrylic resin with (a) amino resins; (b) (poly)isocyanates; (c) (poly)acrylates; R = organic rest.

The reaction of acetoacetoxy groups with isocyanates is slower than the reaction of hydroxy groups with (poly)isocyanates which extents pot life but film properties are not improved either (Scheme 13b). Acetoacetoxy-functional acrylic resins can also react with (poly)acrylates via a Michael addition at ambient temperature catalysed by amine bases such as 1,8-diazabicyclo[5.4.0]undec-7-ene (DBU) (Scheme 13c).[45] The reaction is too fast for 1K systems but blocking the base with a volatile acid has been reported to extent pot life.[46]

3.1.5 Self-Crosslinking Thermosetting Acrylic Resins

Self-crosslinking thermosetting acrylic resins avoid the presence of a co-reactant and are therefore more economic, easier to handle and often the first choice for manufacturers. Since self-crosslinking resins are supplied as 1K systems, adequate shelf-life is required, meaning that crosslinking takes place only after application to the substrate and, if applicable, subsequent heating, and should be largely suppressed during storage. Due to the stringent requirements, the choice of available crosslinking systems is limited.

The crosslinker *N*-methylol acrylamide (NMA) motive arises in copolymers of acrylamide that was treated with formaldehyde. Resins crosslink by self-condensation at 160-180°C. Alternatively, acrylamide and methacrylamide copolymers can be treated post polymerization with formaldehyde to form methylol groups. The underlying crosslinking chemistry emulates that of amino resins and is catalyzed by acids. Residual N-H groups and methylol groups react with loss of one molecule of water and formaldehyde to form methylene bridges (Scheme 14) and methylol groups react with each other to form dimethylene ether bridges (analogous to the mechanism shown in Scheme 4). 1K Self-crosslinking systems exists since the equilibrium between methylol and amide groups is maintained during storage. Only upon thermal treatment, formaldehyde and water evaporate, thereby driving the reaction toward crosslinking. Etherified methylol acrylamide monomers are also available, e.g. in form of *N*-isobutoxymethyl acrylamide (IBMAA) and react accordingly with cleavage of the corresponding monoalcohol and formaldehyde. A copolymer of BA, MMA and IBMAA is cured through the action of 0.5 wt% pTSA in about 40 min at 80°C.[47] Other sulfonic acid[48,49] and carboxylic acids[50] are known to catalyze this reaction as well. Application is found in coil coatings because of their improved flexibility and weather resistance when compared to hydroxy-functional acrylic resins combined with MF resins. It is assumed that their enhanced flexibility results from the lack of highly crosslinked and rigid clusters of self-condensed MF resins.[11,17,51,52] Their films are chemically more resistant than films formed by hydroxy-functional acrylic resins and amino resins. That is the main reason why they are preferred in certain industrial applications where a good chemical resistance is required such as in refrigerator enamels and washing machine coatings. A disadvantage of this system is the release of formaldehyde, which limits its application due to environmental and health concerns.[17,51]

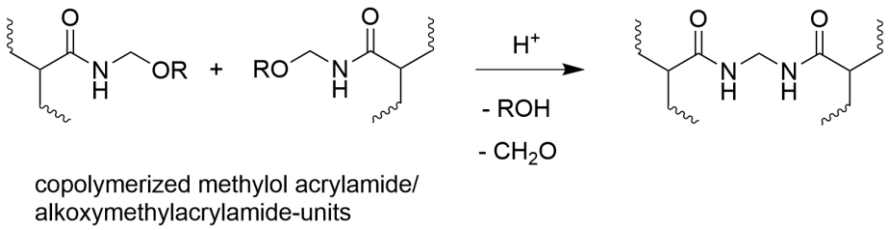

Scheme 14. Self-condensation reaction of copolymerized methylol acrylamide/alkoxymethylacrylamide to a methylene crosslink. R = H, alkyl.

Keto-dihydrazide/diamine chemistry in acrylic resins has been developed starting in the late 1980s with the commercial production of diacetone acrylamide (DAAM) and AAEM. DAAM exhibits excellent stability in water and is therefore primarily used in waterborne coatings. DAAM copolymers crosslink with polyamines and dihydrazides at room temperatures and are often used in combination with adipic acid dihydrazide (**18**). The condensation reaction

between the ketone functionality and the hydrazide is promoted by the loss of water during film formation and results in hydrazone crosslinks (Scheme 15a). Films cure within 7 days at room temperature and exhibit good solvent resistance.[47,51,53]

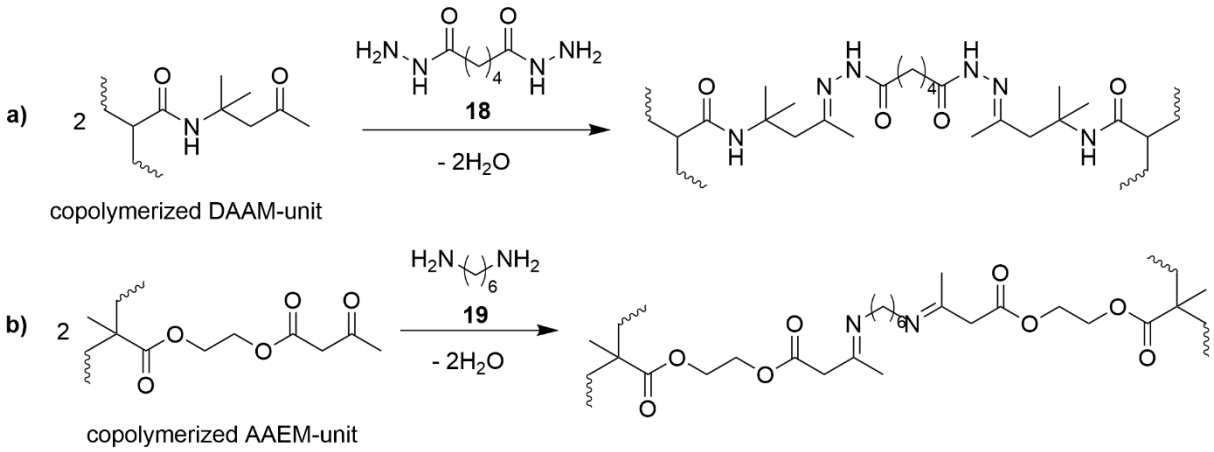

Scheme 15. Crosslinking reaction of (a) copolymerized DAAM with adipic acid dihydrazide **18**; and (b) copolymerized AAEM with hexamethylenediamine **19**.

Resins made from AAEM copolymers are combined with crosslinkers having a variety of functional groups. The most used crosslinker, hexamethylene diamine **19**, forms aminocrotonates (enamines) crosslinks upon reaction with the ketone moiety (Scheme 15b). The reaction proceeds rapidly at room temperature and is catalyzed by acids. However, the system suffers from hydrolytic instability of AAEM and preliminary crosslinking during storage, which can be prevented by neutralizing the resin with ammonia before adding the crosslinker. The resulting enamines are more hydrolytically stable and release the ketone during film formation while ammonia evaporates from the film surface.[47,51]

Alkoxysilanes can also be used to facilitate self-crosslinking of polyacrylates. Copolymerization of methacryl oxypropyl trimethoxysilane or acryl oxypropyl trimethoxysilane with other acrylic monomers yields alkoxysilane-functional acrylic resins that are crosslinked by initial hydrolysis of the alkoxy silane to silanols and subsequent condensation to siloxanes (Scheme 16).

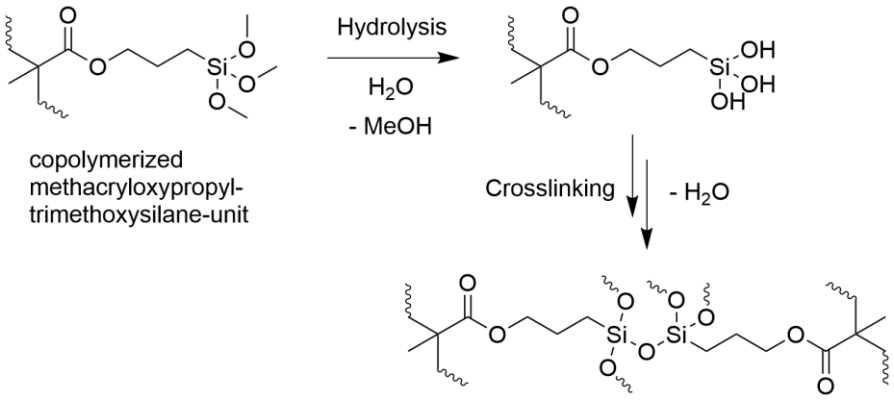

Scheme 16. (Self-)crosslinking reaction of alkoxysilane-functional acrylic resins.

The rate of hydrolysis depends on pH, temperature, and the nature of silane, e.g., isobutoxysilanes hydrolyse much slower than methoxysilanes. Additionally, silanols do not crosslink in the presence of large amounts of water which is why shelf-life of more than one year has been achieved. It is only when the coatings are applied to the substrate and water is allowed to evaporate that extensive crosslinking takes place, in some cases even at ambient temperatures, although curing takes several days. Si-O-Si bonds are robust, conferring good chemical and weather resistance and some hardness to the coatings.[11,51,54]

Metal complexes have been used to crosslink carboxylic acid-functional acrylic resins as early as 1965.[55] Common metals for these coatings are zinc, zirconium, aluminium, titanium, chromium and mixtures of these metals.[56] Typical anions used are phosphate, sulfate, nitrate, carbonate, acetylacetonate, ammonia and tartrate.[57] During storage metal complexes are held in solution and do not react with the carboxyl groups. After the coating is applied to the substrate and the solvent evaporates, crosslinking takes place by displacement of the ligands by carboxylate anions of the acrylic resin (Scheme 17[58]).

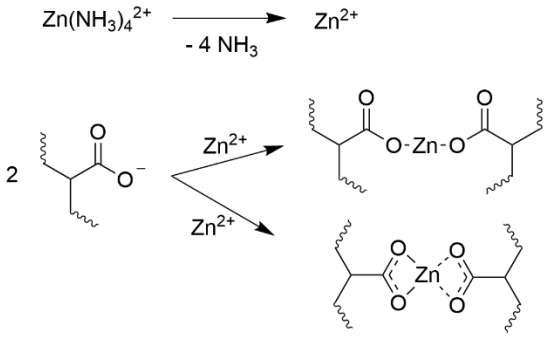

Scheme 17. Crosslinking reaction of carboxylic acid-functional acrylic resins facilitated by $Zn(NH_3)_4^{2+}$.[58]

Chelating effects and volatility of liberated (ammonia) ligands favor the formation of crosslinks. Metal crosslinking enables rapid curing at room temperature and improves film properties of

non-crosslinked coatings in many ways. However, it cannot compete with the robustness of conventional covalent crosslinking, e.g., ammonia-based floor cleaners remove zinc-crosslinked floor coatings because ammonia competes with carboxylates for binding to the zinc ion. However, the use of metals result in opalescent films limiting their application mainly to pressure-sensitive adhesives, wall paints, printing inks and hydrogels.[59]

3.2 Perchlorates

Perchlorates are chemical compounds that contain either the anion ClO_4^- or molecular compounds $ROClO_3$. The history of perchlorate synthesis dates back to 1816 with the preparation of potassium perchlorate from potassium chlorate and sulfuric acid.[60] Today perchlorates, primarily perchloric acid and sodium perchlorate are produced commercially by electrolysis of chlorine[61] or chlorate salts[62]. Other perchlorates are mostly synthesized from the two compounds. The ClO_4^--anion has a tetrahedral symmetry where the chlorine central atom is surrounded by four oxygens (Scheme 18).

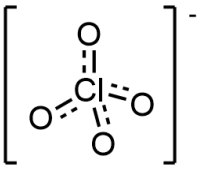

Scheme 18. Chemical structure of the perchlorate anion.

The chlorine atom has the highest oxidation number (+VII) of all chlorine oxides which is why perchlorates are oxidizing agents. However, unlike other commonly used oxidizers most perchlorate salts do not oxidize organic compounds until the mixture is heated. The perchlorate salts usually have a high solvation energy and show a good solubility in water making perchlorates ideal for analytical applications. The binding of the anion to metal ions is weak.

Ever since their first discovery, perchlorates have evolved into a notorious substance class as several of them have a tendency to explode on contact and many incidents have been reported in the past 100 years.[63,64] The explosive power comes from the large pressure increase caused by the gases formed in the decomposition. This is illustrated by the example of the decomposition of ammonium perchlorate, a salt commonly used as rocket propellant and in fireworks (Equation 2). It should be noted that the composition of products formed in the decomposition depends on temperature and can vary greatly.[65]

$$4\ NH_4ClO_4 \rightarrow 4\ HCl + 2\ N_2 + 5\ O_2 + 6\ H_2O \quad (2)$$

Furthermore, perchlorates were found to be harmful to humans, particularly affecting the thyroid function[66], which is why perchlorate concentrations in food and water are now extensively monitored.[67] Nevertheless, if handled responsibly, the exceptional properties of perchlorates can be used in many ways. A variety of applications in both academia and industry are known including electropolishing[68], rocket fuels[69], explosives[70], catalysts[71], drying agents[70], accumulator electrolytes[72] and therapeutics[73].

3.2.1 Perchloric Acid

Perchloric acid ($HClO_4$) is one of the strongest and most corrosive acids known today. It is stronger than sulfuric acid and therefore classified as a super acid. Its pK_a is reported to be -15±2[74], and in aqueous media perchloric acid is completely dissociated up to a concentration of about 4 M. The monohydrate, hydroxonium perchlorate $H_3O^+\ ClO_4^-$, has been described as a relatively stable salt.[75] Perchloric acid is explosive in its pure and anhydrous form (dichlorine heptoxide) but stable and easy to handle as a 70% solution in water, the commercially available product.

70% Perchloric acid is an odorless, colorless, oily, and hygroscopic liquid. The azeotrope boils at atmospheric pressure at 203°C with partly decomposition to chlorine, chlorine oxides and oxygen but can be distilled without decomposition under reduced pressure. During the thermal decomposition of perchloric acid, chloric acid and chlorine dioxide are formed via radical processes (Equation 3-5).[69]

$$HClO_4 + H^{\cdot} \rightarrow ClO_3^{\cdot} + H_2O \quad (3)$$

$$ClO_3^{\cdot} + HClO_4 \rightarrow HClO_3 + ClO_4^{\cdot} \quad (4)$$

$$3\ HClO_3 \rightarrow HClO_4 + H_2O + 2\ ClO_2 \quad (5)$$

Perchloric acid dissolves in water with heat generation. That is the reason for its explosive behaviour when mixed with organic solvents and organic material in general. In some organic solvents including nitromethane[76] and nitrobenzene[77] it is strongly ionic but not necessarily dissociated. An acetic acid/perchloric acid solution will contain a highly reactive acetic acidium perchlorate $[AcOH_2]^+ClO_4^-$ a powerful acylating agent. Other organic solvents including

olefins[78] and primary alcohols[64] react with perchloric acid to form relatively stable adducts (perchlorate esters) or oxonium ions.

At ambient temperatures the properties of perchloric acid are determined by the weak nucleophilicity of the anion, on the other side its oxidizing properties are more pronounced at higher temperatures. Perchloric acid has been used as a catalyst for esterification reactions, cationic polymerizations, rearrangements, acetylation, and isomerization.[71] By dispersion on silica, a heterogeneous catalyst has been developed, expanding its use in the field of green chemistry.[79] Perchloric acid is also an important compound in analytical chemistry.[80]

3.2.2 Perchlorate Esters

The esters of perchloric acid constitute an unusual substance class, first discovered in 1841 with the synthesis of ethyl perchlorate.[81] Most of the research in this field has been conducted between 1930 and 1980, summarized in a comprehensive review.[82] Today alkyl perchlorates are rarely used, neither commercially nor academically. This may be due to their explosive and toxic reputation combined with their essentially non-existent commercial availability, and also limitations in useful precursors.[83] In fact, low molecular weight alkyl perchlorate including methyl and ethyl perchlorate are reported as unstable and explode even at the slightest impact. Methyl perchlorate, b.p.: 52°C, is sensitive to shock and explodes on the hammer test but could successfully be distilled at standard pressure as could ethyl perchlorate.[64] In contrast, higher molecular weight alkyl perchlorates are not as shock sensitive and easier to handle. In fact, *n*-decyl perchlorate, proved to be quite thermally stable in nonpolar solvents up to temperatures of 140°C. Secondary alkyl perchlorates, e.g., *sec*-pentyl perchlorate, rapidly eliminate perchloric acid in nonpolar organic solvents at room temperature, and *tert*-butyl perchlorate is a good source of anhydrous perchloric acid[84].

A main reason why alkyl perchlorates are still not used on an industrial scale is their elaborate synthesis. A first strategy starts from the corresponding alcohol reacting with the anhydride dichlorine heptoxide (Cl_2O_7), or a halide of perchloric acid, e.g., perchloryl fluoride (Equation 6, 7) forming a new bond between an oxygen and the central chlorine atom. This strategy, however, involves handling unfavorable explosive and expensive reagents. The preparation of Cl_2O_7 is laborious. The most convenient method is the dehydration of 70% perchloric acid over phosphorus pentoxide in carbon tetrachloride followed by azeotropic distillation, which gives a solution of Cl_2O_7 in carbon tetrachloride.[85] Also, perchloryl fluoride, an alternative reagent to Cl_2O_7, is not commercially available.[86]

$$ROH + Cl_2O_7 \rightarrow ROClO_3 + HClO_4 \quad (6)$$

$$ROH + FClO_3 \rightarrow ROClO_3 + HF \quad (7)$$

A second strategy is based on the reaction of the nucleophilic perchlorate anion ClO_4^- with an electrophilic carbon atom (Equation 8-9). These reactions require nonpolar media and the absence of any nucleophile that competes with the perchlorate anion. Typical reagents are silver perchlorate, an explosive and expensive salt, and perchloric acid.

$$R_3C^+ + ClO_4^- \rightarrow R_3COClO_3 \quad (8)$$

$$R_3C\text{-}Y + ClO_4^- \rightarrow R_3COClO_3 + Y^- \quad (9)$$

R = H, alkyl, aryl; Y = leaving group

Alkyl perchlorates are obtained from the reaction of primary and secondary alcohols and ethers including cyclic ethers (not shown) with Cl_2O_7 (Scheme 19a+b).[85,87] Free perchloric acid formed in the course of the reaction is reacted with sodium sulfate in an otherwise non-polar medium and which thus is phase separated from the other reactants.

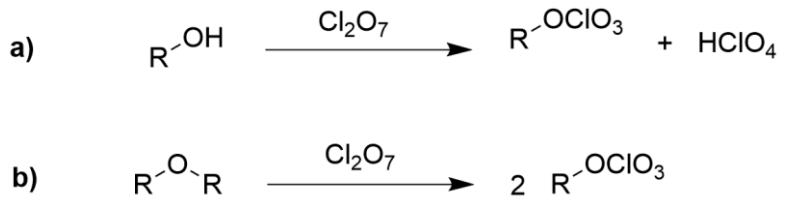

Scheme 19. Synthesis of alkyl perchlorates from the reaction of Cl_2O_7 with (a) alcohols and (b) linear and cyclic ethers; R = alkyl.

Probably the most convenient and widely used synthesis is the reaction of alkyl halides with silver perchlorate in a nonpolar solvent like pentane[88] or benzene[83] (Equation 10). To avoid direct hydrolysis of the alkyl perchlorate silver perchlorate must be dried before use. Commercially available anhydrous silver perchlorate still contains small amounts of water. In the course of the reaction, the silver halide by-product, precipitates from the solution, whereas the alkyl perchlorate remains dissolved, which simplifies workup. After filtration, the alkyl perchlorate is present in solution and as such safe to handle and suitable for long-term storage.

The choice of solvent is of importance as isomerization products have been reported to form in carbon tetrachloride, pentane and 1,1,2-trichlorotrifluoroethane but not in benzene. Complexes of intermediate silver ions with benzene are thought to be the reason for lower reaction rates and for the absence of isomerization products.[89] A number of protocols based

on oxidative iodine elimination/decomposition reactions[90] have been developed to address the disadvantages, but are rather laborious as they require multiple reagents and synthesis steps.

$$RX + AgClO_4 \rightarrow ROClO_3 + AgX \qquad (10)$$

R = alkyl, X = Cl, Br, I

The reaction of olefins with perchloric acid in the presence of sulfuric acid yields secondary perchlorates in very high yield (Scheme 20).[91] A convenient two-phase system simplifies workup but secondary alkyl perchlorates are not stable and readily eliminate perchloric acid even when stored in solution. Primary alkyl perchlorates have not been obtained via this route.

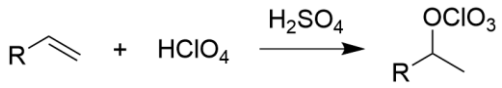

Scheme 20. Synthesis of (unstable) secondary alkyl perchlorates from the treatment of olefines with perchloric acid; R = alkyl.

The addition of Cl_2O_7[92,93] and halogen perchlorates[94] to olefines has also been studied yielding mixtures of alkyl perchlorates. The composition of the reaction products strongly depends on the chemical structure of the olefine. The reaction of olefines with a 10-fold excess of lithium perchlorates in the presence of chlorine, bromine and nitronium fluoroborate is reported to yield β-halogeno and β-nitro perchlorates[95].

A number of fragmentation reactions have been reported for the preparation of alkylperchlorates too. They involve the use of chloroformates[96], betylates[97] and diazo-compounds[98], but the synthetic usefulness is limited, as none of the protocols provides easy and inexpensive access to a broader range of alkyl perchlorates.

The identification of covalently bonded perchlorates was challenging in the beginning of the 20th century. Alkaline hydrolysis of the perchlorate ester followed by analysis of the products was the standard method for quantitative and qualitative analysis. To date, a manifold of techniques are being used including mass spectrometry[94,99], X-ray diffraction analysis[100] and elemental analysis[101]; infrared (IR) spectroscopy and nuclear magnetic resonance (NMR) spectroscopy have proven particularly useful.

Covalently bonded perchlorates show characteristic absorption bands at about 1260 and 1230 [$\nu_{as}(ClO_3)$], from 1100 to 1000 [$\nu_s(ClO_3)$] and near 700 cm^{-1} [ν(Cl-O)]. IR spectra of inorganic perchlorates, on the other hand, do not show bands in the range of 1300-1200 cm^{-1}.[83] NMR spectroscopy is used extensively in qualitative and even quantitative analysis of alkyl

perchlorates. Resonances of the α-protons of *n*-alkyl perchlorates appear in the range 4.2 - 4.6 ppm in chloroform-d_3. The chemical shift of the α-protons in *sec*-alkyl perchlorates is found between 4.9 and 5.6 ppm. These shifts are relatively specific and therefore ideal for analysis, only protons in benzylic position and in olefines have similar chemical shifts.

The perchlorate anion is highly nucleofugitive and easily dissociates from the carbon skeleton forming a temporary carbenium ion pair from which perchloric acid can eliminate (Scheme 21). The resulting olefins rapidly char and polymerize. Compounds that can stabilize the generated carbenium ion through their substituents are the least stable, e.g., tert-alkyl perchlorates[85] and benzyl perchlorates[102]. On the other hand, electron withdrawing substituents confer more stability to the alkyl perchlorate, e.g., perfluoroalkyl perchlorates are stable at room temperature for years[99,103].

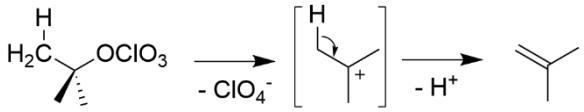

20 **21**

Scheme 21. Elimination of perchloric acid from *tert*-butyl perchlorate (**20**) via carbenium ion **21** to give Isobutylene.

Because of the exceptional good leaving group ability of the ClO_4^- anion[104], multiple orders of magnitude stronger than mesylates and almost as strong as the esters of triflic acid, perchlorate esters are potent alkylating agents.[105] Reasonably stable alkyl perchlorates have, in fact, been used as initiators for cationic polymerization of electron-rich alkenes[106], and ring-opening polymerization of lactones[107] and cyclic ethers[108]. Besides they react rapidly with amines[109] and alcohols[110,111], but even with weaker electrophiles including some aromatic compounds[112], nitriles[113,114] and arenesulfonate ions[115].

The mechanism of nucleophilic substitution of perchlorate esters has been extensively discussed in the literature (Scheme 22).[82] Most evidence support second-order kinetics, except for highly reactive perchlorates such as *tert*-butyl perchlorate whose reactions with nucleophiles proceed via an S_N1 mechanism. Although the reaction involves heterolytic cleavage of the C-O bond, hydrolysis of some sterically hindered primary alkyl perchlorates have been reported to proceed via attack of H_2O at the central chlorine atom and subsequent cleavage of the O-ClO_3 bond[116].

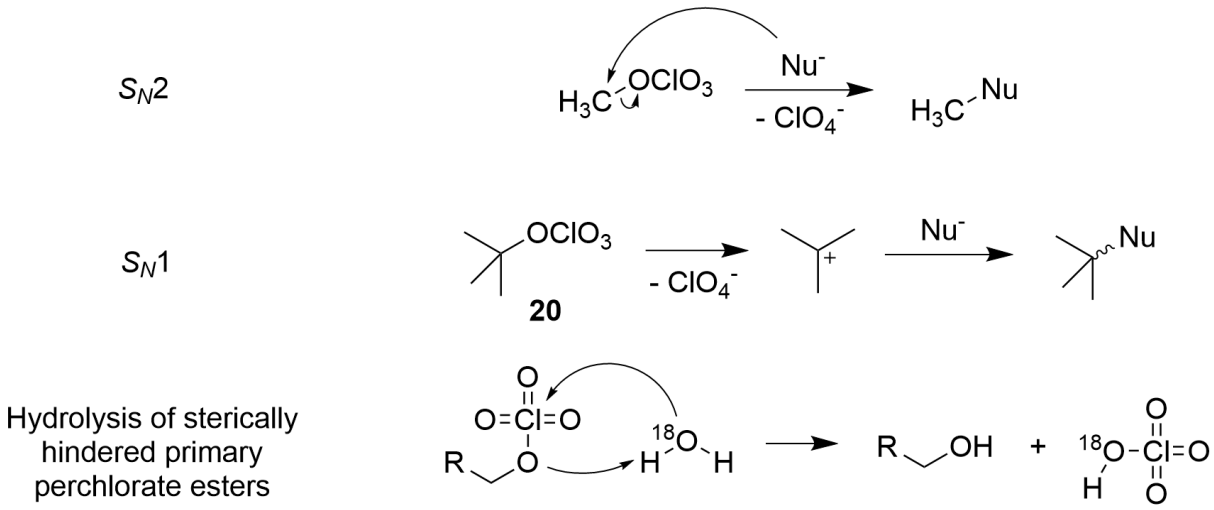

Scheme 22. Type of nucleophilic substitution of primary (top), tertiary (center) and sterically hindered primary (bottom) perchlorate esters.

3.3 Formation of Polymer Networks

3.3.1 Definition of Polymer Networks

Polymer networks will be considered here as a permanent, covalently bonded three-dimensional structure. Unlike linear or branched polymers, whose chains can be separated without breaking covalent bonds, the chains in a true network form a continuous covalent structure that extends in all spatial directions. According to Staudinger's definition[117], such materials cannot be disassembled into individual macromolecules without breaking covalent bonds.

Network formation requires multifunctional monomers, i.e., molecules with more than two reactive groups. Their reaction creates junction points that connect polymer chains into a continuously growing structure. As conversion increases, the system evolves from a soluble, branched ensemble of finite clusters to an infinite, system-spanning cluster. This transition, known as the gel-point, marks the beginning of insolubility and the onset of elasticity.

The chemical formation of networks can proceed through several distinct synthetic concepts (Figure 1). Difunctional or polyfunctional monomers react in step-growth polymerizations by condensation or addition reactions until a critical conversion leads to gelation.[118] Chain-growth polymerizations, for example, free-radical polymerizations of di- or triacrylates, form networks concurrently with chain propagation once crosslinking monomers become incorporated.[119] Alternatively, networks can arise through post-polymerization crosslinking, where preformed

macromolecules bearing pendant reactive groups (e.g., hydroxyl, epoxy, or isocyanate) are covalently joined during a subsequent curing step.[120] Finally, reaction-induced phase separation may occur when the growing network and the unreacted matrix become thermodynamically incompatible, producing heterogeneous or interpenetrating networks.[121] Each of these strategies yields a permanent covalent network, but they differ in reaction kinetics, spatial uniformity, and resulting CD.

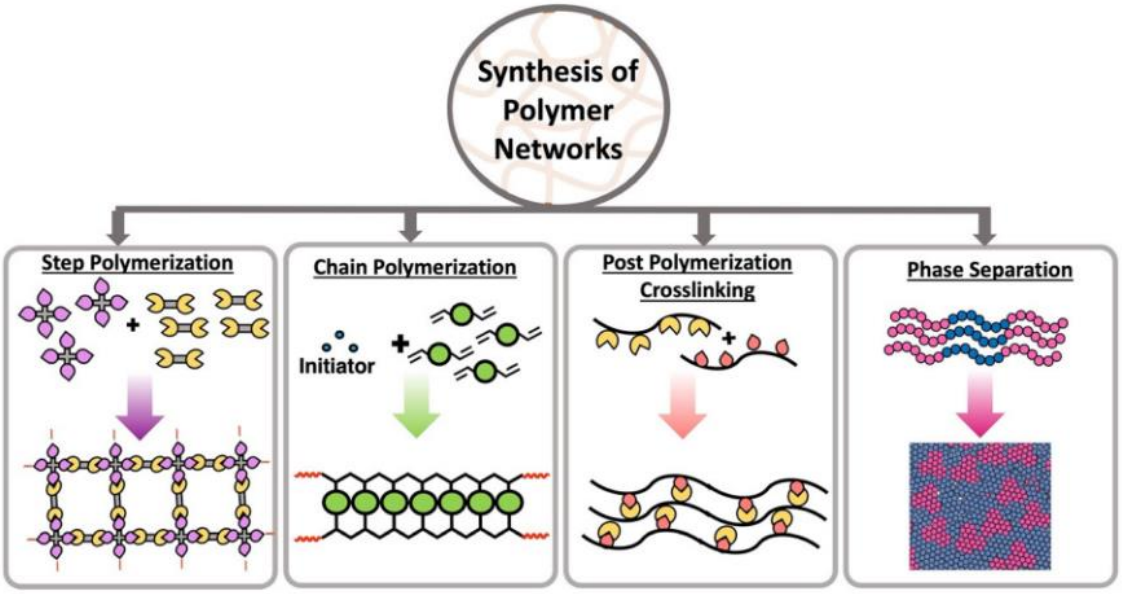

Figure 1. Different strategies to synthesis of polymer networks using step polymerization in the presence of multifunctional monomers, chain polymerization in the presence of multifunctional monomers, post polymerization crosslinking and phase separation.[122] (Reproduced under CC BY-NC 3.0, link to article)

Covalent networks differ fundamentally from physical networks, in which junction points result from reversible interactions such as hydrogen bonding or ionic coordination. Physical networks can often be dissolved or melted, whereas covalent networks cannot. Their macroscopic properties, insolubility, dimensional stability, and elastic recovery after deformation, directly originate from the molecular constraints that each chain segment is permanently anchored between two junctions.

3.3.2 Random Connectivity and Statistical Gelation

The statistical description of polymer network formation originated from the pioneering work of Flory[123,124] and Stockmayer[125]. Their *Flory-Stockmayer theory of gelation* describes network formation as a statistical process in which reactions occur randomly between all functional

groups. Under this assumption, the polymer structure resembles an ideal tree, a branching structure without closed loops.

Two simplifying assumptions define the Flory-Stockmayer theory:

I. all functional groups exhibit equal and independent reactivity, unaffected by molecular size or local environment, and
II. no intramolecular reactions occur between functional groups on the same molecule.

These postulates allow the system to be represented as a tree-like structure composed of branching junctions linked by covalent bonds, excluding closed loops or cycles. Within this framework, each reaction between functional groups occurs with equal probability, and the extent of reaction p governs the probability of forming a 3D network. Under these conditions, the critical conversion of one type of functional groups for gelation is:

$$p_c = 1/(f\text{-}1) \tag{11}$$

with f as the monomer functionality and p_c the gel point. Gelation occurs when M_w diverges to infinity, signaling the emerging of a continuous network. Gelation for trifunctional monomers occurs when half of the reactive groups have reacted ($p_c = 0.5$); for tetrafunctional monomers, one-third conversion is sufficient ($p_c = 0.33$). This theoretical simplicity provided an elegant explanation for the onset of macroscopic network formation and formed the foundation for the statistical theory of gelation.

Although the Flory-Stockmayer model accurately predicts the qualitative features of gelation, it cannot account for unequal group reactivity, sterically hindered reaction sites, diffusion limitations and intramolecular cyclization (loop formation). All these effects shift the gel point and reduce the effective number of load-bearing chains. Nevertheless, the Flory-Stockmayer approach remains the conceptual baseline for all modern descriptions of network formation.[126]

3.3.3 Reaction Kinetics, Diffusion Control, Microenvironment Effects

The formation of a polymer network is strongly influenced by stoichiometry and monomer functionality but also by how easily reactive groups can find each other. At low conversion, the system behaves like a homogeneous liquid with mobile chain segments and reaction proceed under chemically controlled kinetics. The reaction rate depends primarily on the intrinsic reactivity of functional groups, and rate equations follow classical kinetic laws, often of second order. Examples include the polycondensation of diols and diacids, epoxy–amine addition, and

radical polymerization of multifunctional acrylates. Under such conditions, the assumptions of the Flory-Stockmayer model are approximately valid.

As polymerization progresses, molecular weight and viscosity increase. Reactive groups become less mobile and reactions gradually become diffusion-controlled. Reaction rates are no longer determined solely by chemical rate constants but also by the rate at which reactive groups can physically encounter one another[127,128]. Local variations in density and viscosity develop, producing microenvironmental heterogeneity. Reactive groups within dense regions experience slower diffusion and limited accessibility, whereas unreacted sites in less crowded zones remain mobile. These microscopic variations lead to deviations from a mean-field behavior: the apparent reaction order changes, and the overall rate constant decreases as the system approaches the gel point.

Kinetic network models[129] treat network formation as a sequence of time-dependent bond-formation events, with reaction probabilities depending on momentaneous system structure and mobility. The change of key structural parameters during network formation is illustrated using a tetrafunctional system characterized by a negative substitution effect (Figure 2).

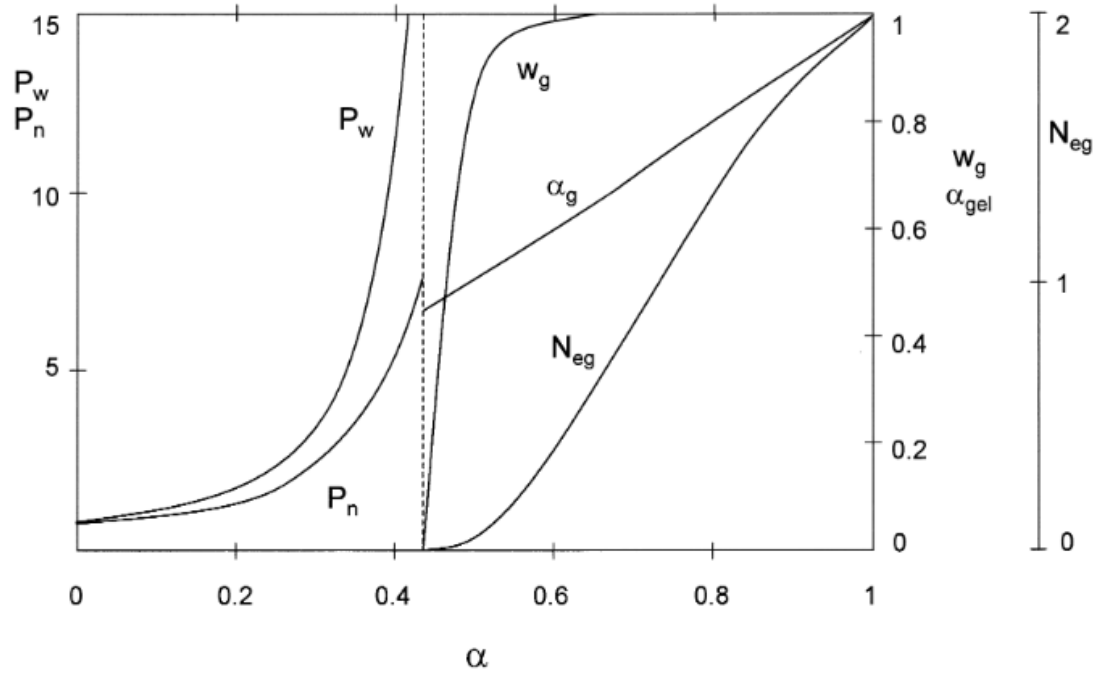

Figure 2. Typical dependencies of structural parameters on the conversion of functional groups in a tetrafunctional system with a negative substitution effect. P_n and P_w denote the number- and weight-average degrees of polymerization; w_g, the gel fraction; N_{eg}, the number of elastically active network chains per monomer unit; and α_g, the conversion within the gel phase.[127] (Reproduced with permission from Elsevier. Copyright © 2000 Elsevier)

The number average and weight average degrees of polymerization P_n and P_w increase continuously during the early stages of the reaction, reflecting unhindered cluster growth. As the system approaches the gel point, the gel fraction w_g rises sharply, marking the formation of the infinite cluster. Beyond the gel point, the number of elastically active network chains per monomer unit N_{eg} increases as additional crosslinks reinforce the infinite network. Meanwhile, the conversion within the gel phase α_g approaches unity only gradually, delayed by diffusion-controlled kinetics and restricted mobility inside the forming network. This behavior directly illustrates how diffusion slows post-gel reactions and locks-in structural features that deviate from ideality.[127] This representation demonstrates that gelation is not a sharp stoichiometric event but a gradual, kinetically-controlled process, determined by local molecular mobility and the evolving microenvironment.

As conversion increases even further, different types of rate-constant evolution appear (Figure 3)[127]. The TE-type behavior corresponds to chemically controlled free-radical crosslinking, where the apparent rate constant remains nearly constant over a wide conversion range and decreases only near vitrification. In TL-type step-growth systems, the rate constant decreases progressively as growing clusters restrict access to functional groups, a purely topological limitation. TGL-type kinetics represent systems where vitrification occurs before high conversion is reached, causing the rate constant to collapse due to the dramatic reduction in segmental mobility as the glass-transition region is approached.

Catalysts and temperature modify this balance by influencing both reactivity and mobility. Higher temperatures shift vitrification to higher conversion, leading to more homogeneous networks. Low curing temperatures promote early vitrification and heterogeneity.

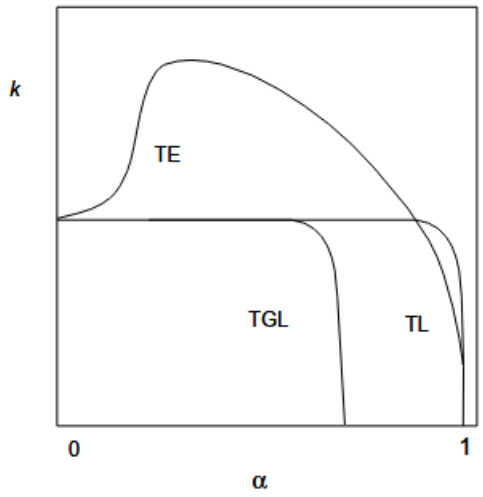

Figure 3. Possible dependencies of the apparent rate constant on conversion for different crosslinking regimes: TE: free-radical crosslinking copolymerization (chemically controlled), TL: stepwise crosslinking reaction limited by topology, TGL: stepwise crosslinking reaction limited by segmental mobility approaching the glass transition[127]. (Reproduced with permission from Elsevier. Copyright © 2000 Elsevier)

3.3.4 Spatial Correlations and Critical Fluctuations

In addition to diffusion limits, the developing network exhibits spatial correlations, regions with different local densities of crosslinks and reactive sites. Near the gel point, these correlations lead to critical fluctuations, where cluster sizes follow power-law distributions and the structure becomes fractal over multiple length scales.

The percolation framework treats gelation as a transition in real space. Each potential bond between reactive sites has a certain occupation probability p. When p exceeds a critical threshold p_c, a system-spanning cluster form.

Percolation introduces several key concepts missing in mean-field theories:

1. Spatial correlations explicitly account for the geometry and spatial distribution of bonds.
2. Macroscopic quantities such as viscosity, modulus, and relaxation time diverge near p_c.
3. Continuous gelation explains the smooth increase of viscoelastic moduli.

By linking molecular events with macroscopic behavior, percolation theory bridges statistical gelation, rheology, and structure evolution, forming the conceptual foundation for later computational and physical models.

3.3.5 Topological Heterogeneity and Defect Formation

Real polymer networks always contain structural defects. These arise from competition between reaction kinetics, diffusion, and entropy, and they are directly observed in simulations and experiments. Some are thermodynamically unavoidable, as, for example, intramolecular cyclization is entropically favored[126]. Important defect classes include (Figure 4):

- Intramolecular loops, where reactive groups on the same chain connect, consuming crosslinks without contributing to elasticity;
- Dangling chains, which terminate prematurely and act as inactive network ends;
- Entanglements, which mechanically couple strands without forming covalent bonds; and
- CD-gradients, produced by diffusion limitations or phase separation during curing.

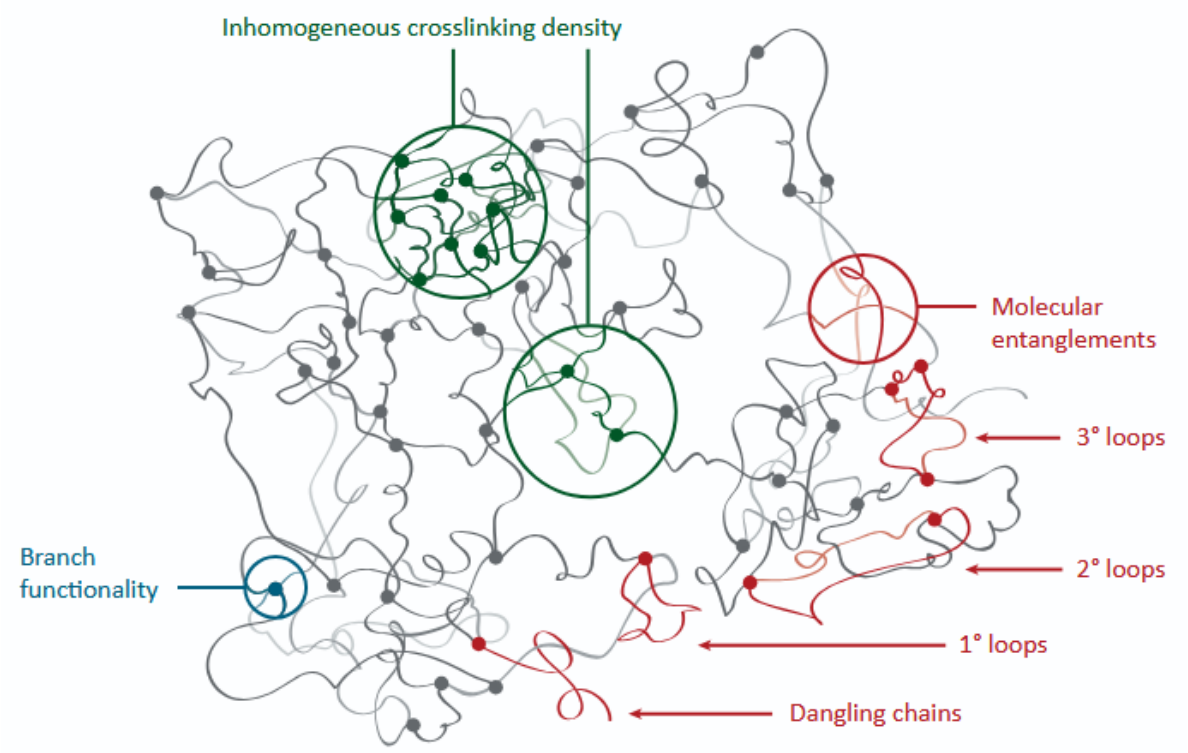

Figure 4. Typical heterogeneities in real polymer networks. Green: inhomogeneity in the distribution of network junctions; red: macromolecular-level structures formed from one or multiple polymer chains; blue: branch functionality[130]. (Reproduced with permission from Elsevier. Copyright © 2019 Elsevier)

Such defects reduce the effective number of load-bearing chains and cause spatial variability in mechanical properties. These effects have been directly quantified through Monte-Carlo[131] and molecular-dynamics simulations[132], which build networks bond-by-bond and measure loop fractions, chain-length distributions, and connectivity maps. These deviations from ideality

explain why real networks often show lower modulus and more complex stress-strain behavior than predicted by simple statistical models.

3.3.6 Elastic Fluctuations, Entanglement and Long-Range Disorder

Even after covalent reactions are complete, the network remains a frozen but fluctuating elastic solid. Crosslink positions vary, strands have different lengths, and chain orientations fluctuate. These variations create elastic heterogeneity on the nanometer scale.

Two key physical phenomena dominate this stage: Long-range entanglement, which restrict chain motion and cause a non-affine deformation, and frozen-in fluctuations, which result from the conditions during network formation. Statistical-mechanical models such as the replica model[133,134] and slip-tube model[134,135] capture these phenomena. The replica model treats the network as a disordered ensemble formed under specific preparation conditions. The slip-tube model describes how chains slide inside virtual tubes defined by surrounding strands. Together, these models connect chemical structure, spatial heterogeneity, and mechanical response. They complete the transition from early statistical theories to a multiscale physical description of real networks.

4 Motivation

Thermosetting acrylic resins are key materials in modern coating technology. Traditionally, they are crosslinked with polyisocyanates or MF-resins, reactions that require acidic or basic catalysts. However, these conventional systems present significant drawbacks: residual catalysts remain in the cured film, promoting degradation and reducing long-term stability[21,48,136]. 2K Coatings require precise mixing shortly before application and have limited pot life, whereas 1K alternatives often rely on complex, expensive formulations involving stabilizers and/or blocked isocyanates.

A crosslinking concept that combines the simplicity of 1K systems with high performance and environmental compatibility of 2K appears highly attractive and valuable. The aim of this work is the development of a novel crosslinking system for thermosetting acrylic resins that meets the following criteria:

(I) be comparable in cost to conventional coatings, preferably even less expensive,
(II) eliminate the need for an external co-reactant through self-crosslinking capability,
(III) form strong and durable networks providing excellent resistance to weathering, temperature, chemicals, and solvents,
(IV) be entirely free of catalyst residues, and
(V) ideally be nontoxic and environmentally friendly.

For this purpose, the exceptional properties of perchlorate esters were utilized.

5 Results and Discussion

5.1 4-Perchloratobutyl Acrylate, a New Monomer for Self-Crosslinking Thermosetting Acrylic Resins

Parts of this chapter were published in: P. Wienefeld and G. A. Luinstra, *J. Appl. Polym. Sci.* **2025**, *142*, e56980. (https://doi.org/10.1002/app.56980)

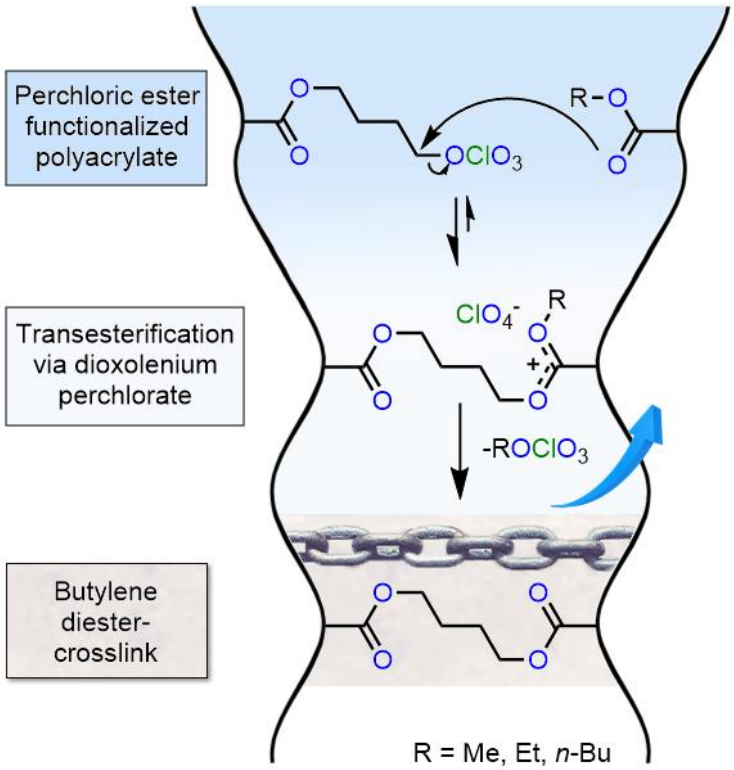

Scheme 23. Schematic illustration of the developed concept[137].

Functional polyacrylates are generally accessible via two common strategies: post-polymerization modification and copolymerization of a bifunctional monomer carrying both a polymerizable group and the desired functional group. Although post-polymerization procedures are especially useful when the desired functional group is incompatible with the polymerization conditions, they are associated with several disadvantages such as incomplete conversion due to steric hindrance, costly purification and difficult analysis. A monomer carrying the perchlorate functional group appeared more attractive and would provide the chemist with extra flexibility. This benefited from the fact that primary alkyl perchlorates were found to be stable in the presence of azobisisobutyronitril (AIBN) at about 70°C in nonpolar solvents. Therefore, the focus was set on the synthesis of a perchlorate ester-functional acrylate and its subsequent copolymerization.

5.1.1 Attempts to Synthesize a Perchlorate Ester-Functional Acrylate

Perchlorates have been previously incorporated into polymers in form of added salts[138,139], covalently perchlorates on binders appear not to have been described. Alternative ideas to incorporate perchlorate esters via a polyfunctional coreactant were discarded as potential crosslinkers such as 1,10-perchloratodecane are expensive in production, usually too volatile, and not atom-economical.

The original approach was adopted from known syntheses of halogen-containing acrylic monomers like 2-chloroethyl acrylate[140] and 2-iodoethyl acrylate[141] from acryloyl chloride and 2-chloro/iodoethanol. Stoichiometric amounts of a base, usually triethylamine or pyridine are required to accelerate the reaction and scavenge free hydrochloric acid that would otherwise add to the acrylic double bond. The analogous 2-perchloratoethanol is accessible by the reaction of 2-iodoethanol and $AgClO_4$. Here it was replaced by 3-chloro-2-hydroxypropyl perchlorate **22**, a precursor having a lesser reactive secondary hydroxyl group. Latter was synthesized from 70% perchloric acid, an inexpensive and commercially available source of perchlorate. The synthesis was carried out using a published procedure:[142] The ring opening of epichlorohydrin with perchloric acid in diethyl ether (Scheme 24**a**). The pure product was obtained in moderate yield after a single filtration step through a pad of silica and used immediately.

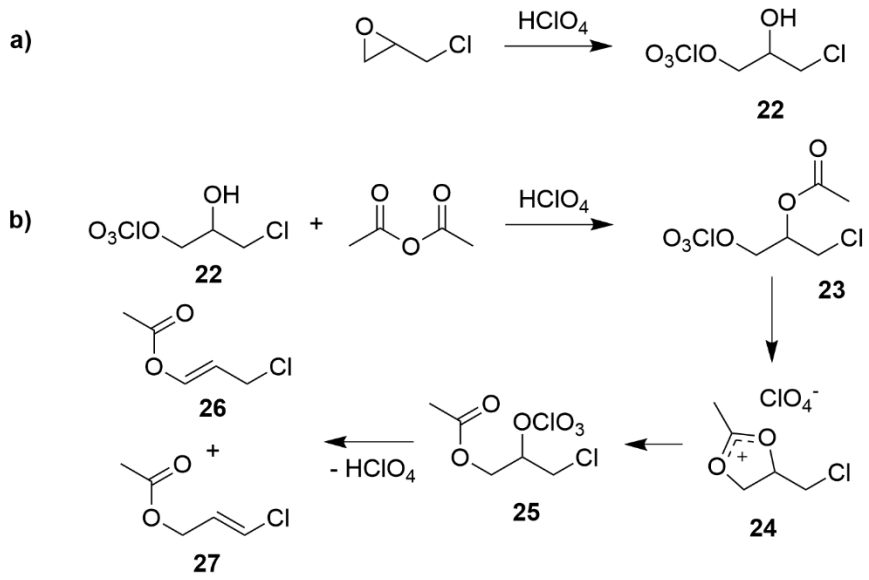

Scheme 24. (a) Synthesis of 3-chloro-2-hydroxypropyl perchlorate (**22**); (b) Synthesis of 3-chloro-1-perchloratopropan-2-yl acetate (**23**) and subsequent rearrangement via dioxolenium ion **24** to secondary perchlorate **25** and elimination to olefines **26** and **27**.

Initial attempts of esterification between **22** and (meth)acryloyl chloride and (meth)acrylic anhydride failed in many ways, using various catalysts and reagents. Therefore, model reactions were carried out with acetyl chloride and acetic anhydride (substitute for acryl analoge without the reactive acrylic functionality). Several non-nucleophilic catalysts that have been reported active in acetylation reactions were tested including Zn[143], ZnO[144], $CoCl_2$[145], $LiClO_4$[146] and $HClO_4$[147]. Reactions were performed in benzene, dichloromethane, tetrahydrofuran (THF), diethyl ether or neat. Several reactions supposedly gave ester **23** with NMR resonances at ~5.27 and ~4.72 ppm, but large amounts of byproducts imparted the yield.

Most promising results were obtained with acetic anhydride in diethyl ether (Scheme 24**b**) yielding ~30% of **23**. The reaction appears to be catalyzed by trace amounts of perchloric acid which might originate from the synthesis of **22** or is formed in-situ by elimination and olefin formation. In fact, the mixture of acetic anhydride/perchloric acid is widely used for acetylation and metal polishing.[148] Their reaction is exothermic and heat evolution facilitates rearrangement to secondary alkyl perchlorate **25** (NMR resonances at 5.13 and 4.36 - 4.20 ppm). Indeed, when a reaction mixture containing **23** was allowed to stand for several hours, the concentration of **25** increased while the that of **23** decreased. The rearrangement to **25** possibly proceeds via the intermediate dioxolenium perchlorate **24**. The formation of elimination products **26** and **27** was also observed. The use of acrylic anhydride instead of acetic anhydride led to further complications due to polymerization. Eventually, the approach

proved impractical due to instability of intermediates and products and generally inconsistent results.

Another approach consisted of the esterification reaction between HEA and Cl_2O_7 to 2-perchloratoethyl acrylate (**28**) (Scheme 25). HEA is a commodity, the anhydride of perchloric acid is not and had to be synthesized.

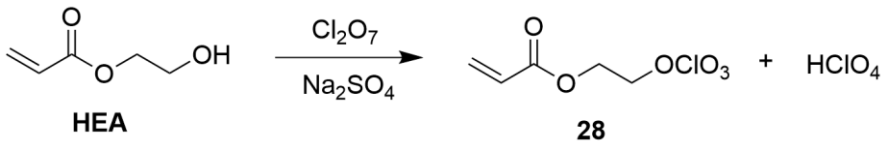

Scheme 25. Synthesis of 2-perchloratoethyl acrylate (**28**).

The synthesis was carried out using co-distilled Cl_2O_7 and carbon tetrachloride originating from a suspension of phosphorus pentoxide in carbon tetrachloride and 70% perchloric acid.[85] The resulting solution was then added to a mixture of HEA and Na_2SO_4 in carbon tetrachloride. Na_2SO_4 was found to absorbs/neutralize perchloric acid that is released during the reaction which would otherwise induce side reactions. Amines, including pyridine are too nucleophilic and react instantly with Cl_2O_7. The resulting mixture must carefully be filtrated through a pad of silica to remove perchloric acid and unreacted HEA. Acrylate **28** is stable in solution and obtained in moderate yields. However, Cl_2O_7 is extremely explosive, and its synthesis is expensive and impractical from an industrial point of view. This approach was therefore not pursued further.

The reaction of 2-bromoethyl acrylate (**29**) with $AgClO_4$ did not give the desired covalently bonded perchlorate but the salt 2-alkenyl-1,3-dioxolenium perchlorate (**30**) as described in a patent from 1968 (Scheme 26).[139]

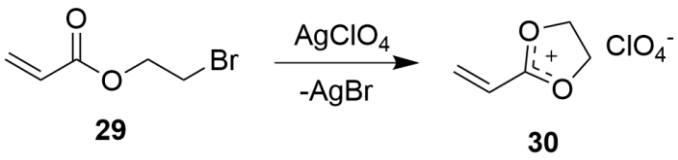

Scheme 26. Synthesis of 2-alkenyl-1,3-dioxolenium perchlorate (**30**).

The salt precipitates from a solution in dichloromethane and is soluble only in polar, non-nucleophilic solvents such as nitromethane which complicates its handling. The covalently bonded perchlorate was not obtained. Even though the author of the patent claims that the salts are easily copolymerized with various acrylates, no such experiments were made as ionic polymers impose special requirements on the coating formulation, especially on the solvent.

5.1.2 Synthesis and Characterization of 4-Perchloratobutyl Acrylate (pCBA)

The reaction of acetyl perchlorate with cyclic ethers including THF has been reported[87] to give almost quantitatively the perchlorate esters via a ring opening reaction. This reaction was taken as a model reaction for the following synthesis of 4-perchloratobutyl acrylate (pCBA). The acrylic monomer pCBA is obtained from acryloyl chloride, $AgClO_4$ and THF in a convenient one-pot reaction (Scheme 27). Treatment of acryloyl chloride with $AgClO_4$ in a nonpolar solvent such as pentane immediately gives a brownish precipitate (AgCl) indicating the formation of acryloyl perchlorate (**31a**), a highly reactive species readily attacked by any nucleophile. Subsequent addition of THF yields oxonium ion (**32a**), which precipitates as a white salt and then further converts to pCBA within seconds by nucleophilic attack of the perchlorate anion at the electrophilic (alpha) carbon adjacent to the positively charged oxygen. The formation of a minor amount of polyTHF, which has been reported[149,150] for comparable conditions, cannot be completely avoided, even when THF is added as a solution in pentane. However, precipitated AgCl and polyTHF are easily removed by filtration through a pad of silica gel and subsequent removal of the solvent under reduced pressure leaves pure liquid monomer in up to 80% yield.

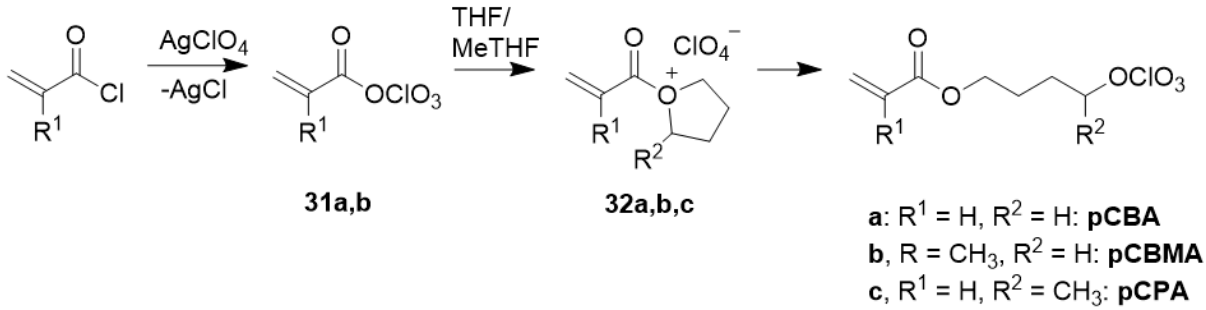

Scheme 27. One-pot synthesis of 4-perchloratobutyl acrylate (pCBA), 4-perchloratobutyl methacrylate (pCBMA) and 4-perchloratopentyl acrylate (pCPA).

pCBA is moisture sensitive and polymerizes rapidly when exposed to air but can be stored as a solution in pentane at room temperature for some days. Its lifespan is further extended by adding a molecular sieve to the solution in order to absorb even trace amounts of water. Although many low molecular weight alkyl perchlorates are explosive, including $AgClO_4$, pCBA did not explode in the hammer-test.[151] Structural proof is provided by ^{1}H and ^{13}C NMR-spectroscopy, IR spectroscopy and elemental analysis. The ^{1}H NMR spectrum of pCBA in $CDCl_3$ revealed a triplet at 4.59 ppm and the ^{13}C NMR spectrum showed a resonance at 75.5 ppm (Figure 5), both characteristic of primary perchlorate ester. This is further supported by the presence of strong bands between 1300 and 1200 cm^{-1} in the IR spectrum (Figure 6,

marked with *), which are characteristic of covalently bonded perchlorates. Mass fractions of C, O and H are within the accepted deviation of 0.3%.

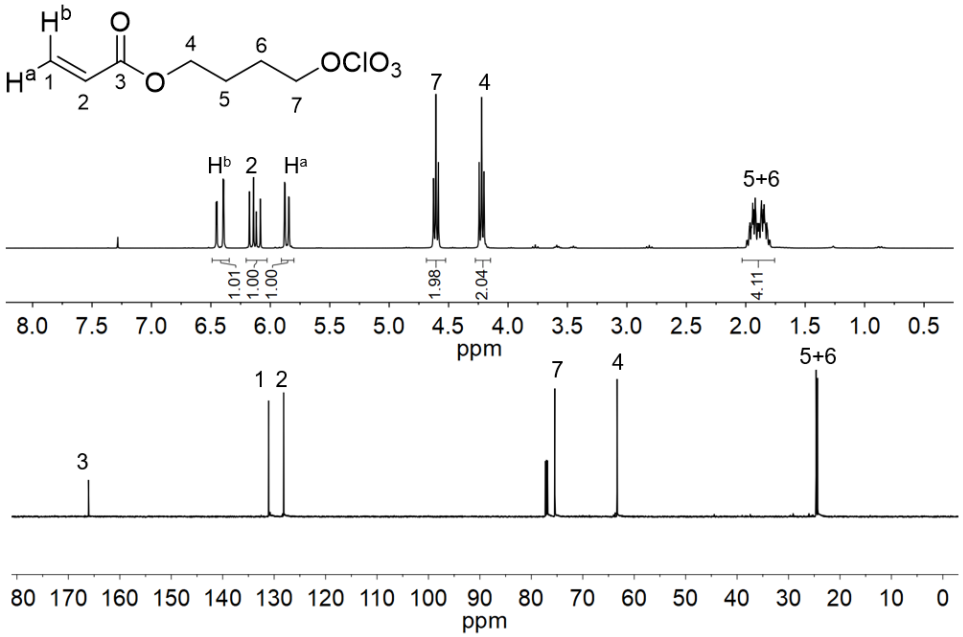

Figure 5. ^{1}H and ^{13}C NMR spectra of pCBA.

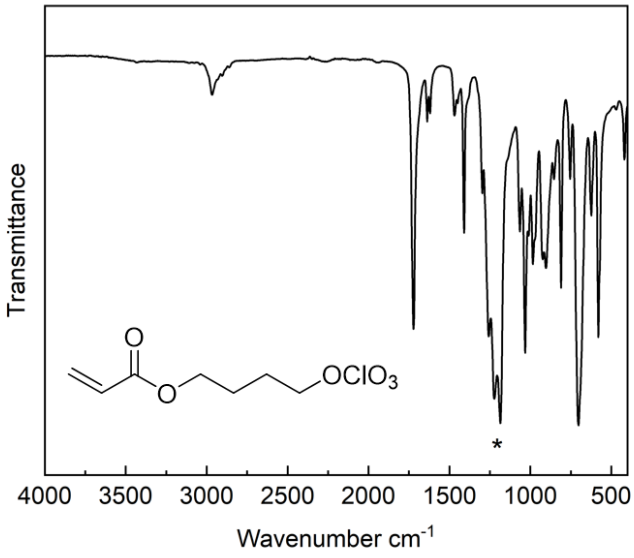

Figure 6. IR spectrum of pCBA; * = typical bands of covalent bound perchlorates.

The corresponding methacrylate and secondary perchlorate were prepared under the same conditions from methacryloyl chloride and 2-methyltetrahydrofuran giving 4-perchloratobutyl methacrylate (pCBMA) and 4-perchloratopentyl acrylate (pCPA), respectively. However, the

secondary alkyl perchlorate pCPA is not stable and readily eliminates $HClO_4$ at room temperature in a solution of chloroform giving a mixture of alkenes.

5.1.3 Free Radical (Co)polymerization of pCBA

Free radical copolymerization of pCBA with various vinyl monomers in toluene solution is straightforward and yield linear polymers. Bulk polymerizations were not attempted but may be possible at low temperatures. Copolymerization with various acrylates, methacrylates and vinyl acetate in 60 wt% toluene at 60°C (Table 1) is unproblematic and polyacrylates with unimodal molecular weight distribution are obtained (Figure 8). Prolonged reaction times or temperatures above 100°C resulted in premature crosslinking which was evident by gelation of the reaction mixture. The progress of the polymerization was conveniently monitored by ^{1}H NMR spectroscopy (Figure 7).

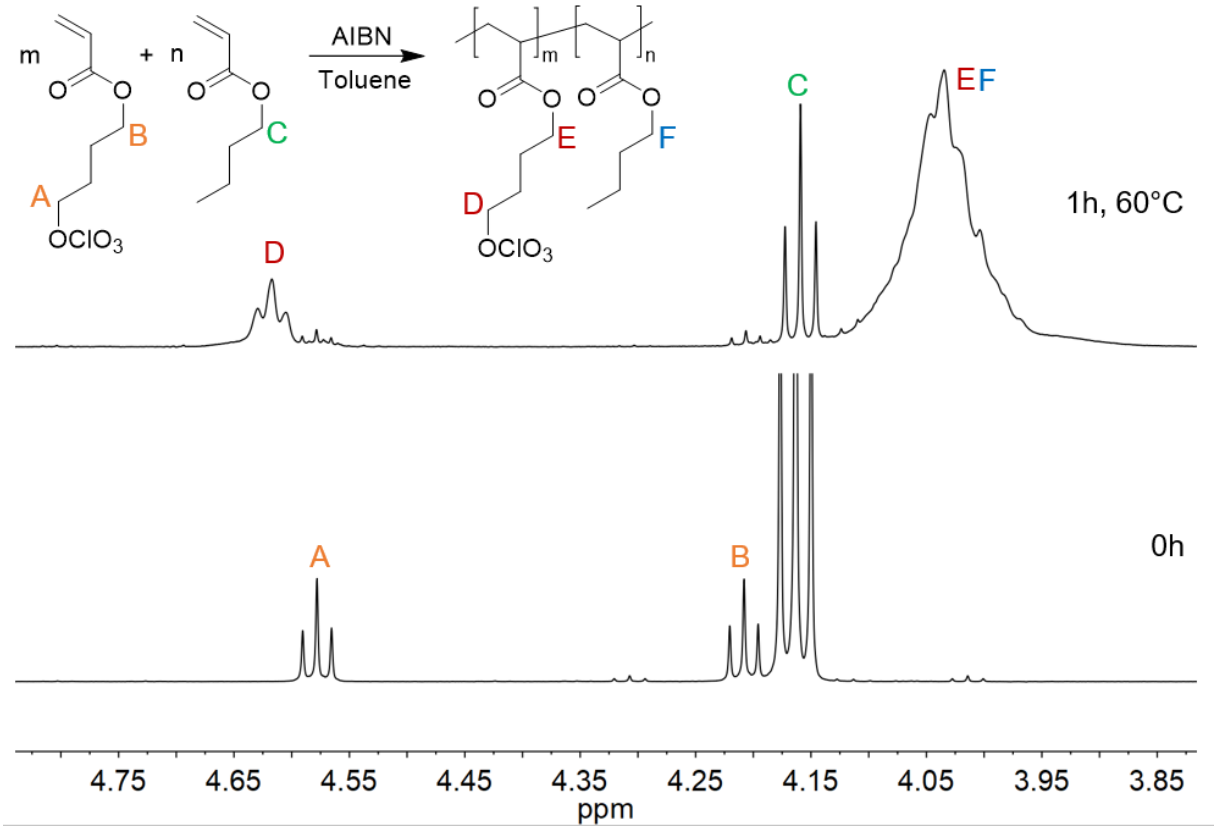

Figure 7. ^{1}H NMR spectra recorded before and after the free radical copolymerization of pCBA and BA in toluene.

The sharp perchlorate resonance A at 4.57 ppm is almost completely replaced by a broader resonance D at 4.62 ppm after 1 hour at 60°C. This resonance is attributed to the polymer analogue of the perchlorate ester. Broad signals are typical of polymers as each monomers

chemical environment is similar but not equal and therefore the signals overlap. Likewise, the broad ester resonances B and C weaken and the broad polymer resonances E and F appear.

The copolymerization reactivity ratio of pCBA is approximately equal to other short-chain alkyl acrylates and statistical random copolymers are obtained. The number average molecular weight (M_n) of the EA and BA copolymers range from 53 to 56 kDa with polydispersity ($Đ$) between 2.0 and 2.9. Copolymers of methyl acrylate (MA) and methyl methacrylate (MMA) have lower molecular weights but a similar polydispersity. The molecular weights of the copolymers are slightly lower than those of the corresponding homopolymers prepared under the same conditions. Additionally, free radical polymerization of EA in the presence of *n*-decyl perchlorate gives PEA with lower M_n than in the absence of *n*-decyl perchlorate under otherwise the same conditions (Table 1, Entry 13). The perchlorate esters thus have some chain regulatory activity. In this context: perchlorate radicals are reported to initiate the free radical copolymerization of MMA and acrylonitrile,[152] and radical processes are reported in the thermal decomposition of perchlorate salts[69] (Chapter 3.2.1).

Molecular weight of pCBA copolymers was controlled using carbon tetrabromide. Environmentally friendly high-solid (low VOC) coatings require polymers with low molecular weight (M_n < 10000 g mol^{-1}) and high functionality (5-25 mol% crosslinker). Molecular weight is typically controlled by adjusting polymerization temperature, monomer to initiator ratio, monomer concentration (monomer starved conditions), solvent, and CTAs. Mercaptans and halocarbons are common agents for free radical polymerizations. Whereas mercaptans are too nucleophilic to be used in combination with perchlorate esters, halocarbons are expected unreactive toward perchlorate esters. Indeed, addition of carbon tetrabromide to the polymerization mixture lowered molecular weights of P(BA-pCBA16) from 60 kDa to ~3 kDa (alkyl acrylate copolymers containing x mol% of pCBA are designated P(YA-pCBAx), with x the mol% of pCBA in the backbone and Y being either M for methyl, E for ethyl or B for butyl acrylate content). Molecular weight was determined by NMR spectroscopy from the signal ratio of end groups to total in-chain monomers.

Table 1. Copolymers of (meth)acrylates and pCBA[137].

Entry	(Co)-monomer	mol% pCBA at start (in the polymer)	(Co)-monomer-conversion (%)	M_n (kg mol^{-1})	M_w (kg mol^{-1})	$Đ$
1	MA	-	55	42	92	2.1
2	MA	3.1 (3.4)	75	27	69	2.5
3	EA	-	48	66	140	2.1
4	EA	1.0 (0.90)	66	56	150	2.7
5	EA	1.8 (1.8)	55	56	140	2.5
6	EA	3.6 (3.7)	61	54	160	2.9
7	EA	4.2 (4.6)	45	53	140	2.7
8	EA	7.3 (8.0)	53	56	140	2.5
9	BA	-	50	46	100	2.1
10	BA	4.2 (4.7)	69	55	110	2.0
11	MMA	-	12	27	57	2.1
12	MMA	3.6 (2.5)	23	12	25	2.1
13*	EA	-	50	47	122	2.6

* = Addition of 100 µL *n*-decyl perchlorate.

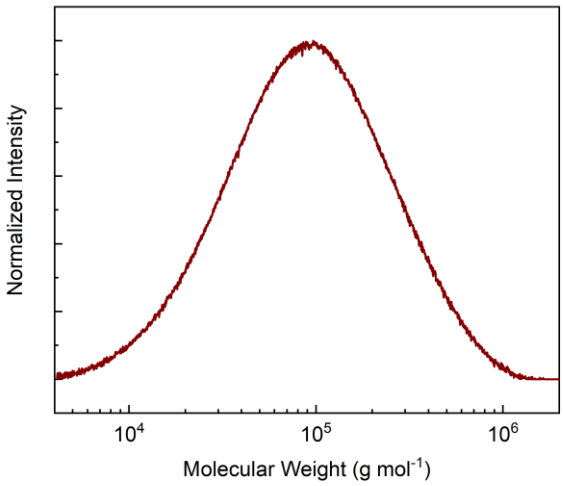

Figure 8. SEC chromatogram of P(EA-pCBA8)[137].

5.1.4 Reactions of BA/pCBA-Copolymers with Various Nucleophiles and Crosslinkers

The reactivity of pCBA copolymers towards various nucleophiles including amines, alcohols and nitriles was tested. Amines and alcohols react readily with the perchlorate ester functionality of the copolymers, whereas nitriles needed harsher conditions. Reactions were carried out in NMR tubes, which allowed a convenient monitoring by ^{1}H NMR spectroscopy. A low molecular weight P(BA-pCBA16) (M_n = ~3000 g mol^{-1}) resin was chosen over high molecular weight copolymers because gelation, which may complicate analysis by NMR spectroscopy, would in general occur in a later stage of crosslinking (in case of difunctional crosslinkers/co-reactants). The resin was dissolved in either $CDCl_3$ or acetonitrile-d_3, followed by addition of the nucleophile.

Primary amines react rapidly with the perchlorate ester functionalities of P(BA-pCBA16). Addition of two equivalents *n*-butylamine, calculated relative to the total amount of perchlorate ester, to a solution of P(BA-pCBA16) in $CDCl_3$ (50 mg/0,7 mL) yields secondary ammonium perchlorate salts with full conversion reached after 20 hours (Figure 9).

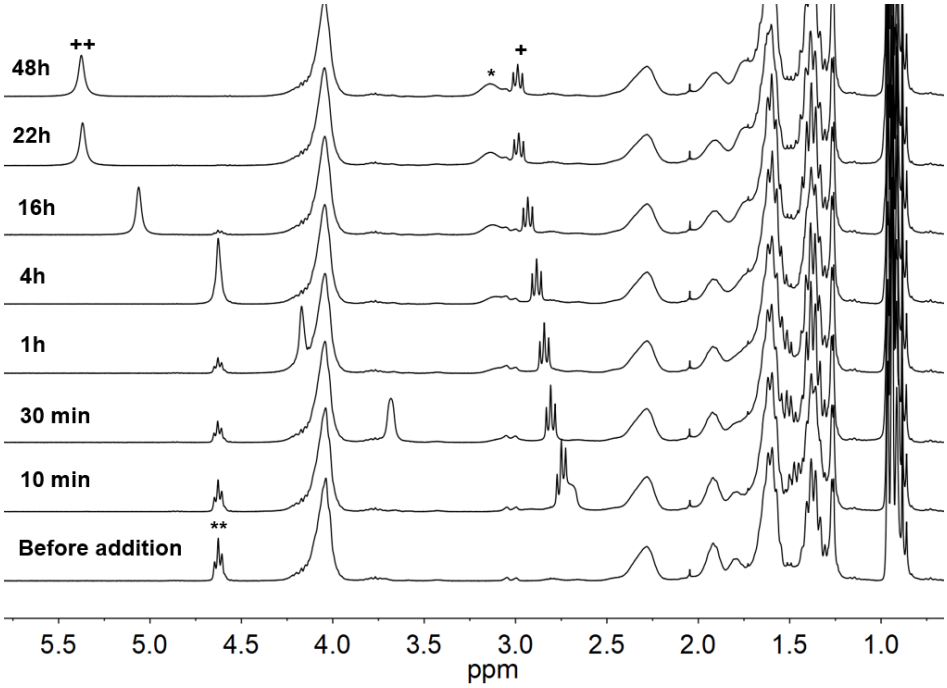

Figure 9. Stacked plot showing ^{1}H NMR spectra of reaction of P(BA-pCBA16) with 2 eq. *n*-butylamine in $CDCl_3$ at room temperature; *: alkylammonium perchlorate salt, **: unreacted perchlorate ester, + and ++: free *n*-butylamine (+: N-CH_2-; ++: -NH_x).

As the reaction proceeds, the triplet at 4.60 ppm assigned to the α-protons of the perchlorate ester disappears and a broad signal at 3.20 ppm (marked with *) appears indicating the formation of alkyl ammonium salts. Both resonances of free *n*-butylamine shift downfield over time, likely caused by proton transfer from the ammonium perchlorate salts to free amines.[153] Washing the solution with saturated $NaHCO_3$-solution gave a multiplet at ~2.60 ppm and HSQC NMR experiments revealed the chemical shift of the adjacent carbon atom at 51 ppm strongly suggesting the presence of a secondary amine. Replacement of *n*-butylamine with 2-aminopentane resulted similarly in the formation of a secondary amine with the corresponding ^{1}H resonance at ~2.60 ppm and ^{13}C resonances at 47 ppm and 51 ppm.

Primary amines, the products of dealkylation of ammonium salts were not detected.[153] Aqueous washed polyacrylates were treated with 3.5-bis(trifluoromethyl)benzaldehyde (BTFBA) and a recorded ^{19}F NMR spectrum showed only the resonance for unreacted BTFBA at -62.9 ppm (Figure 10) confirming the absence of primary amines. Control experiments with *n*-butylamine resulted in a new resonance at 62.8 ppm indicating the formation of an imine. Fluorobenzene was used as an internal reference (113 ppm).

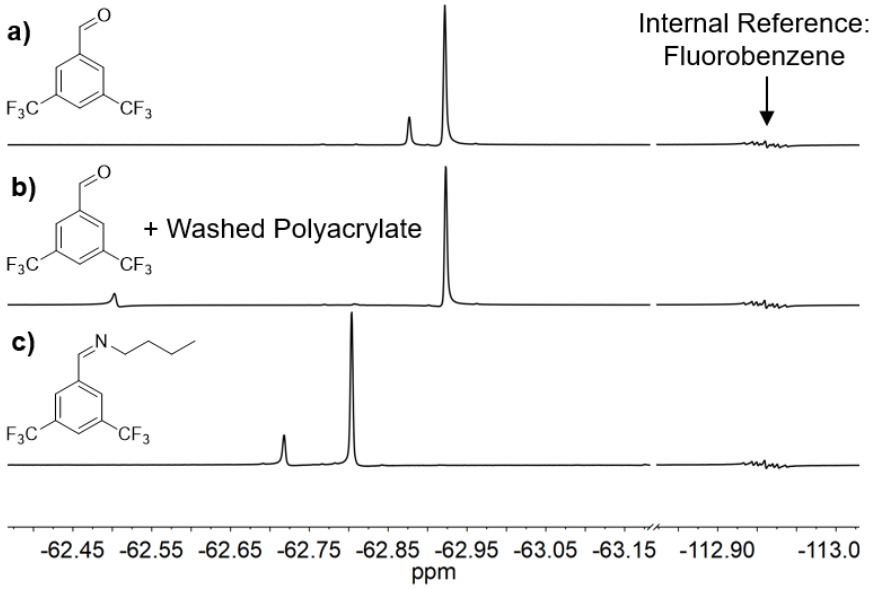

Figure 10. (a) ^{19}F NMR spectrum of BTFBA; (b) BTFBA and water washed polymer; (c) and BTFBA with excess *n*-butylamine.

A classical 2K system would exist in the treatment of P(BA-pCBA16) with one equivalent hexamethylenediamine and *JEFFAMINE*® D-230 (*Huntsman*). Latter is a polyether amine having 2.5 polypropylene oxide units as backbone and two primary amine groups located on secondary carbon atoms at both ends of the aliphatic polyether chain. The treatment resulted in gelation within seconds. More detailed analysis using NMR spectroscopy was hampered by significant peak broadening, but the formation of crosslinks via analogous ammonium salts is envisioned.

Primary alcohols are also reactive towards the perchlorate esters of P(BA-pCBA16) but require slightly harsher conditions. The solvent was therefore changed from $CDCl_3$ to 1,1,2,2-tetrachloroethane-d_2 (TCE-d_2) with a higher boiling point. When 10 eq. *n*-butanol was added to a solution of 50 mg P(BA-pCBA16) in 0.7 mL of TCE-d_2 at 60°C, the reaction proceeds within several hours with virtually complete conversion of the perchlorate ester after 30 hours (Figure 11) or within 3 hours at 100°C. The resonance at 4.60 ppm assigned to the perchlorate ester decreases constantly over the reaction period, while a new multiplet appears at 3.42 ppm assigned to a newly formed ether. Ether formation was further verified by heating P(BA-pCBA16) in methanol-d_4, leading to the appearance of a distinct triplet in the ^1H NMR spectrum.

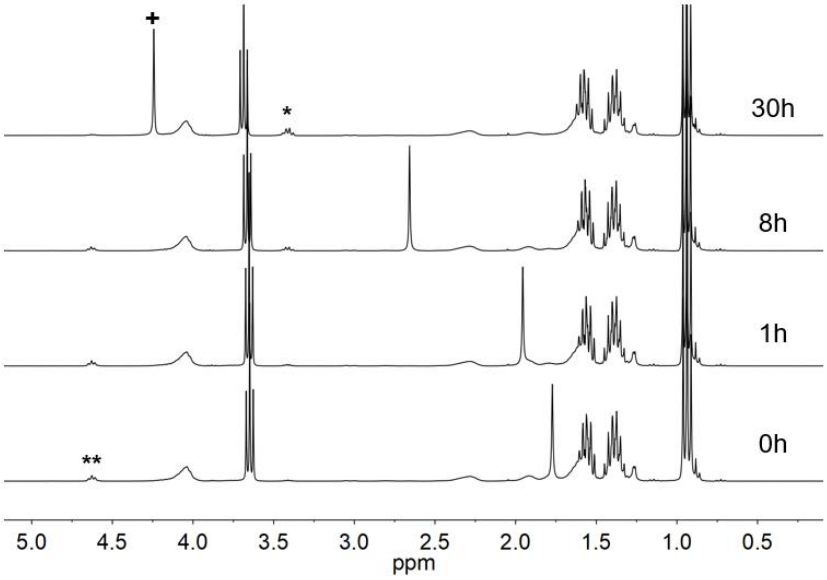

Figure 11. Stacked plot showing ^{1}H NMR spectra of reaction of P(BA-pCBA16) with 10 eq. *n*-butanol in $CDCl_3$ at 60°C; * = ether, ** = perchlorate ester, + = *n*-butanol (O-H).

Perchloric acid is generated in the course of the nucleophilic substitution. It will protonate remaining free *n*-butanol present in the reaction mixture. Proton transfer between *n*-butanol molecules is fast on an NMR time scale as the O-*H* resonance of *n*-butanol shifts downfield from 1.75 ppm to 4.25 ppm (marked by a "+" in Figure 11). When *n*-butanol is replaced by P(ST/BA/HEA13), a hydroxy functional acrylic polyol with M_n = 40,000 g mol^{-1}, in the same OH/perchlorate ester ration of 10:1 and heated to 100°C in TCE-d_2, rapid gelation takes place indicating the formation of crosslinks. The combination of acrylic resins bearing perchlorate ester functionalities with commercially available hydroxy functional acrylic resins may at first appear promising for a 1K thermosetting system, but Arrhenius law still applies and such a system would most likely suffer from poor storage stability.

Nitriles also react with P(BA-pCBA16), albeit under significantly harsher conditions than primary alcohols. P(BA-pCBA16) was heated in a 3:1 mixture of acetonitrile-d_3 and $CDCl_3$ at 60°C (Figure 12). The perchlorate ester resonance at 4.60 ppm disappeared completely over the course of nine hours and a new resonance at 3.43 ppm suggests the presence of an amide.[113,114] This is in accordance with reports that Ritter-type transformations of alkyl perchlorates with nitriles require an excess of the nitrile component.[113,114] The Ritter-type reaction is assumed to proceed in two steps: First the perchlorate group is directly substituted for the nucleophilic nitrogen center of the nitrile group through an S_N2-type of mechanism. The intermediately formed but relatively stable nitrilium perchlorate is then hydrolyzed to the corresponding acetamide and $HClO_4$. This proceeds either by trace amounts of water present

in the reaction mixture (like in this study) or from the surrounding atmosphere, or alternatively in a separated second reaction step with the addition of water to the reaction medium. The latter avoids direct competition between water and nitrile which can lead to alcohol by-products.

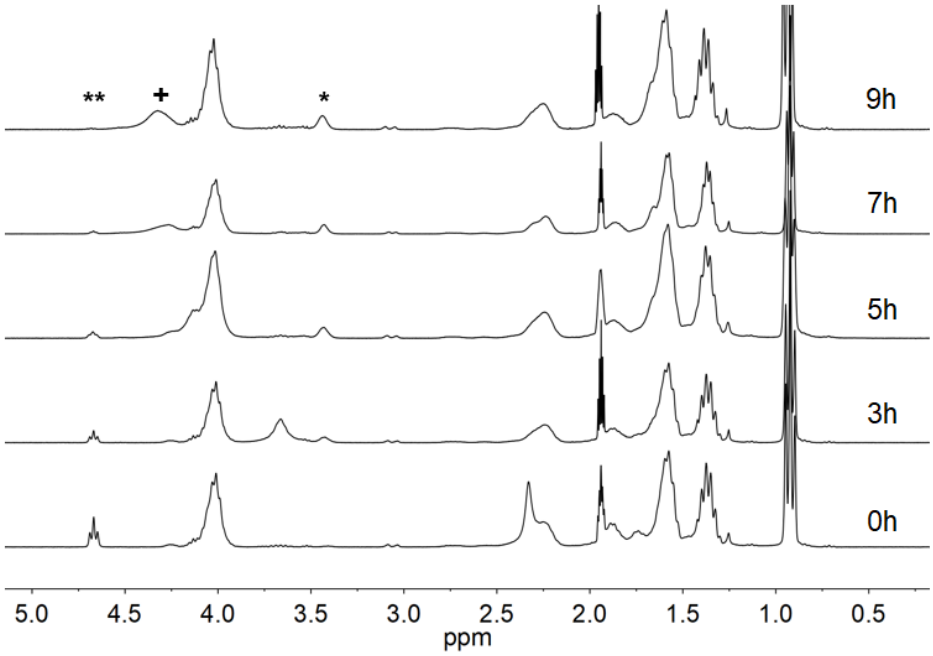

Figure 12. Stacked plot showing ^{1}H NMR spectra of reaction of P(BA-pCBA16) with acetonitrile-d_3 in 3:1 mixture of acetonitrile-d_3 and $CDCl_3$ at 60°C.

When the ratio of acetonitrile-d_3 to $CDCl_3$ was reduced from 3:1 to 1:10, the formation of the amide was too slow, rendering this approach unsuitable for the development of a thermosetting resin. However, under these changed conditions a new type of reaction is favored which is extensively discussed in section 5.1.5.

Although the experiments with amines, alcohols and nitriles provide valuable insights into possible crosslinking pathways involving perchlorate esters, their current limitations namely unfavorable kinetics, reaction products and side-reactions make them less suitable for a 1K formulation. However, these reagents are not necessary for crosslinking the binder as is presented below.

5.1.5 Self-Crosslinking pCBA-Copolymers

It was unexpectedly found that pCBA-copolymers crosslink even in the absence of a hardener by a simple thermal treatment. Copolymers of EA and pCBA with various pCBA content were found to crosslink relatively quickly at room temperature when the solvent was removed. Neat

copolymers showed gelation even after 1h of storage under nitrogen atmosphere. When pCBA-copolymers are applied to glass substrates from 30 wt% xylene solution and heated to 105°C and 135°C, they crosslink to a thermoset material within hours or minutes, respectively.

5.1.5.1 Analysis of Crosslinking Process

Heating thin films of EA/pCBA copolymers over 100°C leads to a thermoset as indicated by swelling studies. The crosslink density (CD) increases for about 4 hours while curing at 105°C to reach a constant level for polymer composition with less than 8 mol% pCBA. Curing at 135°C follows a similar trend reaching completion after 1 hour (Figure 13a,b). Experimental CDs are in alignment with calculated CDs assuming that each perchlorate entity leads to a crosslink.[154] (Figure 13c,d). The crosslinker seems therefore quite effective: every mol of copolymerized pCBA generates a crosslink. This also stands in contrast to most conventional self-crosslinking acrylic resins, who often require two different functionalities in the resin backbone per generated crosslink.

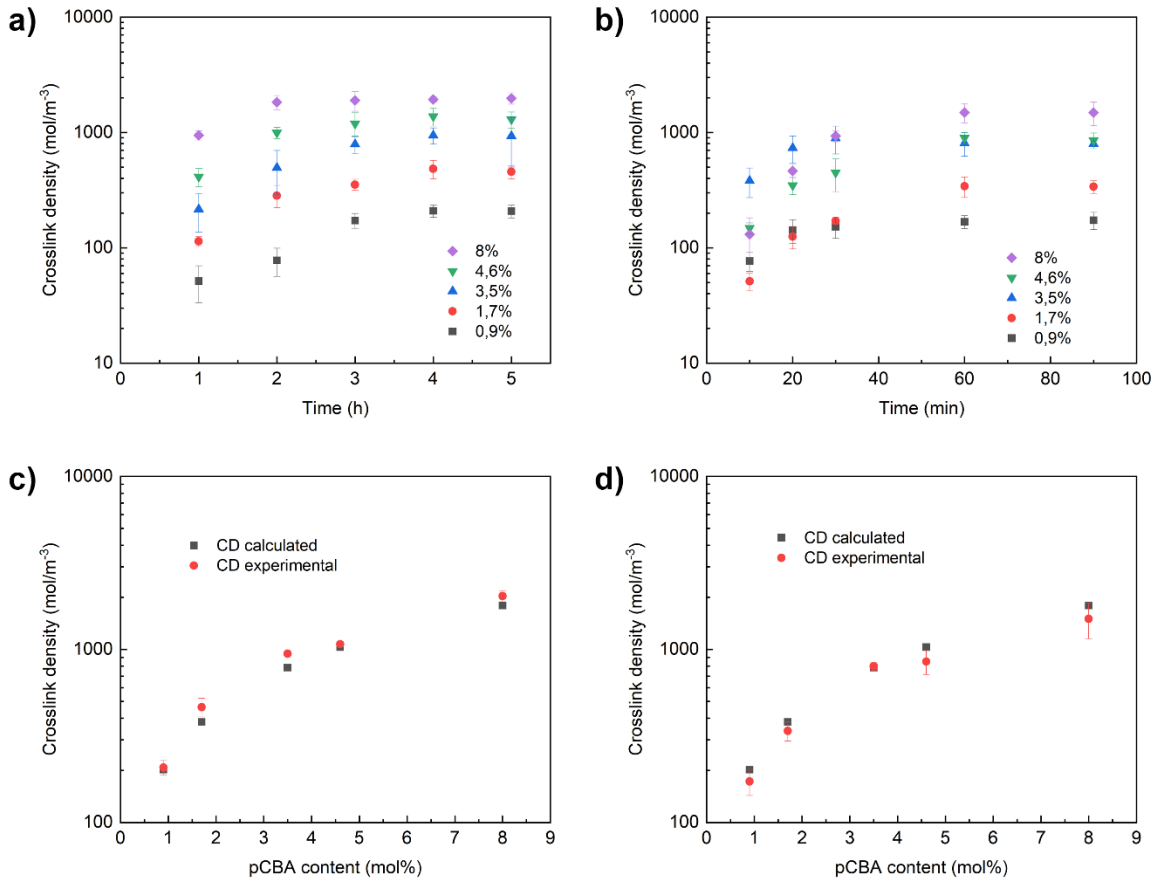

Figure 13. CD of P(EA-pCBA0.9-8) thin films (30-50 µm) cured at (a) 105°C and (b) 135°C. Experimental and calculated CDs of thin films of P(EA-pCBA0.9-8) cured at (c) 105°C and (d) 135°C[137].

The glass transition temperatures (T_g) of completely cured resins were found to increase with increasing pCBA content (Figure 14) as a higher level of crosslinking shortens segments and impedes general mobility. Linear PEA shows a T_g of -23°C[155] and cured P(EA-pCBA0.9-8) has a T_g between -12°C and +20°C.

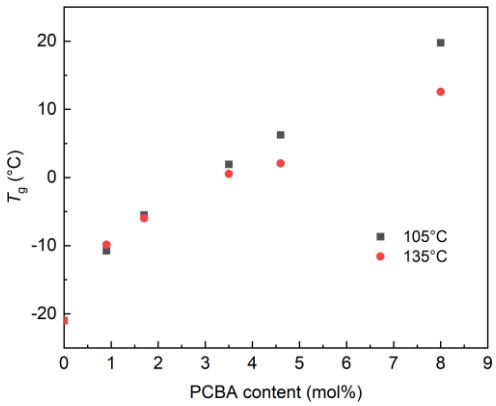

Figure 14. Glass transition temperature (T_g) of cured samples of P(EA-pCBA0.9-8) at 105°C and 135°C[137].

The curing process is conveniently monitored by Attenuated Total Reflection-Fourier Transform Infrared (ATR-FTIR) spectroscopy of the films (Figure 15). The solitary bands at around 585 cm^{-1} and 707 cm^{-1} of the perchlorate anion are a good probe to detect changes related to the perchlorate ester. They show the same changes as the characteristic absorptions of covalently bonded perchlorates at around 1260, 1230 and 1100-1000 cm^{-1}, but lack the partly strong overlap with other absorptions. Even though they have not been reported in the literature[83,85,87,89,92], they are also present in spectra of *n*-decyl perchlorate, pCBA and pCBMA. Calibration relative to the C=O vibration at ~1700 cm^{-1}, using polymers of defined monomer composition, shows an approximately linear dependence of the signal maximum on the pCBA concentration up to 10 mol% (Figure 16).

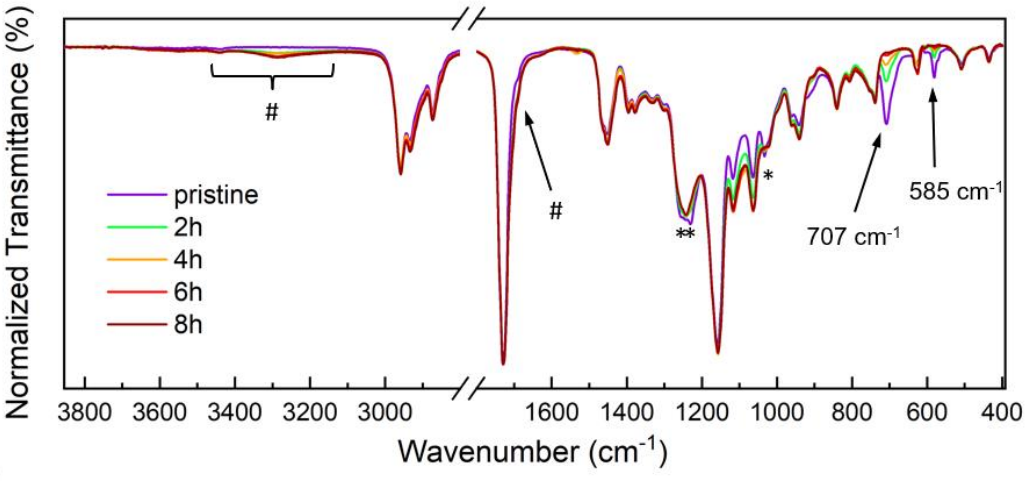

Figure 15. IR-spectra of P(BA-pCBA10) at 2h intervals during curing at 105°C (*: perchlorate ester related absorptions; #: resp. of acid entities)[137].

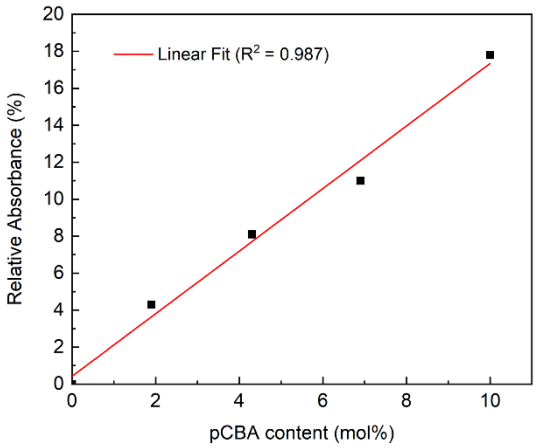

Figure 16. Relative Absorbance of the perchlorate band at ~585 cm^{-1} relative to the C=O vibration at ~1700 cm^{-1} in P(EA-pCBA0-10)[137].

Heating a thin film of P(BA-pCBA10) to 105°C for 8 hours leads to a complete loss of perchlorate entities (Figure 15). The perchlorate species are released from the films as volatile perchlorate ester derivatives rather than through thermal decomposition. This observation is consistent with the known thermal stability of primary alkyl perchlorates[156], some of which can be distilled at temperatures exceeding 100°C[64]. As noted previously, *n*-decyl perchlorate remains stable in 1,1,2,2-tetrachloroethane at 140°C for several hours, further supporting the notion that perchlorate groups in the polymer are eliminated intact as volatile esters rather than undergoing degradation.

The perchlorate loss proceeds with an approximately first-order dependence on its concentration. Similar behavior is observed upon curing at elevated temperatures of 115 and 125°C, albeit with progressively higher rates (Figure 17a,b,c). For instance, P(BA-pCBA11) completes curing within approximately 8, 4 and 2 hours at 105, 115, and 125°C, respectively. Copolymers of pCBA with EA and MA exhibit noticeably faster curing kinetics, with rates increasing in the order BA < EA < MA. At 105°C the respective resins cure within about 8, 2 and 1 hour. Furthermore, the observed curing rates are in good agreement with kinetic parameters derived from swelling experiments.

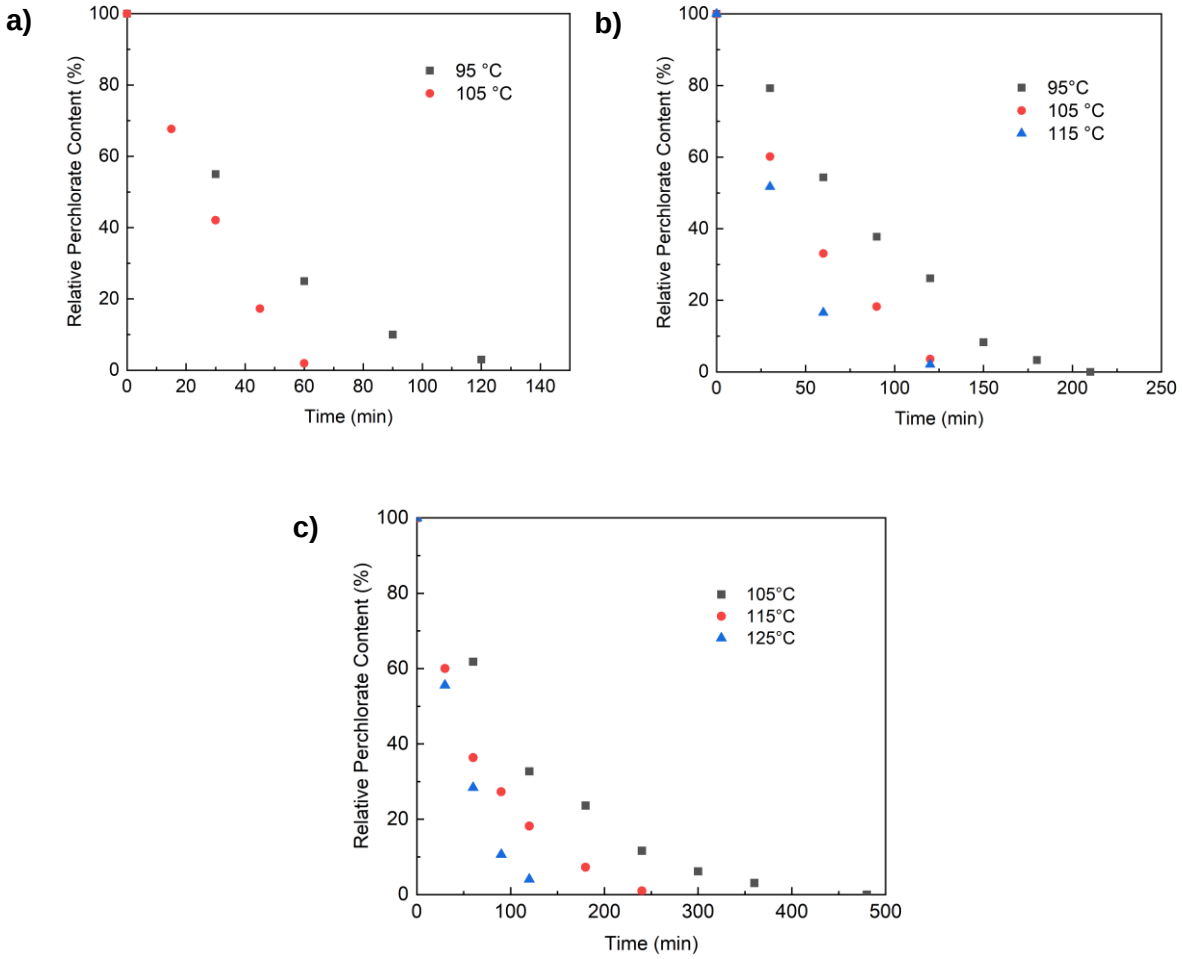

Figure 17. Perchlorate content during the curing process of thin films of (a) P(MA-pCBA11), (b) P(EA-pCBA10), and (c) P(BA-pCBA11) at 95, 105, 115 and 125°C. Data are obtained from the absorption maximum at ~585 cm^{-1} put in relation to the C=O vibration at ~1700 cm^{-1}[137].

Activation energies (E_A) were calculated from an Arrhenius plot by determining the slope of the line when plotting the natural logarithm of the rate constant (ln(k)) versus the inverse of the temperature in Kelvin (1/T). E_A increases in the order of P(MA-pCBA11) < P(EA-pCBA10) < P(BA-pCBA11). The difference in E_A (ΔE_A) between P(MA-pCBA11) and P(EA-pCBA10) is 6 kJ mol^{-1}, it is 30 kJ mol^{-1} between P(EA-PCBA10) and P(BA-pCBA11). The pronounced difference is consistent with data obtained from thermogravimetric analysis.

Table 2. Kinetic data for the curing of P(MA-pCBA11), P(EA-pCBA10) and P(BA-pCBA11) at 95-125°C[137].

pCBA-Copolymer	Temperature (°C)	Rate constant *k* (min^{-1})	Reaction order *n*	Activation energy E_A ($kJ\ mol^{-1}$)	Pre-exponential factor *A* ($((mol\ L^{-1})^{-0.5}/min$)
P(MA-pCBA11)	95	0.029	1	29	27
	105	0.037			
P(EA-pCBA10)	95	0.018	1	35	31
	105	0.026			
	115	0.033			
P(BA-pCBA11)	105	0.0095	1	65	54
	115	0.017			
	125	0.026			

5.1.5.2 Identification of Crosslink Moieties and By-products

Cured copolymers of pCBA with MA and EA feature both 1,4-butylene diester crosslinks and residual carboxylic acid functionalities. Solid state Cross-Polarization Magic Angle Spinning ^{13}C NMR Spectroscopy (^{13}C CP MAS NMR) represents a powerful method for elucidating the chemical structure of crosslinks in thermosetting polymers[157]. The technique requires a powder-like sample that remains solid at the temperature of recording (50°C). Consequently, only copolymers of pCBA with MA and EA were investigated, as the corresponding BA-based copolymers exhibited melting under these conditions and were therefore unsuitable for solid-state analysis.

The ^{13}C CP MAS NMR spectra of cured films of P(MA-pCBA11) (Figure 18a) and P(EA-pCBA8) (Figure 18**b**) do not exhibit any signals corresponding to covalently bound perchlorate moieties, which would be expected at approximately 75 ppm. Instead, new resonances appear at 25, 65 and 181 ppm that are not part of the parent resin (PEA: 174.9, 80.8, 40.8 and 14.6 ppm[158] and PMA: 175.5, 52.3 and 41.9 ppm[159]). The signals at 25 ppm and 65 ppm can be attributed to the newly formed ester crosslinks and are assigned to a symmetrical 1,4-butylene unit connecting two carboxylic ester functionalities. The same resonances are

likewise observed in the corresponding spectra of an independently prepared poly(EA-co-1,4-butanediol diacrylate (BDDA)) reference resin (Figure 18c), thereby confirming the proposed structural assignment.

The resonance at 181 ppm is assigned to carboxylic acid moieties, in confluence with the results obtained from IR spectroscopy. Emerging IR bands at 3280 cm^{-1} (broad) and 1715 cm^{-1} are indicative of carboxylic acid groups, most likely originating from acid-catalyzed hydrolysis or dealkylation of acrylic ester units. In fact, the ^{13}C NMR spectrum of P(MA-pCBA11) cured in the absence of water does not show the resonance at 181 ppm, supporting the proposed assignment and mechanism of acid formation. The in-situ formation of carboxylic acid entities, also has a strong effect on T_g as T_g(PAA) is 109°C[160] considerable higher than that of PEA (-23°C[155]). For instance, hydrolysis of 5% of ethyl ester units in PEA will raise T_g by approximately 5°C as calculated using the Fox-equation (Equation 1).

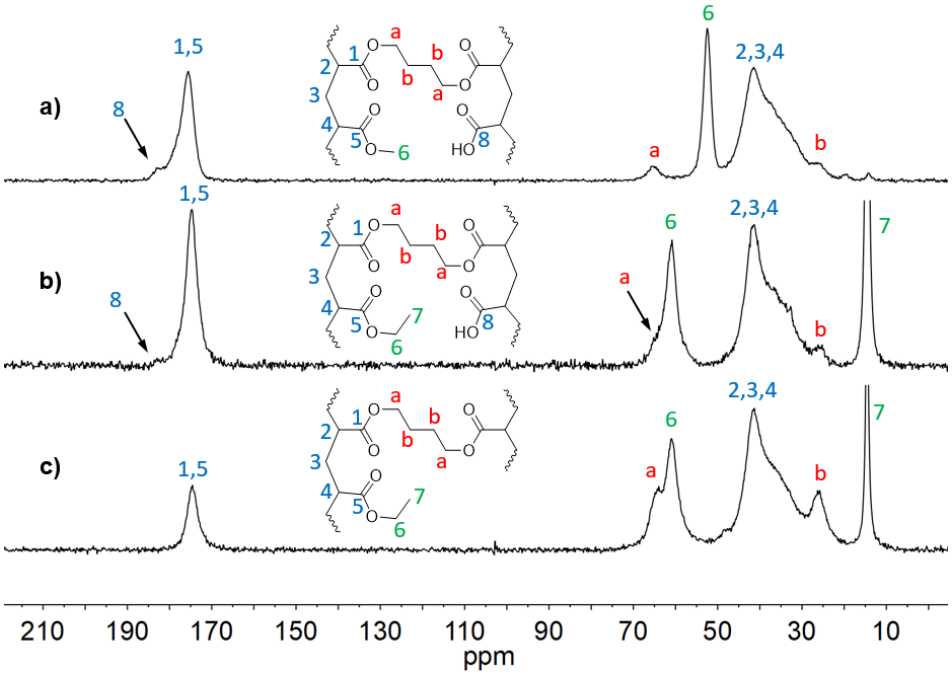

Figure 18. ^{13}C CP MAS NMR spectrum of cured (a) P(MA-pCBA11), (b) P(EA-pCBA8), and (c) P(EA-BDDA16)[137].

Thermogravimetric analysis coupled with FTIR spectroscopy (TGA-FTIR) of copolymers of pCBA with MA, EA and BA reveal a characteristic two-step mass loss when heated at a rate of 10 K min^{-1} under nitrogen atmosphere (Figure 19a). The first mass loss occurs between approximately 140°C and 220°C, followed by a second between 300°C and 500°C. The latter corresponds to the typical thermal degradation of polyacrylates[161]. The loss of mass starting at about 140°C is consistent with the loss of alkyl perchlorates from the samples.

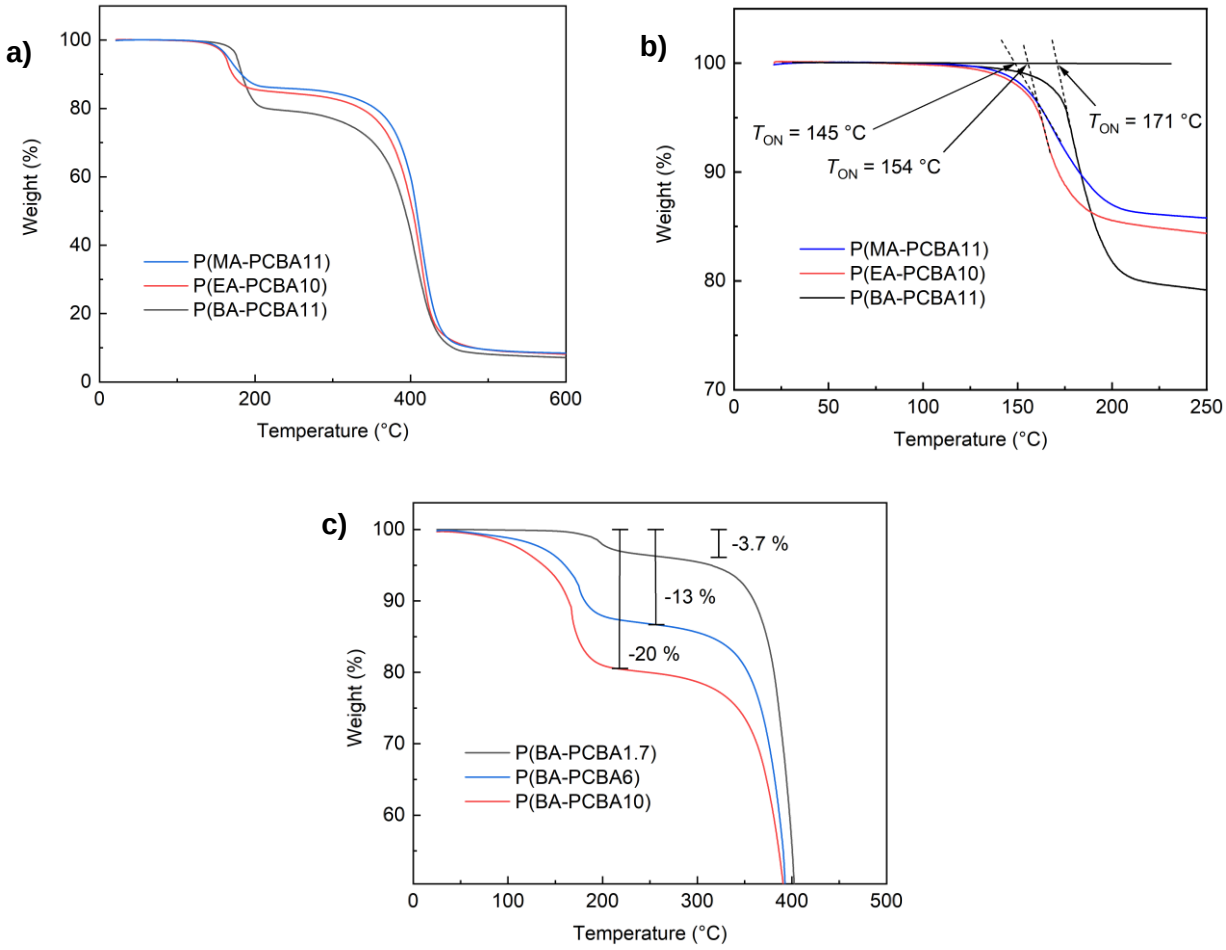

Figure 19. (a) Thermogravimetric analysis of P(MA-pCBA11), P(EA-pCBA10) and P(BA-pCBA11); (b) Thermogravimetric analysis of P(BA-pCBA1.7), P(BA-pCBA6) and P(BA-pCBA10). (c) Binder mass during the curing process of thin films of P(MA-pCBA11), P(EA-pCBA10), and P(BA-pCBA11)[137].

The onset temperatures (T_{ON}) of the first decomposition step follow the same order as the experimentally determined rates of perchlorate release from the films: 171°C for P(BA-PCBA11), 154°C for P(EA-PCBA10) and 145°C for P(MA-PCBA11) (Figure 19b). Additional calorimetric data obtained from differential scanning calorimetry (DSC) are in alignment with the thermogravimetric data and reveal an exothermic peak in the relevant temperature range of 140-230°C (Figure 20). As anticipated, the total mass loss correlates with the pCBA content (Figure 19c) and with the molecular mass of the alkyl side chain in the respective comonomer (Figure 19a).

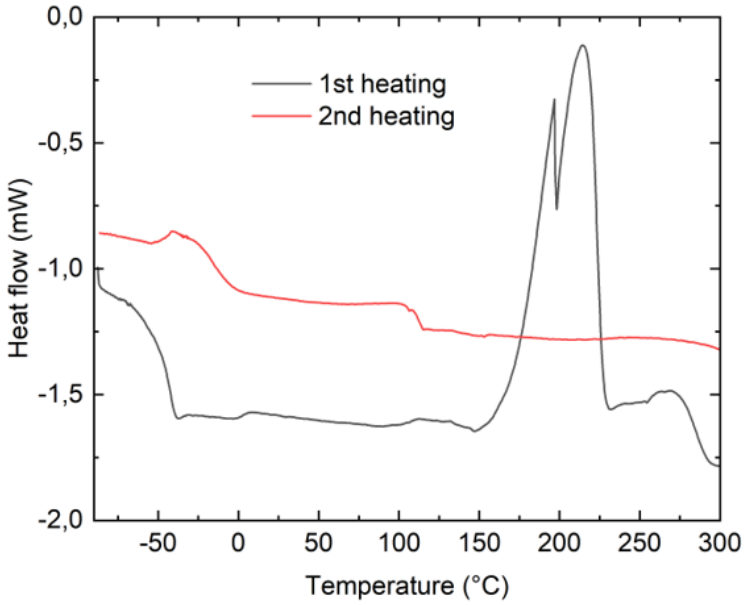

Figure 20. Differential Scanning Calorimetry analysis of P(BA-pCBA7). 1st heating shows a strong exothermic peak at 140-230°C that is missing in the 2nd heating[137].

IR spectra of the off-gases are consistent with a mixture of alkyl perchlorates, THF and CO_2 (Figure 21). Also, smaller amounts of alcohols and ethers were detected. The formation of the mixture of alkyl perchlorates and THF was confirmed by independent trapping experiments. Volatiles released from P(MA-pCBA7), P(EA-pCBA10) and P(BA-pCBA11) upon heating to 200°C under dynamic vacuum were collected in a liquid nitrogen trap and subsequently analyzed by ^{1}H NMR spectroscopy. The spectra of the condensates revealed characteristic signals corresponding to methyl (s, 4.24 ppm), ethyl (q, 4.63 ppm) and butyl perchlorate (t, 4.55 ppm), respectively, as well as trace amounts of THF (Figure 22), thereby corroborating the FTIR findings and confirming the evolution of volatile perchlorate esters during the curing process.

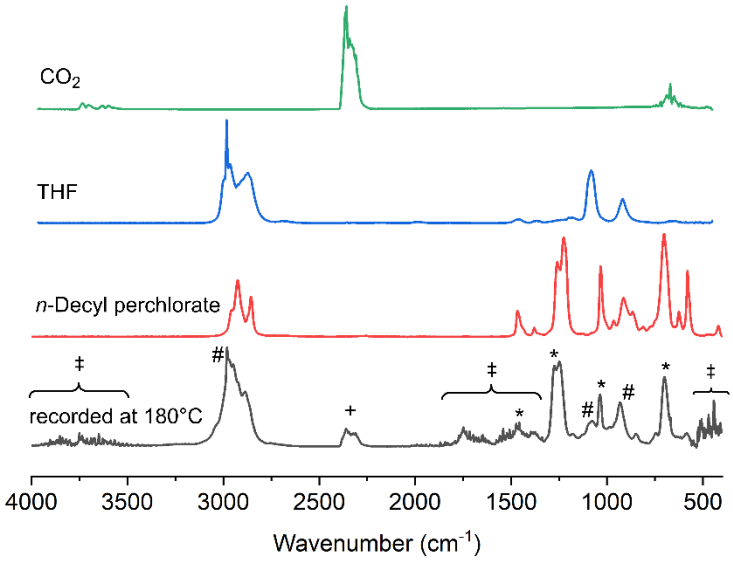

Figure 21. IR-spectra recorded at 180°C (black) of the off-gas during the curing of P(BA-pCBA10) with reference spectra CO_2 (green, gas phase),[162] THF (blue, liquid)[162] and *n*-decyl perchlorate (red, liquid); each band is assigned to the references (+: CO_2; #: THF; *: alkyl perchlorate); ‡: Background H_2O in air[137].

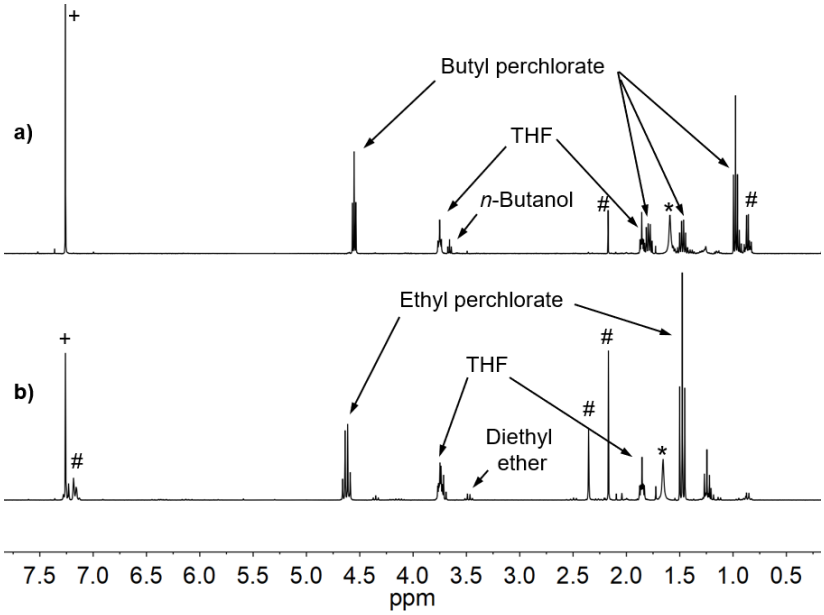

Figure 22. NMR-spectra of emissions trapped during the curing of (a) P(BA-pCBA10) and (b) P(EA-pCBA9); Products are indicated with arrows; #: solvent related impurities; *: water resonance; +: $CDCl_3$ resonance; alkyl perchlorate/THF ratio of about 3:1[137].

The detected CO_2 may, at least in part, originate from the partial decomposition of volatile alkyl perchlorates within the heated transfer line (200°C) connecting the TG-unit and the FTIR detector. This hypothesis is supported by complementary thermogravimetric analysis coupled with mass spectrometry (TGA-MS) experiments conducted on benzene and on mixtures of benzene and ethyl perchlorate, which yielded comparable results. The observed instability of

ethyl perchlorates and possibly other low molecular weight alkyl perchlorates under these experimental conditions is consistent with previous reports[64,80] The thermal decomposition of ethyl perchlorate ($C_2H_5O_4Cl$) proceeds with the evolution of CO_2 , dihydrogen and hydrogen chloride in the expected stoichiometric ratios, confirming that a portion of the CO_2 detected during TGA-FTIR measurements likely arises from secondary decomposition processes occurring in the gas phase rather than from the polymer itself.

5.1.5.3 Description of the Curing Process

The reaction between a perchlorate ester and a carboxylic ester was identified as the predominant crosslinking pathway in pCBA-containing copolymers. This process proceeds via a transesterification mechanism[163], yielding 1,4-butylene diester crosslinks and volatile alkyl perchlorate as byproducts. During the curing of P(EA-pCBA) copolymers, ethyl perchlorate was the only volatile perchlorate ester detected, indicating that the curing mechanism (Scheme 28. Proposed pathways of the crosslinking reaction in the presence (bottom) and absence (top) of moisture (ClO4--anions as charge compensation for the acylium esters are not displayed)[137].) is proposed to involve a transesterification step in which the butyl perchlorate substituent is replaced by an ethyl perchlorate species.

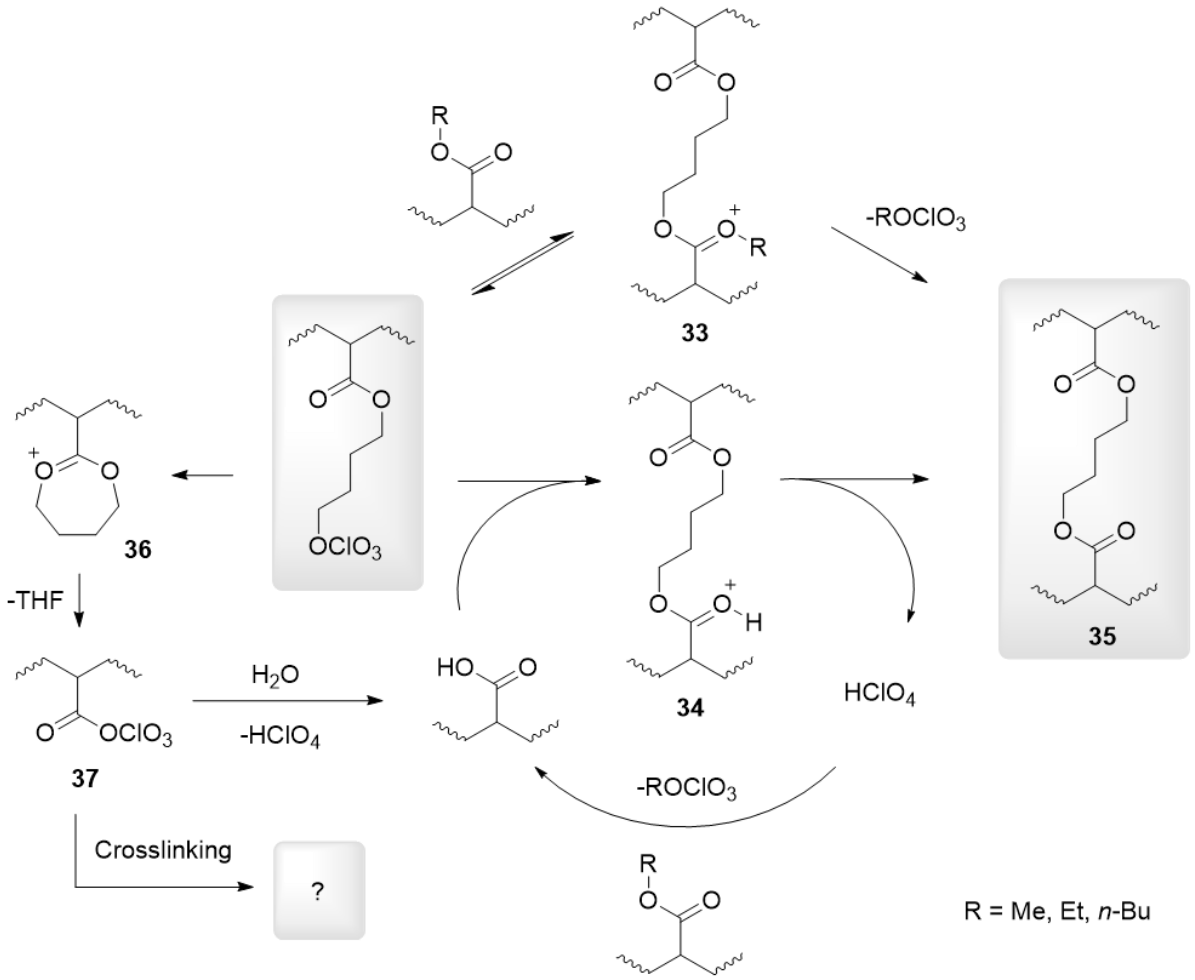

Scheme 28. Proposed pathways of the crosslinking reaction in the presence (bottom) and absence (top) of moisture (ClO_4^--anions as charge compensation for the acylium esters are not displayed)[137].

The overall mechanism of crosslink formation is envisioned to proceed via nucleophilic attack of an ester carbonyl oxygen on the electrophilic carbon center of the perchlorate ester, leading to the formation of a cationic 1,3-dioxolenium intermediate (**33**) (Scheme 28). Such 1,3-dioxolenium perchlorate salts have been reported previously[164] and are known to be reasonably stable compounds in the absence of nucleophiles. Their stability increases with the presence of electron-donating substituents and delocalization of the positive charge. Owing to their high electrophilicity, these species have also been employed as initiator for the cationic ring opening polymerizations of cyclic ethers.[165]

Subsequent reaction of this intermediate with a “free” perchlorate anion regenerates a perchlorate ester either in the form of the starting material or in the form of a volatile alkyl perchlorate. The reaction equilibrium consequently shifts toward the formation of the 1,4-butylene diester crosslink (**35**) as the volatile alkyl perchlorate is continuously removed from the polymer film und dynamic conditions.

In addition to this predominant intermolecular transesterification pathway, a series of minor side reactions were identified to occur during the curing process. An intramolecular variant of the transesterification mechanism is proposed, involving a nucleophilic attack by the ester moiety carrying a butyl perchlorate group. This process regenerates a coordinated THF oxonium ion (**36**), which subsequently decomposes to yield free THF and a polymer-bound acyl perchlorate intermediate (**37**)[149]. Hydrolysis of this intermediate in the presence of trace amounts of water (e.g. from the air during curing) leads to the formation of carboxylic acid substituents and perchloric acid. The formation of carboxylic acid groups was indeed observed experimentally in the ^{13}C CP MAS NMR (Figure 18) and IR (Figure 15) spectra, underscoring the relevance of this side reaction under typical curing conditions.

It can be anticipated that the formation of carboxylic acid groups further promotes crosslink formation, since carboxylic acids are generally more nucleophilic than the corresponding ester functionalities. Moreover, the presence of acidic groups in the final polymer network may be advantageous, as they enhance interfacial adhesion to polar substrates such as metals and glass. Consequently, a limited amount of moisture can be tolerated within the perchlorate ester-based crosslinking system, as it not only participates in side reactions but may also indirectly contribute to improved material performance through the generation of carboxylic acid sites.

Swelling experiments, however, indicate that the acyl perchlorate intermediate (**37**) ultimately contributes to crosslink formation. A conceivable reaction pathway involves the interaction of **37** with an ester functionality, leading to the transient formation of a bridging anhydride and an alkyl perchlorate. The presence of such an anhydride structure could, however, be ruled out, as the ^{13}C CP MAS NMR spectrum of a reference poly(ethyl acrylate-*co*-acrylic anhydride) sample did not coincide with that of the cured product (Figure 46).

Alternatively, perchloric acid generated from the hydrolysis of **37** may either evaporate from the polymer film or participate in an equilibrium reaction with ester moieties, yielding an alkyl perchlorate and an additional carboxylic acid (Scheme 29). The analog transesterification between carboxylic esters and pTSA to give carboxylic acids and sulfonic acid esters, has been reported[166]. The newly formed carboxylic acid can subsequently act as a reactive side for further crosslinking reactions. In particular, it may undergo alkylation by perchlorate esters via intermediate **34**, as confirmed by model reactions, which also demonstrate the concurrent formation of free perchloric acid.

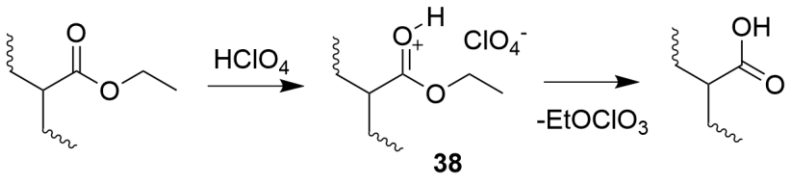

Scheme 29. Proposed mechanism of the carboxylic acid ester dealkylation by perchloric acid[137].

Such a sequence of transformations again results in the establishment of a crosslink when a 1,4-bisperchlorato-butane intermediate is formed. The formation of such an intermediate can be envisioned through the same mechanistic pathway that leads to the 1,4-butylene diester crosslink motif **35** (Scheme 28. Proposed pathways of the crosslinking reaction in the presence (bottom) and absence (top) of moisture (ClO4--anions as charge compensation for the acylium esters are not displayed)[137].). If this reaction occurs between two pCBA units, both the diester crosslink **35** and 1,4-bisperchlorato-butane are produced. The latter can, in turn, regenerate a pCBA unit through the elimination of an alkyl perchlorate or evaporate from the film. This dynamic equilibrium enables the redistribution of crosslinks throughout the polymer.

The observed mass loss during the curing process exceeds the theoretical value calculated under the assumption of exclusive volatilization of alkyl perchlorates from the polymer films (Table 3). As expected, the extent of mass loss correlates with the pCBA content (Figure 19c) as well as with the molecular mass of the alkyl side chain in the respective comonomer (Figure 19a). Moreover, the additional mass loss appears to scale with both the molecular weight of the comonomer and the corresponding onset temperature. Although this observation suggests that partial degradation of the polymer backbone may occur under the applied conditions, direct spectroscopic or analytical evidence for such a process remains limited.

Table 3. Calculated and actual weight loss after curing of copolymers of pCBA[137].

Comonomer	pCBA-content (mol%)	Expected loss of weight (%)[a]	Actual loss of weight (%)
MA	11	12,4	13
EA	10	11,4	15
BA	11	12,4	20

[a]For the elimination of the respective alkyl perchlorate while forming a butylene crosslink **35**.

The involvement of reactions associated with the formation or elimination of THF, which is presumed to be the primary cause of the additional mass loss, particularly at elevated temperatures especially when copolymers of pCBA and BA are cured, remains not fully understood. Nevertheless, it can be concluded that the initial alkylation steps leading to the intermediates **33** and **36** constitute key stages in the crosslinking mechanism, as both THF and alkyl perchlorates are released simultaneously from the heated polymers despite having considerable different boiling points: methyl perchlorate: 52°C[64], ethyl perchlorate: 89°C[64], butyl perchlorate: estimated 130°C, THF: 66°C (Figure 23Figure 24Figure 25). The observation that the onset of curing increases with longer alkyl side chains further suggests that the formation of intermediate **33** proceeds more slowly in sterically hindered systems. As a result, the competing pathway toward intermediate **36** becomes more favorable, potentially promoting partial degradation of the polymer matrix under these conditions.

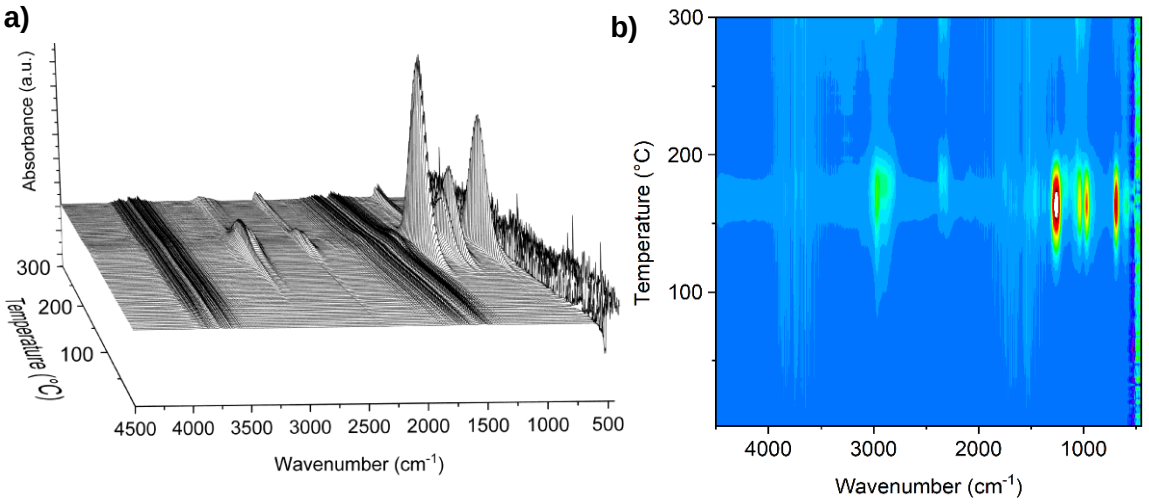

Figure 23. Beaded IR-spectra of emitted compounds recorded during the heating of P(MA-pCBA11); (a) 3D-view; (b) contour-image[137].

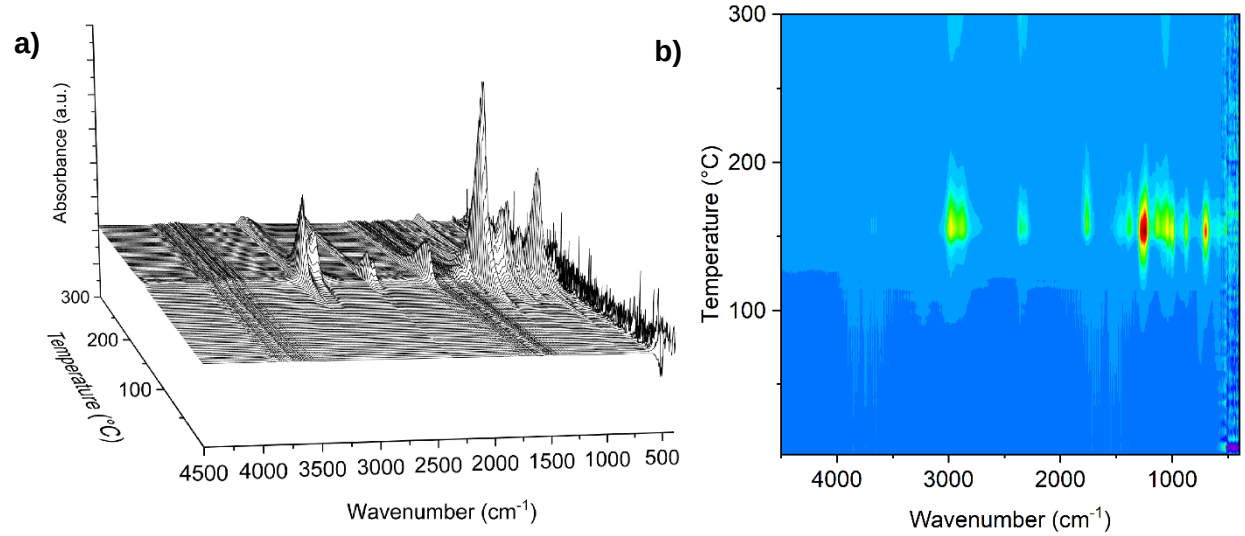

Figure 24. Beaded IR-spectra of emitted compounds recorded during the heating of P(EA-pCBA1); (a) 3D-view; (b) contour-image[137].

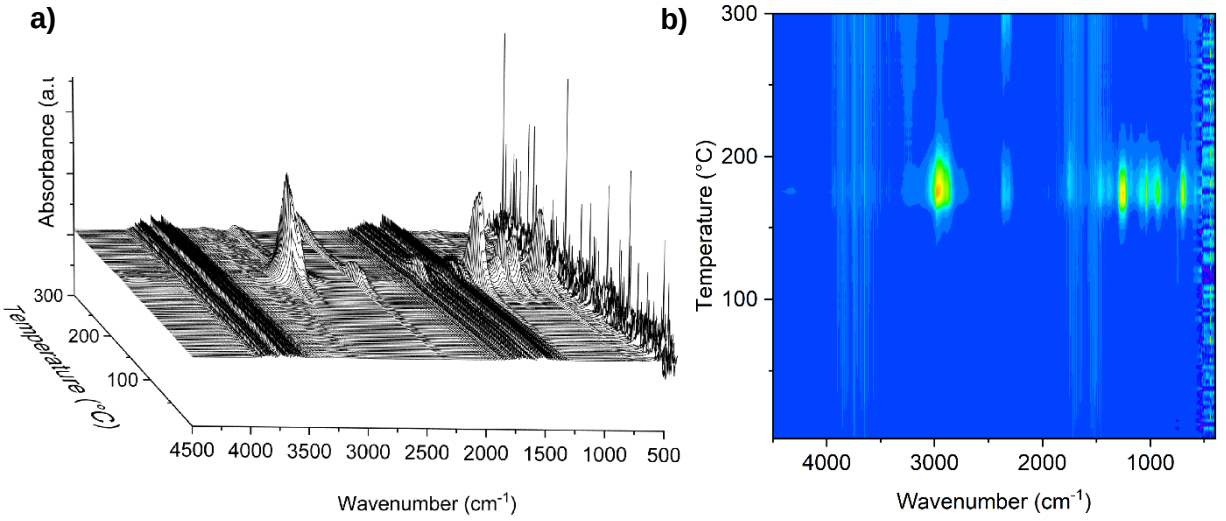

Figure 25. Beaded IR-spectra of emitted compounds recorded during the heating of P(BA-pCBA11); (a) 3D-view; (b) contour-image[137].

Notably, no THF is detected during the curing of P(MMA-pCBMA4), as characteristic THF signals are absent in both IR and NMR spectra. The reactivity of carboxylic ester groups in polyacrylates is known to depend strongly on steric factors, including substituents on the polymer backbone and neighboring monomer units[167]. In this case, the additional methyl substituent in the MMA-based copolymer likely imposes steric hindrance that suppresses the intramolecular reaction pathway responsible for THF formation.

5.1.6 Conclusion

Alkyl esters of perchloric acid were successfully incorporated into poly(meth)acrylates by copolymerization with 4-perchloratobutyl (meth)acrylate (pCBA/pCBMA). The resulting copolymers react with common nucleophiles and co-reactants such as amines, alcohols and nitriles. In the absence of these nucleophiles, pCBA copolymers exhibit self-crosslinking behavior upon thermal treatment between 105 and 135°C, forming robust thermoset materials. Solid-state and solution NMR studies revealed that the perchlorate ester moieties undergo transesterification reactions with carboxylic ester groups within the polymer, leading to the formation of a novel type of crosslink consisting of a 1,4-butylene unit connecting two ester functionalities. Complementary TGA-FTIR analyses confirmed the evolution of volatile alkyl perchlorates as by-products of this process. Their rapid evaporation from the polymer matrix shifts the equilibrium toward crosslink formation, thereby facilitating efficient curing. In addition to alkyl perchlorates, small quantities of THF were detected among the evolved gases, suggesting the presence of secondary reactions that generate carboxylic acid groups and possibly additional crosslinks of yet unidentified structure.

Compared to conventional crosslinks, the butylene diester crosslink represents an exceptionally non-polar linkage that integrates seamlessly into the polyacrylate backbone. The chemical reactivity of its ester groups is indistinguishable from that of the backbone esters, rendering the crosslink chemically inert under most conditions. Consequently, the crosslinked network provides excellent resistance to chemical attack, as the cleavage of all ester bonds would be required to disrupt the structure. This unique feature distinguishes the system from other known crosslinking chemistries for acrylic resins and opens up opportunities for application in the high-end-coatings industry where robust polyacrylates are required. Moreover, the formation of carboxylic acid groups during curing may enhance adhesion to metal substrates and improve the cohesive strength of the coating.

Despite these advantages, the system is not without significant limitations. The synthesis of pCBA requires the use of silver perchlorate, an expensive and explosive reagent, which makes large-scale production economically and logistically challenging. Handling of perchlorate-functionalized monomers and resins would require specialized safety training and strict operational protocols. In addition, the regulatory approval for such materials, particularly within the framework of the European Chemicals Agency (ECHA), appears uncertain due to the intrinsic hazards associated with perchlorates.

A further concern arises from the evolution of short-chain alkyl perchlorates and THF during the curing process. These compounds pose potential health and environmental risks: short-

chain alkyl perchlorates are known to be highly reactive alkylating agents with explosive properties and are suspected carcinogens, while THF has been classified by the International Agency for Research on Cancer (IARC) as a potentially cancerogenic (Group 2B) in 2017[168]. Moreover, the total mass loss of up to 20 wt% observed during curing is inconsistent with current ecological and economic sustainability targets.

To address these limitations, the subsequent chapter explores a catalytic version of the pCBA-based crosslinking system that retains most advantages while eliminating some of the major disadvantages.

5.2 Perchloric Acid, an Effective Catalyst for Thermosetting Self-Crosslinking Hydroxy Acrylic Resins

Parts of this chapter were published in: P. Wienefeld and G. A. Luinstra *J. Appl. Polym. Sci.* **2025**, e58087. (https://doi.org/10.1002/app.58087)

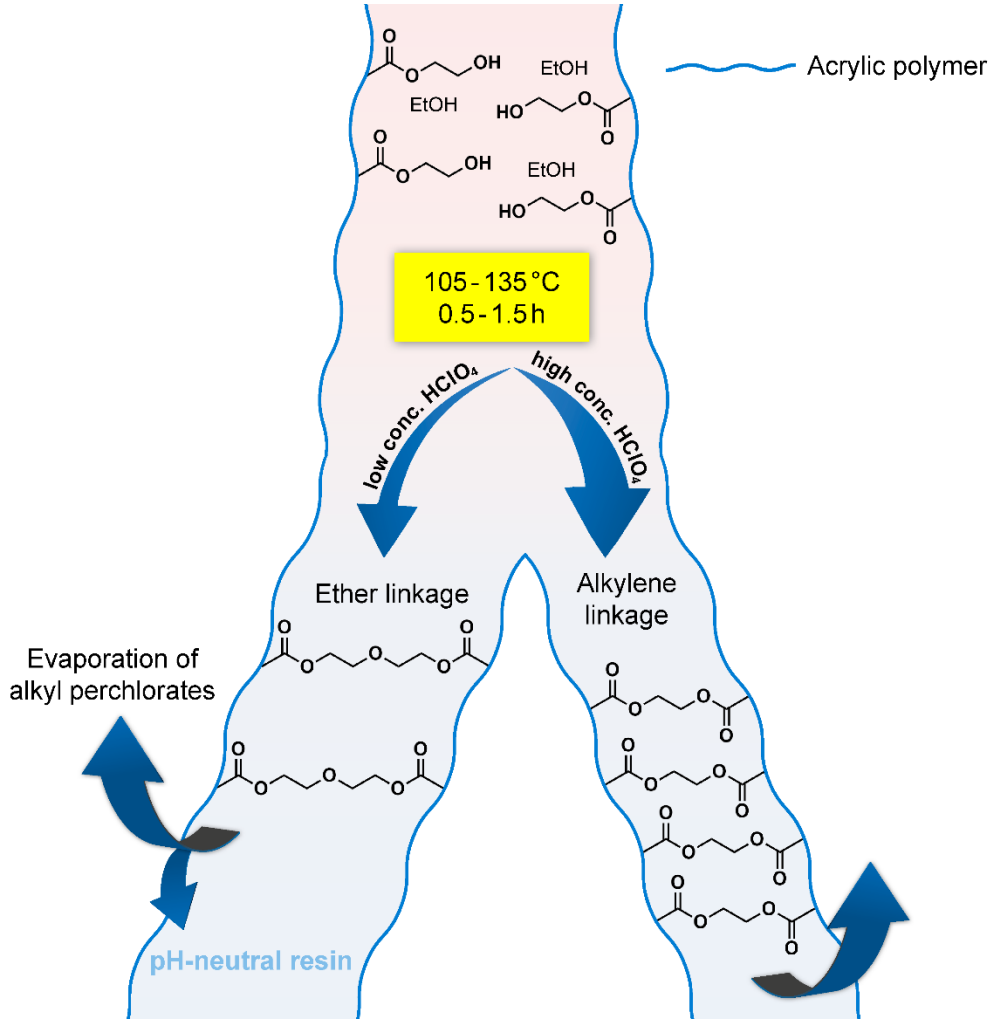

Scheme 30. Schematic illustration of the developed concept[169].

The crosslinking strategy presented in this chapter builds upon the published work presented in the previous chapter on thermosetting, self-crosslinking acrylic resins containing pCBA[137]. A simple thermal treatment of the resin was shown to induce a transesterification between perchlorate and alkyl ester groups, leading to the formation of robust butylene diester crosslinks accompanied by volatile alkyl perchlorates. However, the potential high production costs of the perchlorate monomer and associated health risks, particularly due to the release of substantial amounts of volatile alkyl perchlorates during curing, represent significant drawbacks to the practical application of such systems. In this chapter an improved concept is presented that retains the advantageous perchlorate chemistry but is considerably simpler in execution. The result again is a crosslinked binder with effectively no catalyst residues and expected similar properties.

The basic concept is the in-situ generation of a perchlorate ester via reaction of the binder´s hydroxyl functionalities with concentrated aqueous perchloric acid. Early work relevant to this concept includes the synthesis of ethyl perchlorate by treatment of ethanol with anhydrous perchloric acid in 1936[64] (Scheme 31). Although this reaction is not of any synthetic significance, it may be anticipated that an equilibrium exists in a mixture of alcohol and perchloric acid yielding some ethyl perchlorate, possible proceeding through the presumable intermediate: ethyloxonium perchlorate. Perchloric acid is a super acid ($pK_a \approx -15 \pm 2$[74]) and can be assumed to be substantially dissociated in hydroxyl-containing media. In a coating formulation, such an equilibrium would generate a binder containing a perchlorate moiety which, in principle, can undergo the crosslinking chemistry described above[137].

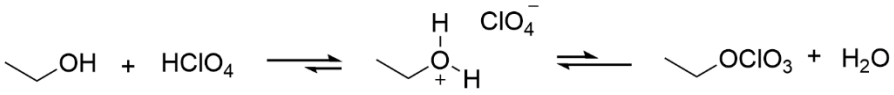

Scheme 31. Postulated equilibrium between ethanol/$HClO_4$ and ethyl perchlorate/H_2O[169].

Although the equilibrium may be shifted predominantly toward an intermediate oxonium salt, drying of the formulation and subsequent thermal treatment can increase the chemical potential of aqueous perchloric acid and thereby promote the in-situ formation of perchlorate ester. The perchlorate esters formed during solvent evaporation and heating are therefore expected to facilitate the anticipated crosslinking reactions such as transesterification[137] (Scheme 32).

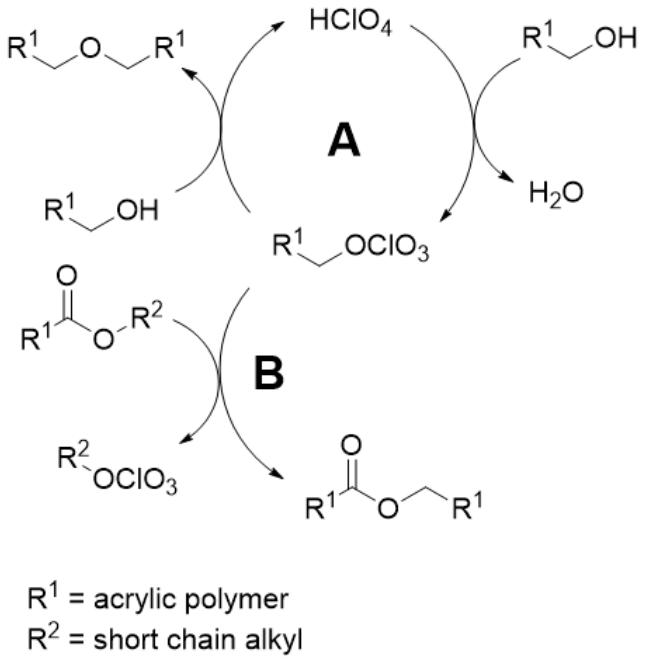

Scheme 32. Catalytic cycle for ether crosslink formation (A) and stoichiometric transesterification to alkene crosslink (B)[169].

The in-situ formation of perchlorate esters from alcohols creates a reaction environment in which an electrophilic carbon center (of the perchlorate ester) and nucleophilic hydroxyl groups coexist. Interaction of these species can give rise to ether linkages while regenerating perchloric acid (Scheme 32)[110,170]. Consequently, an acid-catalyzed condensation of primary alcohols constitutes an additional crosslinking pathway, a reaction that has been documented under the influence of various catalysts[171] including sulfuric acid[172] and hydrochloric acid[173]. Thus, in systems comprising hydroxyl-functional binders and perchloric acid, two principle crosslinking pathways may be operative: formation of ether bridges (pathway A) or formation of alkylene diester bridges via transesterification between perchlorate and alkyl esters (pathway B).

5.2.1 Synthesis of Polyacrylates and Coating Preparation

Hydroxy-functional acrylic copolymers based on EA and either HBA or HEA were synthesized at varying hydroxyl monomer contents. Specifically, EA-HBA copolymers containing 4.6, 7.6, and 14 mol% HBA, and EA–HEA copolymers containing 4.2, 7.5, and 13 mol% HEA were prepared via free-radical polymerization in toluene, using AIBN as an initiator.

Although toluene served as a suitable solvent for the polymerization reactions, ethanol represents a promising alternative due to its lower cost, higher environmental compatibility, and potential to simplify the overall process. The use of ethanol would not only improve the sustainability of the synthesis but also eliminate the need to remove the polymerization solvent prior to resin formulation, an aspect that could significantly streamline processing and enhance efficiency. However, this optimized approach was not investigated within the scope of the present study.

The resulting polyacrylates exhibited M_n between 26 and 34 kg mol^{-1}, polydispersity's in the range of 3.2-4.1, and number average hydroxy functionalities (f_n) from 12 to 43 (Table 4). For clarity, the copolymers are denoted as P_y(EA-HEAx) or P_y(EA-HBAx), where *x* refers to the molar fraction (mol%) of the hydroxy-functional comonomer within the repeating units, and *y* denotes the molar ratio of perchloric acid to hydroxyl groups in the corresponding curing formulation.

Table 4. EA-resins synthesized[169].

Entry	Crosslinker (mol%)	M_n (kg mol^{-1})	$Đ^a$	P_n^b	f_n^c
1	HBA 4.6	29	3.2	284	13
2	HBA 7.6	28	4.1	271	20
3	HBA 14	32	3.8	301	42
4	HEA 4.2	28	3.6	280	12
5	HEA 7.5	26	3.6	257	19
6	HEA 13	34	3.8	333	43

[a] Polydispersity $Đ$ (=$M_w M_n^{-1}$); [b]P_n degree of polymerization; [c]f_n hydroxy functionality per polymer chain.

Ethanol was selected as the application solvent for the resin formulations as it is inexpensive, dissolves the acrylic polymers and tolerates acidity. The large excess of ethanol is further anticipated to suppress premature formation of alkyl perchlorates by immediate solvation and stabilization of protonated species (e.g., $EtOH_2^+$ and H_3O^+). Concentrated perchloric acid was introduced into the ethanolic resin solutions as a commercially available aqueous solution (70 wt% $HClO_4$). The perchloric acid concentration in the ethanolic resin was varied

systematically from 0.6 mol% to 100 mol% with respect to the total number of hydroxyl groups present in the polyacrylate resin (i.e., relative to the mol% of HBA or HEA comonomer in the EA copolymers). Resin formulations were prepared predominantly as 25 wt% polymer solutions in ethanol. Homogeneous, optically clear mixtures were obtained for the polymer/ethanol solutions and for ternary mixtures of polymer, ethanol and aqueous perchloric acid, with miscibility maintained for resin loadings in ethanol up to at least 40 wt%.

The resin solution exhibited good storage stability: when maintained in glass vials at ambient temperature they showed no detectable changes in viscosity or discoloration over a 63-day period (Figure 26) and could be cured reproducibly after storage for up to five months. It is notable that the binary system of concentrated aqueous perchloric acid (70 wt%) and ethanol constitutes a manageable mixture in practical handling. This combination is, for example, routinely employed in metal electropolishing and etching protocols[68].

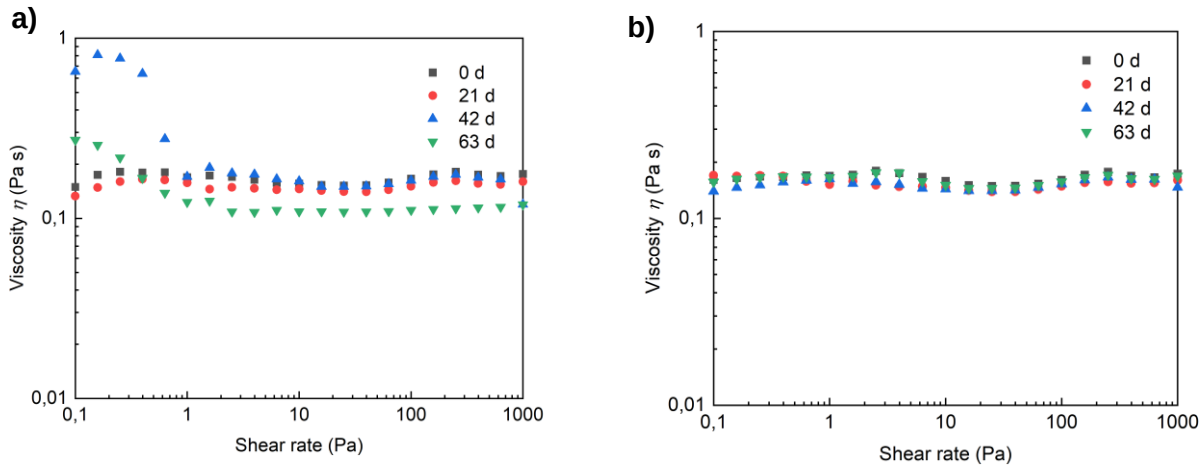

Figure 26. Viscosity curves of 25 wt% ethanolic solutions of (a) P_6(EA-HEA13) and (b) P(EA-HEA13) without perchloric acid[169].

5.2.2 Analysis of Crosslinking Process

Coatings were applied onto glass substrates using a self-made film coating bar (spreader) and were allowed to level and dry for five minutes at ambient temperature prior to thermal curing in a drying oven. The formulated hydroxy-functional polyacrylates cure to insoluble crosslinked networks within 1-3 hours at temperatures between 85°C and 105°C (Figure 27). Curing occurred both in the presence of stoichiometric and catalytic amounts of perchloric acid, whereas comparable formulations containing either non hydroxylated EA resins or hydroxyl-

functional resins without perchloric acid did not form crosslinked films. The resulting cured films were transparent and exhibited thicknesses in the range of 30 – 50 µm. HEA copolymers were completely colorless even with high amounts of perchloric acid, whereas those derived from HBA copolymers showed yellow discoloration that increased with the perchloric acid content in the formulation.

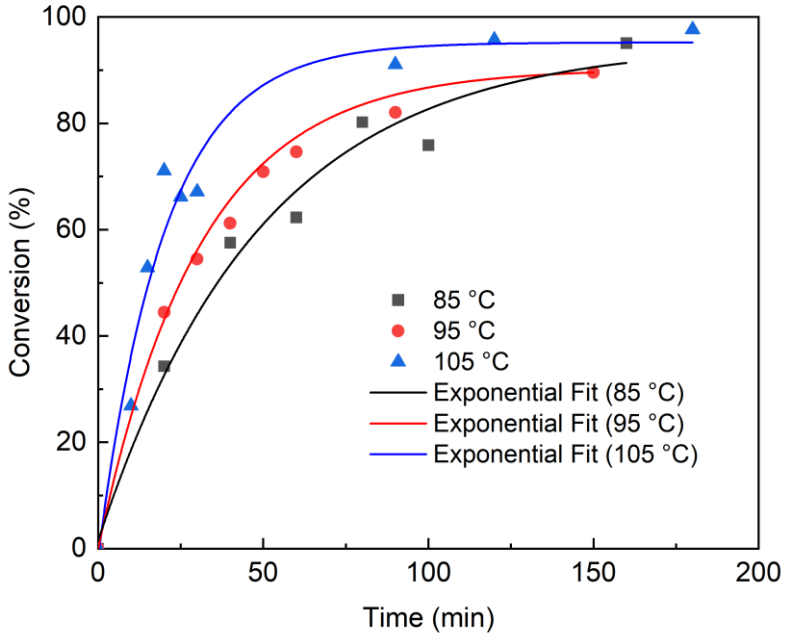

Figure 27. Conversion-time curves of P_3(EA-HEA7.5) cured at 85, 95 or 105°C[169].

Swelling studies in acetone revealed that the CDs of EA-HEA copolymers increase with HEA content and with perchloric acid concentration (Figure 28). Generally, EA-HEA copolymers exhibit higher CDs than the corresponding EA-HBA analogues, with only a small number of exceptions.

For the EA–HBA series, CDs increase with perchloric acid loadings in the range 1.5-12 mol% (expressed relative to the number of hydroxyl functionalities), however, at perchloric acid ratios above this interval the effective CD decreases (Figure 28b). This behavior is attributed to competing side reactions in HBA-containing systems that reduce efficiency of crosslink formation. The extent of these side reactions increases with perchloric acid concentration. The underlying chemistry remains unclear, although some hints were found, like the formation of carboxylic entities. The C4-alkyl perchlorate intermediate may undergo intramolecular reactions to generate THF and a perchlorate ester at the backbone, which remains present in the cured resin in the form of the hydrolyzed carboxylic acid product (vide infra). The longer

C4 side chain of HBA thus appears capable of engaging in additional “backbiting” or intramolecular pathways that are not accessible to the shorter C2-derived intermediates of HEA-containing resins. Comparable, unidentified side reactions for the pCBA-based system were discussed in the previously chapter and have been published[137].

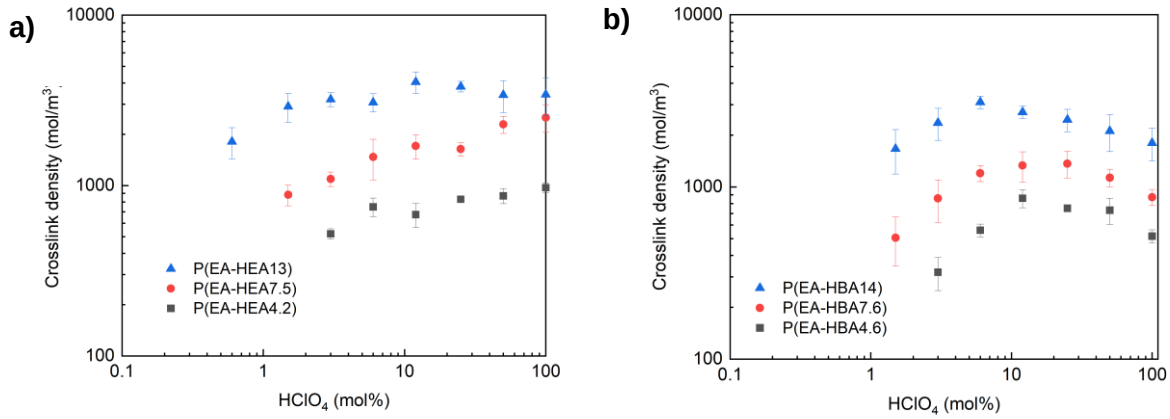

Figure 28. CD values of (a) P_y(EA-HEAx) and (b) P_y(EA-HBAx) thin films cured at 105°C for 6h from swelling measurements in acetone[169].

The minimum perchloric acid concentrations required to obtain a measurable insoluble network were determined as 0.6 mol% for P(EA-HEA13), 1.5 mol% for P(EA-HEA7.5) and 3 mol% for P(EA-HEA4.2). Formulations containing lower equivalents of perchloric acid produced tacky films that prevented reliable CD determination (large errors in Figure 28), likely because volatile alkyl perchlorates (e.g., ethyl perchlorate) formed and evaporated during curing, thereby depleting the active perchlorate species and terminating the crosslinking process.

ATR FTIR spectroscopy was employed to gain a more detailed understanding of the chemical transformations occurring during the curing process. As a representative example, uncured films of P/EA-HBA14) exhibited broad absorption bands in the range of 3700-3300 cm^{-1}, characteristic of hydroxyl stretching vibrations. Upon thermal treatment, these hydroxyl-associated bands diminished in intensity, while new bands emerged between 3300 and 2500 cm^{-1}, indicative of carboxylic acid functionalities (Figure 29). The appearance of these carboxylic species during the curing process suggests partial oxidation or rearrangement of intermediate structures. Although the absorption of carboxylic acids overlaps partially with that of hydroxyl groups, the sequential nature of their formation allows the initial consumption of hydroxyl functionalities to be clearly observed.

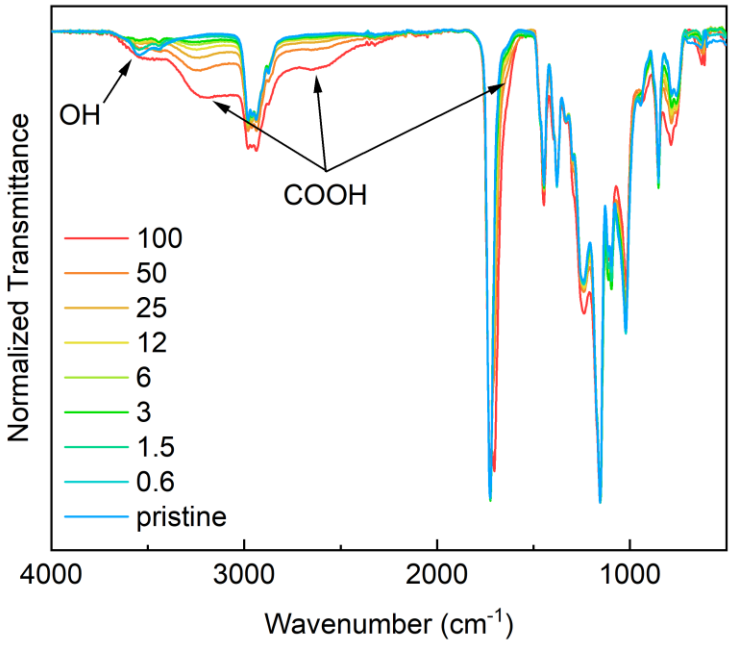

Figure 29. IR spectra of P(EA-HBA14) cured at 105°C for 6h with varies amounts of perchloric acid (normalized to the carbonyl vibration at 1155 cm^{-1})[169].

Quantitative evaluation of the curing process was performed by monitoring the absorbance intensity of the OH band at 3545 cm^{-1} relative to the carboxylic ester vibration at approximately 1155 cm^{-1} (Figure 30). Each data point corresponds to the normalized absorbance ratio of these two bands. From this analysis, it was determined that complete curing, defined as full consumption of hydroxyl groups, requires approximately 3 mol% perchloric acid for HEA copolymers and around 6 mol% for HBA copolymers. At perchloric acid concentrations below these thresholds, residual hydroxyl groups remain detectable in the cured films. These findings are consistent with the trends observed in swelling experiments, confirming the relationship between concentration of perchloric acid and CD.

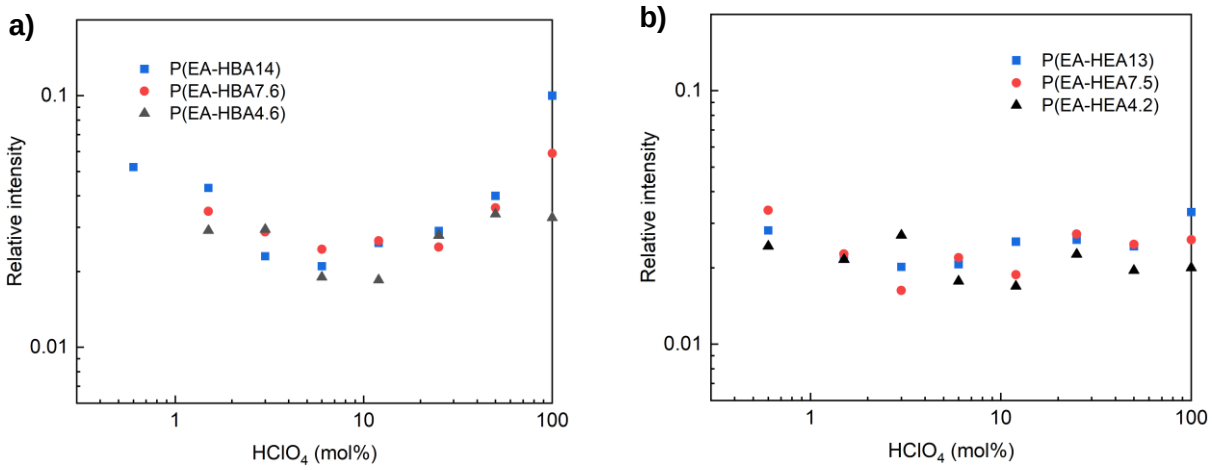

Figure 30. Relative OH band intensity at 3545 cm^{-1} of cured (a) P_y(EA-HBAx) and (b) P_y(EA-HEAx) (6h, T = 105°C)[169].

At acid concentrations >12 mol%, especially in HBA copolymers, intensities of bands attributed to carboxylic acids complicate further analysis. Consequently, the minima in the trends were taken to represent the minimum perchloric acid concentration required for complete curing under the applied conditions.

5.2.3 Thermal Properties of the Cured Resins

The thermal properties of the cured coatings were found to depend strongly on the perchloric acid concentration employed during curing, reflecting variations in the resulting network structure and crosslinking pathway. DSC analysis revealed that the T_gs of the resins increase progressively with increasing perchloric acid content (Figure 31). Resins cured in the presence of 100 mol% perchloric acid exhibited the highest T_g values, indicative of the formation of particularly dense network structures. The dependence of T_g on perchloric acid concentration was most pronounced for copolymers with higher hydroxyl contents, as reflected by the steepest slopes in Figure 31. These differences cannot be attributed solely to variations in the extent of hydroxyl group conversion, since curing was complete in most cases, but rather to changes in the predominant crosslink mechanism.

.

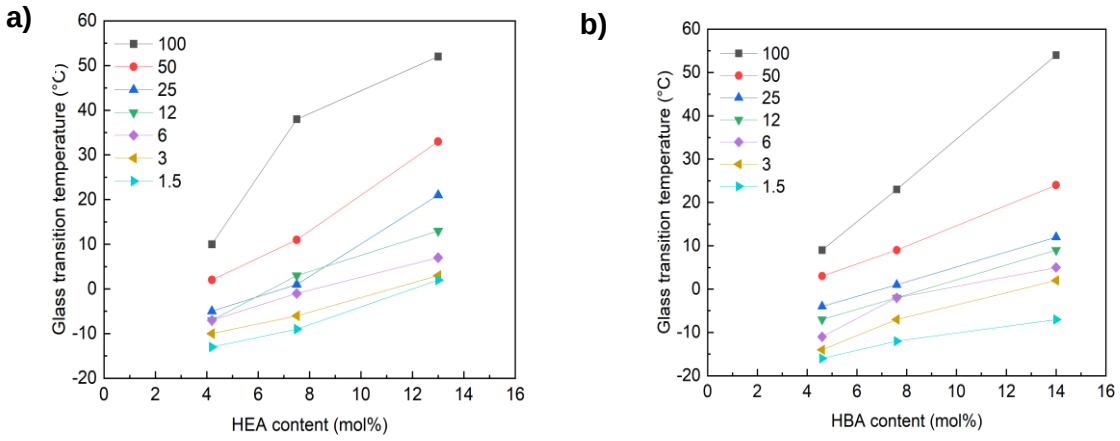

Figure 31. T_g of cured (a) P_y(EA-HEAx) and b) P_y(EA-HBAx), y reaching from 1.5 to 100 mol%, 6h of curing at 105°C[169].

The observed increase in T_g is attributed to both enhanced crosslink formation and the concurrent generation of carboxylic acid groups during curing. The distribution and type of crosslinks significantly influence the thermal response of the polymer network. Shorter alkylene bridges, for example, are expected to yield a more rigid and higher T_g structure than longer or more flexible linkages. Additionally, the contribution of in-situ formed carboxylic acids should not be neglected. According to the Fox equation, incorporation of as little as 5 mol% AA-units into PEA can increase the T_g by approximately 5°C, based on reported values of T_g(PEA) = −21°C[155] and T_g(PAA) = 109°C[160]. This effect likely contributes to the T_g elevation observed in perchloric acid cured systems, where partial oxidation or rearrangement reactions yield carboxylic acid functionalities within the polymer network.

5.2.4 Identification of Crosslink Motives and Side Reactions

To gain deeper insight into the structural characteristics of the cured resins, extensive analytical efforts were undertaken to elucidate the nature and type of crosslinks formed during curing. From these investigations, an averaged structural description of the polymer networks could be derived. However, the precise identification of crosslink types proved challenging for EA-based systems. In particular, the characteristic resonances of the ethyl moiety complicate the interpretation of solid-state NMR spectra, as the methylene signal of the ethyl group appears in the same chemical shift region as that of the potential crosslinker entities, whereas the methyl ester resonance is clearly separated at ~52 ppm.

To overcome this limitation, structurally analogous copolymers based on MA were synthesized and investigated, as these materials exhibit simpler NMR spectroscopic signatures due to the absence of the ethyl substituent. In contrast, BA–based cured resins formed cohesive, highly crosslinked powders that tended to flow and aggregate at operating temperatures, thereby hindering solid-state NMR characterization. Nevertheless, these resins can be prepared via the same synthetic route and exhibit higher T_gs, while being amenable to crosslinking under the same conditions. Accordingly, copolymers of MA with HEA and HBA were selected as model systems and cured using both stoichiometric (100 mol%) and catalytic (12 mol%) quantities of perchloric acid to facilitate a more detailed structural analysis.

The crosslink structures formed in the cured copolymers were identified by ^{13}C CP MAS NMR spectroscopy. The spectrum of cured P_{100}(MA-HEA16) revealed a distinct new resonance at 63 ppm, accompanied by a weak shoulder at approximately 181 ppm (Figure 32a). This resonance is assigned to methylene carbons within ethylene diester (alkylene) crosslinks. The assignment is supported by the spectrum of a separately prepared reference polymer, poly(MA-*co*-ethylene glycol diacrylate) (P(MA-EDGA)), which exhibits an identical signal (Figure 32b). Additional peaks in the P(MA-EDGA) spectrum arise from terminal acrylic double bonds of mono-inserted crosslinker units.

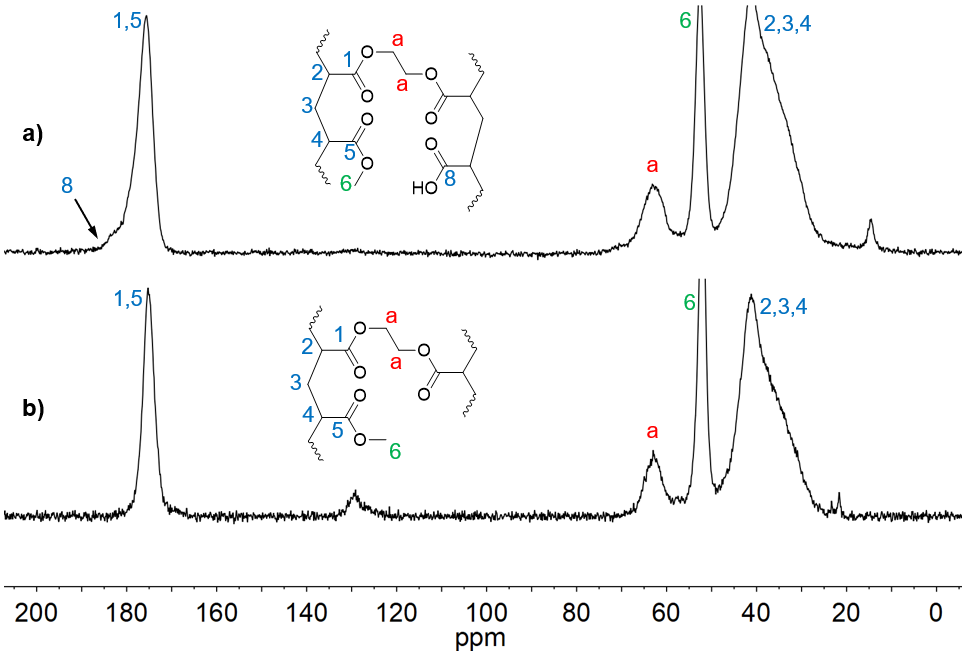

Figure 32. ^{13}C CP MAS NMR spectrum of cured (a) P_{100}(MA-HEA16) and (b) P(MA-EGDA15)[169].

Varying the perchloric acid concentration was found to influence the type of crosslinks formed in the HEA copolymers. The spectrum of P_{12}(MA-HEA16), cured with a catalytic amount of

perchloric acid (12 mol%), display two new resonances at 69 ppm and 63 ppm (Figure 33a). A reference copolymer, poly(MA-*co*-diethylene glycol diacrylate) (P(MA-DEGDA)), exhibits the same two resonances (Figure 33b), confirming the presence of diethylene crosslinks. It is also found that the relative intensities of these resonances differ between P_{12}(MA-HEA16) and P(MA-DEGDA), consistent with the assumption that both linkage types coexist in the cured HEA-based networks. These findings demonstrate that the crosslink mechanism in HEA copolymers is strongly influenced by the perchloric acid concentration, with higher acid level favouring shorter ethylene diester bridges and lower concentrations yielding mixed linkage structures.

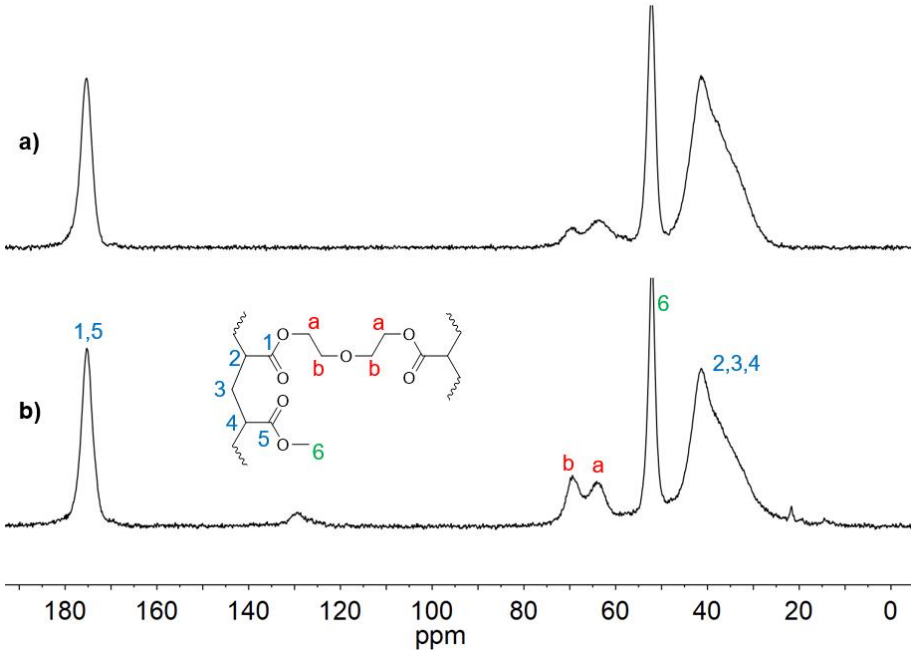

Figure 33. ^{13}C CP MAS NMR spectrum of cured (a) P_{12}(MA-HEA16) and (b) P(MA-DEGDA15)[169].

Curing of the P(MA-HBAx) copolymers, in contrast, appears to generate predominantly butylene diester crosslinks. The ^{13}C CP MAS NMR spectrum of cured P_{100}(MA-HBA14) exhibits resonances at 65 ppm and 25 ppm, which correspond closely to those observed in copolymers of EA and BDDA (Figure 34a,c). A weak resonance at 15 ppm detected in the spectrum of $P_{100/12}$(MA-HBA14) suggests the presence of ethyl groups, likely formed through transesterification between ethanol (used as solvent) and methyl acrylate esters[137]. Owing to a generally lower signal-to-noise ratio, these spectra must be interpreted with caution. Nevertheless, the main resonances provide strong evidence for butylene diester linkage formation.

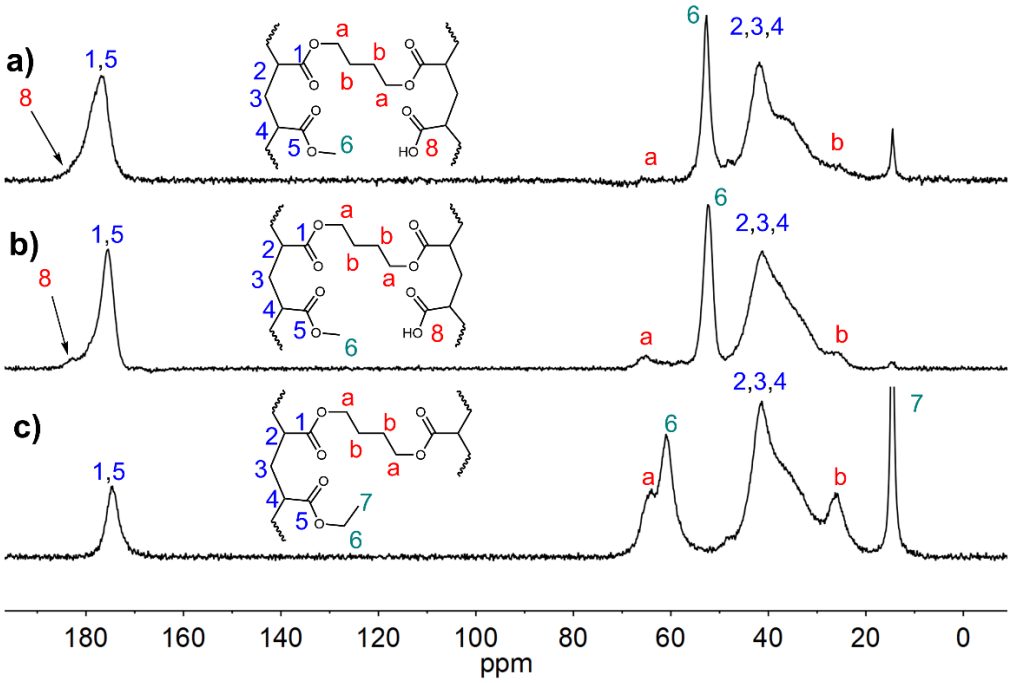

Figure 34. ^{13}C CP MAS NMR spectrum of cured (a) P_{100}(MA-HBA14), (b) P_{12}(MA-HBA14) and (c) P(EA-BDDA)[137].

At catalytic perchloric acid concentrations, HBA copolymers also form the same crosslinks with minor variations. The spectrum of cured P_{12}(MA-HBA14) shows the same characteristic resonances at ~65 ppm and 25 ppm, along with additional weak features in the same spectral regions (Figure 34b). These findings suggest that besides the butylene diester crosslink minor amounts of alternative linkages/structures may have formed.

The spectroscopic data of the cured HEA and HBA copolymers provide clear evidence for the formation of carboxylic acid functionalities during curing. In both systems, a distinct shoulder on the ester carbonyl resonance at approximately 181 ppm was observed in the ^{13}C CP MAS NMR spectra (e.g., for cured P_{100}(MA-HEA16) and P_{100}(EA-HBA14), Figure 32,Figure **35**), consistent with the appearance of carboxylic acid bands in the corresponding IR spectra (Figure 29). The extent of carboxylic acid formation in EA copolymers exhibits a weak positive correlation with perchloric acid concentration, becoming particularly noticeable in formulations with stoichiometric ratios (Figure 36). The formation is attributed to acid-induced dealkylation, effectively a hydrolysis of alkyl esters by perchloric acid and water, or a transesterification reaction between perchloric acid and ethyl esters, which may gain importance at later curing stages. Both ester hydrolysis and transesterification with ethanol are expected to occur within the resin matrix and are expected to become more pronounced at high perchloric acid concentrations.

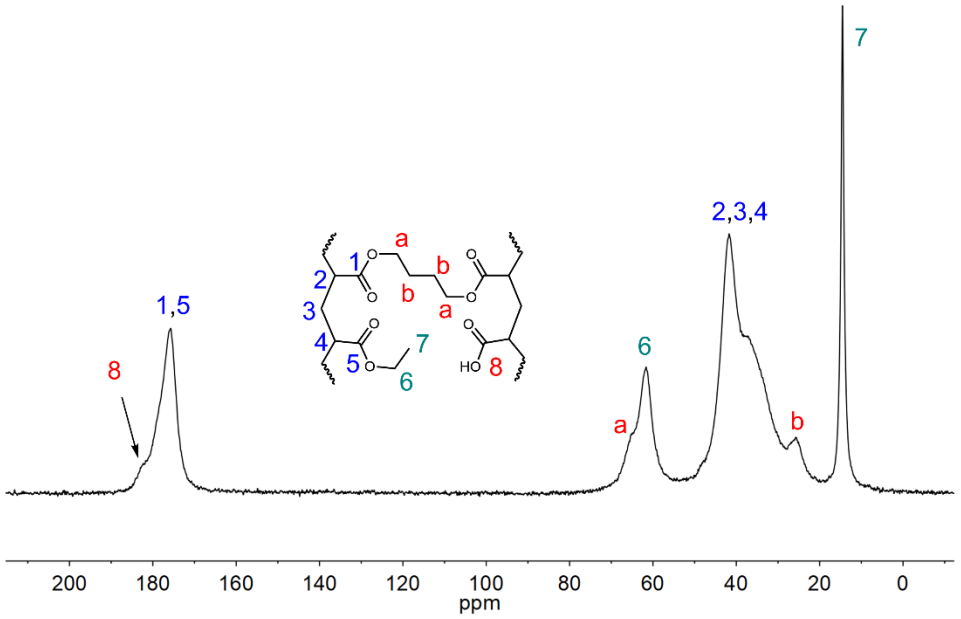

Figure 35. ^{13}C CP MAS NMR spectrum of cured P_{100}(EA-HBA14)[169].

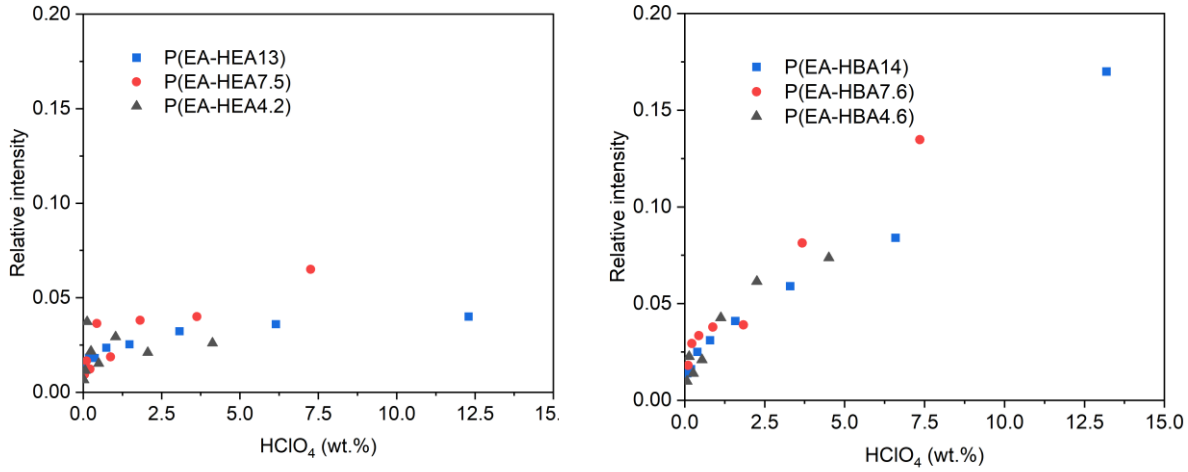

Figure 36. Relative COOH band intensity at 3250 cm^{-1} of cured (a) P_y(EA-HEAx) and (b) P_y(EA-HBAx), 6h of curing at 105°C (the amount of $HClO_4$ is given relative to the weight of the polymer)[169].

Furthermore, the formation of carboxylic acids is significantly more evident in HBA copolymers than in their HEA analogues. The elimination of THF from the butyl hydroxyl moiety via an intramolecular transesterification mechanism, as suggested for the pCBA-based system, may be a key factor, or alternatively by a neighbouring-group-assisted mechanism. Both would generate additional carboxylic functionalities within the polymer network.

The addition of more water to the resin solutions was found to have no measurable influence on the formation of carboxylic acids and CD. The direct relationship between the amount of added aqueous perchloric acid and the extent of carboxylic acid formation in the cured resins

has already been demonstrated (Figure 36). Since the curable acrylic resins are formulated with aqueous perchloric acid, all coating solutions contain small amounts of water, which could, in principle, contribute to carboxylic acid formation. To evaluate the influence of water a series of experiments was conducted using the standard formulations P_6(EA–HEAx), to which increasing amounts of water (10×, 100×, and 1000× the calculated water content of the standard mixture) were added. IR spectra of the cured films showed that the relative band intensities at 3250 cm^{-1} remained constant between 0.01 and 0.04 independent of the amount of added water (Figure 37a), demonstrating that additional water in the formulation does not affect carboxylic acid formation. Swelling experiments further corroborate these findings, showing an unchanged CD even at a 1000-fold increase in water content (Figure 37b). In fact, water and ethanol form an azeotrope and evaporate simultaneously from the film prior to the onset of crosslinking as TGA-MS experiments confirm.

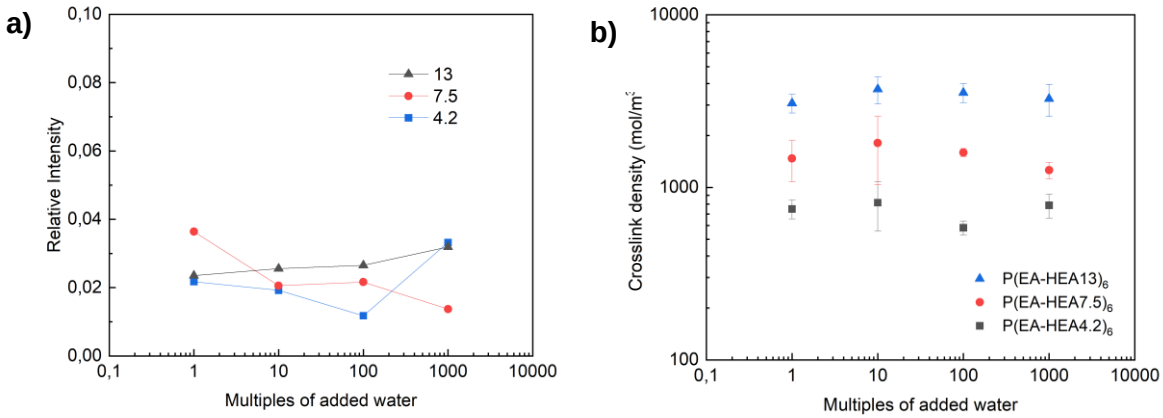

Figure 37. (a) Relative COOH band intensities at 3250 cm^{-1} of cured P_6(EA-HEAx) formulated with various amounts of H_2O; (b) CD values of cured P_6(EA-HEAx) formulated with various amounts of H_2O. Curing conditions: 6h at 105°C[169].

5.2.5 Description of the Curing Process

The curing process starts with the evaporation of ethanol and water. Several azeotropes are present indicating co-evaporation of these compounds. $HClO_4$ is not detected in the mass spectra of the released gases and therefore remains largely in the film. As ethanol and water are removed, the concentration and chemical potential of perchloric acid (boiling point >100°C[174]) increase. With the loss of solvent, perchloric acid interacts more strongly with the hydroxyl groups of the resin (Scheme 31). This shifts the equilibrium between the hydroxyl

groups (**39a/b**) and perchloric acid toward the formation of perchlorate ester (**40a/b**), accompanied by the release of water (Scheme 33).

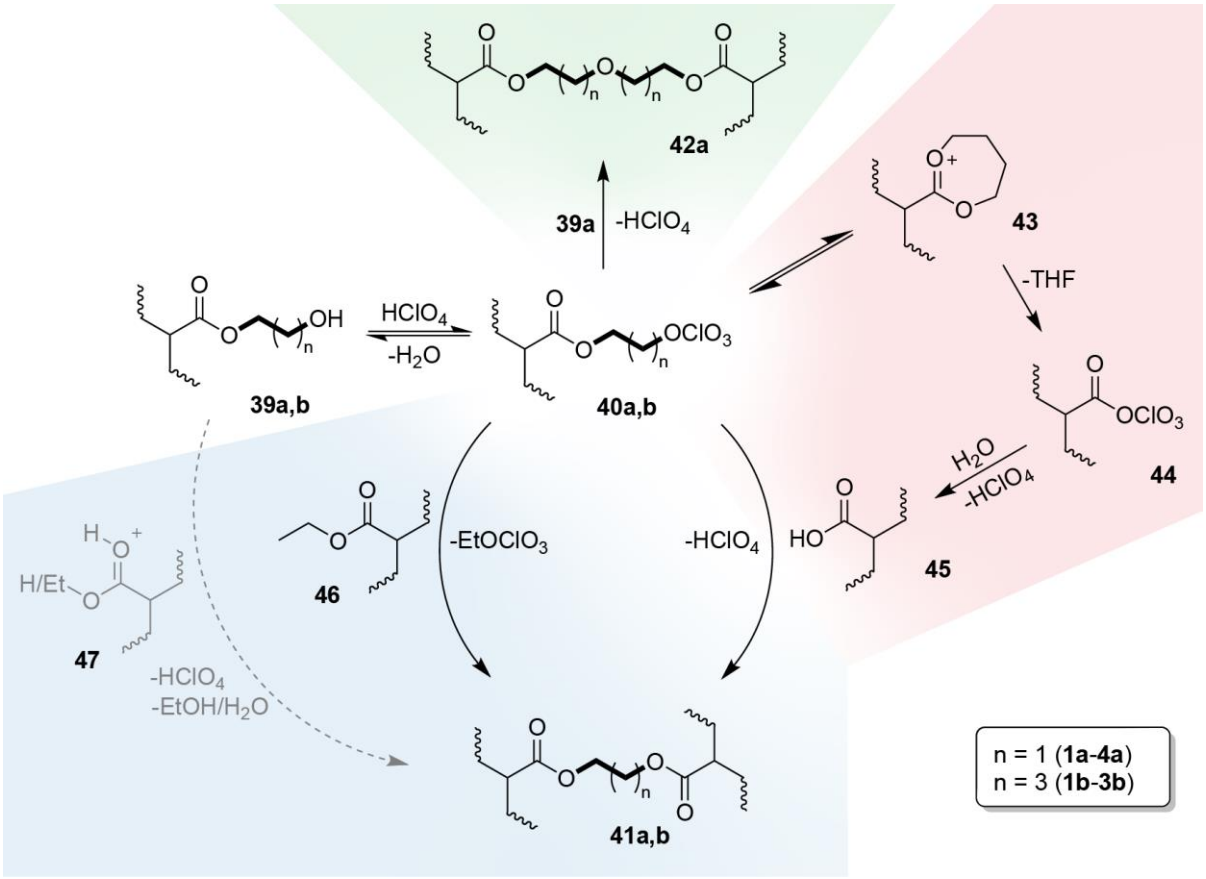

Scheme 33. Reaction pathways in the curing of HEA and HBA copolymers; green underlay: Reaction to ether crosslinks; blue underlay: (Trans)esterification (center/right) and Fischer-Speier-type (trans)esterification (gray text) to ethylene diester crosslink; red underlay: THF expulsion and carboxylic acid formation[169].

The intermediate perchlorate ester **40a/b** reacts preferably with the most nucleophilic functional group in its immediate vicinity. Specifically at low perchloric acid concentrations, ether formation is explained by nucleophilic attack of hydroxyl groups of HEA units (**39a**) in HEA copolymers on the perchlorate ester intermediate. The etherification step regenerates perchloric acid and thus shows the catalytic character of $HClO_4$. The sequence can propagate as long as chain mobility and a sufficient local concentration of hydroxyl groups are maintained. Propagation is impeded once a dense network restricts molecular motion or hydroxyl sites become scarce (Scheme 33, green pathway).

Mechanistically, the reaction corresponds to an acid-catalyzed condensation of two primary alcohols, a type of transformation that is known from the curing of MF resins[175]. Many electron-rich alcohols are activated by relatively weak acids (e.g., carboxylic[50] or sulfonic acids[176]),

whereas perchloric acid is sufficiently strong to promote etherification even of less nucleophilic (electron-poor) alcohols at temperatures compatible with thermosetting.

Alkylene diester crosslink formation becomes increasingly favored at higher perchloric acid concentrations. With higher perchloric acid loadings, the steady-state concentration of perchlorate ester **40a/b** is higher whereas the local concentration of free hydroxyl groups is reduced. Consequently, curing proceeds more rapidly and chain mobility is restricted much earlier. Under these conditions the carboxylic ester group of the acrylate backbone (or carboxylic acid entities formed in-situ) can act as a competing nucleophile. In analogy to the mechanism proposed in the previous chapter for pCBA-based acrylic resins[137], the perchlorate ester **40a/b** reacts with such ester functions to afford alkylene diester crosslinks (**41a/b**) with concomitant formation of volatile alkyl perchlorate (Scheme 33, blue pathway).

The volatility of the alkyl perchlorate leads to two important consequences. First, evaporation of the alkyl perchlorate from the film renders the transesterification effectively irreversible and thus “locks in” the newly formed alkylene crosslink. Second, loss of volatile perchlorate species can deplete active perchlorate in the film and thereby terminate further crosslinking if evaporation is substantial. The identity of the evaporating alkyl perchlorate is determined by the ester substituent of the copolymer: ethyl perchlorate is expected (and observed) from EA copolymers, whereas methyl perchlorate is formed from MA copolymers.

The formation of ethyl perchlorate during curing constitutes direct evidence for transesterification between a perchlorate ethyl ester and an ethyl ester. To verify this, volatile species evolved during thermal treatment of P_{100}(EA-HEA13) and P_{100}(EA-HBA14) were collected: the formulations were heated to 200°C under dynamic vacuum while a dry N_2 stream carried the off-gases into a liquid-nitrogen cold trap. Analysis of the condensates by ^{1}H NMR revealed each a characteristic quartet at 4.62 ppm (Figure 38. ^{1H} NMR spectra of emissions trapped during the curing of (a) P100(EA-HBA14) and (b) P100(EA-HEA13)[169].), which is consistent with ethyl perchlorate and thus supports the proposed transesterification pathway.

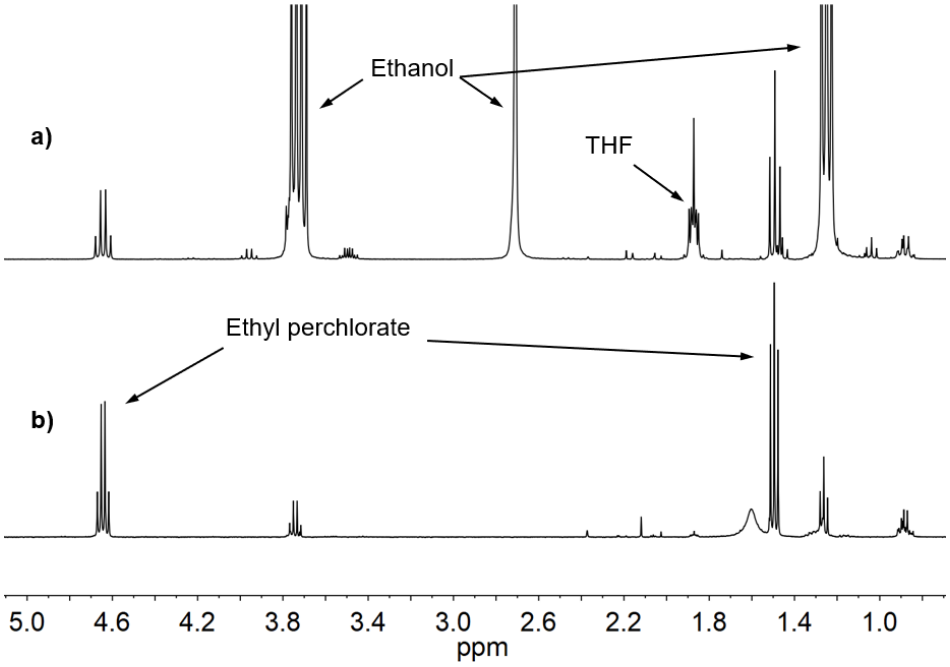

Figure 38. ^{1}H NMR spectra of emissions trapped during the curing of (a) P_{100}(EA-HBA14) and (b) P_{100}(EA-HEA13)[169].

TGA-MS analysis of formulated P_{100}(EA-HEA13) and P_{100}(EA-HBA14) resins confirms the evolution of volatile ethyl perchlorate during the curing process. TGA traces show a major mass loss of approximately 70% between 25 and 100°C, which is assigned to evaporation of ethanol (M_r = 46 Da) and water (Figure 39). A second mass loss event, commencing at ~100°C and persisting to ~200°C, correlates in the MS-data with signals attributable to ethyl perchlorate (*m* of 128 Da). Although the intact molecular ion of ethyl perchlorate was not observed, two characteristic fragment ions were detected: *m*/*z* = 127, resulting from hydrogen radical abstraction $[M\text{-}H]^+$, and *m*/*z* = 113, resulting from methyl-radical abstraction $[M\text{-}CH3]^+$. Each of these fragments is accompanied by the corresponding ^{37}Cl isotope peaks at *m*/*z* = 129 and 115, respectively, with the chlorine-typical intensity ratio of ca. 3:1, supporting the assignment to chlorine-containing perchlorate-derived species. Evolved CO_2 (*m* = 44 Da) and additional pyrolysis fragments consistent with decomposition of perchlorate esters were also detected. In the case of HEA copolymers, further volatile products such as AA and ethyl vinyl ether (both $M_r \approx 72.1$ Da) were detected. The latter likely arises from a reaction between ethanol and ethyl perchlorate and shows predominantly fragment ions at *m*/*z* = 43 and 44.

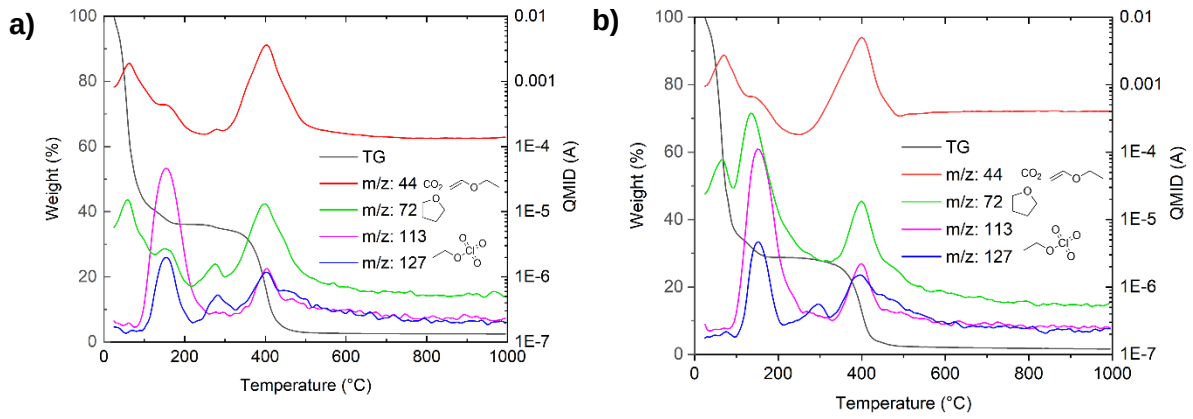

Figure 39. TGA curves (black line) of (a) P_{100}(EA-HEA13) and (b) P_{100}(EA-HBA14), and intensity-temperature profiles for formed volatiles[169].

During the curing of P(EA-HBA) copolymers, volatile compounds are formed that contain not only ethyl perchlorate but also THF (*m* = 72 Da) (Figure 38Figure **39**b). The formation of THF had previously been observed in the curing of copolymers of EA and pCBA (Figure 21Figure **22**)[91]. This can be explained by an intramolecular transesterification of a 4-perchloratobutyl moiety via dioxolenium perchlorate **43**, leading to the formation of THF and acylium perchlorate **44** (Scheme 33, red section), a reactive intermediate. The simultaneous detection of a compound with the mass of THF together with ethyl perchlorate strongly suggests that a butylene perchlorate intermediate is formed in the process. It is known that this intermediate reacts with ethyl carboxylic esters of the acrylic backbone to produce ethyl perchlorate and a butylene diester crosslink. The acylium perchlorate **44** can either react directly with a hydroxyl group of an HBA unit, forming the corresponding butylene crosslink, or it can hydrolyze to yield a carboxylic acid and free $HClO_4$. In contrast, the expected formation of ethylene oxide during the curing of HEA copolymers could not be confirmed. Neither the characteristic singlet in the ^{1}H NMR spectrum at 2.54 ppm[177] nor the expected mass spectral signals (*m*/*z* = 15, 29, 44[178]) were observed.

Both types of cured resins exhibit no measurable weight loss up to 250°C (Figure 39). A further decrease in mass of about 5-8% occurs between 250°C and 320°C. In this temperature range, several unidentified compounds with molecular masses of 55, 99, 127, 143, 155, and 256 Da were detected. The increased signal intensity corresponding to a mass of 127 Da cannot be attributed to ethyl perchlorate, as no signal of its known decomposition product, methyl perchlorate (*m* = 113 Da), was observed. Any free perchloric acid remaining in the film after crosslinking is capable of dealkylating carboxylic esters, leading to the evaporation of an alkyl

perchlorate. This reaction ensures that all perchlorate species are ultimately removed from the polymer film. When the cured resins were immersed in water for several days, no change in pH was detected, indicating the absence of residual acidic species. The continuous mass loss observed from approximately 350°C onward is attributed to the general decomposition of acrylic polymers[161].

Alternatively, alkylene bridges may form by a Fischer-Speier type esterification or by transesterification (Scheme 33, blue section). Early in the curing process, the incremental loss of water and ethanol promotes interaction of perchloric acid with the next most polar entities in the resin, possibly carboxylic esters. This situation represents an inverse Fischer-Speier process: attack of acid on the ester can lead to hydrolysis and thus to formation of carboxylic acids, with concurrent release of ethanol (for EA-based resins) or methanol (for MA-based resins). The resulting protonated carboxylic acid **47** can then react with a hydroxyl group in HEA or HBA copolymers to form an alkylene diester crosslink via a Fischer-Speier esterification. In HBA-containing resins, the acylium perchlorate intermediate will also react with water to yield a protonated carboxylic acid. That protonated species may be converted into neutral carboxylic acids (**45**), which are reasonably good nucleophiles and can themselves react with perchlorate esters to form an alkylene diester crosslink or remain unreacted within the cured resin.

The unequivocal detection of ethyl perchlorate indicates that alkyl perchlorates are formed readily during curing, and because Fischer-Speier (trans)esterification reactions are generally slow, the perchlorate intermediates seem of higher relevance. Replacing perchloric acid with other strong Brønsted acids such as sulfuric acid or triflic acid also yields crosslinked resins, however, these alternatives produce films that suffer pronounced discoloration, and catalyst residues or their esterified derivatives remain in the film after curing because the corresponding esters are either not volatile enough or not formed at all. The resulting materials are hygroscopic and therefore susceptible to accelerated degradation[21,48,136]. In contrast, weaker acids such as carboxylic or phosphoric acids are ineffective: they are too weak to catalyze etherification or transesterification within the film under the curing conditions. These observations emphasize the particular role of perchloric acid and its organic esters: an electrophilic, reactive intermediate is generated in-situ that can attack esters, acids, and hydroxyl groups, a volatile side product that carries away the remnants of the strong acid is lost from the resin, and, under the applied curing conditions, neither perchloric acid nor the formed alkyl perchlorates appear to oxidize the polymer.

5.2.6 Description of the Network Formation

The central assumption in the formation of the polymer network is the reactivity of the initially generated perchlorate ester, which is located at the terminal position of an ethyl linker in HEA copolymers and a butyl linker in HBA copolymers. The competition between the reactions of this perchlorate ester with either hydroxyl or ester groups fundamentally determines the relative proportion of ether and alkyl crosslinks (Table 5). The reaction rates for ether and ester formation differ, whereas the combined amount of hydroxyl and perchlorate groups remains constant, provided that decomposition of the C2 or C4-linker motives is negligible. The ratio of perchloric acid linking to hydroxyl entities is higher at higher perchloric acid concentrations. Consequently, the formation of alkylene diester crosslinks is favored under conditions of high catalyst concentration.

The curing process can be regarded as a batch reaction in which the reaction conditions continuously change over time. The crosslinks formed at the early stages are likely to play a decisive role in the overall network development. A high initial conversion rate may produce small domains with a high local concentration of short crosslinks between individual polymer chains, resulting in localized gelation and the formation of dense, macroreticular structures. These early crosslinks restrict the mobility of the chains within defined regions, where subsequent formation of additional alkylene linkages through reactions involving the continuously generated alkyl perchlorates further increases local density within the cured resin. As crosslinking progresses, the developing network incorporates both longer chain segments and shorter after full conversion of the hydroxyl groups. The resulting reduction in chain mobility leads to a pronounced increase in the T_g, yielding a comparatively rigid resin with a high T_g. This behavior is observed for both HEA and HBA copolymers. A slower initial conversion of the hydroxyl groups promotes a more uniformly distributed ether linkage dominated crosslinking, leading to a more open network with greater segmental mobility between crosslinking points and, consequently, a significantly lower T_g. The dependence of network structure on reaction rate is well established, for example, in resorcinol-formaldehyde and silica-based systems, and is supported by theoretical analysis[123,179].

Table 5. Data on cured EA-HEA and EA-HBA copolymers[169].

Entry	Polymer	CD (exp.) (mol m^{-3})	CD (calc. ether) (mol m^{-3})	CD (calc. ester) (mol m^{-3})	Theoretical ether/alkylene ratio	M_c (exp.) (kg mol^{-1})
1	P(EA-HEA4.2)$_{100}$	970	470	940	0:100	1.1
2	P(EA-HEA4.2)$_3$	520	470	940	82:18	2.1
3	P(EA-HEA7.5)$_{100}$	2500	850	1700	0:100	0.45
4	P(EA-HEA7.5)$_3$	1100	850	1700	55:45	1.0
5	P(EA-HEA13)$_{100}$	3400	1500	2900	0:100	0.33
6	P(EA-HEA13)$_3$	3200	1500	2900	0:100	0.35
7	P(EA-HBA4.6)$_{100}$	520	500	1000	92:8[a]	2.2
8	P(EA-HBA4.6)$_6$	560	500	1000	79:21 [a]	2.0
9	P(EA-HBA7.6)$_{100}$	870	850	1700	96:4 [a]	1.3
10	P(EA-HBA7.6)$_6$	1200	850	1700	42:58 [a]	0.93
11	P(EA-HBA14)$_{100}$	1800	1600	3100	79:21 [a]	0.62
12	P(EA-HBA14)$_6$	3100	1600	3100	4:96	0.36

[a]Observed dealkylation to carboxylic acid entities was not accounted for, leading to substantially higher theoretical ether linkage formation numbers.

The identification of the dominant crosslinking patterns as a function of perchloric acid concentration makes it possible to calculate the CD as a function of the hydroxyl functionality of the resin. Assuming that the types of crosslinks formed in MA- and EA-based resins are comparable, theoretical values for the CD can be determined for fully cured materials. Formation of ether linkages consumes two hydroxyl groups, whereas alkylene bridges originate from only one hydroxyl group together with a backbone ester unit. Consequently, the theoretical CD of a resin cured predominantly through one or the other mechanism differs by a factor of two (Table 5).

It is instructive to compare the CDs obtained from swelling measurements, which rely on several approximations and simplifications, with the theoretical values based on ether linkage formation competing with alkylene bridge formation. For HEA copolymers, lower CDs are observed at lower perchloric acid concentrations. This difference decreases as the HEA

content increases, and at high perchloric acid concentrations the resulting CDs become nearly identical. At high HEA content, the dominant crosslinking mechanism involves alkylene bridge formation, whereas at low HEA content and low perchloric acid concentration, ether bridge formation prevails. This conclusion is supported by the ^{13}C NMR spectrum of sample P_{12}(MA-HEA16), which reveals a mixture of both types of crosslinking motifs (Figure 33a). It should be noted that the reactivity of MA- and EA-based resins toward perchlorate esters differs, as reflected in the distinct reaction rates observed for the pCBA-system (Figure 17).

The evaluation of the CD of cured HBA copolymers from swelling measurements yields results similar to those obtained for the corresponding HEA copolymers, but only when lower amounts of perchloric acid are used as the catalyst. It should be noted that in the nomenclature P_y(EA-HEAx) and P_y(EA–HBAx), where x denotes the amount of comonomer in the resin, the total amount, and thus the concentration of perchloric acid also increases with the same value of y. The variation in T_g as a function of HBA content shows a comparable trend, indicating that a similar type of network structure is formed. The ^{13}C NMR spectrum of cured sample P_{12}(EA–HBA14) shows no resonances attributable to ether linkages; instead, signals assigned to carbons of butylene diester crosslinks are observed. This suggests that the formation of dibutylene ether linkages is significantly less favored than the formation of diethylene ethers in HEA-based resins. A competing crosslinking pathway may involve a Fischer esterification between an HBA crosslinker and a carboxylic ester, as previously proposed for HEA copolymers, resulting in an alkylene linkage. However, the calculated CD values cannot be explained solely by the crosslinking chemistry, since the resin composition undergoes substantial changes during curing, particularly due to the formation of a higher number of carboxylic acid groups. This effect becomes more pronounced with increasing HBA content in the copolymer (Figure 36). The high calculated CD values may therefore represent an artifact of the calculation method, or they may indicate the presence of additional, unaccounted crosslinking reactions.

Crosslinking of HBA copolymers with sub-stoichiometric amounts of perchloric acid produces coatings with relatively high CDs. The NMR spectra indicate facile formation of butylene bridges, which effectively compete with ether formation under conditions of low hydroxyl and perchloric acid concentrations. This behavior is analogous to that observed for HEA copolymers and suggests that decomposition of the hydroxybutyl units and subsequent secondary reactions play only a minor role. The resulting material is uniformly crosslinked and exhibits a T_g below 10°C when the perchloric acid content is below 25 mol% (Figure 31).

The CDs of HBA copolymers cured with 100 mol% perchloric acid are consistently about half those of the corresponding HEA copolymers. This observation could, in principle, be explained by the predominant formation of dibutyl ether linkages. However, the ^{13}C NMR spectrum of cured P_{100}(MA-HBA14) provides little evidence for such structures, as the expected resonance near 70 ppm is absent (Figure 34a). It is therefore more plausible that alkylene bridges are the dominant crosslinking motif and that approximately half of the butyl hydroxyl groups ultimately do not form a crosslink. The resonances assigned to the butylene bridges appear weaker than those observed for P_{12}(MA-HBA14) (Figure 34b). Studies on copolymers of pCBA have shown that butyl perchlorate intermediates can undergo partial decomposition, producing THF and an acyl perchlorate species of largely unknown reactivity[137]. Nevertheless, this decomposition pathway appears to have little influence on the overall CD.

A high concentration of perchloric acid also promotes dealkylation of acrylic acid esters, producing volatile alkyl perchlorates and generating additional carboxylic acid groups. This process effectively reduces the maximum attainable CD by removing hydroxyl functionalities. The effect is more pronounced in HBA copolymers, where it leads to a greater accumulation of carboxylic acid groups on the polymer backbone (Figure 36). Consequently, high perchloric acid concentrations favor alkylene crosslink formation in HBA copolymers. The increased presence of carboxylic acids introduces an additional nucleophilic species, and under these conditions an already formed crosslink may be cleaved. Carboxylic acids also act as intermediates in the formation of alkylene crosslinks: reaction of a carboxylic acid with an alkyl perchlorate side chain produces the same net result as a transesterification with an ethyl ester, albeit accompanied by release of perchloric acid.

5.2.7 Low-VOC Resins - Influence of CTAs on Curing Kinetics and Mechanism

High-solids, low VOC acrylic coatings are commonly offered by paint and coating manufacturers to comply with regulations[180] on VOC levels. Polyacrylates of relatively low molecular weight, often in the oligomeric range, exhibit lower viscosity and hence allow high-solids content at a low solvent content. However, the reduced chain length typically requires more reactive sites per mass unit to reach the same CD as the comparable high molecular weight resins, which increases system complexity and material cost.[181]

CTAs play a decisive role in the synthesis of low-VOC coating systems[182]. They enable the preparation of low-molecular weight polymers, while simultaneously controlling the molecular architecture and end-group functionality of the polymer. CTAs are small reactive molecules

that regulate chain growth in radical polymerization. They induce chain-transfer reactions in which a growing polymer radical abstracts a hydrogen or halogen atom from the CTA, thereby terminating one chain and generating a radical that initiates a new chain. Through this mechanism, molecular weight can be precisely controlled, yielding distributions with moments of Flory-Schulz statistics.[181]

Common CTAs in free radical polymerization are aliphatic or aromatic thiols, such as dodecyl mercaptan (DDM) or *n*-octyl mercaptan. The weak S-H bond inflicts an efficient hydrogen transfer. Halogenated hydrocarbons such as carbon tetrachloride, carbon tetrabromide (CBr_4) or bromotrichloromethane are less frequently used but act in a similar way.

Low-molecular weight HEA copolymers were synthesized in this study using the CTAs DDM and CBr_4. Addition of 2.5 and 3 wt%, respectively, relative to the amount of monomer produced oligomers with an M_n of 4.9 and 6.5 kg mol^{-1} and a respective HEA content of 13 and 11 mol% (Table 6). The molecular weights and HEA contents were adjusted in such a way that the CDs of the cured resins, assuming unrestricted crosslinking, matches those of cured P(EA-HEA7.5). The calculated functionality f_n was 6.8 and 4.9, respectively. Considering that about two hydroxyl groups per chain are required to match the molecular weight of the linear reference polymers, the number of hydroxyl groups available for actual crosslinking are 4.8 and 2.9. This translates to a directly comparable HEA content of 8.7 and 7.7 mol%, close to the targeted 7.5 mol% of the reference polymer P(EA-HEA7.5).

Table 6. Low molecular weight EA-resins synthesized.

Entry	Crosslinker (mol%)	CTA (wt%)[a]	M_n (kg mol^{-1})	$Đ$[b]	P_n[c]	f_n[d]
1	HEA 13	DDM 2.5	4.9	1.7	48	6.2
2	HEA 11	CBr_4 3.0	6.5	2.1	63	4.9

[a] Relative to the total weight of monomers; [b]Polydispersity $Đ$ (=$M_wM_n^{-1}$); [c]P_n degree of polymerization; [d]f_n hydroxy functionality per polymer chain.

The synthesized low molecular weight polyacrylates P(EA-HEA13)DDM and P(EA-HEA11)CBr_4 are transparent but exhibit a significantly lower viscosity than their high molecular weight analogs and could therefore be formulated as 50 wt% solution in ethanol. The resulting

solutions have about the same viscosity as those of high molecular weight resins and were found to be stable in the presence of perchloric acid over a 63-day time period (Figure 40).

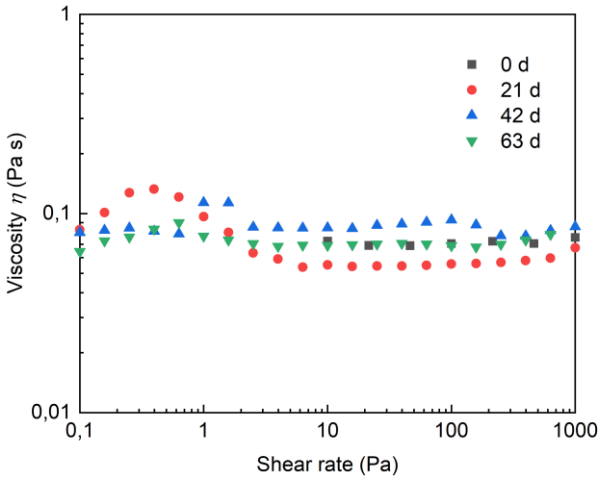

Figure 40. Viscosity curves over time of 50 wt% ethanolic solution of P_6(EA-HEA13)DDM.

Resins formulated with 3 mol% perchloric acid were found to cure into insoluble networks. The curing progress was assessed by swelling the resin at intermediate times in acetone. P_3(EA-HEA13)DDM reached complete curing after 90 min at 105°C, whereas P_3(EA-HEA11)CBr_4 required approximately 10h to achieve a comparable degree of crosslinking (Figure 41). The curing rate of P_3(EA-HEA11)CBr_4 is similar to that observed for high molecular weight polymers, suggesting that the functional groups (e.g., organobromides R-CBr_3 and R-$CHCH_3Br$) introduced through CBr_4 do not interfere with the curing process, in congruence to observations in the pCBA system. In contrast, DDM-derived end groups (mostly thioether) appear to hinder the curing reaction and significantly reduce the curing rate: For P_3(EA-HEA13)DDM, an increase of curing temperature by 50°C is required to reach rates comparable to those of high molecular weight reference polymers. It may be expected that perchloric acid engages preferentially with hydroxyl groups, as they are generally less sterically hindered and more basic (pK_a ($EtOH_2^+$) = -2,4[183]; pK_a ($(CH_3)_2SH^+$) = -5.3[184]), however, kinetic data show that this interaction is not rate determining.

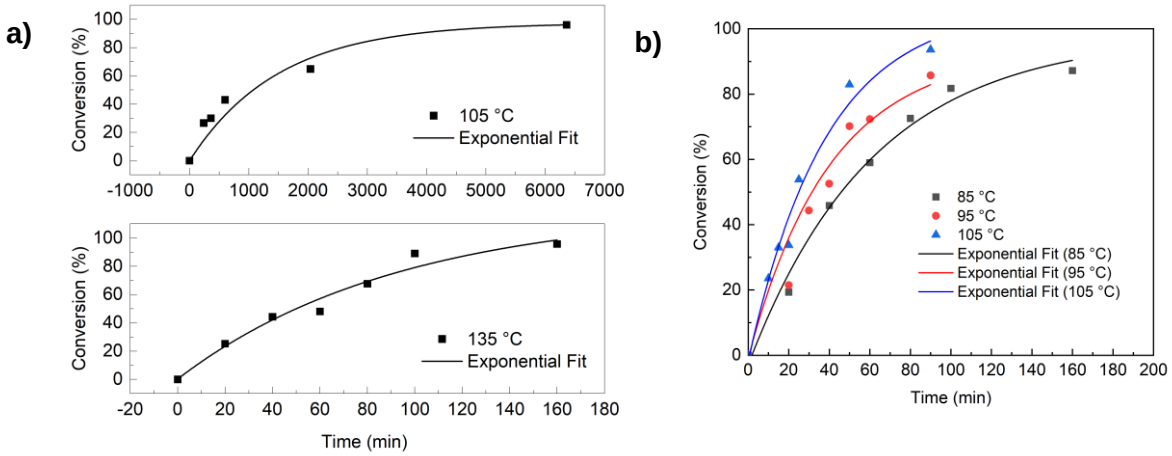

Figure 41. Conversion-time curves of (a) P_3(EA-HEA13)DDM cured at 105 and 135°C and (b) P_3(EA-HEA11)CBr_4 cured at 85, 95 and 105°C; solid lines represent exponential fits.

The curing reaction of formulations based on both low- and high molecular weight resins was found to follow an overall reaction order of 1.5, as indicated by the linear relationship obtained when plotting $(1-X)^{-0.5}$ vs. time (Figure 45a). Kinetic data for both low molecular weight resins and a reference high molecular weight resin were extracted from Arrhenius plots (Table 7). Activation energies are in line with the observed curing rates: E_A (P_3(EA-HEA11)CBr_4) = 41 kJ mol^{-1} and E_A (P_3(EA-HEA13)DDM) = 130 kJ mol^{-1}.

Table 7. Kinetic data of P(EA-HEA7.5)$_3$, P(EA-HEA11)$_3$$CBr_4$ and P(EA-HEA11)$_3$DDM.

Polymer	Cure Temperature (°C)	Rate constant *k* ((mol L^{-1})$^{-0.5}$ min^{-1})	Reaction order *n*	Activation energy E_A (kJ mol^{-1})	Pre-exponential factor *A* ((mol L^{-1})$^{-0.5}$ min^{-1})
P_3(EA-HEA7.5)	85	0.012	1.5	39	8.6
	95	0.017			
	105	0.024			
P_3(EA-HEA11)CBr_4	85	0.011	1.5	41	9.4
	95	0.016			
	105	0.023			
P_3(EA-HEA13)DDM	105	0.0006	1.5	130	36
	135	0.015			

Comparing CDs of resins cured with varying amounts of perchloric acid (1.5-100 mol%) reveals that low molecular weight formulations reach essentially the same final CD as high molecular weight P_y(EA–HEA7.5) (Figure 42), suggesting that the presence of CTAs does not hinder network formation. The characteristic relationship between catalyst concentration and CD is maintained in the curing of both low molecular resins: low perchloric acid levels seem to favor the formation of ether crosslinks and result in lower CDs, whereas higher amounts promote alkylene crosslinks and lead to higher CDs. It is noteworthy that, although thioether-based end groups reduce the curing rate, they do not affect the final degree of crosslinking, indicating that the curing mechanism proceeds to completion regardless of the CTA structure. This perhaps is not unexpected as they constitute only a small percentage of the reactive groups.

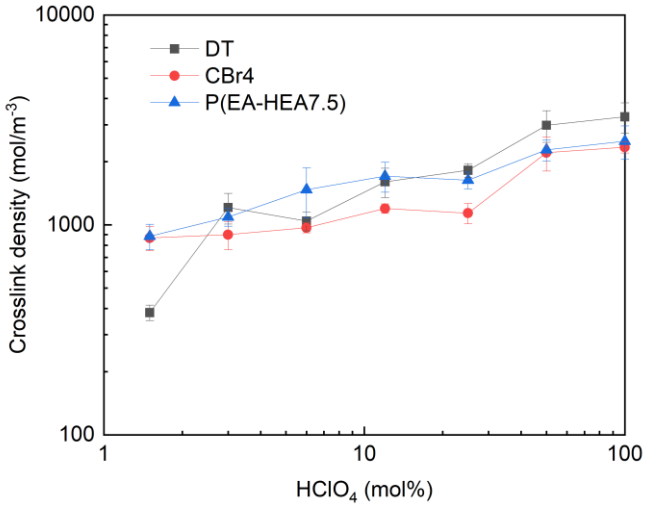

Figure 42. CDs of cured high molecular weight P_y(EA-HEA7.5) and low molecular weight P_y(EA-HEA11)CBr_4 and P_y(EA-HEA13)DDM.

Thioether end groups originating from chain transfer reactions of DDM are readily protonated by perchloric acid, establishing an acid-base equilibrium. Kinetic data indicate that organobromide end-groups derived from CBr_4 do not interfere with the curing process, whereas thioether end groups incorporated via DDM do. In contrast to the majority of hydroxyl groups, the thioethers remain in the film during the curing process and do not evaporate. Their weakly basic character allows them to compete with the hydroxyl functionalities of the crosslinkers HEA and HBA for interaction with perchloric acid, resulting in an equilibrium between the unprotonated thioether **48** and free $HClO_4$ and the corresponding sulfonium perchlorate **49** (Scheme 34). As a consequence, a portion of the acid is temporarily unavailable for catalysis.

The relevance of this equilibrium is therefore governed by the stoichiometric relationship between thioether end groups and perchloric acid. The molar ratio of thioether functionalities to $HClO_4$ spans a wide range, from approximately 1:6.2 for P_{100}(EA-HEA)DDM and 1:4.9 for P_{100}(EA-HEA)CBr_4 to as low as 1:0.18 and 1:0.15 for P_3(EA-HEA)DDM and P_3(EA-HEA)CBr_4. Comparable molar amounts of thioether groups are present at perchloric acid loadings of 12 and 25%, demonstrating that, depending on both molecular weight and catalyst concentration, the system may experience either an excess or a deficiency of acid relative to the thioether functionalities.

It is speculated that, at elevated perchloric acid concentrations, the apparent activation energy of the curing reaction decreases and a concomitant increase in the curing rate may occur. In such a scenario, this trend might be rationalized by assuming that protonation of thioether end groups does not quantitatively sequester all available $HClO_4$, leaving a fraction of the acid catalytically active and accessible for the crosslinking reaction. Consequently, the inhibitory effect associated with thioether protonation would be expected to become less pronounced at higher acid loadings. Furthermore, considering the elevated curing temperature required for P_3(EA-HEA13)DDM, and literature reports on sulfonium perchlorate formation and stability[185], the equilibrium is likely shifted toward sulfonium **49**.

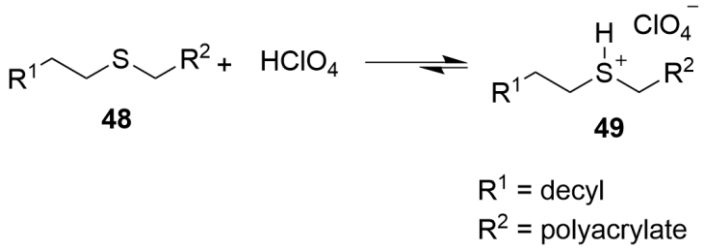

Scheme 34. Proposed equilibrium between thioether **48**/free perchloric acid and sulfonium perchlorate **49**.

Thioethers may also participate directly in the crosslinking reaction through transalkylation reactions. The proposed reaction pathway for P_{12}(EA-HEA13)DDM starts with the reaction of intermediately formed perchlorate ester **40a** with a thioether to yield trialkylsulfonium perchlorate **50** (Scheme 35). Subsequent dealkylation by nucleophilic attack of the perchlorate anion at the alpha-carbon of the decyl moiety generates dodecyl perchlorate and thioether crosslink **51**. Indirect evidence for the formation of dodecyl perchlorate was obtained from TGA-MS analysis of P_{12}(EA-HEA13)DDM, where two distinct mass signals at *m*/*z* 140 and 168 were detected between 150 and 250°C, slightly delayed to other typical volatile side products (alkyl perchlorates). The observed signals are attributed to 1-dodecene, formed by elimination of perchloric acid from dodecyl perchlorate, and match the reference mass spectrum[178]. Since

no corresponding peaks are present when the high molecular weight HEA copolymers are cured and the volatile parent DDM would evaporate before the onset of crosslinking, the detected 1-dodecene must result from secondary reactions occurring during the curing or analytic procedures. The resulting thioether **51** constitutes a newly formed crosslink. The sulfonium salt **50** may behave similar to a dioxolenium intermediate in the pCBA system: The perchlorate anion can attack any of the alkyl substituents and nucleophilic attack at positions other than the decyl group would regenerate o polymer-bound perchlorate species.

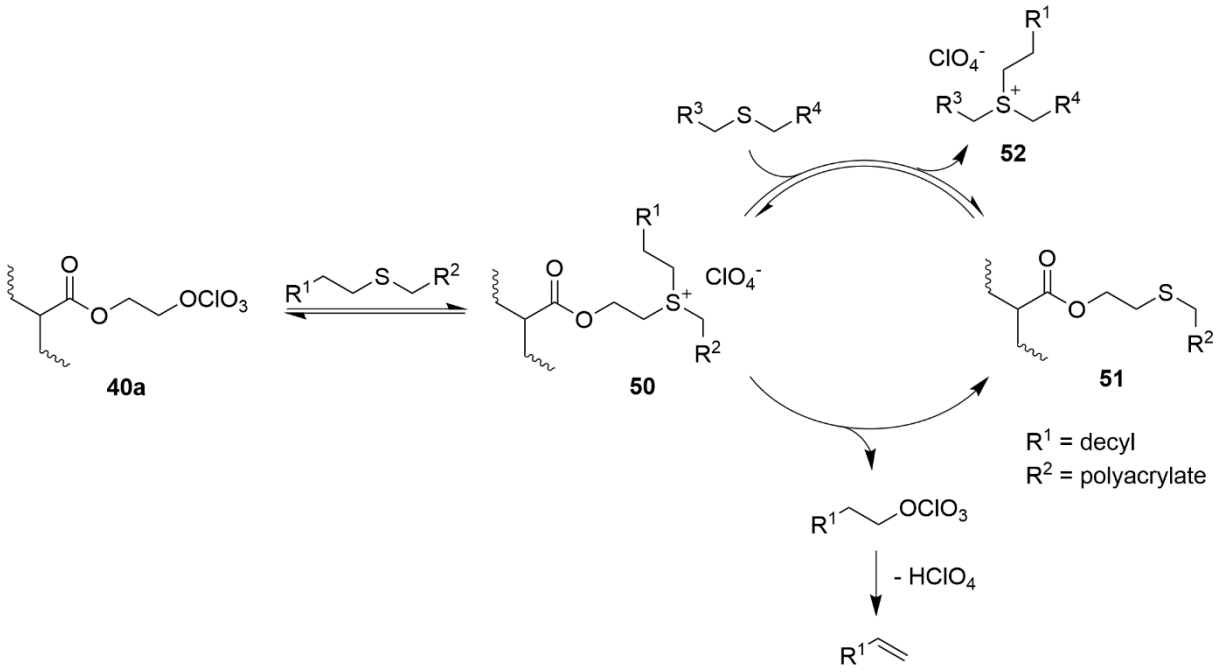

Scheme 35. Proposed reaction pathway for the transalkylation of thioethers and alkyl perchlorates.

An exchange of alkyl groups between sulfonium salt **50** and thioethers is also conceivable (Scheme 35). Such a transalkylation would proceed via nucleophilic attack of a thioether at the alpha-carbon of one of the alkyl substituents of the sulfonium salt, resulting in the formation of a new thioether crosslink (**51**) together with a new sulfonium salt (**52**). A comparable transalkylation has been reported for brosylates[186], where the activation energy of 108±4 kJ mol^{-1} for the exchange between tributylsulfonium brosylate and dihexyl sulfide is in the same ballpark as the value of 130 kJ mol^{-1} determined for the crosslinking reaction of P_3(EA-HEA13)DDM. The dynamic exchange continues until it is terminated either by nucleophilic attack of perchlorate ions, yielding alkyl perchlorates, or by reaction with hydroxyl groups from incorporated HEA units. This underscores the dynamic nature of the crosslinking process, promoting a homogenous distribution of crosslinks throughout the network.

Reaction products resulting from the use of alternative CTAs such as carbon tetrachloride, bromotrichloromethane, pentaphenylethane, *n*- or *iso*-propanol, and ethanol are not expected to interfere significantly in the curing process, whereas any other mercaptan is likely to display behavior similar to that observed for DDM.

5.2.8 Short Evaluation of an Application in the Coil Coatings Industry

Considering the requirements, a commercial application of the chemistry developed in this study may tentatively be found in the coil coating industry. Coil coating is a continuous process for coating steel or aluminum sheets on one or both sides. The coil coating process consists of (i) uncoiling of coiled metal strips up to a width of 2.6 meters that are free from greases and oils applied to protect the surface after production, and (ii) chemically passivation before (iii) application of an adhesion promoter (primer) and topcoat (if needed; Figure 43). The curing of the coating layers takes less than 30 seconds in modern systems. In this short time, the metal is heated to 200 to 290°C, predominantly in circulating air dryers with high energy output. Fast heating is essential to limit the total length of the curing oven at high line speed. At a normal line speed of 150 m min^{-1}, a curing time of 20 seconds already means an oven length of 50 meters. Typical binders used for coil coating application are bisphenol A-epoxy resins, epoxy-ester and epoxy-MF resins, polyester-MF and alkyd-MF resins. Also, thermosetting acrylic MF coatings have been used over primers.[11,187] These systems are curable usually in the same temperature range as the perchloric acid system. However, perchlorates might not withstand curing temperatures around 200°C, even for a short period of time, as their oxidative power increases rapidly above 100°C.[80,83] Curing could be performed at a lower temperature.

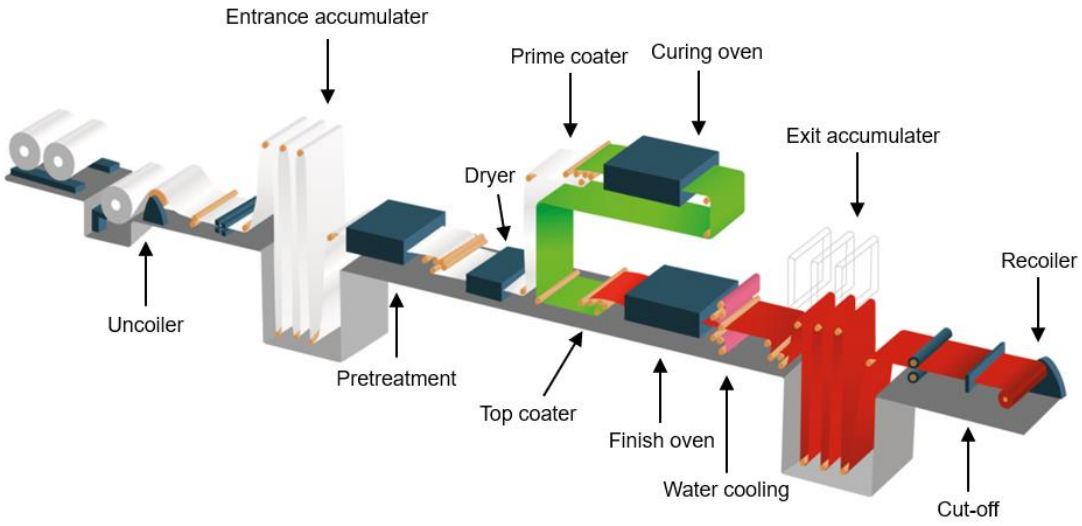

Figure 43. Schematic illustration of a coil coating line.[188]

One advantage of the coil coating process is the presence of an exhaust air system. The exhaust air, which is enriched with solvents, leaves the dryer/oven at a temperature of 250 to 350°C. It is then purified in a thermal oxidizer in which the exhaust air from the dryers is heated to over 750°C. At these temperatures, the hydrocarbons (VOC) are safely converted into water and CO_2. The heat generated in this process is reused to heat the oven. In this way, the actual curing process in the coil coating line can be operated with a very low input of primary energy.[11,187]

Any alkyl perchlorate released during the curing is likely to decompose at these temperatures. The main combustion products are expected to be H_2O, CO_2, CO, HCl, Cl_2 and $COCl_2$, with HCl and Cl_2 accounting for the majority of chlorine-containing compounds. The hydrogen content in the exhaust air determines the ratio between those two. High hydrogen content favors HCl formation whereas low hydrogen content favors Cl_2 formation.[189] By burning the off gas, VOC emissions are largely avoided, and the heating value of the solvent is recovered. As a result, there is less incentive to switch to waterborne or high-solid coatings in coil-coating applications than in other applications. This might benefit an application of the perchloric acid system if the use of mercaptans is abandoned in favor of the curing kinetics.

To ensure the operational reliability of the dryer, the solvent concentration in the individual dryer zones is continuously monitored. By regulating the necessary hot air quantities, exceeding the lower explosion limit is avoided. Due to the presence of alkyl perchlorates, a re-evaluation of explosion limits and explosion hazards may be necessary, but the necessary facilities are generally already in place.[11,187]

5.2.9 Concluding Remarks

Concentrated perchloric acid is an effective crosslinking reagent for hydroxy-functional acrylic resins. In this study, representative copolymers of EA with HEA or HBA were formulated in ethanol and catalyzed with 70% aqueous perchloric acid. The formulations remain stable for weeks and can be cured at elevated temperatures; practical curing was achieved at 105°C within 90 minutes, producing transparent and, for sub-stoichiometric perchloric acid amounts, colorless films. The measured CDs (Table 5) summarize the dependence of network formation on comonomer composition and catalyst loading.

A characteristic and useful feature of the perchloric acid curing chemistry is the volatilization of perchloric entities as alkyl perchlorates. This dealkylation removes acidic species from the film, yielding a neutral coating that is expected to be resistant to hydrolytic attack over long timescales. Mechanistically, curing proceeds by formation of a strongly electrophilic alkyl perchlorate intermediate, generated in-situ from perchloric acid and a hydroxyl group. This intermediate reacts either with another hydroxyl to form ether crosslinks or with ester/carboxyl moieties to produce alkylene (diester) crosslinks. Therefore, the concentration of perchloric acid relative to hydroxyl functionality controls both the rate of crosslink formation and the balance between ether and alkylene crosslinks: faster curing and higher acid concentrations favor alkylene crosslink formation, whereas lower acid loadings and shorter hydroxyl-terminated chains (as in HEA) favor ether formation, at least until local network density becomes limiting.

HEA copolymers generally form more diethylene-type ether linkages at low perchloric acid concentrations, producing networks with lower T_g. At higher HEA contents and/or higher perchloric acid concentrations, alkylene crosslinks become dominant, producing locally denser crosslinking and correspondingly higher T_g's. In contrast, HBA copolymers tend to yield butylene diester crosslinks. They also produce THF under curing, analogous to pCBA systems, consistent with partial decomposition of butyl perchlorate intermediates. The overall effect in the HBA systems is a lower effective CD, which reflects both the relative number of available hydroxyl monomers and side-reactions that alter backbone composition (notably formation of additional carboxylic acids).

The combination of catalytic (small) amounts of perchloric acid with HEA copolymers is attractive in an application: 70% aqueous perchloric acid is industrially available at scale[62,190], avoiding the need for less common reagents such as silver perchlorate when used in an alternative approach. Formulating in ethanol rather than xylene reduces the environmental impact of the coating formulation. Emissions of short-chain alkyl perchlorates were markedly

reduced in optimized HEA systems, and THF emissions can be avoided by appropriate choice of hydroxy functional monomer. For commercial deployment (for example, in coil coating), capturing volatile alkyl perchlorates during curing will be essential to meet safety and regulatory requirements.

Low molecular weight HEA copolymers synthesized with DDM and CBr_4 enable the formulation of high-solids, low-VOC acrylic coatings with CDs comparable to high molecular weight analogues. Both CTAs permit complete network formation, but differ in their rates: brominated end groups introduced by CBr_4 do not affect the curing process, whereas thioether end groups from DDM slow the reaction down, probably by acid consumption in a thioether-sulfonium perchlorate equilibrium. Evidence from TGA-MS further suggests that thioethers participate in transalkylation reactions via possible sulfonium intermediates, dynamically contributing to network rearrangement. Despite lower curing rates, the final CD remains unaffected, demonstrating that CTA structure primarily influences curing kinetics rather than the extent of crosslink formation.

Revisiting the five criteria defined before in chapter 4 (motivation), the system with the highest potential for application, i.e. the $HClO_4$/HEA copolymer system,

(I) is comparable in cost to conventional coatings, maybe even less expensive,
(II) is self-crosslinking and does not need a co-reactant,
(III) forms strong ether and ethylene diester crosslinks,
(IV) is entirely free of catalyst residues,
(V) forms volatiles, which, even though formed in catalytic amounts, evaporate from the film and are potentially harmful to humans and the environment.

Although the original target profile (I-V) could not be met in full, the present work clarifies which criteria are realistically achievable with perchlorate chemistry and where fundamental safety and regulatory barriers arise. Future work should explore process and formulation levers to further tailor coating properties. Candidate directions include the deliberate addition of polyols (glycerol, pentaerythritol, 1,4-butanediol) or saccharides to modulate network architecture and toughness, systematic studies of catalyst loading versus kinetics and domain formation, long-term hydrolytic and oxidative stability tests, and development of practical volatile-capture strategies for scale-up. Such investigations will clarify the tradeoffs between network chemistry, processing, performance, and environmental/safety management, and will determine the most promising paths toward industrial application.

6 Experimental Part

6.1 Materials

MA (BASF SE, technical grade), MMA (BASF SE, technical grade), EA (BASF SE, technical grade), BA (BASF SE, technical grade), acetyl chloride (technical grade), benzene (BASF SE, technical grade), ethanol (Sigma Aldrich, 99.5%), pentane (Thermo Fisher Scientific, 95%), styrene (BASF SE, technical grade), triethylamine (Sigma Aldrich, USA, 99.5%), vinyl acetate (BASF SE, technical grade), and dichloromethane (Sigma Aldrich, technical grade) were distilled prior to use.

Acetic anhydride (Sigma Aldrich, ≥98%), Acetone (technical grade), acetonitrile-d_3 (Merck, 99%), acrylic acid (Sigma Aldrich, ≥ 99%), acryloyl chloride (Sigma Aldrich, ≥ 97%), AIBN (Sigma Aldrich, 98%), 2-aminopentane (Sigma Aldrich, 97%), BDDA (Sigma Aldrich, technical grade), 3,5-bis(trifluoromethyl)benzaldehyde (TCI-Chemicals, >95%), n-butanol (Sigma Aldrich, ≥99.4%), n-butylamine (Sigma Aldrich, ≥99%), 1-bromodecane (Sigma Aldrich, ≥ 98%), carbon tetrabromide (CBr4, Sigma Aldrich, 99%), carbon tetrachloride (Sigma Aldrich, 99.5%), chloroform-d_1 ($CDCl_3$, Deutero GmbH, 99.8%, +0.03% TMS), cobalt(II) chloride ($CoCl_2$, Merck, 97%), diethyl ether (Sigma Aldrich, technical grade), diethylene glycol (Sigma Aldrich, 99%), ethanol (technical grade), dodecyl mercaptan (DDM, Merck, ≥98%), (±)-epichlorohydrin (Merck, ≥99%), fluorobenzene (TCI-Chemicals, ≥99%), hexamethylenediamine (Sigma Aldrich, ≥99%), HBA (TCI-Chemicals, > 97%), HEA (Acros Organics, 97%), 70% $HClO_4$ (Fluka Chemie GmbH, 70% in H2O), JEFFAMINE D-230 (Huntsman,), lithium perchlorate (Sigma Aldrich, ≥95%), methacryloyl chloride (Merck, 97%), methanol-d_4 (Deutero, 99.8%), 2-methyltetrahydrofuran (Acros Organics, >99%), phosphorus pentoxide (P_2O_5, Merck, 99%), sulfuric acid (Sigma Aldrich, ≥96%), THF (Acros Organics, dry, 99.85%) and dry toluene (Acros Organics, 99.85%), trifluoromethanesulfonic acid (Alfa Aesar, ≥98%), zink (dust, Sigma Aldrich, ≥98%), zink oxide (ZnO, Sigma Aldrich, 99.9%) were used without further purification.

Xylene and 1,1,2,2-tetrachloroethane-d_2 were dried under nitrogen atmosphere over a molecular sieve 4 Å.

Anhydrous silver perchlorate was purchased from Alfa Aesar, dissolved in dry toluene, and precipitated by the addition of pentane. The solvent mixture was decanted, and residual silver perchlorate was dried under reduced pressure and stored under nitrogen in the absence of light.

Reactions involving Cl_2O_7, $AgClO_4$ and pCBA were performed under a nitrogen atmosphere.

6.2 Characterization

6.2.1 FTIR Spectroscopy

FTIR measurements were performed using a Vertex 70 spectrometer (*Bruker*) in ATR-mode. Measurements were conducted in the spectral range of 4000-400 cm^{-1} with a resolution of 8 cm^{-1}, averaging 18 scans per spectrum. The spectrometer was operated with the OPUS software package. Thin films of 30-50 µm were applied with a spreader on glass substrate and cured at 85-135°C. The polymer was scraped off the glass substrate and placed in the spectrometer for analysis.

6.2.2 Nuclear Magnetic Resonance Spectroscopy

^{13}C CP MAS Measurements were performed at 25°C with an Avance II 400 MHz solid-state spectrometer (*Bruker*) equipped with a 4 mm double resonance ^{1}H/X-MAS probe head. Spectra were recorded at the resonance frequency of approximately 100 MHz. ^{13}C Chemical shifts were calibrated through the tertiary carbon resonance of alanine as an external reference at 51 ppm. Samples were prepared by grinding polymer films at liquid nitrogen temperature.

^{1}H and ^{13}C NMR spectra were recorded on *Bruker* AV400, AV500, or AV600 MHz spectrometers in $CDCl_3$ at room temperature; approximately 20 mg of substance was dissolved in 0.7 mL $CDCl_3$ and transferred into 5 mm NMR tubes (*Wilmad Labglass*). ^{1}H NMR data are referenced to TMS at 0 ppm using the residual proton signals of the deuterated solvent.

6.2.3 Differential Scanning Calorimetry

Glass transition temperatures (T_g) were measured on a *Mettler Toledo* equipment (DSC1). Samples of 5-15 mg were weighted into 40 µL aluminum crucibles, cold welded with aluminum foil lids, and cooled to -90°C at a rate of 20 K min^{-1}. After they were kept constant for 3 min, the samples were heated to 350°C at a heating rate of 10 K min^{-1}. Glass transition temperatures were determined as the center point between the tangential baseline before and after the glass transition range.

6.2.4 Size-Exclusion Chromatography

The number/weight average molecular weight (M_n/M_w) and polydispersity ($Đ = M_w M_n^{-1}$) values of the polymers were determined by size-exclusion chromatography (SEC) in THF at room temperature (flow rate = 1.0 mL min^{-1}) on a Thermo Separation Products AS1000 auto sampler (*Thermo Fisher Scientific*) equipped with a Schambeck RI 2012 refractive index detector (*Schambeck SFD GmbH*) and a SDV (styrene-divinylbenzene) GPC linear column (5 µm). Samples were measured at a concentration of 5 mg mL^{-1} after filtration through a 0.45 µm pore-size membrane. Calibration was performed using polystyrene standards.

6.2.5 Trapping of Evaporating Compounds

Volatile compounds were analyzed by means of NMR spectroscopy. Therefore, a 10 mL Schlenk flask loaded with 200 mg of polymer was connected through 5 cm of tubing to a cold trap. After 30 min of dynamic vacuum, the cold trap was dipped into liquid nitrogen and the valve of the flask was slightly opened to make sure that a nitrogen stream ran from the flask through the cold trap. The resin was heated at a rate of approximately 10 K min^{-1} to a final temperature of 200°C.

6.2.6 TGA-FTIR

The thermal properties and the detection of the emerging gases, which are produced when the samples were heated, were measured with a thermobalance (STA 409C/CD from *Netzsch*) coupled with a Fourier Transform InfraRed Spectrometer (FTIR TENSOR 27 with external gas cell from *Bruker*) in 0.3 ml Al_2O_3 DTA/TG-crucibles. The samples were measured under a nitrogen (5.0) flow (50 mL/min) from room temperature to 900°C with a heating rate of 10 K min^{-1}.

6.2.7 TGA-MS

The thermal properties and the detection of the emerging gases, which are produced when the samples were heated, were measured by means of TGA-MS with a thermobalance (TG 209

F1 Libra, *Netzsch*) in the dynamic mode with a heating rate of 10 K min^{-1} under nitrogen (5.0) flow (20 mL min^{-1}) from room temperature to 900°C. Evolving gases were analyzed by a coupled quadrupole mass spectrometer (QMS 403 D Aëolos, *Netzsch*) equipped with electron ionization and a Faraday detector. Gases were transferred via a heated adapter (200°C) and through a heated quartz glass capillary (200°C) connecting the TGA furnace outlet with the MS gas inlet.

6.2.8 Viscometry

Dynamic viscosities were measured on an AR-G2 rheometer (*TA Instruments*, 159 Lukens Drive, New Castle, DE 19720, USA) with cone plate geometry using a cone angle of 2° and a cone diameter of 60 mm. All experiments were conducted at 25°C and viscosities measured at steady-state flow at shear rates (1/s) from 0.1 to 1000.

6.2.9 Crosslink Density

Swelling experiments based on the equilibrium swelling of crosslinked polymers in a suitable solvent were conducted to determine the number average molecular weight between crosslinks, M_c, and CD of the PEA-based resins. When a crosslinked polymer network is placed in a good solvent, it will absorb solvent molecules and expand until an equilibrium is reached between the osmotic driving force and the elastic retraction forces of the network chains. The final degree of swelling depends largely on the CD and the affinity between solvent molecules and polymer. These measurements provide insight into the efficiency and underlying mechanism of the crosslinking reactions taking place in the material.

M_c was calculated from the Flory-Rehner-equation:

$$\ln(1-V_2) + V_2 + \chi V_2^2 = (-\rho V_1 / M_c)(V_2^{1/3}\ 0.5V_2) \qquad (12)$$

where V_2 is the volume fraction of the polymer in the swollen gel at equilibrium, χ is the polymer-solvent interaction parameter, ρ is the polymer density, and V_1 is the molar volume of the solvent.

For both systems, P_y(EA-HEA/HBA)/acetone and P(EA-pCBA)/acetone the equation can be written as:

$$M_c = -1.12\ \text{g cm}^{-3} * 106.26\ \text{cm}^3\ \text{mol}^{-1}\ (V_2^{1/3}\ 0.5\ V_2) / \ln(1-V_2) + V_2 + 0.36\ V_2^2 \qquad (13)$$

For simplification, ρ was set to the density of the base polymer (PEA). χ (0.36) was calculated using Bristow and Watson semi-empirical equation (Equation 14):

$$\chi = \beta_1 + (V_1 / RT)\ (\delta_s - \delta_p)^2 \qquad (14)$$

where β_1 is the lattice constant (0.34), R is the universal gas constant, T is absolute temperature and δ_s and δ_p are the Hansen solubility parameters of the solvent and polymer respectively.

Acetone was selected as swelling solvent over toluene, as its Hansen solubility parameter (19.9 $\text{Mpa}^{1/2}$) is in between that of PEA (19.1 $\text{Mpa}^{1/2}$) and PAA (23.3 $\text{Mpa}^{1/2}$). The substantial change in polarity of the base polymer through formation of carboxylic acid groups especially for high ClO_4-content formulations is better balanced by acetone than by for example, toluene (18.3 $\text{Mpa}^{1/2}$), in which some highly crosslinked films did not swell, complicating further analysis.

The volume fraction of the polymer was calculated by a method reported by Hill.[154] Films of 30-50 µm thickness were applied on PTFE/glass fiber composite sheets (*Rehm Dichtungen Ehlers GmbH*, Gaußstraße 4, 31224 Peine, Germany) or glass substrates (*VWR International*) and cured between 85 and 135°C. Round platelets of approximately 1 mm diameter were punched out using a hollow puncher, placed onto a microscope slide, and covered with a thin coverslip. The diameter of the unswollen sample was measured with a microscope (Leica DMi8A, *Leica Mikrosysteme Vertrieb GmbH*, Ernst-Leitz-Strasse 17-37, 35578 Wetzlar, Germany) equipped with a digital measuring device set at 2.5 magnification. A few solvent drops were placed at the slide/coverslip interface whereupon the solvent was drawn into the small gap between the two glasses. As soon as the samples came in contact with the solvent, they began to swell until an equilibrium was reached, usually within 2 min. The fractional increase in diameter (f) was calculated according to:

$$f = (x_2 - x_1) / x_1 \qquad (15)$$

where x_1 is the diameter of the sample before swelling, and x_2 is the diameter of the sample in equilibrium swollen state.

When isometric swelling is assumed, V_2 can then be calculated from:

$$V_2 = 1 / (1 - f)^3 \quad (16)$$

CD was derived from M_c and the density of PEA (1.12 g cm^{-3}):

$$\text{CD (mol cm}^{-3}) = 1.12 \text{ g cm}^{-3}\ M_c^{-1} \quad (17)$$

Each data point is the average of six diameter measurements from 3 individual samples. Selected measurements were collected more than once, showing a deviation <10% from each other, indicating generally good reproducibility.

The calculated CD of cured pCBA copolymers and HEA/HBA copolymers with a 1:1 OH/perchloric acid ratio were calculated from the following statistical approach:

$$M_{c,cal} = M_{EA} \text{ (100 mol\%)} / 2Q \quad (18)$$

Where $M_{c,cal}$ is the calculated number average molecular weight between crosslinks, M_{EA} is the molecular weight of ethyl acrylate, and Q is the percentage molar ratio of pCBA/HEA/HBA in the polymer.

CDs of HEA/HBA copolymers cured with 12 mol% perchloric acid were calculated as follows:

$$M_{c,cal} = M_{EA} \text{ (100 mol\%)} / Q \quad (19)$$

6.2.10 Activation Energy E_A

The crosslinking reaction of pCBA copolymers was found to follow an overall reaction order of 1, as indicated by the linear relationship obtained when plotting ln(1-conversion) vs. time for P(BA-pCBA11) (Figure 44). The same applies to all other studied pCBA-copolymers.

The rate constant k is equal to the negative of the slope of the plot. The Arrhenius equation (Equation 20) connects reaction rate with absolute temperature T and activation energy (E_A).

$$k = A \exp(-E_A/RT) \quad (20)$$

Taking the natural logarithmic and subsequent rearrangement yields:

$$\ln(k) = -E_A/R\ (1/T) + \ln(A) \quad (21)$$

Plotting the rate constants against the reciprocal reaction temperature allows the activation energies to be determined from the straight-line slope and the gas constant *R*. The pre-exponential factor *A* is determined from the intersection with the Y-axis.

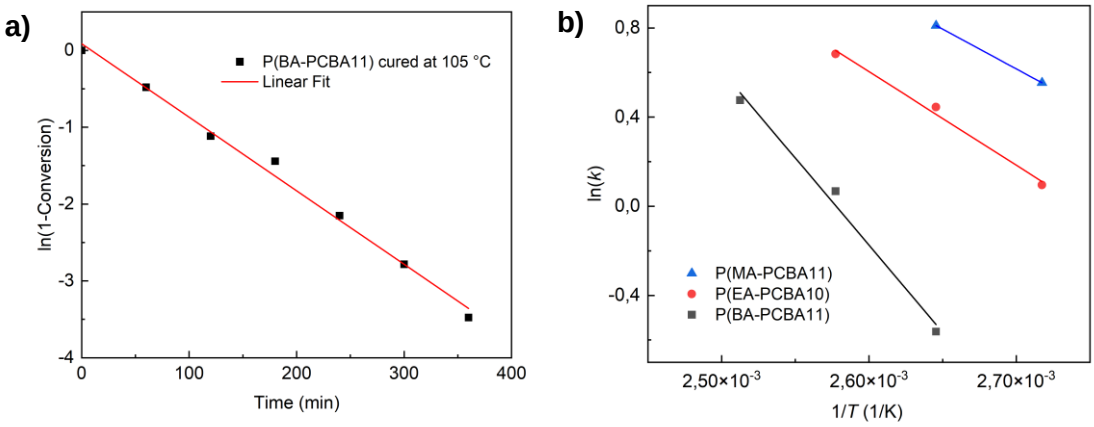

Figure 44. (a) Exemplary linear plot for P(BA-pCBA11) and (b) Arrhenius plots for the curing of P(MA-pCBA11), P(EA-pCBA10), and P(BA-pCBA11), lines represent linear fits to determine E_A and *A*.

The crosslinking reaction of EA/HEA copolymers was found to follow an overall reaction order of 1.5, as indicated by the linear relationship obtained when plotting $(1\text{-}X)^{-0.5}$ vs. time (Figure 45a). First- and second-order kinetics can be excluded, since the corresponding plots of ln(1-*X*) and 1/(1-*X*) against time do not yield linear dependencies. Likewise, an autocatalytic mechanism is unlikely as the conversion-time profiles do not exhibit the characteristic sigmoidal shape. The rate law is defined as:

$$-d[1\text{-}X]/dT = k[1\text{-}X]^{-0.5} \qquad (22)$$

Rate constant *k* is determined from the slope of the linear plots. E_A is calculated from the rate constant *k* using the Arrhenius equation (Equation 20):

By plotting ln(*k*) vs. 1/*T* (Figure 45b), E_A can be calculated from the slope of the linear regression and *A* from the intersection of the regression line with the y-axis.

$$E_A = -R \text{ slope} \qquad (23)$$

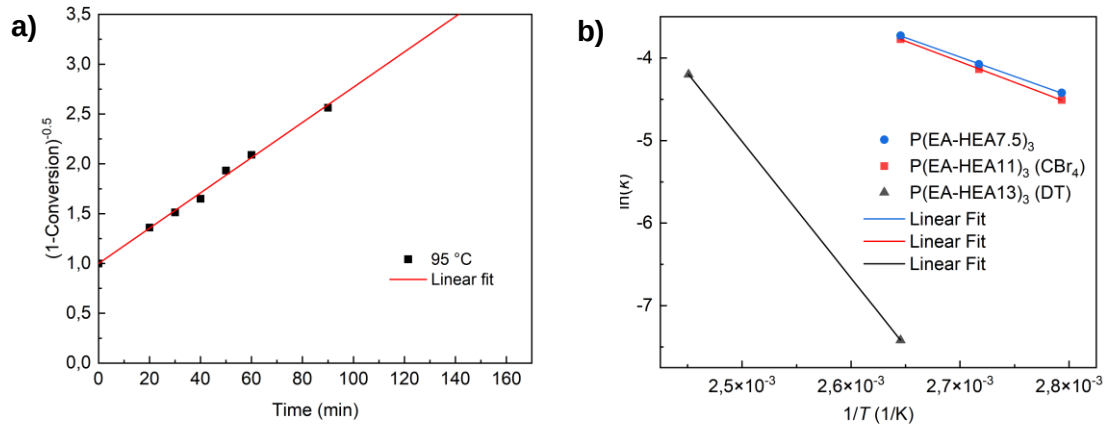

Figure 45. (a) Exemplary linear plot for P_3(EA-HEA7.5) at 95°C and (b) Arrhenius plots for the curing of P_3(EA-HEA7.5), P_3(EA-HEA11)CBr_4, and P_3(EA-HEA13)DDM, lines represent linear fits to determine E_A and A.

6.3 Preparative Procedures

Preparation of 3-Chloro-2-hydroxypropyl Perchlorate (22)

3-Chloro-2-hydroxypropyl perchlorate was prepared from epichlorohydrin and perchloric acid following a procedure from Hoffmann.[142] To a stirred mixture of epichlorohydrin (1.0 mL, 10 mmol, 1.0 eq.) and diethyl ether (4 mL) at -20°C was carefully added 70% perchloric acid (1.6 g, 10 mmol, 1.0 eq.). The solution was allowed to warm to room temperature and diethyl ether (5 mL) was added. The organic phase was washed with H_2O (5 mL) and dried over Na_2SO_4. The organic solvent was removed under reduced pressure and the residue dissolved in ethyl acetate and filtrated through a pad of silica gel. The solvent was removed under reduced pressure to afford **22** as a clear liquid in 70-90% yield.

^{1}H NMR (300 MHz, $CDCl_3$): δ 4.62 (dd, J = 5.4, 1.5 Hz, 2H), 4.26 (p, J = 5.3 Hz, 1H), 3.69 (dd, J = 5.2, 3.8 Hz, 2H).

Preparation of Dichlorine Heptoxide

Dichlorine heptoxide was prepared from phosphorus pentoxide and perchloric acid following the procedure of Baum.[85] Phosphorus pentoxide (25 g, 0.17 mol) was suspended in carbon tetrachloride (50 mL) and the mixture was cooled to 0°C. 70% perchloric acid (2.6 mL, 30 mmol) was dropwise added over 1h and the mixture subsequently refluxed for 20 min. The mixture was co-distilled under vacuum at 25°C. A clear liquid was obtained that fumes upon

exposure to air. The Cl_2O_7 concentration has not been determined but was assumed to match those of the literature (0.03 mmol mL^{-1}).

Preparation of 2-Perchloratoethyl Acrylate (pCEA, 28)

To a suspension of HEA (10 µL, 94 µmol) and Na_2SO_4 (0.1 g, 0.7 mmol) in $CDCl_3$ (1.0 mL) was added the solution of Cl_2O_7 (4.0 mL, 0.12 mmol). The solid was filtered off and the solution analyzed by ^{1}H NMR spectroscopy.

^{1}H NMR (600 MHz, $CDCl_3$): δ 6.49 (dd, *J* = 17.3, 1.3 Hz, 1H), 6.15 (dd, *J* = 17.3, 10.4 Hz, 1H), 5.93 (dd, *J* = 10.5, 1.3 Hz, 1H), 4.80 - 4.73 (m, 2H), 4.54 - 4.47 (m, 2H).

Preparation of 2-Bromoethyl Acrylate (29)

A mixture of 2-bromoethanol (6.7 g, 54 mmol, 1.0 eq.), triethylamine (8.2 mL, 58 mmol, 1.1 eq.) in dichloromethane (30 mL) was cooled to 0°C and acryloyl chloride (4.4 mL, 54 mmol, 1.0 eq.) added. The mixture was allowed to warm up and stirred over night at room temperature. The precipitate was filtered off and the resulting solution washed with H_2O (2x50 mL) and brine (20 mL) and subsequently dried over Na_2SO_4, filtered and the organic solvent removed under reduced pressure. The residue was vacuum distilled to afford **29** (3.5 g, 36% yield) as a clear liquid.

^{1}H NMR (600 MHz, $CDCl_3$): δ 6.52 – 6.36 (m, 1H), 6.23 – 6.01 (m, 1H), 5.93 – 5.80 (m, 1H), 4.47 (t, *J* = 6.2 Hz, 2H), 3.55 (t, *J* = 6.2 Hz, 2H) [191].

Preparation of 4-Perchloratobutyl Acrylate (pCBA)

Silver perchlorate (0.85 g, 3.7 mmol, 1.3 eq.) was suspended in pentane (24 mL) and cooled to -20°C. Under vigorous stirring, acryloyl chloride (0.24 mL, 2.9 mmol, 1 eq.) was added, and the reaction mixture was allowed to warm to room temperature. The suspension was stirred for 1 h, and brownish silver chloride precipitated. The mixture was again cooled to -20°C before THF (0.24 mL, 2.9 mmol, 1 eq.) in pentane (2 mL) was added dropwise, and the reaction mixture was subsequently stirred for another hour at room temperature. The formed salt was removed by filtration through a pad of silica gel, and the resulting clear solution was dried over molecular sieve 4 Å for at least 12h before further use. The solution was again filtered, and the solvent was removed under reduced pressure. pCBA is obtained as a clear liquid in 50-80%

yield. It is water sensitive and was stored in a solution of pentane under nitrogen atmosphere at -36°C. It does not explode in the hammer test[151].

^{1}H NMR (600 MHz, $CDCl_3$): δ 6.39 (d, *J* = 18.2 Hz, 1H), 6.10 (dd, *J* = 17.3 Hz, 1H), 5.83 (d, *J* = 10.4 Hz, 1H), 4.57 (t, *J* = 6.3 Hz, 2H), 4.19 (t, *J* = 6.2 Hz, 2H), 1.95-1.87 (m, 2H), 1.85-1.78 (m, 2H). ^{13}C NMR (150 MHz, $CDCl_3$): δ 166.1, 131.1, 128.2, 75.5, 63.4, 24.7, 24.4. IR (cm^{-1}) v = 2966, 1721, 1637, 1409, 1296, 1222, 1185, 1064, 1032, 984, 903, 810, 702, 623, 579. EA calculated for $C_7H_{11}ClO_6$ (226.02): C 37.10, H 4.89, O 42.36; found: C 37.33, H 4.91, O 42.20.

Preparation of 4-Perchloratobutyl Methacrylate (pCBMA)

Silver perchlorate (0.85 g, 3.7 mmol, 1.3 eq.) was suspended in pentane (24 mL) and cooled to −20°C. Under vigorous stirring, methacryloyl chloride (0.24 mL, 2.9 mmol, 1 eq.) was added, and the reaction mixture was allowed to warm to room temperature. The suspension was stirred for 1 h and brownish silver chloride precipitated. The mixture was again cooled to -20°C before THF (0.24 mL, 2.9 mmol, 1 eq.) in 2 mL of pentane was added dropwise. The reaction mixture was subsequently stirred for another hour at room temperature. The salt was removed by filtration through a pad of silica gel, and the resulting clear solution was dried over molecular sieve 4 Å for at least 12 h before further use. The solution was again filtered, and the solvent was removed under reduced pressure. pCBMA was obtained as a clear liquid in 30 % yield. It is reactive towards water and was stored in a solution of pentane under nitrogen atmosphere at -36°C. It does not explode in the hammer test[151].

^{1}H NMR (600 MHz, $CDCl_3$): δ 6.09 (s, 1H), 5.57 (t, *J* = 1.5 Hz, 1H), 4.59 (t, *J* = 6.3 Hz, 2H), 4.19 (t, *J* = 6.2 Hz, 2H), 1.95-1.89 (m, 5H), 1.86-1.80 (m, 2H). ^{13}C NMR (150 MHz, $CDCl_3$): δ 167.4, 136.2, 125.8, 75.5, 63.6, 24.8, 24.5, 18.3. IR (cm^{-1}) v = 2963, 1715, 1637, 1404, 1296, 1224, 1160, 1032, 914, 814, 703, 625, 579. EA calculated for $C_8H_{13}ClO_6$ (240.04): C 39.93, H 5.45, O 39.89; found: C 43.29, H 5.57, O 38.46.

Preparation of 4-Perchloratopentyl Acrylate (pCPA)

Silver perchlorate (0.67 g, 3.2 mmol, 1.1 eq.) was suspended in pentane (12 mL) and cooled to -10°C. Under vigorous stirring acryloyl chloride (0.24 mL, 2.9 mmol, 1 eq.) was added and the reaction mixture was allowed to warm to room temperature. The suspension was stirred for 1h and brownish silver chloride precipitates. The mixture was again cooled to -20°C before 2-methyltetrahydrofuran (0.3 mL, 2.9 mmol, 1 eq.) was added dropwise and the reaction mixture subsequently stirred for another hour at room temperature. The salt was removed by

filtration through a pad of silica gel and the resulting clear solution dried over molecular sieve 4 Å for at least 24 h. pCPA was obtained as a clear liquid but decomposes quickly even in solution of $CDCl_3$ at room temperature.

^{1}H NMR (600 MHz, $CDCl_3$): δ 6.42 (dd, *J* = 17.3, 1.5 Hz, 1H), 6.15 (t, *J* = 17.3, 10.4 Hz, 1H), 5.87 (t, *J* = 10.4, 1.5 Hz, 1H), 5.19 – 5.07 (m, 1H), 4.26 – 4.12 (m, 2H), 1.92 - 1.73 (m, 4H), 1.53 (d, *J* = 6.3 Hz, 3H).

General polymerization procedure for the preparation of pCBA copolymers

A solution of (meth)acrylate (1.4 mL), pCBA and AIBN (40 mg, 0.25 mmol) in toluene (6.5 mL) was purged for 30 min with nitrogen and subsequently heated to 60°C for 30 min. The mixture was allowed to cool to room temperature and poured into cold pentane. The overlaying solution was discarded, polymers were redissolved in dichloromethane, and the procedure was repeated one more time. The precipitated polymers were dried under reduced pressure until a constant weight was attained.

General polymerization procedure for the preparation of high molecular weight HEA/HBA copolymers

A solution of EA (3.0 mL, 28 mmol), hydroxy-functional acrylate and AIBN (80 mg, 0.48 mmol) in toluene (13 mL) was purged for 30 min with nitrogen and subsequently heated at 65°C for 60 min. The mixture was allowed to cool to room temperature and poured into cold pentane. The polymer was collected, redissolved in dichloromethane, and the procedure was repeated one more time. The precipitated polymers were dried under reduced pressure until constant weight was attained.

General polymerization procedure for the preparation of low molecular weight HEA copolymers

A solution of EA (6.0 mL, 56 mmol), HEA (0.9 mL, 8.3 mmol), AIBN (200 mg, 1.2 mmol) and CTA (DDM (0.2 mL, 0.8 mmol) or CBr_4 (0.2 g, 0.6 mmol)) in ethanol (6 mL) was added dropwise over a period of 180 min to degassed ethanol (6 mL) at 78°C. The mixture was allowed to cool to room temperature and poured into cold pentane. The polymer was collected, redissolved in dichloromethane, and the procedure was repeated one more time. The precipitated polymers were dried under reduced pressure until constant weight was attained.

Preparation of Acrylic Anhydride

AA (1.9 mL, 27 mmol, 1.0 eq.) was added dropwise to a mixture of acryloyl chloride (2.5 mL, 30 mmol, 1.1 eq.), triethylamine (3.8 mL, 27 mmol, 1.0 eq.) and THF (50 mL) at 0°C. The suspension was stirred at 40°C for 2 h. THF was removed under reduced pressure and dichloromethane (100 mL) was added to the residue. The organic layer was washed with $NaHCO_3$-solution (2 x 100 mL) and brine (1 x 50 mL), dried over Na_2SO_4 and the solvent was removed under reduced pressure. The residue was vacuum distilled at 60°C to afford acrylic anhydride (1.5 g, 44% yield) as a clear liquid.

^{1}H NMR (300 MHz, $CDCl_3$): δ 6.57 (dd, *J* = 16.9, 1.3 Hz, 2H), 6.19 (dd, *J* = 16.9, 10.5 Hz, 2H), 6.04 (dd, *J* = 10.4, 1.4 Hz, 2H)[192].

Preparation of Poly(ethyl acrylate-*co*-acrylic anhydride)

A solution of EA (1.4 mL, 13 mmol), acrylic anhydride (0.32 mL, 2.7 mmol), AIBN (40 mg, 0.25 mmol) in toluene (6.5 mL) was purged for 30 min with nitrogen and subsequently heated to 70°C for 24 h. The mixture was allowed to cool to room temperature and washed several times with dichloromethane. The polymer was dried under vacuum at 70°C until constant weight was attained. The resulting polymer was characterized by means of ^{13}C CP MAS NMR spectroscopy (Figure 46).

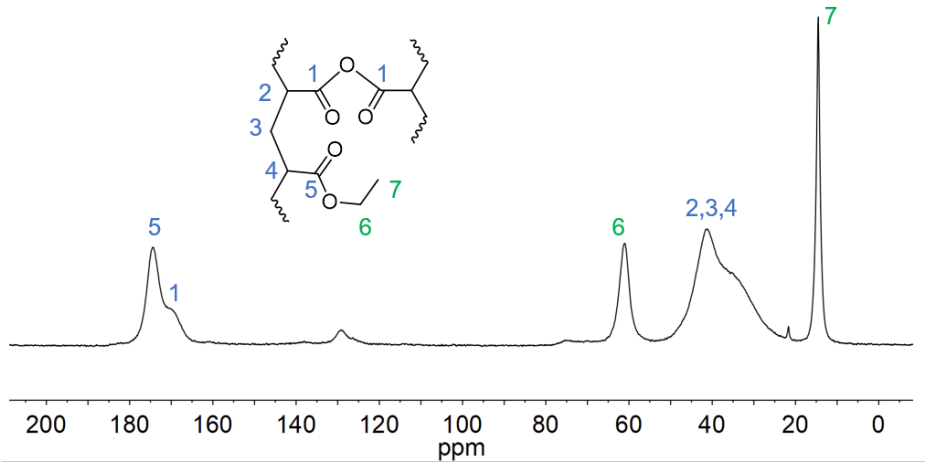

Figure 46. ^{13}C CP MAS NMR spectrum of poly(EA-*co*-acrylic anhydride); Residual signals at ~130 ppm originate from unreacted acrylic double bonds[137].

Preparation of Poly(ethyl acrylate-*co*-1,4-butanediol diacrylate)

A solution of EA (1.4 mL, 13 mmol), BDDA (0.48 mL, 2.5 mmol), AIBN (40 mg, 0.25 mmol) in toluene (6.5 mL) was purged for 30 min with nitrogen and subsequently heated to 70°C for 24h. The mixture was allowed to cool to room temperature and washed several times with dichloromethane. The polymer was dried under vacuum at 70°C until constant weight was attained. The resulting polymer was analyzed by means of ^{13}C CP MAS NMR spectroscopy (Figure 18. ^{13C} CP MAS NMR spectrum of cured (a) P(MA-pCBA11), (b) P(EA-pCBA8), and (c) P(EA-BDDA16)[137].).

Preparation of Ethylene Glycol Diacrylate

Acryloyl chloride (5.3 mL, 65 mmol, 1.1 eq.) was added dropwise to a mixture of HEA (6.3 mL, 59 mmol, 1.0 eq.), triethylamine (10 mL, 71 mmol, 1.2 eq.), and dichloromethane (50 mL) at 0°C. The suspension was stirred for 24h at room temperature. Dichloromethane (100 mL) was added, and the organic layer was washed with $NaHCO_3$-solution (2 × 100 mL) and brine (1 × 50 mL), dried over Na_2SO_4. The solvent was removed under reduced pressure, and the residue was distilled at 60°C in vacuum to afford ethylene glycol diacrylate (6.5 g, 65 % yield) as a clear liquid.

^1H NMR (300 MHz, $CDCl_3$): δ 6.44 (dd, *J* = 17.3, 1.5 Hz, 2H), 6.15 (dd, *J* = 17.3, 10.4 Hz, 2H), 5.87 (dd, *J* = 10.4, 1.5 Hz, 2H), 4,41 (s, 4H) [193].

Preparation of Poly(methyl acrylate-*co*-ethylene glycol diacrylate)

A solution of MA (1.4 mL, 15 mmol), EGDA (0.45 mL, 2.8 mmol) and AIBN (40 mg, 0.25 mmol) in toluene (6.5 mL) was purged for 30 min with nitrogen and subsequently heated to 70°C and kept at that temperature for 22h. The mixture was allowed to cool to room temperature and washed several times with dichloromethane. The resulting polymer was dried under vacuum at 70°C until constant weight was attained.

Preparation of Diethylene Glycol Diacrylate

Acryloyl chloride (8.5 mL, 0.10 mol, 4.0 eq.) in dichloromethane (50 mL) was slowly added to a mixture of diethylene glycol (2.4 mL, 25 mmol, 1.0 eq.), triethylamine (17 mL, 0.12 mol, 4.8 eq.), and dichloromethane (150 mL) at room temperature. After complete addition, the mixture was heated to 40°C and kept at that temperature for 2h. The precipitate was filtered off, and the

solvent was removed under reduced pressure. The residue was dissolved in a 3:1 ratio of pentane and ethyl acetate and filtered through a pad of silica gel. The solvent was removed under reduced pressure to afford diethylene glycol diacrylate (3.4 g, 60% yield) as a clear liquid.

^{1}H NMR (300 MHz, $CDCl_3$): δ 6.43 (dd, *J* = 17.3, 1.5 Hz, 2H), 6.15 (dd, *J* = 17.3, 10.4 Hz, 2H), 5.85 (dd, *J* = 10.4, 1.5 Hz, 2H), 4.35 – 4.29 (m, 4H), 3.79 – 3.73 (m, 4H) [194].

Preparation of Poly(methyl acrylate-*co*-diethylene glycol diacrylate)

A solution of MA (1.4 mL, 15 mmol), DEGDA (0.50 mL, 2.3 mmol), AIBN (40 mg, 0.25 mmol) in toluene (6.5 mL) was purged for 30 min with nitrogen and subsequently heated to 70°C and kept at that temperature for 22h. The mixture was allowed to cool to room temperature and washed several times with dichloromethane. The remaining polymer was dried under vacuum at 70°C until a constant weight was attained.

Preparation of *n*-Decyl Perchlorate

1.0 mL 1-Bromodecane (4.6 mmol, 1.0 eq.) was added to a stirred suspension of 1.2 g silver perchlorate (5.9 mmol, 1.3 eq.) in 15 mL benzene and the mixture stirred for 14 days at room temperature before it was heated to 60°C for 24h. The mixture was filtered through a pad of silica gel to remove the precipitated salt and traces of perchloric acid. The solvent was removed under reduced pressure to afford *n*-decyl perchlorate (1.0 g, 92% yield) as a clear liquid.

^{1}H NMR (300 MHz, $CDCl_3$): δ 4.54 (t, *J* = 6.6 Hz, 2H), 1.86 – 1.74 (m, 2H), 1.48 – 1.20 (m, 14H), 0.88 (t, *J* = 6.5 Hz, 3H)[113]. IR (cm^{-1}) v = 2923, 2856, 1467, 1378, 1259, 1224, 1031, 962, 914, 867, 703, 624, 580, 416.

7 Bibliography

[1] a) M. Webb, *Lacquer: technology and conservation*. *a comprehensive guide to the technology and conservation of Asian and European lacquer*, Butterworth-Heinemann, Oxford, **2000**; b) F. S. Kleiner, *Gardner's Art Through The Ages: A Global History*, Wadsworth Publishing Co Inc, Boston: Wadsworth, **2012**; c) J. Hang, Q. Guo, *Chinese arts & crafts*, Cambridge University Press, Beijing: China, **2012**.

[2] can be found under https://megalodon.jp/2020-0707-0601-44/https://en.visit-hokkaido.jp:443/what-to-do/kakinoshima-jomon-archaeological-site/, **2022**.

[3] Koncept Analytics, *Global Paints and Coatings Market Report: Insights, Trends and Forecast (2019-2023)*, **2019**.

[4] Fortune Business Insights, *Paints and Coatings Market Size, Share and COVID-19 Impact Analysis*, **2021**.

[5] R. Talbert, *Paint technology handbook*, CRC Press Taylor & Francis, Boca Raton, Fla., **2007**.

[6] A. A. Tracton (Ed.) *Coatings Materials and Surface Coatings*, CRC Press, Boca Raton, Fla., **2006**.

[7] U. Poth, R. Schwalm, M. Schwartz, *Acrylic Resins*, Vincentz Network, Hanover, Germany, **2011**.

[8] H.-J. Streitberger, K.-F. Dössel, *Automotive Paints and Coatings*, Wiley, **2008**.

[9] a) H. Dodoiuk, S. H. Goodman (Eds.) *Handbook of Thermoset Plastics*, Elsevier, **2014**; b) R. Lambourne, T. A. Strivens, *Paint and surface coatings*. *Theory and practice*, Woodhead Pub. Ltd, Cambridge Eng., **1999**.

[10] R. Sharma, *Thermosetting Acrylic Resin Market Research Report 2033*, **2024**.

[11] F. N. Jones, *Organic coatings*. *Science and technology*, John Wiley & Sons Inc, Hoboken, NJ, USA, **2017**.

[12] K. Zhang, Z. Wang, Y. Luo, *Colloids Surf. A: Physicochem. Eng. Asp.* **2024**, *683*, 133045.

[13] T. Güthner, B. Hammer, *J. Appl. Polym. Sci.* **1993**, *50*, 1453.

[14] S. Liu, Z. Shen, J. Li, Z. Sun, W. Cui, Y. Li, Q. Liu, E. Yu, Y. Shen, Q. Liu et al., *Small* **2025**, *21*, e2408968.

[15] M. N. Ashraf, S. M. Khan, S. Munir, R. Saleem, *J. Am. Leather Chem. Assoc.* **2020**, *115*, 132.

[16] D. Gonçalves, J. M. Bordado, A. C. Marques, R. Galhano Dos Santos, *Polymers* **2021**, *13*, 4086.

[17] B. Müller, U. Poth, *Coatings formulation*. *An international textbook*, Vincentz Network, Hanover, Germany, **2011**.

[18] G. Y. Tilak, *Progress in Organic Coatings* **1985**, *13*, 333.

[19] R. W. Ryan, M. B. Walt (Eds.) *Proc. Waterborne High-Solids Powder Coat. Symp.*, New Orleans, LA, **1994**.

[20] S.-H. Guo, US5480943A, **1996**.

[21] W. J. Blank, *J. Coat. Technol.* **1979**, *51*, 61.

[22] a) F. Börner, M. Jobmann, M. Hahn, EP3041875A1, **2013**; b) R. Saleem, A. Adnan, A. F. Qureshi, US20170058073A1, **2015**; c) J. Zhou, P. Li, J. Zhou, X. Liao, B. Shi, *J. Am. Leather Chem. Assoc.* **2018**, *113*, 198.

[23] M. Szycher, *Szycher's handbook of polyurethanes*, Taylor & Francis, Boca Raton FL, **2013**.

[24] a) P. A. Berlin, et al., *Kinet. Katal.* **1993**, *34*, 640; b) N. Yu, et al., *Kinet. Catal. (Engl. Ed.)* **1995**, *36*, 612.

[25] a) Y. Hira, S. Tsuzuku, M. Gotoh, H. Yokono, M. Hatano, *Polym. Mater. Sci. Eng.* **1983**, *49*, 336; b) M. Sato, *J. Am. Chem. Soc.* **1960**, *82*, 3893.

[26] W. J. Blank, Z. A. He, E. T. Hessell, *Prog. Org. Coat.* **1999**, *35*, 19.

[27] a) E. P. Squiller, J. W. Rosthauser, *Mod. Paint Coat.* **1987**, 28; b) S.-G. Luo, H.-M. Tan, J.-G. Zhang, Y.-J. Wu, F.-K. Pei, X.-H. Meng, *J. Appl. Polym. Sci.* **1997**, *65*, 1217; c) S.-W. Wong, K. C. Frisch, *J. Polym. Sci. A Polym. Chem.* **1986**, *24*, 2867.

[28] L. Thiele, R. Becker, H. Frommelt, *Zeitschr. für Polymerforschung* **1977**, *28*, 405.

[29] a) D. A. Wicks, Z. W. Wicks, *Prog. Org. Coat.* **1999**, *36*, 148; b) D. A. Wicks, Z. W. Wicks, *Prog. Org. Coat.* **2001**, *41*, 1; c) Z. W. Wicks, *Prog. Org. Coat.* **1975**, *3*, 73; d) Z. W. Wicks, *Prog. Org. Coat.* **1981**, *9*, 3.

[30] W. J. Mijs, W. J. Muiebelt, J. B. Reesingk, *J. Coat. Technol.* **1983**, *55*, 45.

[31] G. Daude, P. Girard, US4623592A, **1996**.

[32] U. Rockrath, G. Wigger, U. Poth, US5516559A, **1996**.

[33] M. Ooka, H. Ozawa, *Prog. Org. Coat.* **1994**, *23*, 325.

[34] T. Agawa, E. D. Dumain in *Proc. Waterborne High-Solids Powder Coat. Symp,* New Orleans, LA, **1997**, 342.

[35] W. J. Blank, Z. A. He, M. Picci, *J. Coating Technol.* **2002**, *74*, 33.

[36] A. Fushimi, Y. Okude, S. Ishikura, *Prog. Org. Coat.* **2001**, *42*, 159.

[37] C. Flosbach, W. Schubert, *Prog. Org. Coat.* **2001**, *43*, 123.

[38] S. Sun, P. Sun, D. Liu, *Eur. Polym. J.* **2005**, *41*, 913.

[39] D. Stanssens, R. Hermanns, H. Wories, *Prog. Org. Coat.* **1993**, *22*, 379.

[40] a) J. W. Rehfuss, D. L. St. Aubin, US5356669A, **1994**; b) M. L. Green, *J. Coat. Technol.* **2001**, *73*, 55; c) J. W. Rehfuss, D. L. St. Aubin, US5474811A, **1992**.

[41] R. S. Porzio, et al. in *Proc. Waterborne High-Solids Powder Coat. Symp.,* New Orleans, LA, **2003**, pp. 129–143.

[42] J. E. Goldstein, H. van Boxtel, S. P. Pauls, EP2106469A1, **2008**.

[43] D. C. Webster, *Prog. Org. Coat.* **2003**, *47*, 77.

[44] a) W. H. Ohrborn, T. S. December, P. J. Harris, US5856382; b) T. S. December, P. J. Harris, US5431791A; c) T. S. December, P. J. Harris, US6184273B1, **2001**.

[45] P. J. Geurink, L. van Dalen, L. G. van der Ven, R. R. Lamping, *Prog. Org. Coat.* **1996**, *27*, 73.

[46] J. C. Graham, T. Li, *J. Coat. Technol.* **1993**, *65*, 64.

[47] J. W. Taylor, M. A. Winnik, *J Coat. Technol. Res.* **2004**, *1*, 163.

[48] D. R. Bauer, *Prog. Org. Coat.* **1986**, *14*, 193.

[49] L. J. Calbo, *J. Coat. Technol.* **1980**, *52*, 75.

[50] M. G. Lazzara, *J. Coat. Technol.* **1984**, *56*, 19.

[51] S. Parvate, P. Mahanwar, *J. Disper. Sci. Technol.* **2019**, *40*, 519.

[52] S. Fourdrin, M. Rochery, M. Lewandowski, M. Ferreira, S. Bourbigot, *J. Appl. Polym. Sci.* **2006**, *99*, 1117.

[53] C. Koukiotis, I. D. Sideridou, *Prog. Org. Coat.* **2010**, *69*, 504.

[54] a) T. Johansson, L. Weidolf, F. Popp, R. Tacke, U. Jurva, *Drug. Metab. Dispos.* **2010**, *38*, 73; b) Z.-G. Sun, D.-Q. Fan, S.-Q. Huang, *J. Appl. Polym. Sci.* **2009**, *111*, 185.

[55] a) J. R. Rodgers, US3320196A, **1965**; b) J. R. Rodgers, US3308078A, **1965**.

[56] a) Z. Czech, A. Butwin, U. Głuch, J. Kabatc, *J. Appl. Polym. Sci.* **2012**, *123*, 118; b) Z. Czech, M. Wojciechowicz, *Eur. Polym. J.* **2006**, *42*, 2153; c) J. M. Shaffer, T. L. Eifolla, US8236903B2, **2012**.

[57] a) R. T. Gray, J. M. Owens, H. S. Killam, US5574090A, **1996**; b) J. W. Taylor, M. Brink, A. Meer, US7470751B2, **2008**; c) R. E. Zdanowski, J. M. Owens, US4517330, **1985**.

[58] W. Yan, X. Zhang, Y. Zhu, H. Chen, *Iran Polym. J.* **2012**, *21*, 631.

[59] a) T. Friedrich, B. Tieke, F. J. Stadler, C. Bailly, *Soft Matter* **2011**, *7*, 6590; b) Z. Pu, Y. Chen, Le Zhang, L. Wang, Q. Zhang, *Rare Met.* **2011**, *30*, 657; c) W. Rongmin, Z. Wenzhong, H. Chen, H. Yufeng, Q. Wenzhen, CN104829775A, **2015**.

[60] F. Stadion, *Ann. Phys. (Leipzig)* **1816**, *22*, 197.

[61] W. Müller, P. Jönck, *Chem. Ing. Tech.* **1963**, *35*, 78.

[62] H. Vogt, J. Balej, J. E. Bennett, P. Wintzer, S. A. Sheikh, P. Gallone in *Ullmann's Encyclopedia of Industrial Chemistry*, Wiley-VCH Verlag GmbH & Co. KGaA, Weinheim, Germany, **2000**.

[63] a) O. Hackl, *Fresenius Z. Anal. Chem.* **1936**, *107*, 385; b) R. C. Nester, G. F. Vander Voort, *Safety in the Metallographic Laboratory*, ASTM Standardization News, **1992**; c) J. W. Reed, *Analysis of the Accidental Explosion at Pepcon, Henderson, Nevada, May 4, 1988*, **1988**; d) E. G. Young, R. B. Campbell, *Science* **1946**, *104*, 353; e) V. Zahn, *Ind. Eng. Chem., News Ed.* **1937**, *15*, 214.

[64] J. Meyer, W. Spormann, *Z. Anorg. Allg. Chem.* **1936**, *107*, 341.

[65] a) M. Dode, *Bull. Soc. Chim. France* **1938**, *5*, 170; b) M. Dode, *Bull. Soc. Chim. France* **1938**, *5*, 176.

[66] a) R. E. Tarone, L. Lipworth, J. K. McLaughlin, *J. occup. environ. med.* **2010**, *52*, 653; b) F. Wu, H. Chen, X. Zhou, R. Zhang, M. Ding, Q. Liu, K. Peng, *Arch. environ. occup. h.* **2013**, *68*, 161; c) L. E. Braverman, X. He, S. Pino, M. Cross, B. Magnani, S. H. Lamm, M. B. Kruse, A. Engel, K. S. Crump, J. P. Gibbs, *J. clin. endocr. metab.* **2005**, *90*, 700.

[67] S. Susarla, T. W. Collette, A. W. Garrison, N. L. Wolfe, S. C. McCutcheon, *Environ. Sci. Technol.* **1999**, *33*, 3469.

[68] M. Di, S. Li, C. Liang, *Corros. Sci.* **2009**, *51*, 713.

[69] V. V. Boldyrev, *Thermochim. Acta* **2006**, *443*, 1.

[70] U.S. Environmental Protection Agency, National Center for Environmental Assessment, *Perchlorate Environmental Contamination: Toxicological Review and Risk Characterization (External Review Draft)*, Washington, DC, **2002**.

[71] R. Dalpozzo, G. Bartoli, L. Sambri, P. Melchiorre, *Chem. Rev.* **2010**, *110*, 3501.

[72] J. C. Schumacher, *Perchlorates: Their Properties, Manufacture, and Uses*, Reinhold Publishing Corporation, New York, **1960**.

[73] A. M. Leung, E. N. Pearce, L. E. Braverman, *Best Pract. Res. Cl. En.* **2010**, *24*, 133.

[74] A. Trummal, L. Lipping, I. Kaljurand, I. A. Koppel, I. Leito, *J. Phy. Chem. A* **2016**, *120*, 3663.

[75] a) G. F. Smith, O. E. Goehler, *Ind. Eng. Chem., Anal. Ed.* **1931**, *3*, 58; b) F. S. Lee, G. B. Carpenter, *J. Phys. Chem.* **1959**, *63*, 279.

[76] C. P. Wright, D. M. Murray-Rust, H. Hartley, *Analyst* **1931**, 199.

[77] D. M. Murray-Rust, H. J. Hadow, H. Hartley, *Analyst* **1931**, 215.

[78] D. M. Hoffman, *J. Org. Chem.* **1971**, *36*, 1916.

[79] M. A. Bigdeli, M. M. Heravi, G. H. Mahdavinia, *J. Mol. Catal. A: Chem.* **2007**, *275*, 25.

[80] H. Burton, P. F. G. Praill, *Analyst* **1955**, *80*, 4.

[81] Hare, C. Boye, M. H., *Phil. Mag.* **1841**, *19*, 370.

[82] N. S. Zefirov, V. V. Zhdankin, A. S. Koz'min, *Russ. Chem. Rev.* **1988**, *57*, 1041.

[83] J. Radell, J. W. Connolly, A. J. Raymond, *J. Am. Chem. Soc.* **1961**, *83*, 3958.

[84] W. R. Longworth, P. H. Pleasch, *Proc. Chem. Soc.* **1958**, 117.

[85] K. Baum, C. D. Beard, *J. Am. Chem. Soc.* **1974**, *96*, 3233.

[86] C. A. Wamser, W. B. Fox, D. Gould, B. Sukornick, *Inorg. Chem.* **1968**, *7*, 1933.

[87] K. Baum, C. D. Beard, *J. Org. Chem.* **1975**, *40*, 81.

[88] Y. Pocker, D. N. Kevill, *J. Am. Chem. Soc.* **1965**, *87*, 5060.

[89] C. D. Beard, K. Baum, *J. Org. Chem.* **1974**, *39*, 3875.

[90] a) R. I. Davidson, P. J. Kropp, *J. Org. Chem.* **1982**, *47*, 1904; b) N. S. Zefirov, V. V. Zhdankin, G. V. Makhon´kova, *J. Org. Chem.* **1985**, *50*, 1872; c) K. B. Wiberg, W. E. Pratt, M. G. Matturro, *J. Org. Chem.* **1982**, *47*, 2720; d) G. A. Olah, J. Welch, *Synthesis* **1977**, 419.

[91] D. M. Hoffman, *J. Org. Chem.* **1971**, *36*, 1716.

[92] K. Baum, *J. Org. Chem.* **1976**, *41*, 1663.

[93] S. J. Tauber, A. M. Eastham, *J. Am. Chem. Soc.* **1960**, *82*, 4888.

[94] C. J. Schack, K. O. Christe, *Inorg. Chem.* **1979**, *18*, 2619.

[95] N. S. Zefirov, A. S. Koz'min, V. V. Zhdankin, A. V. Nikulin, N. V. Zyk, *J. Org. Chem.* **1982**, *47*, 3679.

[96] D. N. Kevill, W. A. Reis, J. B. Kevill, *Tetrahedron Lett.* **1972**, *13*, 957.

[97] a) J. F. King, S. M. Loosmore, M. Aslam, J. D. Lock, M. J. McGarrity, *J. Am. Chem. Soc.* **1982**, *104*, 7108; b) J. F. King, S. M. Loosmore, J. D. Lock, M. Aslam, *J. Am. Chem. Soc.* **1978**, *100*, 1637.

[98] J. Engberts, B. Zwanenburg, *Tetrahedron Lett.* **1967**, *8*, 831.

[99] C. J. Schack, D. Pilipovich, K. O. Christe, *Inorg. Chem.* **1975**, *14*, 145.

[100] V. I. Bondar´, T. F. Rau, V. G. Rau, *Cryst. Struct. Somm.* **1981**, *10*, 587.

[101] A. Bruggink, B. Zwanenburg, J. Engberts, *Tetrahedron* **1969**, *25*, 5655.

[102] H. Burton, P. F. G. Praill, *J. Chem. Soc.* **1953**, 827.

[103] C. J. Schack, K. O. Christe, *Inorg. Chem.* **1974**, *13*, 2374.

[104] D. N. Kevill, G. M. L. Lin, *Tetrahedron Lett.* **1978**, *19*, 949.

[105] a) C. D. Beard, K. Baum, US4165332A, **1979**; b) J.-R. Pougny, U. Kraska, P. Sinaÿ, *Carbohyd. Res.* **1978**, *60*, 383; c) A. R. Katritzky, J. W. Suwinski, *Tetrahedron* **1975**, *31*, 1549; d) L. Bohé, D. Crich, *Carbohyd. Res.* **2015**, *403*, 48.

[106] a) J. P. Hermans, G. Smets, *J. Polym. Sci. A Gen. Pap.* **1965**, *3*, 3175; b) T. Higashimura, O. Kishiro, *J. Polym. Sci. Polym. Chem. Ed.* **1974**, *12*, 967; c) B. MacCarthy, W. P. Millrine, D. C. Pepper, *Chem. Commun.* **1968**, 1442.

[107] R. L. D. Whitby, L. C. Smith, G. Dichello, T. Fukuda, T. Maekawa, S. V. Mikhalovsky, *Mat Express* **2014**, *4*, 242.

[108] a) DE2356531A; b) E. Baeder, H. Amann, DE2003270A; c) B. Sander, US3775370A.

[109] D. N. Kevill, B. W. Shen, *J. Am. Chem. Soc.* **1981**, *103*, 4515.

[110] D. N. Kevill, H. S. Posselt, *J. Chem. Soc., Perk. T. 2* **1984**, 909.

[111] D. N. Kevill, H. R. Adolf, *Tetrahedron Lett.* **1976**, *17*, 4811.

[112] M. C. Cauquil, M. H. Barrera, *Bull. Soc. Chim. France* **1951**, 124.

[113] N. V. Yashin, E. B. Averina, Y. K. Grishin, T. S. Kuznetsova, N. S. Zefirov, *Russ. Chem. Bull.* **2016**, *65*, 1873.

[114] N. V. Yashin, P. O. Markov, K. N. Sedenkova, D. A. Vasilenko, Y. K. Grishin, T. S. Kuznetsova, E. B. Averina, *Russ. Chem. Bull.* **2020**, *69*, 980.

[115] D. N. Kevill, G. M. L. Lin, M. S. Bahari, *J. Chem. Soc., Perk. T. 2* **1981**, 49.

[116] A. S. Koz´min, V. V. Zhdankin, G. V. Komolova, P. B. Terentev, *Zjur. Org. Khim.* **1983**, *19*, 1892.

[117] H. Staudinger, *Die Hochmolekularen Organischen Verbindungen - Kautschuk und Cellulose* -, Springer Berlin Heidelberg, Berlin, Heidelberg, **1932**.

[118] V. Schamboeck, P. D. Iedema, I. Kryven, *Sci. Rep.* **2019**, *9*, 2276.

[119] J. L. Mann, R. L. Rossi, A. A. A. Smith, E. A. Appel, *Macromolecules* **2019**, *52*, 9456.

[120] G. Tillet, B. Boutevin, B. Ameduri, *Prog. Polym. Sci.* **2011**, *36*, 191.

[121] M. S. Silverstein, *Polymer* **2020**, *207*, 122929.

[122] C. W. H. Rajawasam, O. J. Dodo, M. A. S. N. Weerasinghe, I. O. Raji, S. V. Wanasinghe, D. Konkolewicz, N. de Alwis Watuthanthrige, *Polym. Chem.* **2024**, *15*, 219.

[123] P. J. Flory, *J. Am. Chem. Soc.* **1941**, *63*, 3083.

[124] P. J. Flory, *J. Phys. Chem.* **1942**, *46*, 132.

[125] W. H. Stockmayer, *J. Chem. Phys.* **1943**, *11*, 45.

[126] E. B. Trostyanskaya, P. G. Babaevskii, *Russ. Chem. Rev.* **1971**, *40*, 64.

[127] K. Dušek, M. Dušková-Smrčková, *Prog. Polym. Sci.* **2000**, *25*, 1215.

[128] K. Dušek, *Polym. Gels Networks* **1996**, *4*, 383.

[129] a) K. S. Anseth, C. N. Bowman, *Chem. Eng. Sci.* **1994**, *49*, 2207; b) A. G. Mikos, C. G. Takoudis, N. A. Peppas, *Macromolecules* **1986**, *19*, 2174; c) H. Tobita, A. E. Hamielec, *Makromol Chem. Macromol. Symp.* **1988**, *20-21*, 501.

[130] Y. Gu, J. Zhao, J. A. Johnson, *Trends Chem.* **2019**, *1*, 318.

[131] S. Dutton, R. F. T. Stepto, D. J. R. Taylor, *Angew. Makromol. Chem.* **1996**, *240*, 39.

[132] a) D. C. Doherty, B. N. Holmes, P. Leung, R. B. Ross, *Comput. Theo. Polym. Sci.* **1998**, *8*, 169; b) K.-J. Lee, B. E. Eichinger, *Polymer* **1990**, *31*, 406.

[133] a) S. Panyukov, Y. Rabin, *Phys. Rep.* **1996**, *269*, 1; b) R. T. Deam, S. F. Edwards, *Phil. Trans. R. Soc. Lond. A* **1976**, *280*, 317.

[134] S. Panyukov, *Polymers* **2020**, *12*.

[135] M. Rubinstein, S. Panyukov, *Macromolecules* **2002**, *35*, 6670.

[136] T. Okumuto, H. Mizuno, K. Watanabe, *Nippon Gomu Kyokaishi* **1995**, *68*, 244.

[137] G. A. Luinstra, P. Wienefeld, *J. Appl. Polym. Sci.* **2025**, *142*, e56980.

[138] a) M. Abedini, F. Shirini, M. Mousapour, *Res. Chem. Intermed.* **2016**, *42*, 2303; b) E. Ülker, M. Kavanoz, *J. Brazil. Chem. Soc.* **2015**, *26*, 1947; c) N. G. Khaligh, F. Shirini, *Ultrason. Sonochem.* **2013**, *20*, 26.

[139] D. A. Tomalia, US3417062, **1968**.

[140] S. J. Kim, B. S. Min, H. B. Jeon, H. J. Baek, J. Y. Jung, G. H. Kim, D. S. Jang, Y. Y. Kang, S. H. Lee, H. I. Ju, KR20210075577A, **2021**.

[141] Y.-H. Chang, P.-Y. Lin, M.-S. Wu, K.-F. Lin, *Polymer* **2012**, *53*, 2008.

[142] K. A. Hofmann, G. A. Zedtwitz, H. Wagner, *Ber. Dtsch. Chem. Ges.* **1909**, *42*, 4390.

[143] M. A. Pasha, M. B. M. Reddy, K. Manjula, *Eur. J. Chem.* **2010**, *4*, 385.

[144] M. H. Sarvari, H. Sharghi, *Tetrahedron* **2005**, *61*, 10903.

[145] J. Iqbal, R. R. Srivastava, *J. Org. Chem.* **1992**, *57*, 2001.

[146] G. Bartoli, M. Bosco, E. Marcantoni, M. Massaccesi, S. Rinaldi, L. Sambri, *Tetrahedron Lett.* **2002**, *43*, 6331.

[147] A. J. Liston, P. Toft, *J. Org. Chem.* **1968**, *33*, 3109.

[148] a) S. D. Nicholas, F. Smith, *Nature* **1948**, *161*, 349; b) E. P. Painter, *J. Am. Chem. Soc.* **1953**, *75*, 1137; c) B. Whitman, E. Schwenk, *J. Am. Chem. Soc.* **1946**, *68*, 1865.

[149] R. Alamo, J. Guzmán, J. G. Fatou, *Makromol. Chem.* **1981**, *182*, 725.

[150] Y. Eckstein, P. Dreyfuss, *J. Inorg. Nucl. Chem.* **1981**, *43*, 23.

[151] K. L. Williams, B. W. Harris, *Sensitivity of once-shocked, weathered high explosives*, **1998**.

[152] S. Nakahama, K. Hashimoto, N. Yamazaki, *Polym. J.* **1973**, *4*, 437.

[153] S. K. Sen Gupta, *J. Phys. Org. Chem.* **2017**, *30*, e3605.

[154] L. N. Hill, *J. Coat. Technol.* **1992**, *64*, 28.

[155] S. Aksakal, C. Remzi Becer, *Polym. Chem.* **2016**, *7*, 7011.

[156] G. S. Pearson, *Perchlorates: A Review of their Thermal Decomposition and Combustion, with an Appendix on Perchloric Acid*, Westcott, **1986**.

[157] a) J. R. Ebdon, B. J. Hunt, W. T. S. O'Rourke, J. Parkin, *Brit. Poly. J.* **1988**, *20*, 327; b) M. El Hariri El Nokab, P. C. A. van der Wel, *Carbohyd. Polym.* **2020**, *240*, 116276; c) R. V. Law, D. C. Sherrington, C. E. Snape, I. Ando, H. Kurosu, *Macromolecules* **1996**, *29*, 6284; d) I. A. Udoetok, L. D. Wilson, J. V. Headley, *Ultrason. Sonochem.* **2018**, *42*, 567.

[158] a) A. R. Lim, Y.-J. Kwark, J.-S. Kim, *J. Appl. Phys.* **2003**, *94*, 7351; b) A. Natansohn, C. G. Bazuin, X. Tong, *Can. J. Chem.* **1992**, *70*, 2900.

[159] A. Lim, J.-S. Kim, *Solid State Commun.* **2000**, *115*, 179.

[160] A. R. Greenberg, R. P. Kusy, *J. Appl. Polym. Sci.* **1980**, *25*, 1785.

[161] N. Grassie, J. G. Speakman, *J. Polym. Sci. A1* **1971**, *9*, 919.

[162] I. Coblentz Society in *NIST Chemistry WebBook, NIST Standard Reference Database Number 69* (Eds.: P. J. Linstrom, W. G. Mallard), Gaithersburg MD.

[163] J. Otera, *Chem. Rev.* **1993**, *93*, 1449.

[164] a) Z. I. Zelikman, T. P. Kosulina, V. G. Kul´nevich, G. N. Dorofeenko, L. V. Mezheritskaya, *Chem. Inform.* **1976**, *7*, no-no; b) H. Paulsen, R. Dammeyer, *Chem. Ber.* **1976**, *109*, 1837; c) L. V. Mezheritskaya, G. N. Dorofeenko, *Chem. Heterocycl. Compd.* **1975**, *11*, 761.

[165] a) Y. Yamashita, K. Chiba, *Polym. J.* **1973**, *4*, 200; b) Y. Yamashita, S. Kozawa, M. Hirota, K. Chiba, H. Matsui, A. Hirao, M. Kodama, K. Ito, *Makromol. Chem.* **1971**, *142*, 171; c) K. Matyjaszewski, S. Penczek, E. Franta, *Polymer* **1979**, *20*, 1184; d) P. Dreyfuss, M. P. Dreyfuss in *Advances in Polymer Science* (Eds.: A. Abe, A. Albertsson, G. W. Coates, Genzer. J.), Springer Verlag, **1967**, pp. 528–590.

[166] Y. Nitta, Y. Arakawa, *Chem. Pharm. Bull.* **1985**, *33*, 1380.

[167] F. C. Baines, J. C. Bevington, *J. Polym. Sci. A1* **1968**, *6*, 2433.

[168] Y. Grosse, D. Loomis, K. Z. Guyton, F. El Ghissassi, V. Bouvard, L. Benbrahim-Tallaa, H. Mattock, K. Straif, *Lancet Oncol.* **2017**, *18*, 1003.

[169] G. A. Luinstra, P. Wienefeld, *J. Appl. Polym. Sci.* **2025**, e58087.

[170] H. E. Roscoe, *Annalen* **1862**, *124*, 124.

[171] a) J.-L. Yu, H. Wang, K.-F. Zou, J.-R. Zhang, X. Gao, D.-W. Zhang, Z.-T. Li, *Tetrahedron* **2013**, *69*, 310; b) G. A. Olah, T. Shamma, G. Prakash, *Catal. Lett.* **1997**, *46*, 1; c) S. Karuppannasamy, *J. Catal.* **1980**, *66*, 281; d) B. Boyer, E.-M. Keramane, J.-P. Roque, A. A. Pavia, *Tetrahedron Lett.* **2000**, *41*, 2891; e) J. A. Ballantine, M. Davies, I. Patel, J. Purnell, M. Rayanakorn, K. J. Williams, J. M. Thomas, *J. Mol. Catal.* **1984**, *26*, 37.

[172] G. Oddo, E. Scandola, *Gazzetta Chimica Italiana* **1908**, *38*, 603.

[173] S. S. Mochalov, A. N. Fedotov, E. V. Trofimova, N. S. Zefirov, *Russ. J. Org. Chem.* **2015**, *51*, 1217.

[174] a) K. P. Baran, S. Gad in *Encyclopedia of Toxicology* (Ed.: P. Wexler), Academic Press, Oxford, **2014**, pp. 796–798; b) A. I. Karelin, Z. I. Grigorovich, V. Rosolovskii, *Spectrochim. Acta A: Mol. Biomol. Spectrosc.* **1975**, *31*, 765.

[175] D. J. Merline, S. Vukusic, A. A. Abdala, *Polym. J.* **2013**, *45*, 413.

[176] a) K. Holmberg, *Polym. Bull.* **1984**, *11*, 81; b) D. Garcia, S. R. Sandler, J. Brennan, O. Bousque, *J. Coat. Technol.* **2000**, *72*, 89.

[177] N. J. R. van Eikema Hommes, T. Clark, *J. Mol. Model.* **2005**, *11*, 175.

[178] P. J. Linstrom, W. G. Mallard, *NIST Chemistry WebBook, NIST Standard Reference Database 69*, National Institute of Standards and Technology, **1997**.

[179] a) C.J. Brinker, G.W. Scherer, *J. Non-Cryst. Solids* **1985**, *70*, 301; b) A. Coniglio, H. E. Stanley, W. Klein, *Phys. Rev. Lett.* **1979**, *42*, 518; c) O. Payanda Konuk, Alsuhile, Ala A. A. M., H. Yousefzadeh, Z. Ulker, S. E. Bozbag, C. A. García-González, I. Smirnova, C. Erkey, *Front. Chem.* **2023**, *11*, 1294520; d) R. W. Pekala, D. W. Schaefer, *Macromolecules* **1993**, *26*, 5487.

[180] *Directive 2004/42/EC of the European Parliament and of the Council of 21 April 2004 on the limitation of emissions of volatile organic compounds due to the use of organic solvents in certain paints and varnishes and amending Directive 1999/13/EC*, **2004**.

[181] M. Slinckx, N. Henry, A. Krebs, G. Uytterhoeven, *Prog. Org. Coat.* **2000**, *38*, 163.

[182] L. W. Hill, Z. W. Wicks, *Prog. Org. Coat.* **1982**, *10*, 55.

[183] K. P. C. Vollhardt, N. E. Schore, *Organic Chemistry*. *Structure and Function*, W. H. Freeman & Company, New York, **1998**.

[184] E. M. Arnett in *Progress in Physical Organic Chemistry* (Eds.: S. G. Cohen, A. Streitwieser, R. W. Taft), Wiley, **1963**, pp. 223–403.

[185] T. W. Milligan, B. C. Minor, *J. Org. Chem.* **1963**, *28*, 235.

[186] B. Hendriks, J. Waelkens, J. M. Winne, F. E. Du Prez, *ACS Macro Lett.* **2017**, *6*, 930.

[187] A.-S. Jandel, B. Meuthen, *Coil Coating*, Springer Fachmedien Wiesbaden, Wiesbaden, **2013**.

[188] can be found under https://helios-industrialcoatings.com/.

[189] A. K. Gupta, *Chem. Eng. Commun.* **1986**, *41*, 1.

[190] N. N. Greenwood, A. Earnshaw (Eds.) *Chemistry of the Elements*, Butterworth-Heinemann, Oxford, **1997**.

[191] K. Ding, F. Wang, F. Wu, *J. Photoch. Photobio. A* **2011**, *220*, 64.

[192] C. Pugh, B. Raveendra, A. Singh, R. Samuel, G. Garcia, *Synlett* **2010**, *2010*, 1947.

[193] C. Jiao, L. Gao, B. Yu, H. Cong, Y. Shen, *RSC Adv.* **2019**, *9*, 40455.

[194] M.-M. Xun, Y.-P. Xiao, J. Zhang, Y.-H. Liu, Q. Peng, Q. Guo, W.-X. Wu, Y. Xu, X.-Q. Yu, *Polymer* **2015**, *65*, 45.

[195] "Merck | Germany", can be found under https://www.sigmaaldrich.com/DE/de, **2022**.

8 Appendix

8.1 Safety Data

Table 8. Safety instructions for the chemicals used.[195]

Substance (CAS-No.)	Pictogram	H Phrases	P Phrases
(±)-Epichlorohydrin (106-89-8)		226, 301, 311+331, 314, 317, 350	201, 210, 280, 303+361+353, 304+340+310, 305+351+338
1,1,2,2-Tetrachloroethane-d_2 (33685-54-0)		310+330, 411	262, 273, 280, 302+352+310, 304+340+310
1,4-Butanediol diacrylate (1070-70-8)		302, 332, 311, 314, 317, 412	273, 280, 301+312, 303+361+353, 3ß4+340+310, 305+351+338
1,6-Hexamethylenediamine (124-09-4)		302+312, 314, 335	260, 270, 280, 301+312, 303+361+353, 305+351+338
1-Bromodecane (112-29-8)		315, 319	302+352, 305+351+338
2-Aminopentane (63493-28-7)		226, 314	210, 280, 301+330+331, 303+361+353, 305+351+338+310
2-Bromoethanol (540-51-2)		301+311+331, 314	261, 270, 280, 303+361+353, 304+340+310, 305+351+338
2-Bromoethyl acrylate		315, 319, 335	261, 264b, 271, 280, 302+352, 304+340, 305+351+338, 312, 332+313, 362, 501c
2-Hydroxyethyl acrylate (818-61-1)		302, 311, 314, 317, 410	261, 273, 280, 301+312, 303+361+353, 305+351+338
2-Methyltetrahydrofuran (96-47-9)		225, 302, 315, 318	210, 233, 280, 301+312, 303+361+353, 305+351+338
3,5-bis(trifluoromethyl)benzaldehyde (401-95-6)		315, 319, 335	261, 264, 271, 280, 302+352, 305+351+338
4-Hydroxybutyl acrylate (2478-10-6)		302, 315, 317, 318	261, 264, 280, 301+312, 302+352, 305+351+338

Acetic anhydride (108-24-7)		226, 302, 314, 330	210, 280, 301+312, 303+361+353, 304+340+310, 305+351+338
Acetone (67-64-1)		225, 319, 335	210, 233, 240, 241, 242, 305+351+338
Acetonitrile-d_3 (2206-26-0)		225, 302, 312, 319, 331	210, 280, 301+312, 303+361+353, 304+340+311, 305+351+338
Acetyl chloride (75-36-5)		225, 314	210, 233, 240, 280, 303+361+353, 305+351+338
Acrylic acid (79-10-7)	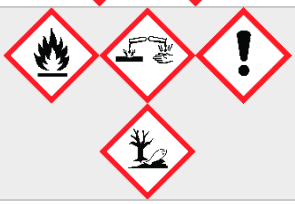	226, 302+312+332, 314, 335, 410	210, 273, 280, 303+361+353, 304+340+310, 305+351+338
Acryloyl chloride (814-68-6)		225, 290, 302, 314, 330	210, 280, 301+312, 303+361+353, 304+340+310, 305+351+338
Azobisisobutyronitrile (78-67-1)		242, 302, 332, 412	210, 235, 273, 304+340+312, 370+378, 403
Benzene (71-43-2)		225, 304, 315, 319, 340, 350, 372, 412	210, 273, 301+310, 303+361+353, 305+351+338
Butyl acrylate (141-32-2)		226, 315, 317, 319, 332, 335, 412	210, 273, 280, 303+361+353, 304+340+312, 305+351+338
Carbon tetrabromide (558-13-4)		302, 315, 318, 335	261, 264, 280, 301+312, 302+352, 305+351+338
Carbon tetrachloride (56-23-5)		301+311+331, 317, 351, 372, 412, 420	273, 280, 301+310, 302+352+312, 304+340+311, 502
Chloroform-d_1 (865-49-6)		302, 315, 319, 331, 336, 351, 361d, 372	202, 301+312, 302+352, 304+340+311, 305+351+338, 308+313
Cobalt(II) chloride (7646-79-9)		302, 317, 318, 334, 341, 350i, 360F, 410	273, 280, 301+312, 302+352, 305+351+338, 308+313
Dichloromethane (75-09-2)		315, 319, 336, 351	202, 261, 264, 302+352, 305+351+338, 308+313
Diethyl ether (60-29-7)		224, 302, 336	210, 24, 240, 241, 301+312+403+233

Diethylene glycol (111-46-6)		302	264-270-301+312, 501
Dodecyl mercaptan (112-55-0)		314, 317, 410	261, 272, 273, 280, 303+361+353, 305+351+338
Ethanol (64-17-5)		225, 319	210, 233, 240, 241, 242, 305+351+338
Ethyl acrylate (140-88-5)		225, 302+312, 315, 317, 319, 331, 335, 412	210, 273, 280, 301+312, 303+361+353, 304+340+311
Fluorobenzene (462-06-6)		225, 318, 411	210, 233, 240, 273, 280, 305+351+338
JEFFAMINE D-230 (9046-10-0)		314, 318, 412	264, 273, 280, 301+330+331, 303+361+353, 304+340+310, 305+351+338, 363, 405, 501
Lithium perchlorate (7791-03-9)		272, 302, 315, 319, 335	210, 220, 261, 301+312, 302+352, 305+351+338
Methacryloyl chloride (920-46-7)		225, 302, 314, 317, 330, 412	210, 273, 280, 303+361+353, 304+340+310, 305+351+338
Methanol-d_4 (811-98-3)		225, 301+311+331, 370	210, 233, 280, 301+310, 303+361+353, 304+340+311
Methyl acrylate (96-33-3)		225, 302+312, 315, 317, 319, 331, 335, 412	210, 273, 280, 301+312, 303+361+353, 304+340+311
Methyl methacrylate (80-62-6)		225, 315, 317, 335	210, 233, 240, 241, 280, 303+361+353
n-Butanol (71-36-3)		226, 302, 315, 318, 335, 336	210, 233, 280, 301+312, 303+361+353, 305+351+338
n-Butylamine (109-73-9)		225, 290, 302, 311+331, 314	210, 280, 301+312, 303+361+353, 304+340+310, 305+351+338
Pentane (203-692-4)	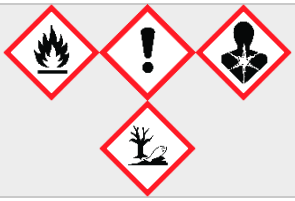	225, 304, 336, 411	210, 233, 240, 273, 301, 310, 331

Perchloric acid (7601-90-3)		271, 290, 302, 314, 373	210, 280, 301+312, 303+361+353, 305+351+338, 314
Phorsphorus pentoxide (1314-56-3)		314	280, 303+361+353, 305+351+338+310
Silver Perchlorate (7783-93-9)		272, 314	210, 220, 260, 280, 303+361+353, 305+351+338
Styrene (100-42-5)		226, 315, 319, 332, 361d, 372	202, 210, 303+361+353, 304+340+312, 305+351+338, 308+313
Sulfuric acid (conc.) (8014-95-7)		314, 330, 335	260, 271, 280, 303+361+353, 304+340+310, 305+351+338
Tetrahydrofuran (109-99-9)		225, 302, 319, 335, 336, 351	201, 202, 210, 301, 312, 305+351+338, 308+313
Toluene (108-88-3)		225, 304, 315, 336, 361d, 373, 412	202, 210, 273, 301+310, 303+361+353, 331
Triethylamine (204-469-4)		225, 302, 311, 331, 314, 335	210, 280, 301+312, 303+361+353, 304+340+310, 305+351+338
Trifluoromethanesulfonic acid (1493-13-6)		290, 302, 314, 335	234, 261, 280, 301+312, 303+361+353, 305+351+338
Vinyl acetate (108-05-4)		225, 332, 335, 351, 412	201, 202, 210, 273, 304+340+312, 308+313
Xylene (1330-20-7)		226, 304, 312+332, 315, 319, 335, 373, 412	210, 273, 280, 301+310, 303+361+353, 331
Zink (dust) (7440-66-6)		410	273, 391, 501
Zink oxide (1314-13-2)		410	273, 391, 501

Table 9. Quantity, application and categorical classification of carcinogenic, mutagenic and reprotoxic (CMR) chemicals used.[195]

Substance (CAS-No.)	Quantity	Application	Category
(±)-Epichlorohydrin	~30 mL	Reagent	Carcinogenicity: 1b
Benzene (71-43-2)	~500 mL	Solvent	Carcinogenicity: 1A Germ Cell Mutagenicity: 1B
Carbon tetrachloride (56-23-5)	~300 mL	Solvent	Carcinogenicity: 2
Chloroform-d_1 (865-49-6)	~3 L	Analysis	Reproductive toxicity: 2 Carcinogenicity: 2
Cobalt(II) chloride (7646-79-9)	~10 mg	Reagent	Carcinogenicity: 1b Germ Cell Mutagenicity: 2 Reproductive toxicity: 1b
Dichloromethane (75-09-2)	~50 L	Solvent	Carcinogenicity: 2
Styrene (100-42-5)	~100 mL	Reagent	Reproductive toxicity: 2
Tetrahydrofuran (109-99-9)	~5 L	Solvent	Carcinogenicity: 2
Toluene (108-88-3)	~10 L	Solvent	Reproductive toxicity: 2
Vinyl acetate (108-05-4)	~5 mL	Reagent	Carcinogenicity: 2

8.2 Spectra and Chromatograms

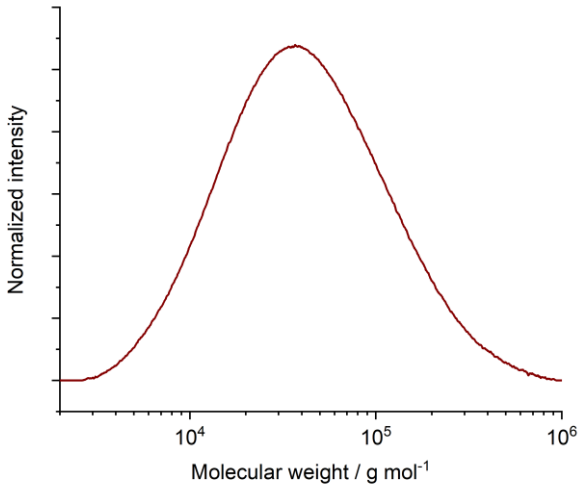

Figure 47. SEC chromatogram of P(MA-pCBA3.4)[137].

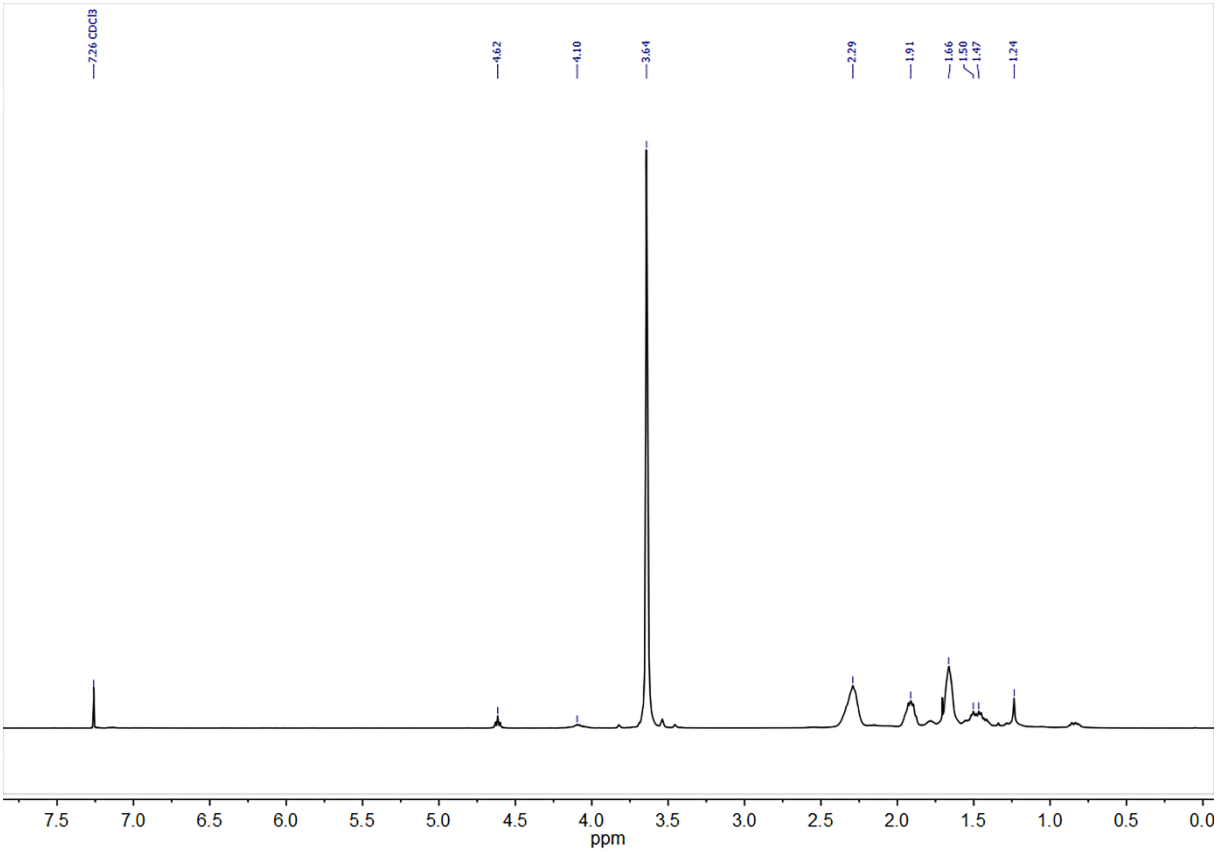

Figure 48. ^{1}H NMR spectrum of P(MA-pCBA3.4)[137].

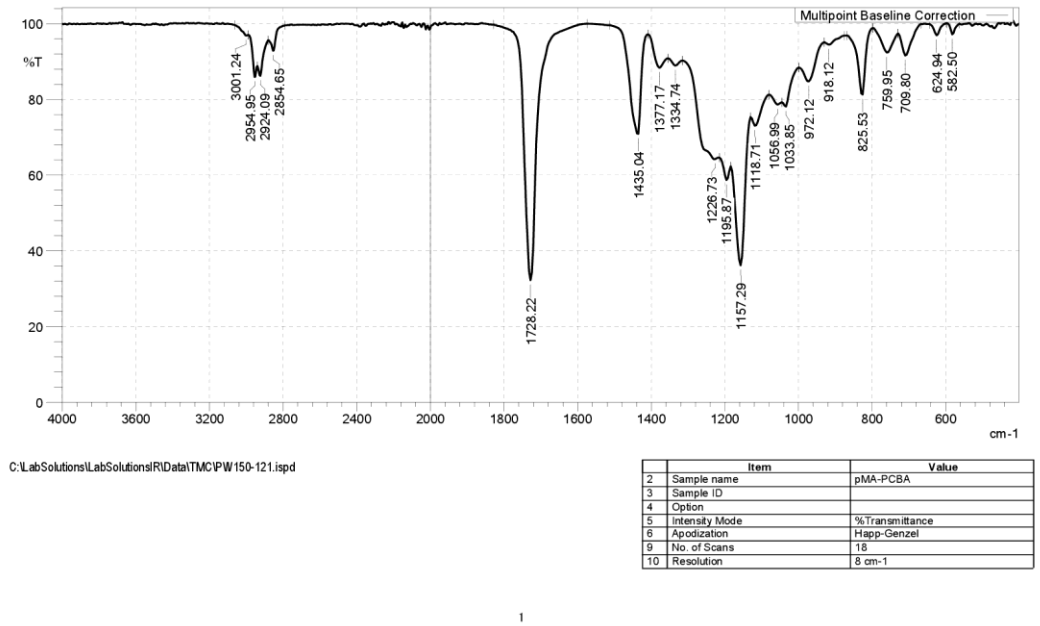

Figure 49. IR spectrum of P(MA-pCBA3.4)[137].

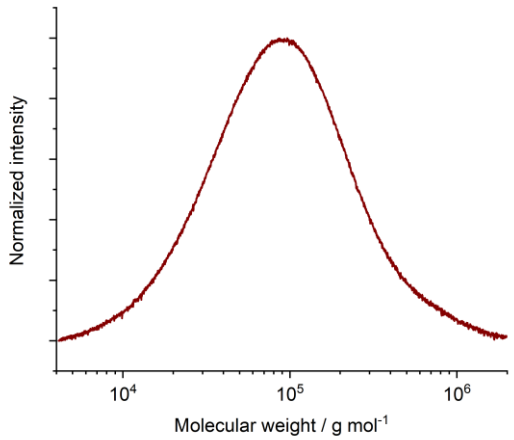

Figure 50. SEC chromatogram of P(EA-pCBA0.9)[137].

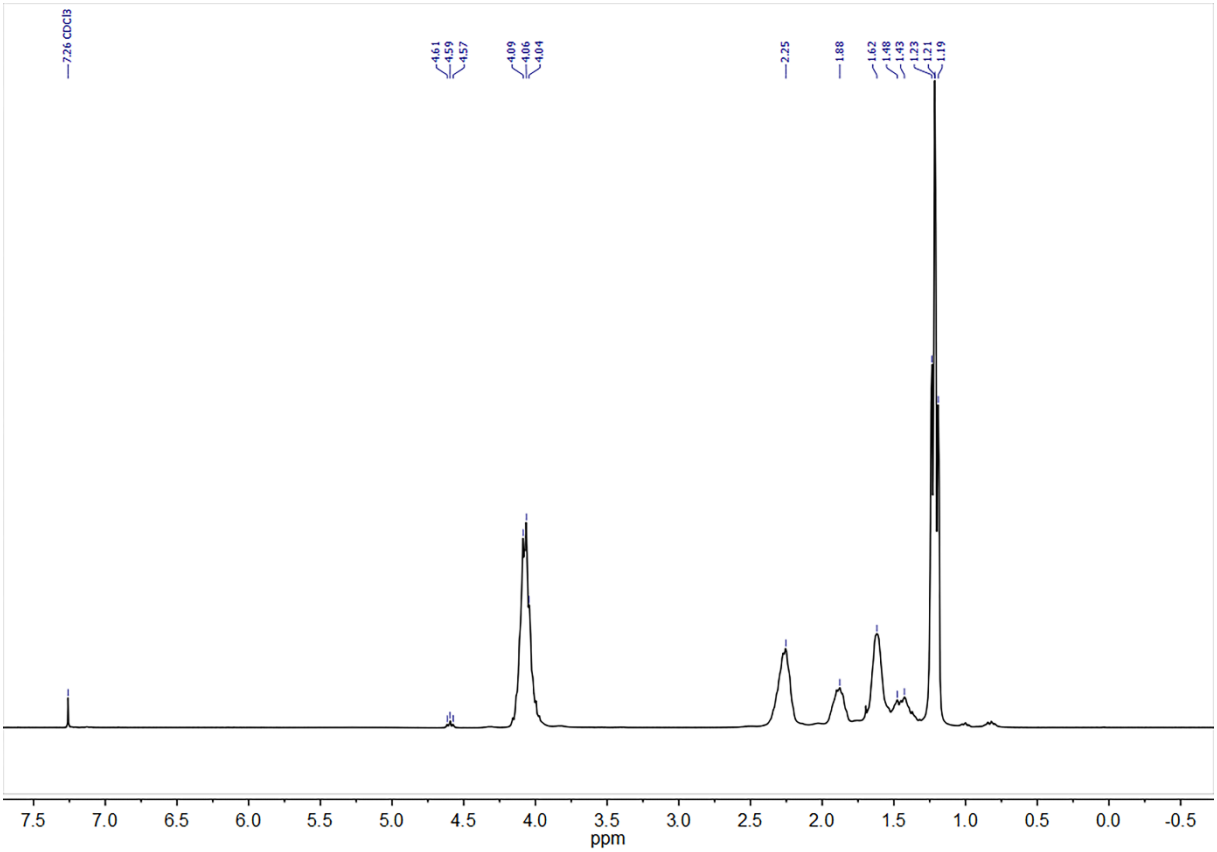

Figure 51. ^{1}H NMR spectrum of P(EA-pCBA0.9)[137].

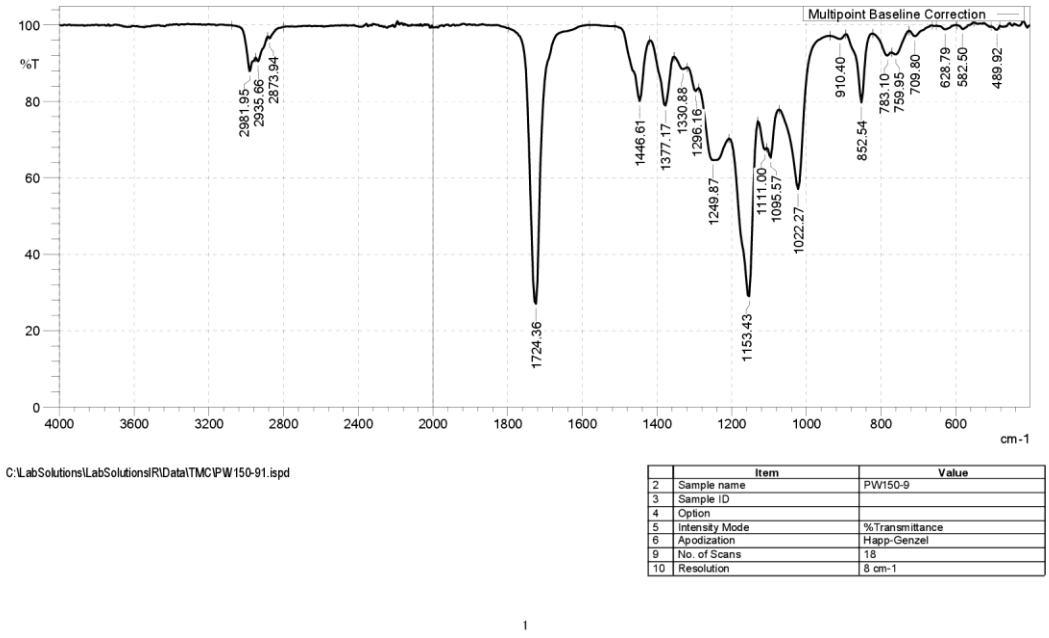

Figure 52. IR spectrum of P(EA-pCBA0.9)[137].

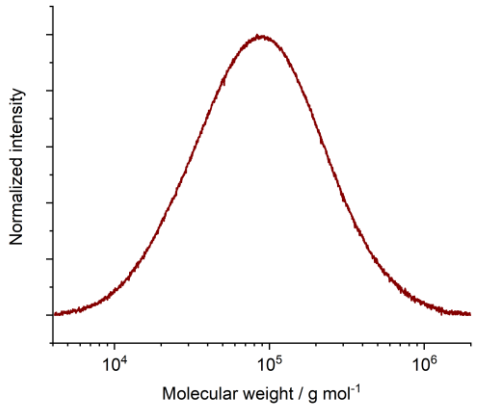

Figure 53. SEC chromatogram of P(EA-pCBA1.7)[137].

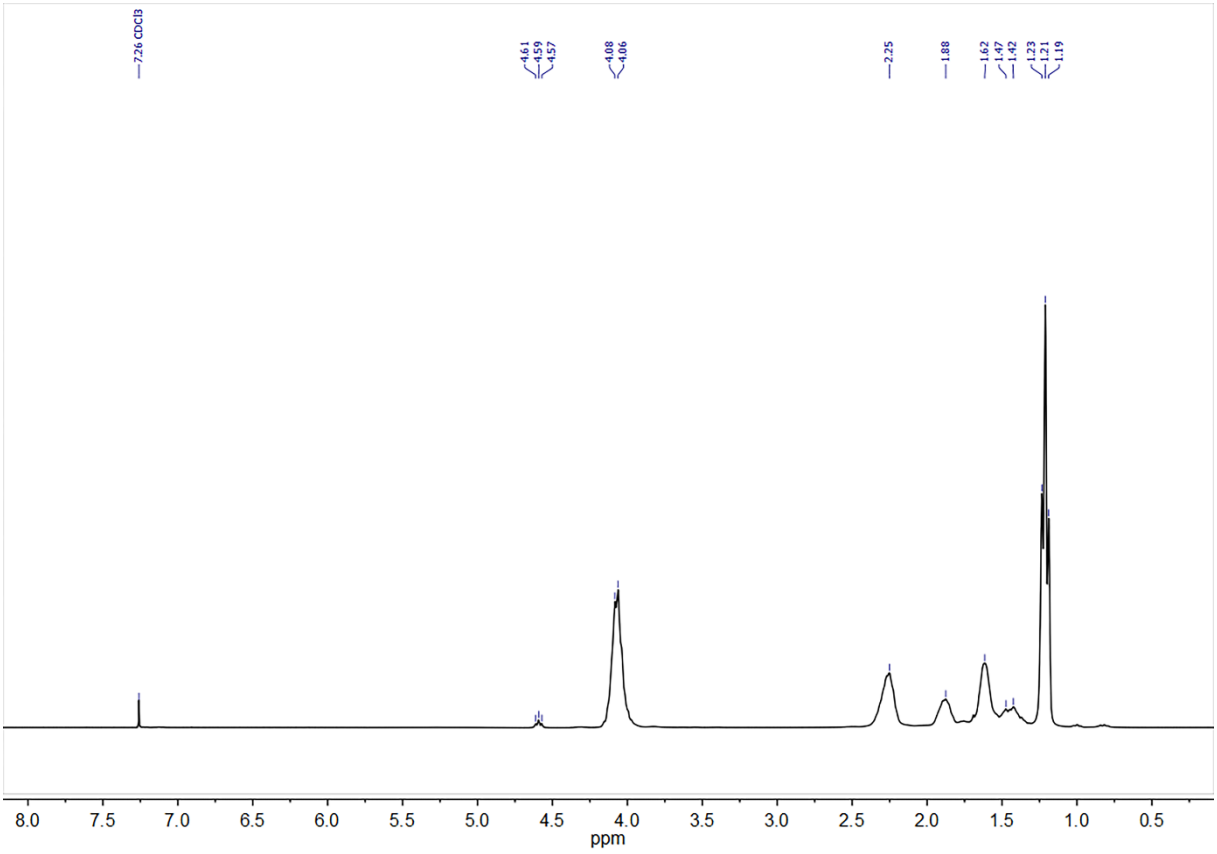

Figure 54. ^{1}H NMR spectrum of P(EA-pCBA1.7)[137].

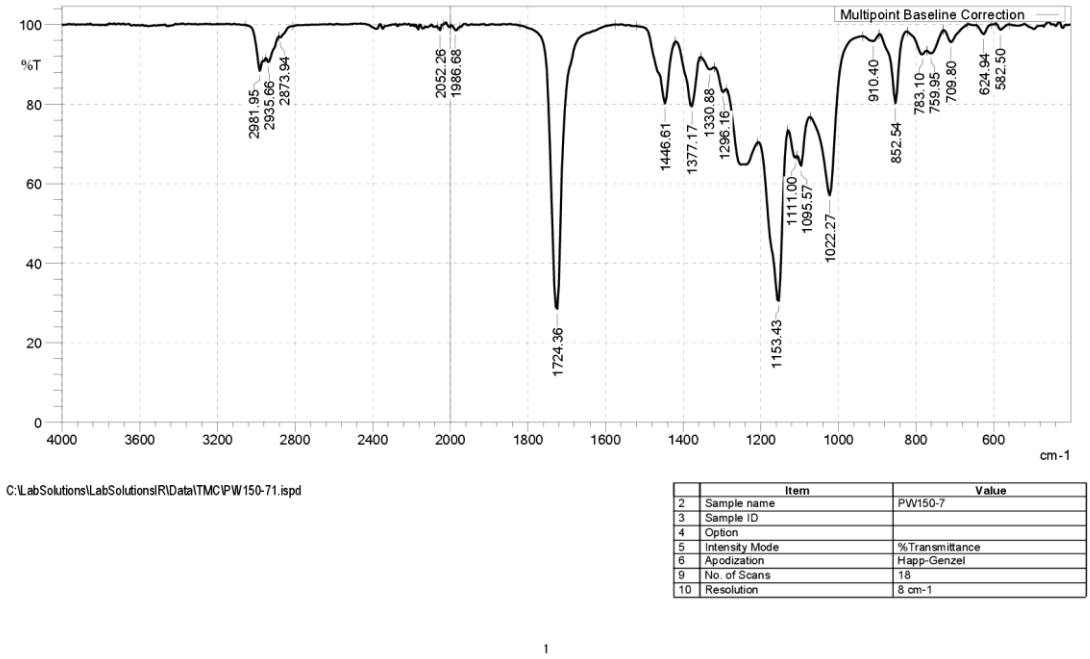

Figure 55. IR spectrum of P(EA-pCBA1.7)[137].

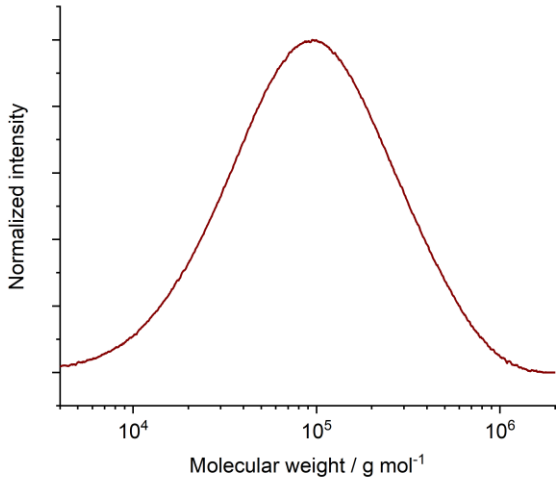

Figure 56. SEC chromatogram of P(EA-pCBA3.5)[137].

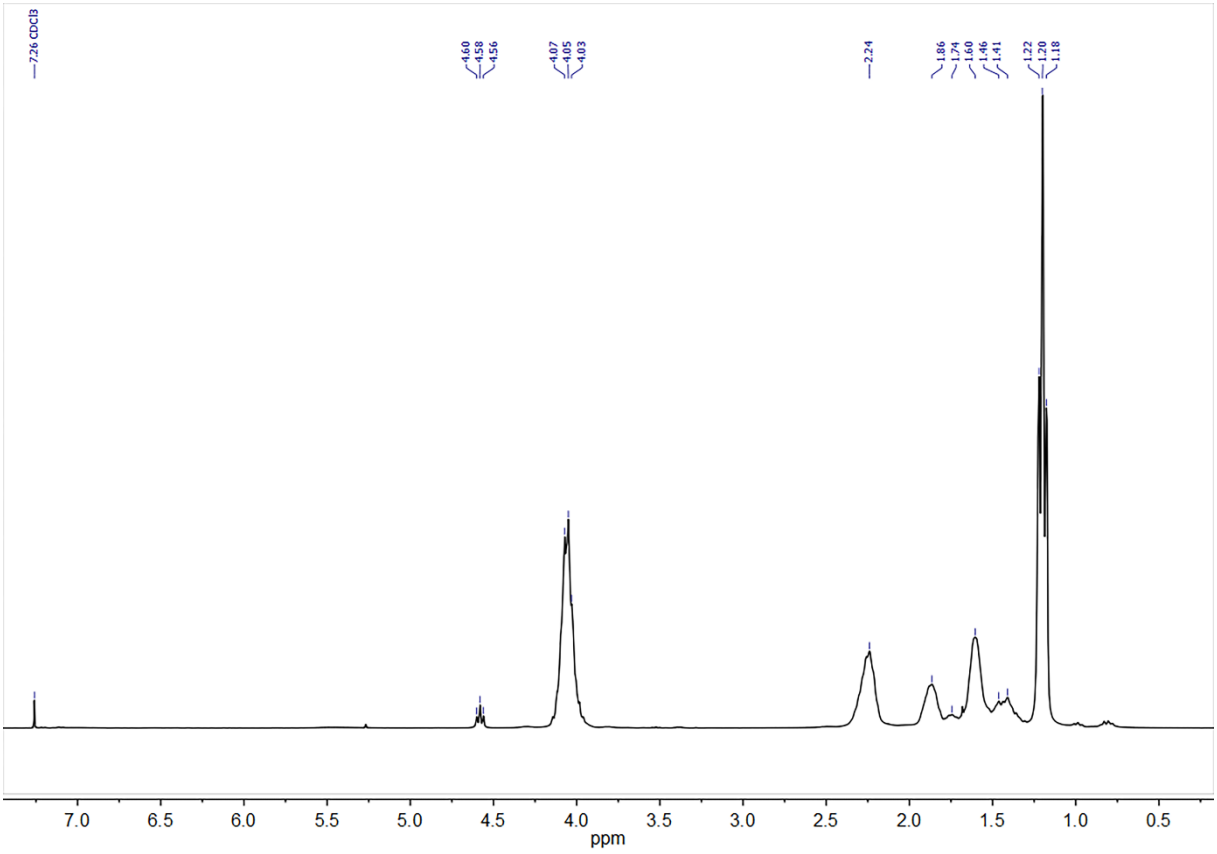

Figure 57. ^{1}H NMR spectrum of P(EA-pCBA3.5)[137].

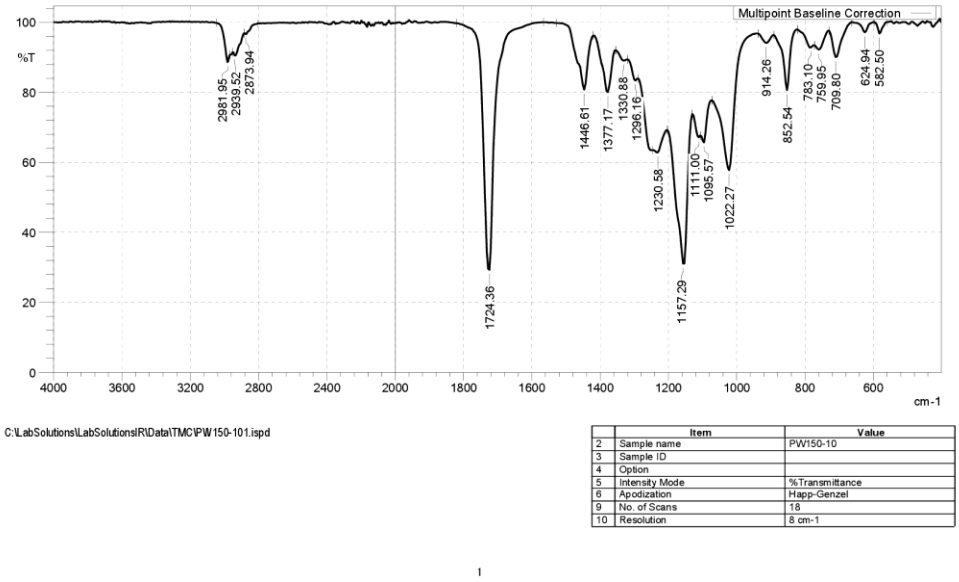

Figure 58. IR spectrum of P(EA-pCBA3.5)[137].

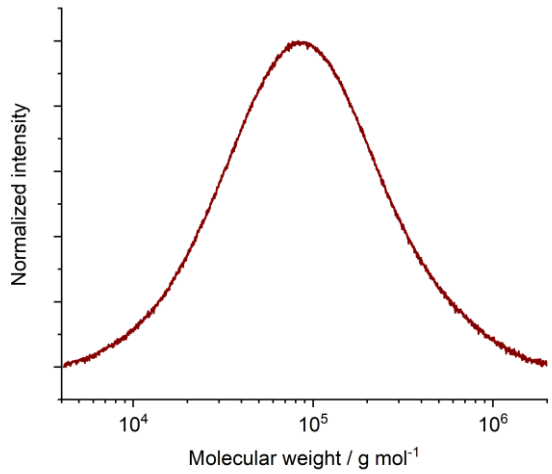

Figure 59. SEC chromatogram of P(EA-pCBA4.6)[137].

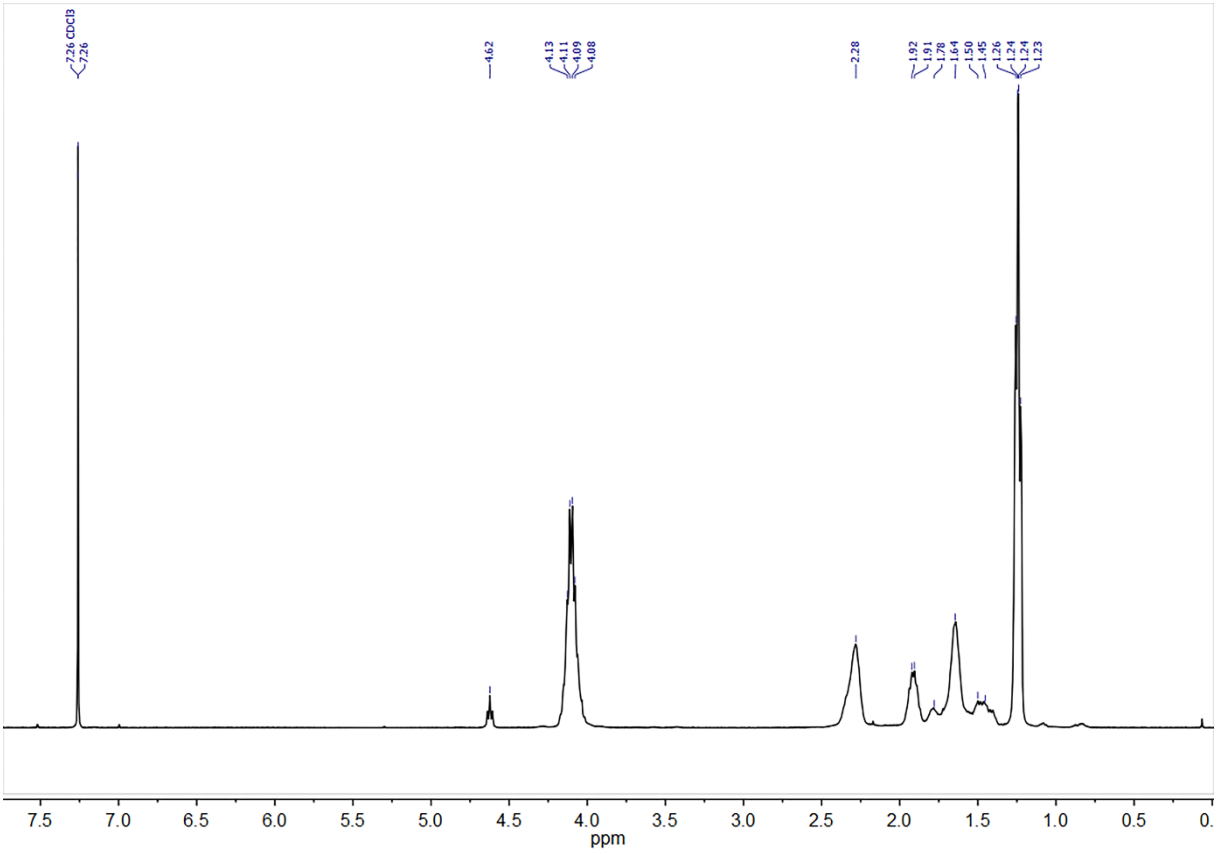

Figure 60. ^{1}H NMR spectrum of P(EA-pCBA4.6)[137].

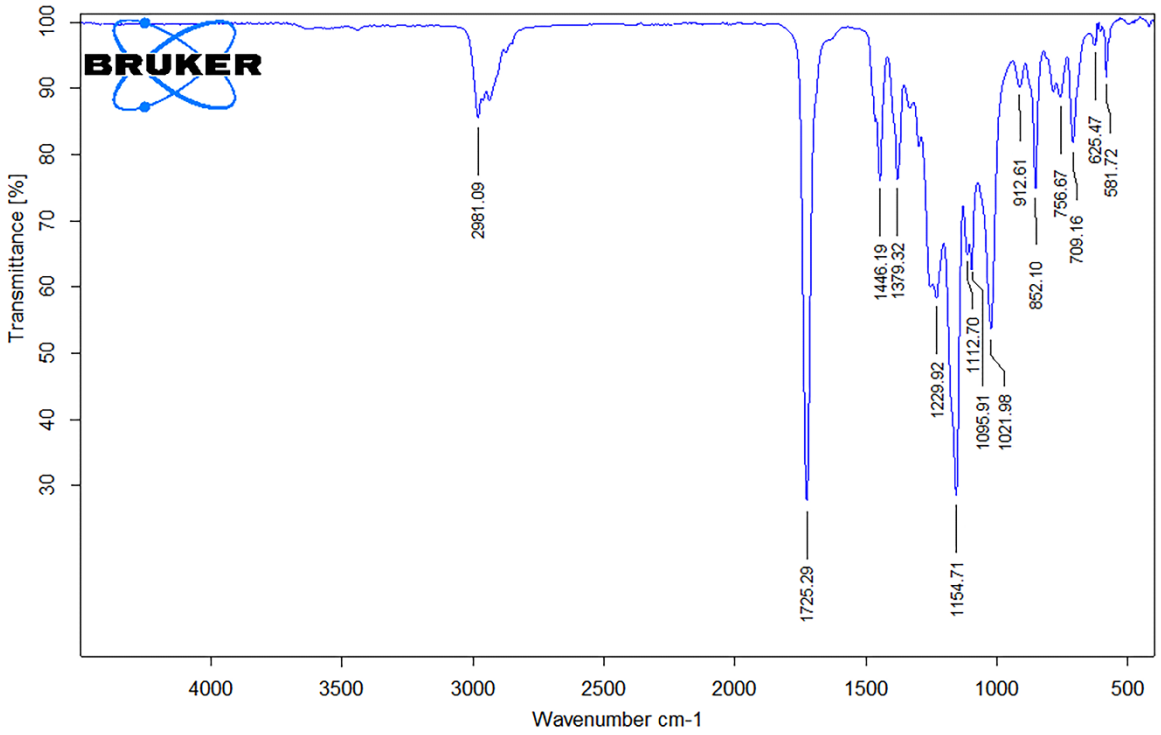

Figure 61. IR spectrum of P(EA-pCBA4.6)[137].

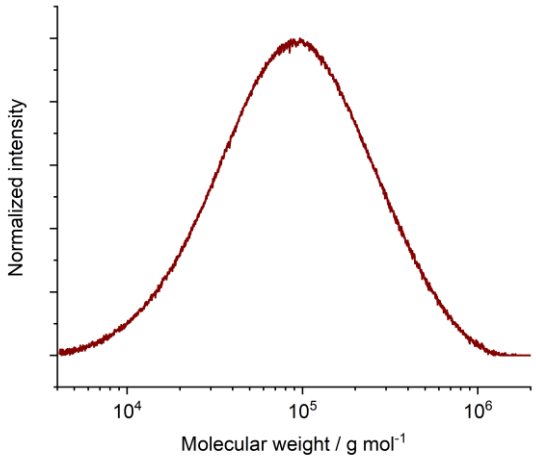

Figure 62. SEC chromatogram of P(EA-pCBA8.0)[137].

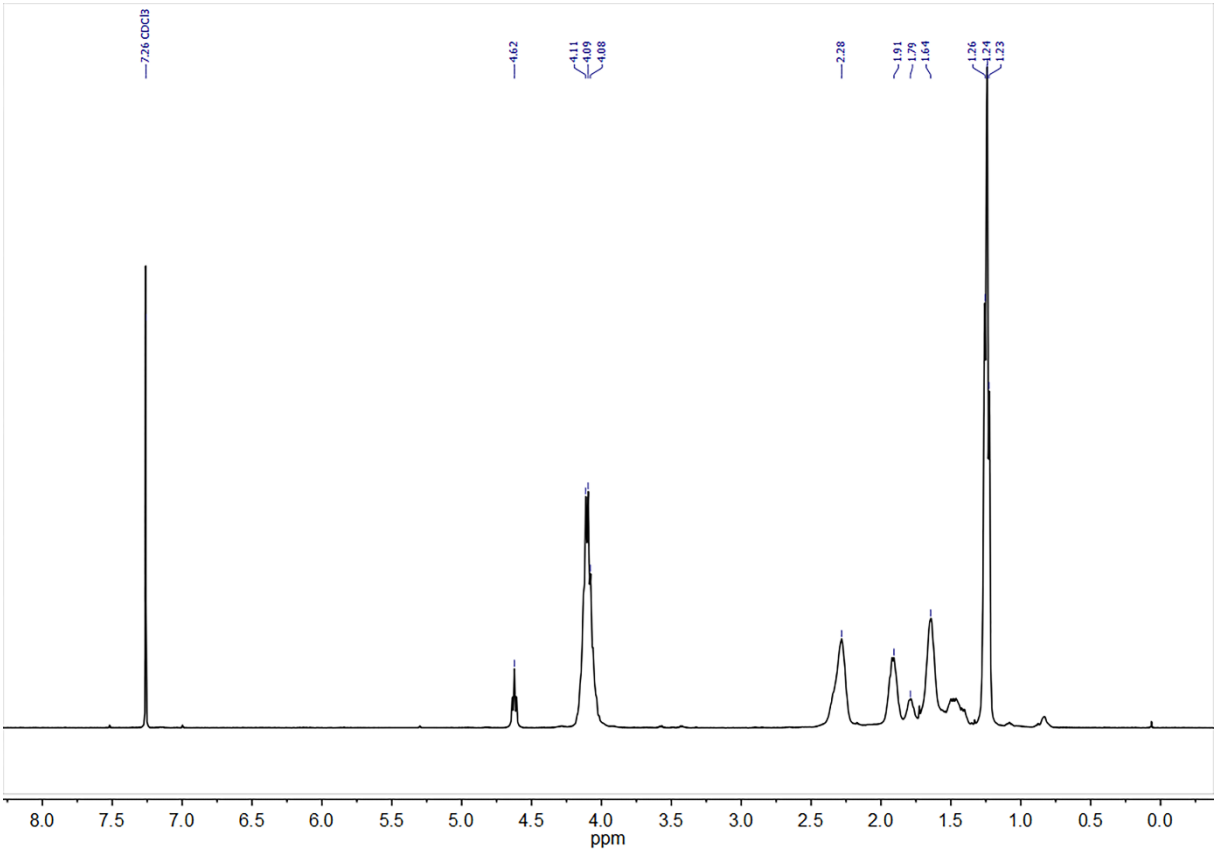

Figure 63. ^{1}H NMR spectrum of P(EA-pCBA8.0)[137].

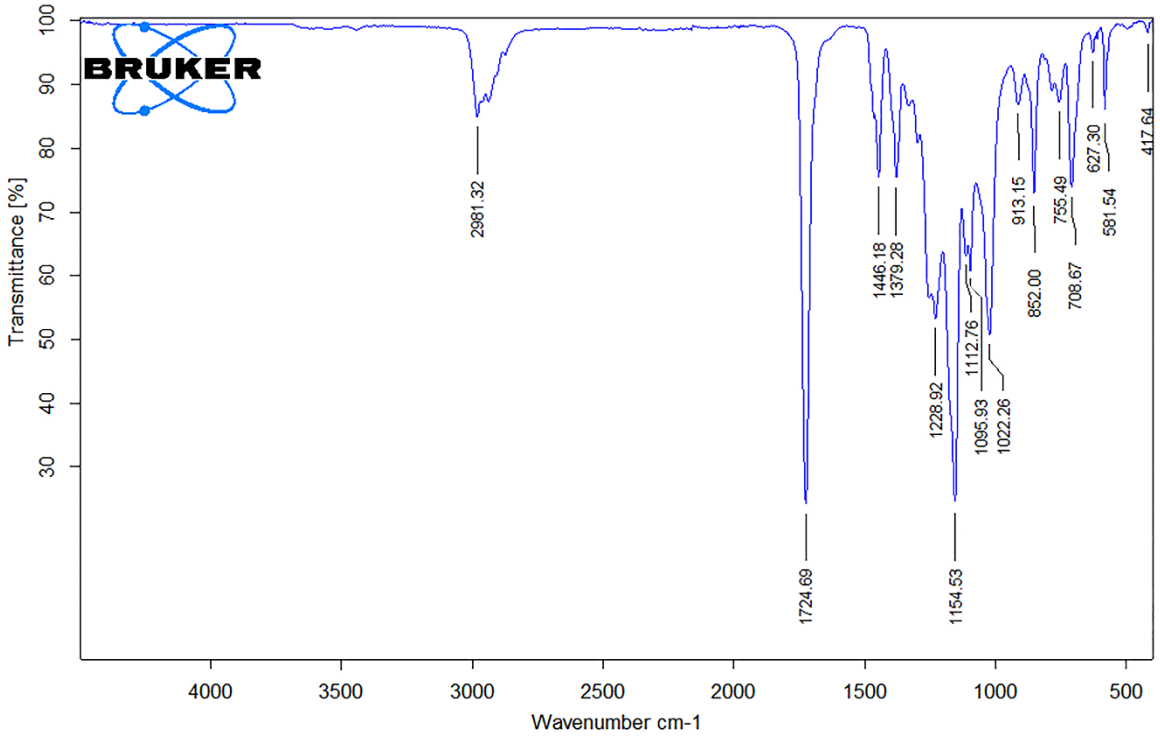

Figure 64. IR spectrum of P(EA-pCBA8.0)[137].

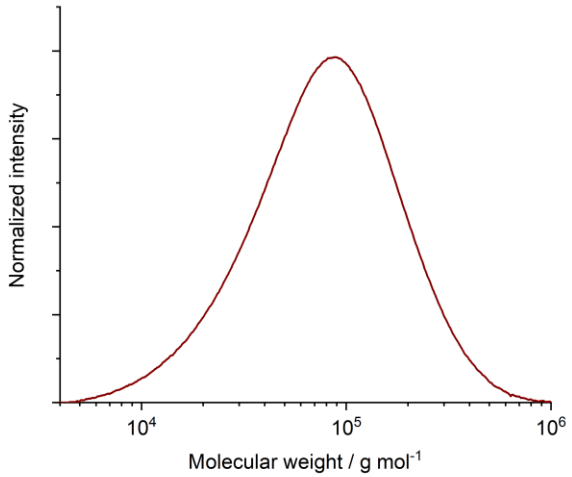

Figure 65. SEC chromatogram of P(BA-pCBA4.7)[137].

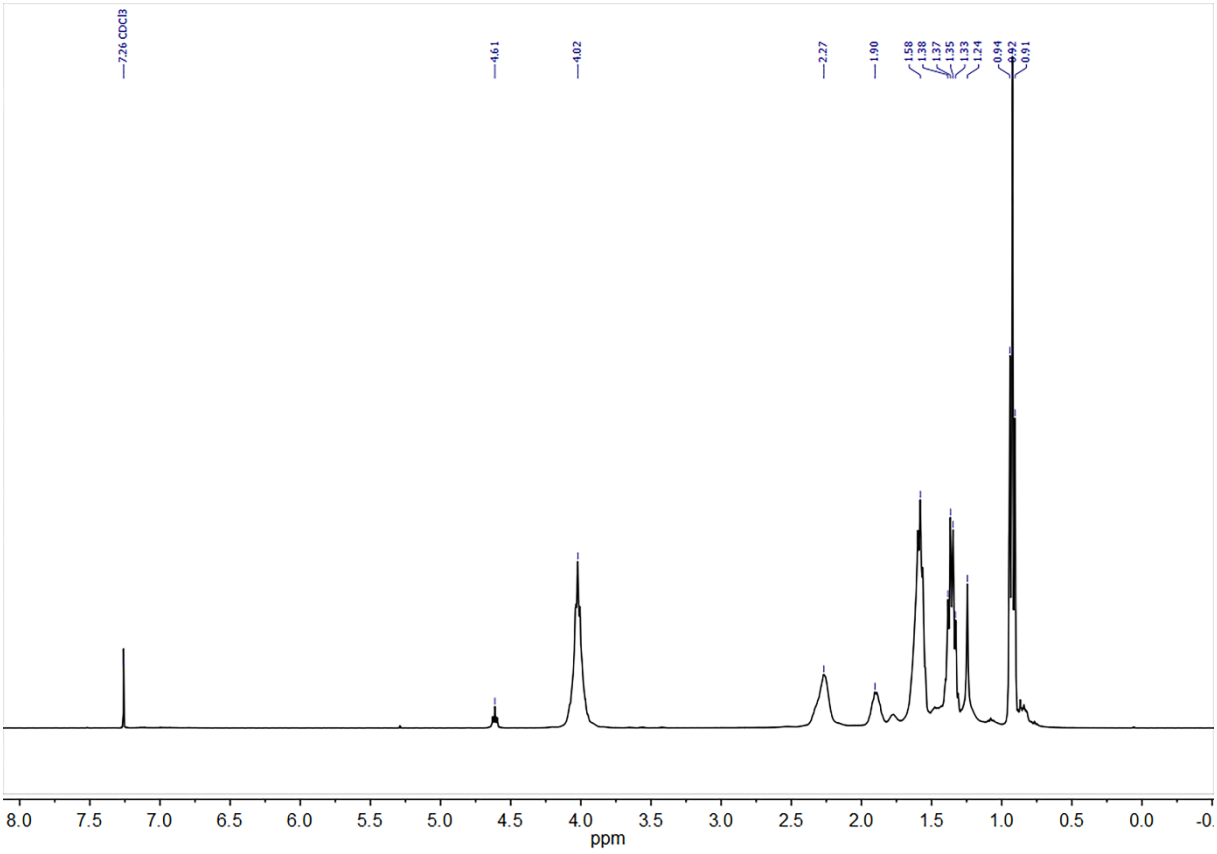

Figure 66. ^{1}H NMR spectrum of P(BA-pCBA4.7)[137].

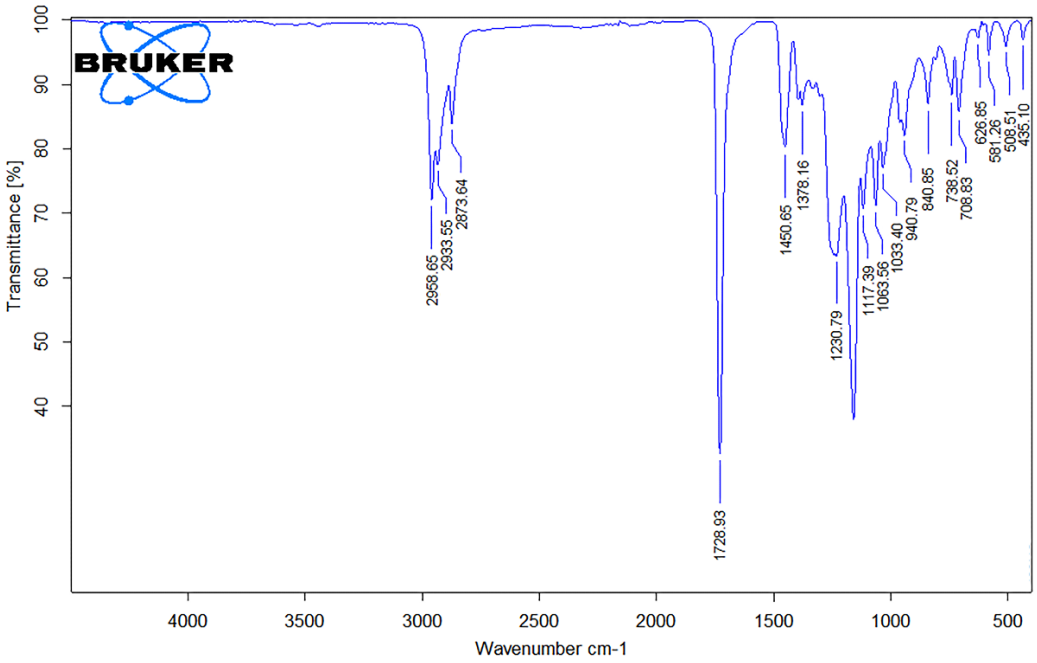

Figure 67. IR spectrum of P(BA-pCBA4.7)[137].

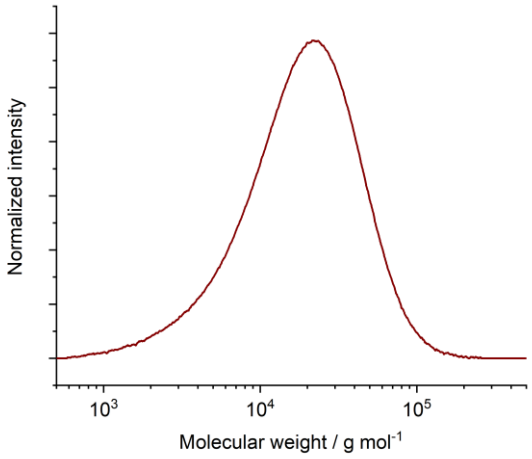

Figure 68. SEC chromatogram of P(MMA-pCBA2.5)[137].

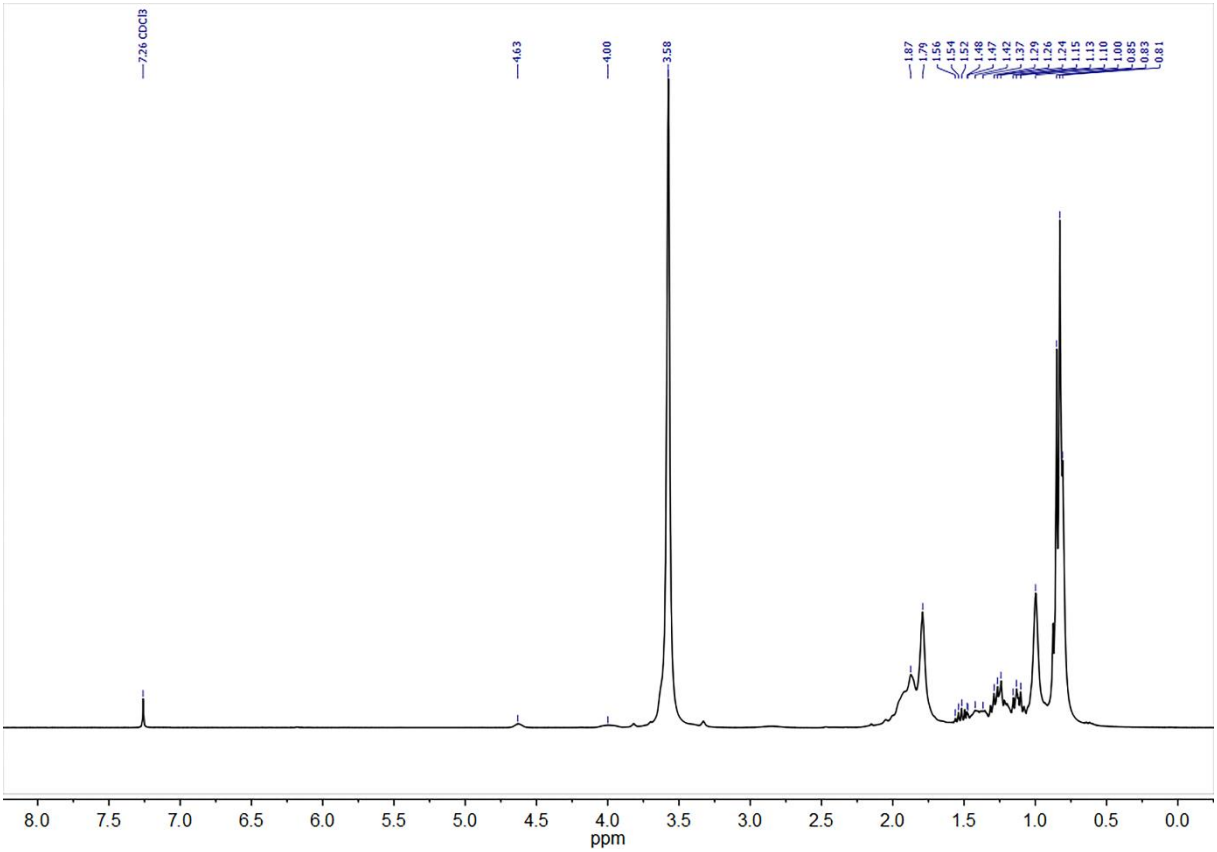

Figure 69. ^{1}H NMR spectrum of P(MMA-pCBA2.5)[137].

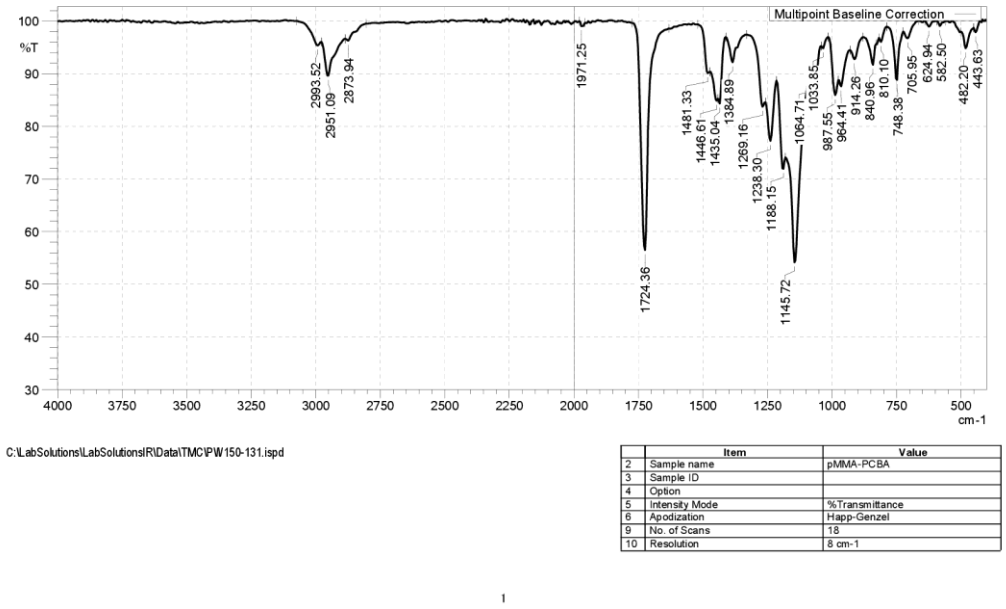

Figure 70. IR spectrum of P(MMA-pCBA2.5)[137].

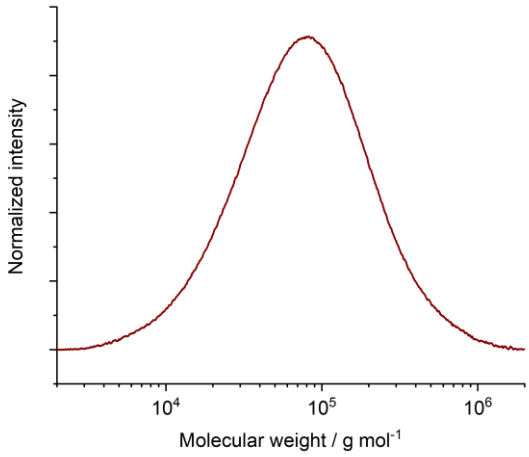

Figure 71. SEC chromatogram of PEA polymerized in the presence of *n*-decyl perchlorate[137].

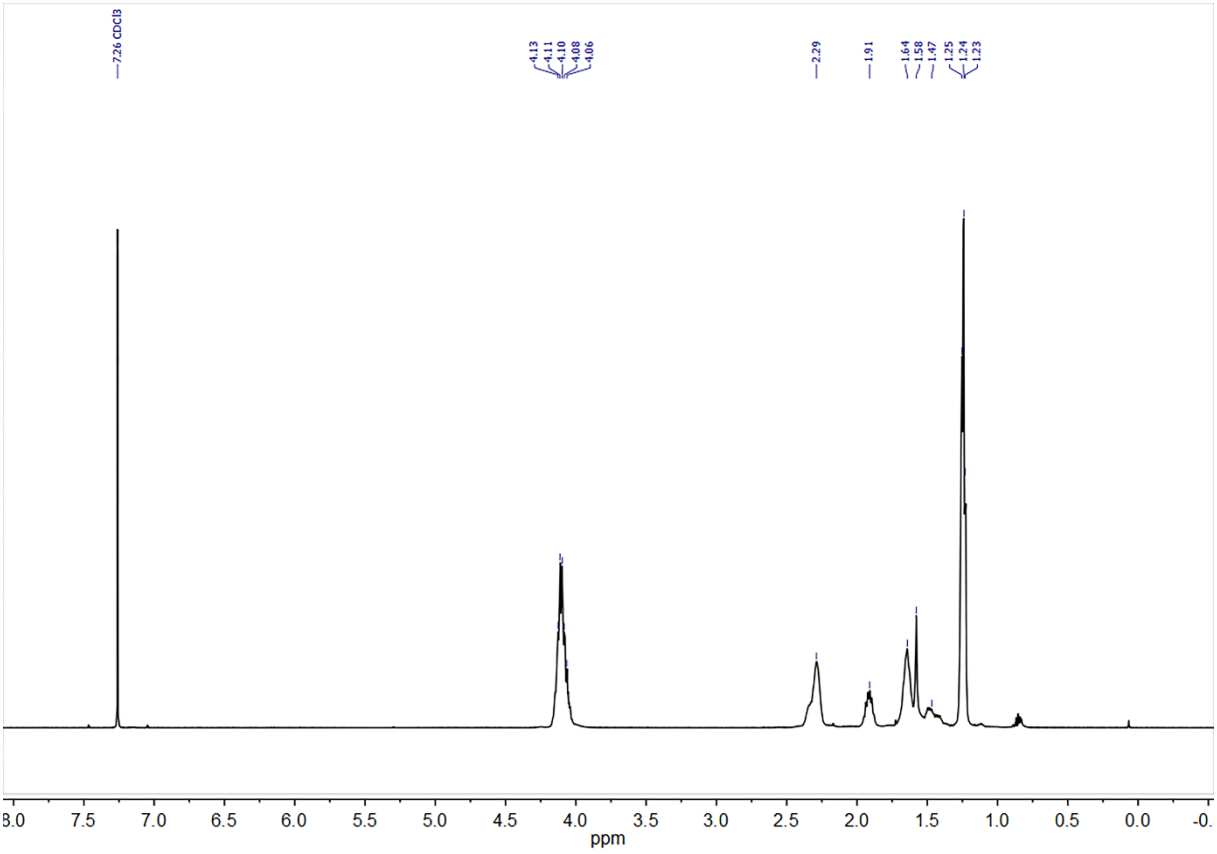

Figure 72. [1]H NMR spectrum of PEA polymerized in the presence of *n*-decyl perchlorate[137].

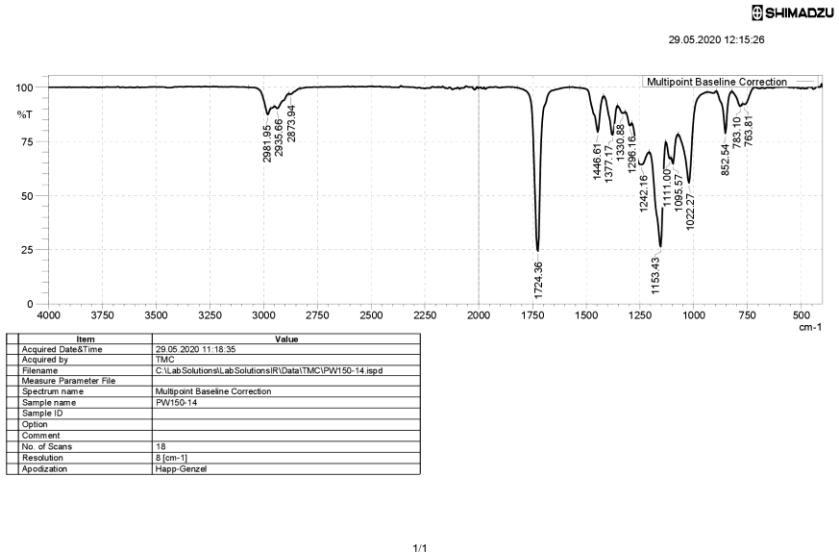

Figure 73. IR spectrum of PEA polymerized in the presence of *n*-decyl perchlorate[137].

Eidesstattliche Erklärung

Hiermit versichere ich an Eides statt, die vorliegende Dissertationsschrift selbst verfasst und keine anderen als die angegebenen Quellen und Hilfsmittel benutzt zu haben. Sofern im Zuge der Erstellung der vorliegenden Dissertationsschrift generative Künstliche Intelligenz (gKI) basierte elektronische Hilfsmittel verwendet wurden, versichere ich, dass meine eigene Leistung im Vordergrund stand und dass eine vollständige Dokumentation aller verwendeten Hilfsmittel gemäß der Guten wissenschaftlichen Praxis vorliegt. Ich trage die Verantwortung für eventuell durch die gKI generierte fehlerhafte oder verzerrte Inhalte, fehlerhafte Referenzen, Verstöße gegen das Datenschutz- und Urheberrecht oder Plagiate.

18.04.2026, Bönningstedt

Acknowledgments

I would like to take this opportunity to thank the many people who supported me over the past years on the way to the completion of this dissertation. This section is written in German.

An erster Stelle gilt mein besonderer Dank meinem Doktorvater Professor Dr. Gerrit A. Luinstra für die Aufnahme in seinen Arbeitskreis, die fachliche Betreuung sowie die Möglichkeit, an spannenden und anspruchsvollen Forschungsthemen zu arbeiten. Ich danke außerdem Privatdozent Dr. Christoph Wutz für die Übernahme des Zweitgutachtens.

Ein großer Dank gilt meinen Laborkollegen Lukas und Theresa für die sehr gute Zusammenarbeit, den fachlichen Austausch und die angenehme Arbeitsatmosphäre. Insbesondere danke ich Lukas für die sorgfältige Korrektur dieser Doktorarbeit. Ebenso möchte ich mich beim gesamten Labor für die Zusammenarbeit und die vielen gemeinsamen guten Stunden im Arbeitsalltag bedanken.

Ich bedanke mich außerdem bei meinem Praktikanten Bastian Fischer für seine experimentelle Unterstützung. Dr. Felix Scheliga danke ich für die Durchführung der zahlreichen GPC-Messungen sowie Stefan Bleck für die Durchführung der DSC-Messungen. Darüber hinaus danke ich Dr. Young Joo Lee für die Durchführung der ^{13}C CP MAS NMR-spektroskopischen Untersuchungen. Ein besonderer Dank gilt Professor Dr. Michael Fröba für den Zugang zum TGA-IR-Instrument sowie Frau Sazama für die Durchführung zahlreicher Messungen.

Ein ganz besonderer Dank gilt meinen Eltern und meiner Familie, die mich über all die Jahre hinweg bedingungslos unterstützt und mir diesen Weg überhaupt erst ermöglicht haben. Vielen Dank für das Vertrauen, die Geduld und das Verständnis, auch über die Zeit an der Universität hinaus.

Der abschließende Dank gilt meiner Frau Lara sowie unseren Kindern Sophia und Milan für ihren Rückhalt, ihre Geduld und ihre Unterstützung. Vielen Dank für euer Verständnis und dafür, dass ihr immer an meiner Seite steht.